Epigenetic regulation in rodent primordial germ cells
and
preimplantation embryos

Aristea Maria Magaraki

ISBN: 978-94-6299-519-2

Cover: Eirini Gerogianni e.gerogianni@gmail.com

Layout: Eirini Gerogianni e.gerogianni@gmail.com, Aristea Magaraki

Printing: Ridderprint BV, Ridderkerk, the Netherlands

The work described in this thesis was performed at the Department of Developmental Biology at the Erasmus MC in Rotterdam, the Netherlands.

Printing of this thesis was financially supported by Erasmus University Rotterdam, and Department of Reproduction and Development, Erasmus MC.

Copyright © 2017 by A.M. Magaraki. All rights reserved. No part of this book may be reproduced, stored in a retrieval system or transmitted in any form or by any means, without prior permission of the author.

Epigenetic regulation in rodent primordial germ cells
and
preimplantation embryos

Epigenetische regulatie in primordiale kiemcellen
en
pre-implantatie embryo's van knaagdieren

Thesis

to obtain the degree of Doctor from the Erasmus University Rotterdam
by command of the rector magnificus

Prof.dr. H.A.P. Pols

and in accordance with the decision of the Doctorate Board.

The public defense shall be held on
Tuesday 17 January 2017 at 15.30 hrs

by

Aristea Maria Magaraki
born in Heraklion Crete, Greece

Erasmus University Rotterdam

DOCTORAL COMMITTEE

Promotor: Prof.dr. J.H. Gribnau

Other members: Prof.dr. A.H.F.M. Peters
Prof.dr. C.P. Verrijzer
Prof.dr. A.B. Houtsmuller

Copromotors: Dr. M. Eijpe
Dr.ir. W.M. Baarends

TABLE OF CONTENTS

Chapter 1	General Introduction	7
	Aim and scope of this thesis	55
Chapter 2	Round spermatid injection rescues female lethality of a paternally inherited *Xist* deletion in mouse	57
Chapter 3	Silencing markers are retained on pericentric heterochromatin during murine primordial germ cell development	91
Chapter 4	Generation of a novel *in vitro* differentiation strategy to study the dynamics of X chromosome inactivation in rat	125
Chapter 5	A robust protocol for simultaneous DNA-RNA FISH in mouse preimplantation embryos	149
Chapter 6	General discussion	169
Addendum	Summary	189
	Samenvatting	194
	List of abbreviations	199
	Curriculum Vitae	202
	List of publications	203
	Ph.D. portfolio	204
	Acknowledgements	205

Chapter 1

GENERAL INTRODUCTION & SCOPE OF THIS THESIS

1. General introduction

In mammals, each individual arises from the successful fusion of two competent gametes: the sperm and the oocyte, derived from the father and the mother, respectively. Following fertilization, a single totipotent cell, called the zygote, will divide mitotically to generate numerous genetically identical cells. These will eventually give rise to the roughly 200 different cell types of the mammalian adult organism through several steps of specification. During these steps, certain genes are switched on or off to give each cell its unique function within the organism. In somatic cells (defined as all the cells that make the body, except the (developing) germ cells), DNA is wrapped around histone octamers, named nucleosomes, and this compacts the DNA to form the 30nm chromatin fibers. The switching on or off of genes is regulated through various mechanisms, usually involving modifications of histones or DNA, or both. Together, these are referred to as epigenetic modifications. An important property of epigenetic modifications is that they can be inherited through cell divisions, and even sometimes from parent to child, and to subsequent generations, through processes called inter- and trans-generational inheritance, respectively.

Throughout mouse development, major epigenetic reorganization events characterize certain developmental phases. Four major events, relevant in the context of this thesis, are illustrated in Figure 1. The first is evident immediately after fertilization, when the paternal pronucleus is drastically remodelled, because the DNA of sperm nucleus that entered was tightly packaged by protamines instead of histones. Upon fertilization these protamines are removed and replaced by maternal histones to generate a canonical chromatin structure, built from nucleosomes (see 1.2.1). This leads to an epigenetic asymmetry between the paternal (unmodified histones) and maternal (modified histones) pronucleus within the zygote. The epigenetic asymmetry between the two parental genomes persists until around the 2- to 4-cell stage of the pre-implantation embryo. Until that stage the maternal and paternal chromosomes remain compartmentalized and therefore the maternally derived histone marks are present in only half the nuclear area (reviewed in Burton & Torres-Padilla 2010).

Second, in the preimplantation female embryos, X chromosome inactivation is a major event (see 1.2.2). Maleness in mammals is determined by the presence of the Y chromosome. This chromosome is relatively gene-poor but evolutionary derived from the X chromosome that is gene rich. The X and the Y chromosome are the sex chromosomes, whereby male cells carry an X and a Y chromosome, and female cells have two X chromosomes but no Y. All other chromosomes (numbered based on their length, 1 being the longest) come in pairs. The presence of two X chromosomes per diploid genome in females and only one in males creates a difference in the dosage of X-linked genes versus autosomal genes between males and females. To compensate for this difference, a mechanism has evolved that ensures inactivation of one complete X chromosome already in female mouse pre-implantation embryos.

Third, after implantation, the future germ line is set apart and its epigenome is reset (see 1.2.5). The germline emerges from epiblast cells, which are cells already programmed towards a somatic fate. In the germline cells, specific changes in histone and DNA modifications will reset the epigenome of those cells and ensure that competent gametes can arise later, when the animal reaches puberty.

Finally, in males, the histone to protamine transition reprogramming event takes place in the final stage of spermatogenesis, called spermiogenesis. During this phase, the histones of the developing sperm are genome-widely replaced by protamines, which are small, positively charged proteins. The replacement of histones by protamines in the sperm will compact the DNA, to protect the genome during its journey to the oocyte (see 1.2.8). Generation of mature oocytes and sperm in females and males, respectively, may then be followed by fertilization and development thus ensuring that the cycle of life never stops.

In this chapter, I will first give a general overview of chromatin organization, with most emphasis on the detailed organisation of pericentric heterochromatin. Then I will describe each of the above mentioned reprogramming events that accompany the cycle of life in more detail, starting with the epigenetic asymmetry in the mouse zygote.

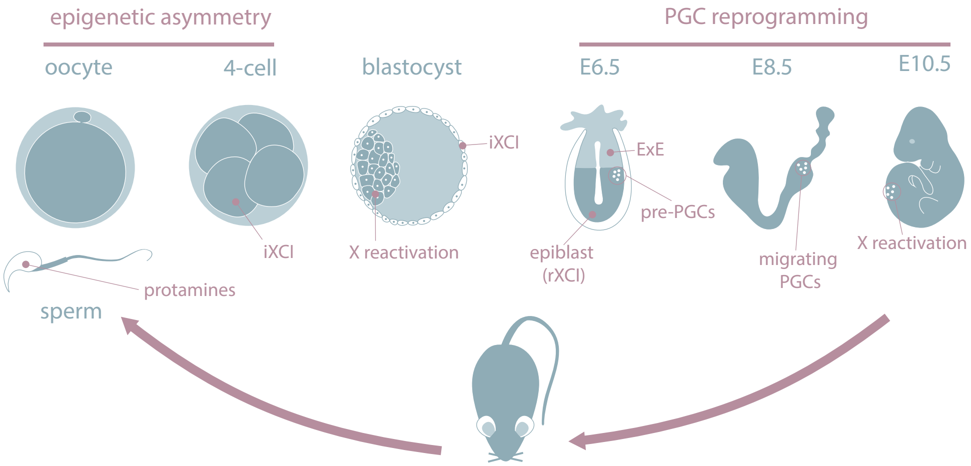

Figure 1: Major epigenetic reorganisation events during the mouse life cycle

The genome of sperm is tightly packaged by protamines, while the oocyte retains a nucleosome based chromatin. Shortly after fertilization, protamines are replaced by unmodified histones provided by the oocyte. This generates a genome-wide epigenetic asymmetry between the paternal and maternal pronucleus. The asymmetry persists approximately until the 4-cell stage of mouse embryo development. At this stage, if the embryo is female, the paternal X chromosome will become inactivated (iXCI). Reactivation of the paternal X takes place in the inner cell mass (ICM) of the blastocyst (followed by random XCI (rXCI) in the developing embryo), while iXCI is retained in the trophectoderm (TE). Later on, PGC precursor cells (pre-PGCs) are specified in the epiblast by signals emerging from the extra-embryonic ectoderm (ExE), where XCI remains imprinted. During migration of PGCs to the developing gonads, genome wide reprogramming occurs, which includes changes in histone marks, DNA modifications and reactivation of the inactive X if the embryo is female.

1.1. A general overview of chromatin organization

1.1.1 The overall assembly of chromatin

The diploid mouse genomic DNA is organized into 20 pairs of chromosomes, of which 19 pairs are autosomal and one pair determines the sex (XY or XX). Human diploid cells also contain one pair of sex chromosomes (XY or XX), but 22 pairs of autosomes. Haploid cells (sperm and ova) of all species contain one copy of each autosome and either an X (all ova and half of the sperm) or a Y chromosome (sperm only).

The DNA of each diploid cell in the mouse consists of approximately 5 billion (5.8 billion in human) bases (adenine (A), thymidine (T), cytocine (C) and guanine (G)) (Mouse Genome Sequencing Consortium et al. 2002) and if stretched, it reaches up to approximately 1.7 meters in length (2 meters in human). In order for such a lengthy molecule to fit into a microscopic nucleus (~10μm) several layers of compaction must take place (Figure 2). Important compaction mediators are the histones, positively charged proteins steadily binding the negatively charged DNA, which form the histone octamer complex. Specifically the octamer complex consists of two of each of the four different canonical histone types: H2A, H2B, H3 and H4 (Eickbush & Moudrianakis 1978). In particular cases, canonical histones can be replaced by non-canonical histone variants such as H2A.Z, in a replication independent manner (reviewed in Skene & Henikoff 2013). The first layer of DNA compaction is achieved by the wrapping of the DNA around the histones. Specifically, a DNA segment of approximately 150bp wraps around the histone octamer and an additional histone, the linker H1, binds the DNA connecting tandem histone octamers, but it is not part of these octamer complexes (Kornberg 1974). The wrapped DNA around the octamer, the octamer itself and the linker H1 form a unit termed as nucleosome (Luger et al. 1997). In general, the DNA and all associated proteins are termed as chromatin.

In addition to the folding of the DNA that is mediated by the nucleosomes, histone post-translational modifications provide an extra layer of compaction and play an important role in the regulation of gene expression. The histone post-translational modifications are usually established on the N-terminal tails of histones, which protrude from the nucleosomal core. Different enzymes add acetyl-, methyl-, phosphate- and other groups to histone tails and depending on the position and the type of each modification the chromatin will appear in a more or less condensed form and can be transcriptionally silenced or activated.

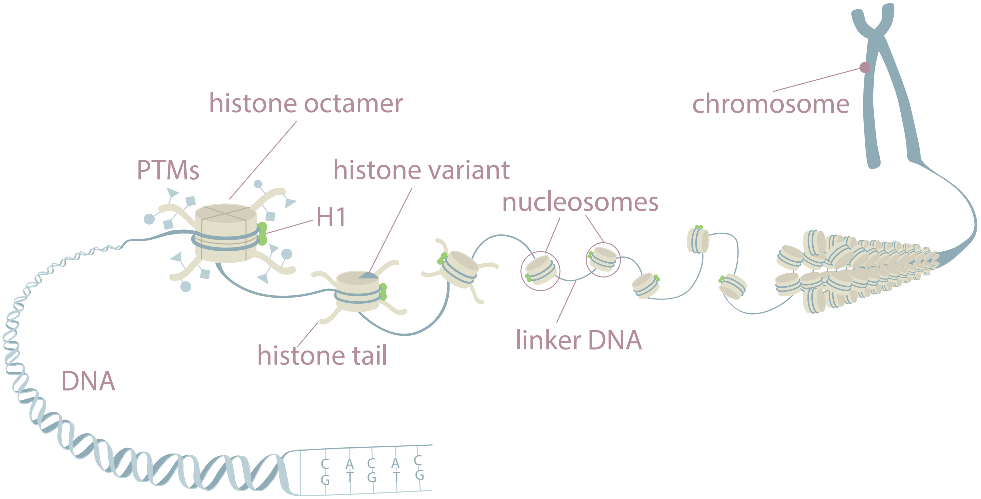

Figure 2: Chromatin structure

In order for the long double stranded DNA molecule (blue - green lines) to fit into the microscopic nucleus the DNA has to fold thousands of times. The folding is mediated by the coiling of the DNA around positively charged proteins that form a barrel-shaped octamer (histone octamer). The complex of the DNA, the histone octamer and the linker H1 (green) form the nucleosome. The linker DNA links consecutive nucleosomes. Further folding is facilitated by post-translational modifications (PTMS) on the histone tails protruding from the nucleosome. In certain cases, canonical histones can be replaced by histone variants. As cells enter mitosis, their chromatin reaches the maximum level of compaction to form visually distinct chromosomes.

1.1.2 The distinction between euchromatin and heterochromatin

In 1928 Heitz was already able to distinguish two chromatin states through cytological analysis of DNA with nuclear dyes. He distinguished a heavily stained state, named heterochromatin, and DNA that was not stained; the euchromatin. From that moment on, researchers have tried to determine the different features and functions of these two chromatin states. In particular research has focused on how different chromatin structures are established and how dynamic they are.

In general, euchromatin is typically gene-rich, relatively decondensed, and contains certain histone modifications such as tri-methylation of H3 on lysine 4 (H3K4me3) and lysine acetylation on H3 and H4 tails that ensure accessibility of the DNA to the transcriptional machinery (Zhang et al. 2015).

Heterochromatin on the other hand forms a condensed and transcriptionally silent environment. Two distinct types of heterochromatin exist: facultative and constitutive. Facultative heterochromatin can be found in various chromosomal regions and is viewed as a flexible heterochromatin form, since its chromatin compaction state may vary (Trojer & Reinberg 2007). This means that facultative heterochromatin can switch from a transcriptionally inactive to an active state in certain contexts, such as during specific developmental stages upon certain cues (Trojer & Reinberg 2007). An example is the inactive X chromosome that switches between active and inactive states during mouse pre-implantation embryo development (see 1.2.2). The most common post-translational modifications characterizing facultative heterochromatin are tri-methylation of lysine 27 of H3 (H3K27me3) and ubiquitination of lysine 119 of H2A (H2AK119Ub), mediated by the Polycomb Repressor Complexes (PRC) 1 and 2, respectively (Di Croce & Helin 2013).

In contrast, constitutive heterochromatin appears to be less flexible compared to facultative heterochromatin and it is formed at specific genomic regions like telomeres, centromeres and pericentromeres in every cell type (Figure 3). The bulk of constitutive heterochromatin forms in the pericentric regions. These areas are largely devoid of genes, but are rich in tandem repetitive elements (reviewed in Saksouk et al. 2015; Déjardin 2015). Traditionally, constitutive heterochromatin has been considered as transcriptionally inert; however, recent evidence suggests that tightly controlled transcription of the underlying repetitive elements can take place (Terranova et al. 2005; Grewal & Elgin 2007; Probst et al. 2010; Casanova et al. 2013). Similar to facultative heterochromatin, constitutive heterochromatin is also characterized by specific epigenetic features, which are discussed in more detail below.

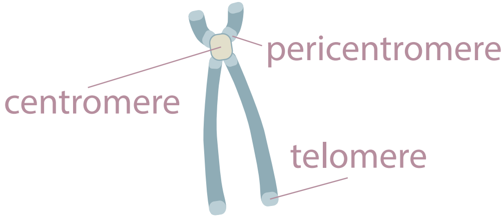

Figure 3: Constitutive heterochromatin
Regions of the chromosome, where constitutive heterochromatin forms.

1.1.3 Chromatin formation at pericentromeres: components and specific features

Despite the fact that the existence of pericentric heterochromatin (PHC) has been known for a long time, the true mechanisms by which it contributes to proper chromosomal function is still not clear. However, it is clear that these regions must maintain their heterochromatic identity, since defects in PHC structure due to the absence of some component or regulator, cause genomic instability and increase the risk for tumorigenesis (Peters et al. 2001; De Koning et al. 2009).

Although the DNA of coding genes is generally highly conserved among mammals, the underlying DNA of PHC is highly different both in size and sequence identity when compared among various organisms. Still, a common feature is the fact that pericentric DNA mainly consists of tandem repeats. In the mouse, these reach up to several megabases in length. The repeat unit of the mouse pericentric DNA array is a 234 bp AT-rich unit, also called major satellite (Vourc'h & Biamonti 2011; Saksouk et al. 2015). In human, pericentric DNA sequence is composed of three different repetitive element classes termed as satellites I, II and III. In addition, the composition of PHC DNA sequence in human differs between different chromosomes. For example, satellite III is not equally distributed over all chromosomes. It is mainly found in PHC of chromosome 1, 5, 9, 10, 17, 20 and Y, but this repeat sequence contributes much less to the PHC of the other chromosomes (Vourc'h & Biamonti 2011).

In the nuclei of mouse cells, PHC from different chromosomes clusters together to form specific, more or less round-shaped structures, termed chromocenters. The centromeres of these chromosomes localize in the periphery of the chromocenters and chromocenters can easily be visualized since they are typically heavily stained for DNA dyes, such as 4',6-diamidino-2-phenylindole (DAPI) (Guenatri et al. 2004) (Figure 4). When comparing different somatic cell types, the size and number of chromocenters differ between different nucleus types (Cerda et al. 1999).

A number of proteins have been identified as being generally enriched at pericentromeres, where they are thought to facilitate the organization of PHC. The list includes histone variants, chromatin remodelers, transcription factors, replication related or cell cycle control proteins, DNA methylation binding proteins, and enzymes such as histone modifiers as well as cohesin. In addition, certain modifications, both of the DNA itself and of the histones, contribute to the compact nature of PCH. For example, a very classical feature of heterochromatinisation is DNA methylation, and in mammals, this mark is generally placed in so-called CpG islands. Three enzymes have been identified as DNA methyltransferases: DNMT1 is responsible for maintaining DNA methylation during replication. In contrast, *de novo* DNA methylation is established by another set of proteins, which includes the *de novo* DNA methyltransferases DNMT3A and DNMT3B, as well as the catalytically inactive protein DNMT3L, that facilitates recruitment of DNMT3A/B to their DNA targets (Hata et al. 2002; Ooi et al. 2007).

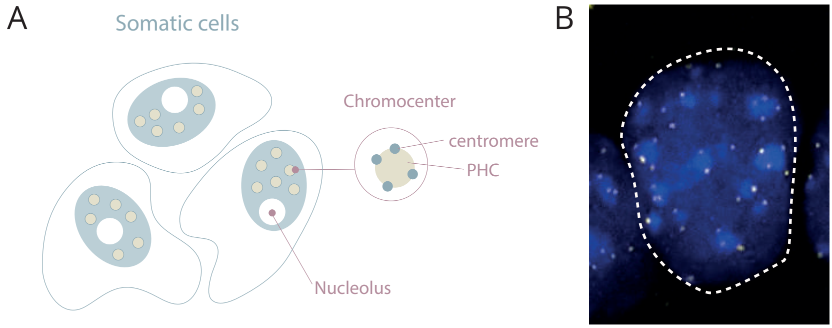

Figure 4: Chromocenters in mouse somatic cells
A Schematic representation of pericentric heterochromatin organization into chromocenters within the nucleus of somatic cells. Each chromocenter consists of pericentric heterochromatin of different chromosomes (PHC). The centromeres of the corresponding chromosomes are localized in the periphery of each chromocenter. B Representative image of chromocenter organization in a somatic nucleus (marked by white dash line). The nucleus is counterstained by DAPI and chromocenters are identified as DAPI dense regions. The centromeres (yellow) are located in the periphery of the chromocenters and are identified by CREST, a centromere marker.

In addition to an enhanced DNA methylation level, PHC is characterized by the presence or absence of certain histone modifications that confer an extra layer of compaction. The most typical post-translational histone modifications that are known to be enriched in PHC include tri-methylation of H3 on lysine 9 (H3K9me3), tri-methylation of H4 on lysine 20 (H4K20me3), tri-methylation of H3 on lysine 64 (H3K64me3) and mono-methylation of H3 on lysine 27 (H3K27me1). Additionally, histones of PHC are hypoacetylated, since acetylation in general promotes a more open and accessible chromatin environment (Görisch et al. 2005).

Despite the fact that the presence (or absence) of these histone marks in PHC has been thoroughly characterized, the molecular mechanism of their biogenesis is not fully clear. Most detailed information is available about H3K9me3 biogenesis in PHC. In a first step, PRDM3 and PRDM16 catalyse formation of mono-methylation of H3 on lysine 9 (H3K9me1) before its incorporation into the chromatin (Pinheiro et al. 2012), and this is followed by SUV39H1/2 methyltransferase mediated di- and tri-methylation at PHC only (Peters et al. 2003). Interestingly, SUV39H1 has a dual activity: one as a SUMO E3 ligase and one as a histone methyltransferase (Maison et al. 2011). No additional function has been reported for SUV39H2. The mechanism of initial recruitment of these methyltransferases to PHC is not clear, but once they are present, H3K9me3 sustains their continuous targeting (Grewal & Moazed 2003). Loss of SUV39H activity leads to specific absence of H3K9me3 at pericentromeres, but not in other regions, suggesting that these two enzymes specifically act at PHC (Peters et al. 2003). In a similar way, H4K20me3 is generated by recruitment of SUV4-20H1/2 methyltrasferase enzymes through one of the most important components of PHC, Heterochromatin Protein 1 (HP1), the "reader" of H3K9me3 (Schotta et al. 2004; Schotta et al. 2008). Still, the mechanisms of generation of H3K27me1 and of the newly identified histone mark H3K64me3 at PHC are currently unclear.

Among factors that were identified as components of the PHC, members of the Heterochromatin Protein family 1 (HP1) stand out. HP1a was first discovered in *Drosophila melanogaster* as a major non-histone component of heterochromatin (James & Elgin 1986). Following its initial identification, HP1 protein isoforms and homologues were also rapidly identified and characterized in other organisms (reviewed in Eissenberg & Elgin 2000). In mammals, there are three HP1 isoforms: HP1α, HP1β and HP1γ, encoded by the *Cbx5*, *Cbx1* and *Cbx3* genes, respectively. In general, HP1 proteins are highly conserved and based on their structural and biochemical characteristics three domains can be identified in all HP1 proteins. The N-terminal chromodomain (CD), recognizes and binds di- or tri-methylated H3K9 (Lachner et al. 2001; Bannister et al. 2001). The C-terminal chromoshadow domain (CSD), mediates dimerization of HP1 proteins with each other or with other proteins containing the PxVxL pentapeptide motif (Smothers & Henikoff 2000; Lechner et al. 2005). The CD and the CSD are highly conserved between HP1 isoforms and homologues. The third and less well-conserved region which separates the CD and CDS domains is the hinge or linker region. This domain has been reported to mediate binding of HP1 proteins to PHC together with the CD and also to interact with RNA, an activity that contributes to the formation and maintenance of the higher order chromatin structure in pericentromeres (Maison et al. 2002; Muchardt et al. 2002).

HP1 proteins carry different post-translational modifications, which allow them to interact with various partners, and to have different localization patterns within the nucleus, while they exert their various functions. So, HP1 proteins are not solely coupled to gene silencing and heterochromatinisation. For example, in NIH3T3 cells, a subpopulation of HP1γ, which is phosphorylated at serine 38, localizes uniquely at euchromatic regions that are coupled with transcriptional elongation. The non–phosphorylated HP1γ is enriched in DAPI dense regions, but it is also present in euchromatic areas (Lomberk et al. 2006; Vakoc et al. 2005; Minc et al. 2000). Also, HP1β has been found to regulate expression of rDNA genes by RNA PolI (Horáková et al. 2010).

With regard to cellular functions, HP1 proteins have been implicated in genome stability (Aucott et al. 2008), DNA damage response (reviewed in Dinant & Luijsterburg 2009) and regulation of alternative splicing (Lev Maor et al. 2015). Interestingly, the HP1 isoforms are not functionally redundant, since single HP1 isoform knockout experiments have revealed different phenotypes. This indicates that the different HP1 isoforms possess different functions within the cell. *Cbx1* (encoding HP1β) null mutation leads to perinatal lethality and to genomic instability (Aucott et al. 2008), while absence of HP1γ has a milder effect, since *Cbx3* knockout mice are viable, albeit sterile (Takada et al. 2011; Abe et al. 2011). No *Cbx5* (encoding HP1α) knockout mice have been reported.

How HP1 proteins are targeted to PHC was very recently published. In spite of the general knowledge that HP1α binds H3K9me3 via its CD domain (Lachner et al. 2001; Bannister et al. 2001), this interaction does not necessarily qualify H3K9me3 as the *de novo* targeting mechanism of HP1α in PHC. Pull down experiments in NIH-3T3 cells revealed that HP1α (and the other HP1 isoforms) carries a SUMO-1 moiety attached to its hinge domain and this post-translational modification, together with the interaction of HP1α with pericentric transcripts (or major satellite transcripts), is an absolute prerequisite for the targeting of HP1α to PHC, even in the absence of H3K9me3. This suggests that sumoylation promotes the *de novo* HP1α targeting to heterochromatin (Maison et al. 2011). A surprising discovery was that SUV39H1 methyltransferase, is not only responsible for catalyzing H3K9me3 formation in those regions, but also for enhancing SUMO-1 deposition on HP1α, thereby acting as a SUMO E3 enzyme in the HP1α-specific SUMO pathway (Maison et al. 2016). Maintenance of HP1α on PHC is mediated by the presence of H3K9me3, as well as of other components, such as SENP7, a SUMO-protease enriched in PHC, which carries two PxVxL motifs that robustly bind and maintain HP1 molecules from neighboring nucleosomes on PHC (Romeo et al. 2015).

Another protein that is often found enriched at pericentric heterochromatin is ATRX (alpha thalassemia/mental retardation syndrome X-linked). This protein is a chromatin remodeler and was first identified in human. Mutations within this gene result in a very profound phenotype characterized by various developmental defects, cognitive disability and mild α-thalassemia (Bérubé 2011). In the mouse, *Atrx* knock out is embryonic lethal, due to developmental defects of the placenta (Garrick et al. 2006).

The ATRX protein contains domains that are critical for its proper function. At the N–terminal part of the protein, three regions pack together and form the ADD (ATRX-DNMT3-DNMT3L) domain, which facilitates targeting of ATRX to the chromatin. At the C-terminal part seven-helicase motifs comprise the Snf2 ATPase domain, which gives ATRX its ATPase activity. Apart from these two domains, ATRX contains a number of other motifs, which mediate binding with various partners, such as H3K9me3 and HP1α.

Immunofluorescence and ChIP-seq data revealed that ATRX localizes not only to PHC but also to genome wide heterochromatic regions such as transposable elements and to the methylated allele of imprinted DMRs (McDowell et al. 1999; Goldberg et al. 2010; Voon et al. 2015). The important function of ATRX at heterochromatic sites is to recruit DAXX, which can incorporate the histone variant H3.3. The deposition of H3.3 is critical for the *de novo* formation of PHC during early preimplantation development in mice (Santenard et al. 2010) and for the general maintenance of heterochromatin at a number of genomic sites, such as at the locations of imprinted genes (Voon et al. 2015).

Apart from its role in heterochromatin formation and maintenance, ATRX has been found to be involved in a number of different cellular processes such as in maintaining genome integrity during meiosis and mitosis, DNA replication and damage repair, transcriptional regulation, X chromosome inactivation and more (reviewed in Bérubé 2011; De La Fuente et al. 2011; De La Fuente et al. 2012; Sarma K et al. 2014).

The general epigenetic profile of PHC led to the general consensus that transcription from these regions would never occur. Today, with the development of various sensitive molecular technologies, it has become evident that transcription of pericentric repeats does occur, in a regulated manner. It is necessary for and linked to various regulatory processes, for example during early pre-implantation development (Probst et al. 2010), cell proliferation (Lu & Gilbert 2007), for heterochromatin formation (Maison et al. 2016; Santenard et al. 2010) and differentiation (Martens et al. 2005; Terranova et al. 2005). However, as with many other noncoding RNAs, the transcriptional regulation of these repetitive elements must be tightly controlled, since overexpression has been coupled to pathological conditions such as cellular stresses (Jolly et al. 1997; Rizzi et al. 2004), cancer (Eymery et al. 2009; Ting et al. 2011), and genetic disorders (Shumaker et al. 2006; Ehrlich et al. 2008).

1.2 Major reprogramming events in the cycle of life

Chromatin structure is not static, and drastic remodeling occurs at specific moments in development. Although the cycle of life inherently does not have a real beginning, I will start my journey in the zygote, the point in the cycle where a new genetically unique individual has just formed. However, it will immediately become clear that everything in the cycle of life is connected. Events that occurred during development of the germ cells that fused to form the zygote, determine the epigenetic constitution and regulation of the paternal and maternal genomes during their first joint efforts to regulate early development. Therefore it is inevitable that I have to refer to other phases of the life cycle, no matter where I begin.

1.2.1 Epigenetic asymmetry in the mouse zygote

The very first drastic chromatin reconfiguration in an individual's life takes place just after the fusion of two highly specialized cells: the sperm and the oocyte (gametes). The successful fusion of the gametes will generate the totipotent one-cell zygote. This is the stage, where chromatin differences between the parental genomes are the most prominent, despite the fact that they share the same environment (ooplasm). Some of these differences are directly mediated by the gametes. For example, at the time of fertilization, the sperm's genome is roughly two times more heavily methylated compared to that of the oocyte (Peat et al., 2014). In addition to such intrinsic differences between the parental genomes, differences between them are generated after fertilization, leading to a remarkable epigenetic asymmetry at several levels of chromatin organization for example in histone modifications and DNA methylation. In general, the maternal chromatin is reminiscent of that of a somatic cell, while the paternal chromatin (after the replacement of protamines by maternal histones - see below) displays a more open and transcriptionally permissive chromatin. In line with this feature, transcription from the paternal genome has been documented to occur before the general activation of the embryonic genome, that takes place around the 2- to 4-cell stage (Aoki et al., 1997).

The most striking difference in chromatin structure between the maternal and paternal genome is induced by the replacement of the sperm's protamines by unmodified histones provided by the oocyte, in order to create a nucleosome-based chromatin structure. The deposition of the histones on the DNA of the paternal genome takes place before the first S phase (van der Heijden et al. 2005), therefore only the non-canonical histone variant H3.3 can be introduced, since incorporation of nucleosomes containing this H3 variant can occur via a DNA replication-independent mechanism (Torres-Padilla et al. 2006). At the same time, the maternal genome, which mostly maintains the same chromatin state as it had in the oocyte, and does not need to exchange histones, contains nucleosomes built with the canonical H3 histones, H3.1 and H3.2 (van der Heijden et al. 2005). Asymmetry in the histone code between the two parental genomes is clearly illustrated by the paternal-specific pattern of acetylation of certain residues in H4 and H3 histones (H4K16, H4K5 and H3K27) (Adenot et al. 1997; Stein et al. 1997; Hayashi-Takanaka et al. 2011), which at the same hypomethylated. While, the maternal chromatin displays mono-, di- and tri-methylation marks in certain H3 and H4 histone residues (e.g. H3K4, H3K9, H3K27 and H4K20), the paternal pronucleus only contains the mono-methylated versions of these histones (Lepikhov & Walter 2004; van der Heijden et al. 2005).

When focusing on specific regions of the genone, PHC is differentially modified in the two parental genomes. In general, the structure of PHC in the early mouse pre-implantation embryo is in a completely different organization form compared to that of somatic cells and typical somatic chromocenters in the early pre-implantation embryo start forming only after the 4-cell stage (Martin et al. 2006). Before this stage, chromosomal pericentric heterochromatin of different chromosomes is organized in the periphery of the Nucleolus Precursor Bodies (NPBs) and forms a ring around them, with the centromeres located between the pericentric domains (Figure 5). NPBs are an atypical kind of nucleoli (reviewed in Fulka & Aoki 2016) and in spite of the morphological dissimilarities of somatic and early embryo heterochromatin, the heterochromatic ring in the early embryo is also heavily stained by DNA dyes, just like the chromocenters (Martin et al. 2006).

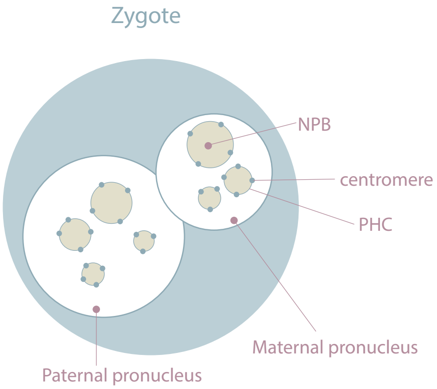

Figure 5: Pericentric heterochromatin in the mouse zygote

In the zygote pericentric heterochromatin (PHC) of the parental genomes (maternal and paternal pronucleus) is organized in the periphery of the nuclear precursor bodies (NPB). The centromeres of the corresponding chromosomes are also located in the periphery of these bodies, between the pericentric heterochromatic regions (green lines connecting centromeres).

The maternal PHC is enriched for the classical constitutive heterochromatin features, such as H3K9me3, H4K20me3, H3K64me3 and HP1β; whereas paternal PHC shows enrichment for facultative heterochromatin markers (Liu et al. 2004; Puschendorf et al. 2008; Kourmouli et al. 2004; Daujat et al. 2009). Histone modifications mediated by the Polycomb Repressive Complex 2 (PRC2), H3K27me2 and H3K27me3, clearly define the paternal ring-shaped PHC, that is also enriched for components of the canonical Polycomb Repressive Complex 1 (PRC1) such as RNF2, BMI1, CBX2 and PHC2, accompanied by H2AK119Ub (Puschendorf 2008). Recruitment of PRC1 components on the maternal PHC is blocked by the presence of HP1β (Tardat et al. 2015).

As mentioned at the beginning of this paragraph, epigenetic asymmetry between the paternal and maternal pronucleus also includes DNA methylation differences, whereby the paternal genome is more heavily methylated than the maternal genome (Peat et al., 2014). Soon after fertilisation, a genome wide DNA demethylation wave starts that lasts until the early blastocyst stage, where methylation reaches the lowest levels (Mayer et al. 2000). It should be noted, that during the global demethylation wave, not all methylation marks are removed. In particular, methylation patterns of imprinted genes are maintained. For imprinted genes, the expression pattern is determined by an epigenetic mark (usually DNA methylation) placed during male or during female gametogenesis in the parent.

In general, the global demethylation wave during early preimplantation development is thought to involve both active and passive mechanisms. However, the initiation of DNA demethylation in the zygote is accompanied with signatures of active demethylation observed primarily on the paternal and not on the maternal genome. Thus, in addition to differences in overall levels of DNA methylation between the paternal and maternal genome, the processing of the parental methylomes is also differentially regulated. The molecular components of active DNA demethylation were largely unknown, but the recent discovery of the Tet-Eleven-Translocation (TET) proteins, oxygenases that catalyze the oxidation of 5-methylcytosine (5mC) to 5-hydroxymethylcytosine (5hmC) and the other derivatives 5-formylcytosine (5fmC) and 5-carboxylcytosine (5cmC) (Ito et al. 2011), was a major breakthrough in the mechanistic unravelling of the active DNA demethylation mechanisms that operate at different steps of the life cycle. Subsequent research proposed that the 5fmC and 5cmC metabolites are intermediates in the process of active demethylation, where they are enzymatically recognized and removed from the genome by components of the DNA repair machinery, such as by thymine–DNA–glycosylase (TDG). Thereafter, an unmodified cytosine is replacing the excised base (reviewed in Kohli & Zhang 2013; Dawlaty et al. 2014). Based on the information provided above, immunofluorescence experiments using antibodies against 5mC and 5hmC revealed astonishingly evident differences between the maternal and paternal genomes with respect to the presence of these modifications, already before the first zygotic mitotic division. 5hmC formation is prominent in the paternal pronucleus, suggesting that an active mechanism of DNA demethylation is ongoing, while the maternal pronucleus is rich for 5mC and shows no apparent signs of demethylation (Santos et al. 2002; Santos & Dean 2004). It has been established that oxidation of 5mC to 5hmC on the paternal genome in the zygote is catalyzed by TET3, which is highly expressed in the oocyte and sperm and it is therefore abundantly present in the zygote. Accordingly, TET3 also shows preferential localization on the paternal genome (Gu et al. 2011). However, genetic TET3 ablation has little effect on the paternal DNA methylome, indicating that TET3 mediated formation of 5hmC might not be as critical for the active demethylation of the paternal genome as was suggested previously (Shen et al. 2014; Gu et al. 2011). Indeed, both parental 5mC (maternal) and 5hmC (paternal) marks undergo replication-mediated dilution in the zygotic S-phase and during subsequent divisions (Inoue & Zhang 2011; Inoue et al. 2011). At this stage, the additional absence of the DNA methylation maintenance machinery components (DNMT1) from the nuclei of the developing embryo favours a passively mediated demethylation process (Hirasawa et al. 2008; Inoue et al. 2011). Recently, Amouroux et al. (2016), carefully timed 5mC disappearance and 5hmC appearance during early pronuclear development. Using ultrasensitive liquid chromatography/mass spectrometry and immunofluorescence, the authors observed a clear 5mC reduction in the early paternal pronucleus, but no concomitant 5hmC increase. Again, inhibition of TET3 did not affect the process, which is also replication independent. Furthermore, no significant 5mC loss was detected at this early zygotic stage from the maternal genome. Their results indicate that an alternative DNA – replication as well as TET3 independent - demethylation pathway is active in the very early embryo specifically targeting the paternal genome. In fact, *de novo* DNA methylation also occurs (by maternally provided DNMT3A & DNMT1), and only the newly formed 5mC is subjected to TET3 mediated oxidation at the late stages of the zygote development (Amouroux et al. 2016; Messerschmidt 2016).

At present, insight into the functional significance of the specific active demethylation, and the TET3-mediated formation of 5hmC on the paternal genome of the preimplantation embryo is lacking. In addition, it is not known if the differences in the histone code between the two parental genomes have any specific function. An attractive scenario is that all these forms of epigenetic asymmetry may be important for proper regulation of gene expression and development of the embryo (Gu et al. 2011 and reviewed in Feil 2009). What is important to consider, though, is that the majority of studies on epigenetic reprogramming at these early stages of development have used mainly the mouse embryo as a model and these results cannot be generalized and assumed for all mammalian species. The early preimplantation embryo stage is considered to be particularly crucial for further development and therefore different species may require distinct epigenetic mechanisms to regulate expression of developmental genes at specific time points. For example, in the human early pre-implantation embryo the epigenetic asymmetry in the PHC as observed in the mouse does not apply; classical pericentric heterochromatin histone marks (e.g. H3K9me3) are retained in the human sperm and transferred to the oocyte at fertilization (van de Werken et al. 2014). In line with this evidence, no enrichment for the PRC1/PRC2 components is apparent in the paternal human pronucleus like it is in the mouse (van de Werken et al. 2014). Even in human somatic cell nuclei, chromocenters cannot be easily identified by DNA dyes, as is the case for mouse (Mayer et al. 2005).

1.2.2 Dosage compensation in the preimplantation embryo

Additionally to the epigenetic differences between the maternal and the paternal pronucleus in the zygote, there is also a difference in the chromosomal composition (sex chromosomes) between female and male embryos. The maternally provided genome always consists of a set of autosomes and the X chromosome and female mammalian individuals always carry two X chromosomes. In contrast, male mammals carry two different sex chromosomes, the X and Y, whereby the Y chromosome carries the male-determining *Sry* gene. This means that half of the sperm cells carry the Y chromosome and upon fusion with the oocyte will generate an XY male embryo, whereas the other half will carry the X chromosome and generate a female embryo.

The difference between male and female cells, whereby female cells carry two copies of all X-linked genes, and males only have a single copy of all these genes (>1000), generates a dosage problem in X-linked gene expression between the two sexes that needs to be equalized. During evolution, this problem has occurred in many animal lineages, since genetic sex determining mechanisms are usually associated with gradual loss of genes from the chromosome that carries the sex determining locus (the Y chromosome in mammals), due to reduced recombination and other evolutionary relevant processes. In mammals, the X-linked gene dosage problem is solved by inactivation of one of the two X chromosomes in all female somatic nuclei by a mechanism termed X chromosome inactivation (XCI). Already in the late 1940s differences in the cytological morphology of somatic male and female nuclei were described, with the latter having an extra 'body' or 'nucleolar satellite' present (Barr & Bertram 1949). A few years later it was proposed that this nucleolar satellite in female cells might correspond to an inactive X chromosome and that this inactivation would be a natural phenomenon taking place specifically in female cells (Ohno & Hauschka 1960; Lyon 1961) in order to compensate for the genetic imbalance between heterogametic males and homogametic females.

In mouse preimplantation embryos, XCI is imprinted (Figure 1). Around the four-cell stage, imprinted XCI (iXCI) is initiated and inactivates always the paternal X chromosome in female mouse embryos. iXCI is essential for development, since female embryos that are incapable of inactivating the paternal X die in utero due to placental defects (Marahrens et al. 1997; Lee 2000; Sado et al. 2001; Wang et al. 2001; Shin et al. 2010). iXCI is maintained in the extraembryonic cell lineage, but is reversed in the inner cell mass of the blastocyst, that will give rise to the embryo proper. XCI is then re-initiated in a random fashion in the developing embryo, stably inactivating either the paternal or maternal X with roughly equal probabilities. The inactive X which is inherited by daughter cells upon cell division. A defined X-linked locus, termed the X-inactivation center is required for the establishment of XCI. The X-inactivation center contains mostly genes that produce non-coding RNAs, and the noncoding *Xist* and *Tsix* RNAs are the major players in the XCI process. When XCI is initiated, *Xist* becomes highly expressed only from the future inactive X chromosome, covers this X in *cis* and becomes detectable as a cloud in the nucleus using RNA FISH (Clemson et al. 1996). This is then followed by addition of repressive histone modifications (e.g. H3K27me3, H4K20me1 and H2AK119ub1) to ensure the faithful establishment of XCI (reviewed in Payer 2016). *Tsix* is partly overlapping with *Xist*, it is transcribed in the opposite direction and acts as an *Xist* antagonist. This means that on the future inactive X chromosome, the levels of *Tsix* are reduced when *Xist* is highly expressed, in order for XCI to initiate (Lee & Lu 1999; Sado et al. 2001). In contrast, on the active X chromosome, *Tsix* is actively transcribed, and interferes with expression of *Xist*, leading to subsequent inactivation of the gene, and maintenance of an active X chromosome (Luikenhuis et al. 2001; Stavropoulos et al. 2001).

In iXCI, *Xist* expression from the paternal allele only initiates at the late 2-cell stage, concomitant with the ZGA (Zuccotti et al. 2002; Kay et al. 1994; Patrat et al. 2009). Following *Xist* accumulation at the 4-cell stage, other marks start to become established on the inactive paternal X chromosome, in order to ensure its robust silencing. These marks include H3K4 hypomethylation, and H3K9 hypoacetylation, followed by H3K27 tri-methylation and H3K9 di-methylation. Additionally, RNA PolII is excluded from the inactive X chromosome (Okamoto et al. 2004).

Inactivation of the Xp takes place in two steps. In the first step, intergenic regions of Xp become inactivated in a *Xist* independent manner. This step is then followed by silencing of X-linked genes in a manner that does depend on *Xist* (Namekawa et al. 2010).

But what determines the absolute choice for Xp inactivation in favor of Xm in the pre-implantation embryo? Studies with uniparental embryos suggested that there may be two types of imprints on the parental X chromosomes required for specific inactivation of Xp, and maintenance of an active Xm. Specifically, when androgenetic embryos were generated (XpXp, XpY or XpO), *Xist* expression and accumulation took place from all X chromosomes, and importantly, the time point of initiation of *Xist* expression was identical to that of wild type XpXm embryos (Okamoto et al. 2000; Matsui et al. 2001). This suggests that the paternal X chromosome is programmed to become inactivated in the pre-implantation embryo regardless of the number of X chromosomes the embryo carries. The other way around, when parthenogenetic embryos were generated (XmXm) expression of *Xist* was never observed until the early morula stage, suggesting that the maternal *Xist* is imprinted to resist expression in the early pre-implantation embryo and that this imprint is overridden later in development (Kay et al. 1994; Nesterova et al. 2001).

It is well accepted that the imprint resisting X inactivation on the maternal X is set during oogenesis. This view is based on observations of parthenogenetic embryos derived by serial nuclear transplantations, resulting from the combination of haploid non-growing (ng) and fully grown (fg) oocyte genomes. These early preimplantation embryos and their extra embryonic tissues preferentially inactivate the X chromosome derived from the ng oocyte, similar to Xp inactivation in normally fertilized wild type XmXp embryos (Tada et al. 2000). This indicates that the genome of the ng oocyte still lacks the imprint on Xm that makes it resistant to XCI up to the morula stage. Deposition of H3K9me3 at the promoter of *Xist* was thought to be responsible for blocking *Xist* expression from Xm (Fukuda et al. 2014), but closer examination of H3K9me3 levels on *Xist* during oogenesis did not reveal any differences between non-growing and fully-grown oocytes (Fukuda et al. 2015). However, DNA FISH experiments suggested that the chromatin organization of the *Xist* locus in a fully-grown oocyte is more compact compared to that of a non-growing oocyte and this could influence *Xist* expression from the maternal X (Fukuda et al. 2015). It still remains an open question what exactly is the imprint on the maternal X, and how it is established. In any case, the imprint appears to differ from the DNA methylation imprints found in association with classic imprinted genes such as *Igf2*, in the sense that it is not stably maintained throughout embryonic development.

With respect to possible epigenetic marks that may actually facilitate *Xist* transcription from the paternal X, two hypotheses have been put forward. First, it has been suggested that the overall lack of histone modifications on the paternal genome (the epigenetic asymmetry described in 1.2.1) may actually facilitate transcription of paternal genes, including *Xist* (Okamoto et al. 2005). Secondly, it has been suggested that the specific silencing of the X (and the Y) chromosome during meiotic and postmeiotic male germ cell development, mediated by the process of Meiotic Sex Chromosome Inactivation (MSCI) and by the formation of Postmeiotic Sex Chromosome chromatin (PMSC) (for details see 1.2.7) somehow may be important in mediating an initial *Xist*-independent silencing of intergenic regions of the paternal X (Namekawa et al. 2010). In addition, or alternatively, these two processes may generate epigenetic marks that somehow facilitate paternal *Xist* gene expression. MSCI and PMSC are thought to be triggered by the lack of homology between the X and Y chromosomes, that are stably connected through a very limited area during meiotic prophase, when all autosomes pair fully with their homologous partner. Taking this into account, recent experiments tested the effect of having a transgenic *Xist* locus and the surrounding region, in multiple copies, in a homozygous or a heterozygous setting, mimicking the presence or absence of a pairing partner, respectively. When the transgene array was inherited from a heterozygote transgene array carrier, the transgenic *Xist* gene was induced during the preimplantation period in the offspring. This was not the case when the parent was homozygous for the transgene. Thus, in the absence of a pairing partner, meiotic silencing may be induced, similar to MSCI, and this may result in an imprint that recapitulates the normal Xp specific *Xist* expression in early preimplantation embryos (Sun et al. 2015). However, in an earlier study, similar experiments were conducted, but in this case, only one copy of the transgene was incorporated in an autosome. In that setting, paternally imprinted expression of the transgenic *Xist* took place, independent of hetero-or homozygosity of the transgene. These authors suggested that the open chromatin of the paternal genome immediately after fertilization, due to the protamine to histone transition, might favor *Xist* expression from the Xp (Okamoto et al. 2005). In conclusion, despite the fact that there is evidence for the existence of both Xm and Xp imprints during the pre-implantation period, knowledge on how these imprints are set and what their exact molecular nature is, is still missing.

The paternal XCI is only transient for most cells, because at around embryo implantation (~E4.5), the paternal X chromosome becomes reactivated. This occurs only in the cells that express the pluripotency factor NANOG, thereby corresponding to the inner cell mass (ICM) cells of the blastocyst, and will give rise to the embryo proper (Mak et al. 2004; Okamoto et al. 2004). Subsequently, random XCI is initiated, whereby both parental X chromosomes have an equal chance to become silenced and this then ensures stable and proper X linked gene dosage compensation in the tissues of developing female embryos relative to XY males (Lee & Lu 1999). The mechanism by which random XCI is initiated should be viewed as a stochastic mechanism in which multiple players -in addition to *Xist* and *Tsix*- that can be X-linked or autosomal, participate to modify the chance of initiation of XCI on a particular X chromosome. This mechanism also clearly depends on the number of X chromosomes that are present, relative to the autosomes.

In addition to the non-coding, acting in *cis* non coding RNAs *Xist* and *Tsix* other factors have been identified to participate in XCI. One critical XCI-trans activator is the X-linked *Rnf12* gene. RNF12 is an E3 ubiquitin ligase which ubiquitinates the pluripotency factor REX1, and thereby targets it for proteasomal degradation (Jonkers et al. 2009; Shin et al. 2010, Gontan et al. 2012). An autosomal gene encodes REX1, which binds DNA and acts to repress XCI in pluripotent stem cells (Gontan et al. 2012).

Lastly, despite the fact that extra embryonic lineages maintain iXCI, a number of genes located on the inactive X escape silencing, and therefore it appears that iXCI is less robust compared to random XCI that takes place in the soma of the embryo (Hadjantonakis et al. 2001; Corbel et al. 2013; Merzouk et al. 2014).

1.2.3 iXCI in species other than mouse

Most of our knowledge today about iXCI comes from the mouse model. However, studies conducted in other eutherian species suggest that what we know about iXCI in mice may not be applicable to other mammals. For example, detailed analysis of *XIST*/*Xist* expression in human and rabbit preimplantation embryos revealed dissimilarities in the time of *XIST*/*Xist* upregulation compared to the mouse, but also in its expression pattern, possibly reflecting different regulatory XCI trajectories between eutherian species. While in the mouse *Xist* accumulation takes place around the 4-cell stage and only from the Xp, in human and rabbit preimplantation embryos *XIST*/*Xist* accumulates later (~morula stage), potentially reflecting differences in the ZGA between species. Strikingly different, though, is the observation that both in human and rabbit embryos expression of *XIST*/*Xist* takes place from both X chromosomes. In the rabbit, this situation is resolved in the ICM of the blastocyst, where both X chromosomes become active, similar to the mouse. However, in human blastocysts *XIST* RNA accumulates on all X chromosomes regardless of the embryo's sex. Remarkably, *XIST* accumulation does not result in X-linked gene silencing as examined by RNA FISH experiments (Okamoto et al. 2011; Petropoulos et al. 2016). This observation is similar to what has been described for the rhesus monkey, where also *XIST* is expressed from both X chromosomes in females and the single X in males as examined by RT-PCR, and chromosome-wide XCI has not yet been induced in female blastocysts (Tachibana et al. 2012). All these data suggest that the mouse model as a system may not be an optimal representative of the XCI process especially when studying diseases related to XCI in humans.

Addressing the question whether iXCI takes place in pre-implantation embryos and extra embryonic tissues in other species than the mouse is frequently quite challenging due to lack of data regarding polymorphisms that can reveal parent specific X-linked gene expression. In any case, using alternative methods and genetic approaches, iXCI has been shown to take place in rat yolk sac, an extra embryonic membrane (Wake et al. 1976). In addition, iXCI has also been reported for both cow pre-implantation embryos (morula only) and placentas (Xue et al. 2002; Ferreira et al. 2010), but in these studies only one gene was analysed. On the other hand, analysis of mule and horse placentas revealed that random XCI takes place in the extra embryonic tissues of these animals (Wang et al. 2012). In human the issue remains unresolved since both imprinted and random XCI have been reported to occur in the placenta (Goto et al. 1997; Moreira de Mello et al. 2010).

Taken together, and despite some contradictory findings that still need to be resolved, it is clear that different eutherian mammals have evolved different strategies for XCI. However, the end result in the soma of all mammals is the achievement of dosage compensation visualized by the presence of the Barr body, representing the inactivated X chromosome. The only cell type that actively reverses this situation is the female primordial germ cell.

1.2.4 Primordial germ cells: specification of a unique population of cells

Primordial germ cells (PGCs) are unique for their ability to generate gametes (oocytes and spermatozoa) that pass the genetic and epigenetic information from one generation to the next, thereby ensuring species survival. In general, PGCs in diverse species are specified during early embryonic development via two different mechanisms: through preformation or via epigenesis (or induction).

In the case of preformation the oocyte contains cytoplasmic components such as mRNA transcripts and proteins (known as nuage or germ plasm) at a specific location. Upon fertilization and subsequent mitotic divisions, cells that will physically inherit these determinants will become PGCs (Bertocchini & Chuva de Sousa Lopes 2016). In the epigenesis scenario, no germ plasm is transmitted from the oocyte, but rather secreted molecules from the tissue surrounding the site of PGC formation will induce the specification of PGCs to that site (Bertocchini & Chuva de Sousa Lopes 2016). In the mouse, PGCs' (mPGCs) specification takes place through induction around embryonic day 6.0 (E6.0). Specifically, signaling emerging from the extra-embryonic ectoderm (ExE) upon the proximal epiblast will induce cells at this region to adopt a PGC fate (Lawson & Hage 1994; Tam & Zhou 1996) (Figure 1). By default, epiblast cells are destined towards a somatic fate and by receiving an inductive signal to do otherwise, the molecular and epigenetic signature of these cells must change drastically.

The inductive signaling includes members of the TGFβ signaling pathway such as various Bone Morphogenetic Protein ligands (BMP) and SMAD proteins, as well as WNT3A. Particularly, BMP4, BMP2 and BMP8b have been shown to be important for PGC specification with BMP4 being absolutely crucial, since *Bmp4* knockout mouse embryos, among other abnormalities, do not present any PGCs (Lawson et al. 1999). *Bmp2* and *Bmp8b* knock out mouse embryos form PGCs, albeit in lower numbers compared to their wild type littermates (Ying et al. 2000; Ying & Zhao 2001). WNT3A has been proposed to be essential for responsiveness of the epiblast to BMP4 (Ohinata et al. 2009). Additionally, SMAD1 and SMAD5 have also been shown to be vital for PGC specification in the mouse (Hayashi et al., 2002; Tremblay et al., 2001).

Nonetheless, despite the overall extensive research in PGC biology over the years and the identification of a plethora of factors participating in the process of PGC specification, the intriguing question on how the transcriptional network of epiblast cells can change from somatic to pluripotent and how specific fates are determined remained unclear. Biochemical studies in PGCs with the current technologies are challenging or not feasible, due to the small size population of these cells in the initial steps of germline development, reaching approximately ~40 cells per (early) embryo in the mouse. The development of *in vitro* systems based on naïve embryonic stem cells (ESCs) sufficiently recapitulating the process of PGCs' specification, and at the same time having the potential to mature to fully functional gametes, has provided a solid platform for the characterization of the signaling principle of mPGC specification. In accordance with this Aramaki et al. (2013), using such an *in vitro* system (Hayashi et al. 2011; Hayashi et al. 2012), identified that a synergistic activity of the BMP/SMAD and WNT3 pathways in the posterior part of the proximal epiblast induces germ cell fate. WNT3A expressing cells at this specific position are exposed to high levels of BMP4 coming from the ExE. WNT3A induces expression of *T* (also known as *Brachyury*), a mesodermal transcription factor, which in the absence of BMP4 activates the expression of mesodermal somatic genes (Martin & Kimelman 2010). However, in the presence of BMP4, this activity of T is blocked, and instead, T activates key transcription factors for germ cell development: PRDM1 (also known as BLIMP1) and PRDM14 (Aramaki et al. 2013; Cantú & Laird 2013). PRDM1 and PRDM14 play a decisive role in PGC development, since both individual mutant mice display loss of germ cells (Ohinata et al. 2005; Vincent et al. 2005; Kurimoto et al. 2008; Yamaji et al. 2008; Grabole et al. 2013). Together, these two transcription factors suppress the somatic program already imposed in the future PGCs and at the same time they promote re-installment of a pluripotent status, expression of germ cell specific genes, as well as initiation of the PGC program-coupled epigenetic reprogramming (Bikoff & Robertson 2008; Nakaki et al. 2013; Magnúsdóttir et al. 2013; Grabole et al. 2013; Saitou & Yamaji 2012). In addition, they activate genes important for PGCs' maintenance, such as *Tfap2c* (Weber et al. 2010). The mechanism that initiates the process of germ cell specification in human is still unknown. Due to obvious ethical restrictions, human embryos older than two weeks old can not be kept in culture (Bertocchini & Chuva de Sousa Lopes 2016), precluding development of useful models, since it is speculated that germ cell specification takes place around this time point (Tang et al. 2015). However, it should be noted that the organization of the extra-embryonic and embryonic layers in the early post-implantation human embryo is very different compared to that of the mouse, indicating a possible different germ cell – line inductive signaling mechanism in humans (Bertocchini & Chuva de Sousa Lopes 2016; Saitou et al. 2016).

Many attempts have been made to generate hPGCs *in vitro* (Chen et al. 2007; Clark et al. 2004; West et al. 2010) to study the molecular mechanisms beyond time points for which human material is unavailable (between 2 to 4 weeks). However the potential germ cells derived from these studies were poorly characterized and the efficiency of obtaining such cells was low. Recently, scientists applied a strategy similar to the method that generated the robust *in vitro* system established in the mouse, using human ESCs, and they identified SOX17, an endodermal factor, as the key regulator for inducing hPGCs (Irie et al. 2015). In the mouse SOX17 has no apparent inductive role in mPGC specification (Hara et al. 2009). Interestingly, single cell transcriptome analysis of *in vivo* hPGCs from week 4 to week 19 confirmed expression of *SOX17*, but also of *SOX15*, which is expressed earlier and more robustly than *SOX17*, indicating a possibly more pivotal role of *SOX15* in hPGCs' development (Guo et al. 2015). Despite the fact that *in vitro* hPGCs have not been tested for their full potential, which would determine their functionality, their usage has confirmed previous skepticism for significant differences in the germline signaling network between human and mouse (reviewed in Surani 2015). These differences underscore the necessity for usage of non-human primate models. Such models may prove to be beneficial for understanding germ cell development in humans, as well as provide knowledge for establishing human gametogenesis *in vitro*, a tool valuable for both basic and applied scientific purposes.

1.2.5 Epigenetic reprogramming of primordial germ cells: the first reprogramming event in the gametic line

After the inductive wave for PGC specification, a small population of nascent PGCs becomes apparent at ~E7.0 as a small cluster of around 40 cells in the extra-embryonic mesoderm (primitive streak) at the base of allantois (Chiquoine 1954; Ginsburg et al. 1990). In order for the PGCs to become part of the developing gonads, they migrate from the extra-embryonic mesoderm to the developing hindgut endoderm and finally they reach the genital ridges by E10.5 (Tam & Snow 1981; Molyneaux et al. 2001; Seki et al. 2007; Richardson & Lehmann 2010). Their migratory pathway is accompanied by cell proliferation, but most importantly by epigenetic reprogramming, that targets genome wide histone modifications, as well as DNA methylation. The dynamics of histone modifications in PGCs has been mainly studied by immunofluorescence analyses covering all stages of germ cell development. However, the recent application of ChIP-seq technologies using small numbers of cells (Ng et al. 2013; Sachs et al. 2013) aimed for a more precise characterization of the PGCs' epigenome. At the same time the use of *in vitro* systems (Kurimoto & Saitou 2015) has opened the road for elucidating the functional significance of PGC reprogramming and possibly it will decipher the regulatory networks that mediate PGC reprogramming, in more detail.

The earliest (around E8.0) observed chromatin change that PGCs encounter is the global loss of H3K9me2, most likely triggered by the downregulation of its catalyzing enzymes GLP and G9a (Seki et al. 2007). The genome wide loss of H3K9me2 is accompanied by a temporal transcriptional quiescence as assessed by immunofluorescent detection of phosphorylated RNA PolII. This global silencing acts presumably to protect PGCs from deregulated transcription until enriched levels of H3K27me3 are well established in PGCs

(Seki et al. 2007; Kagiwada et al. 2013). Concomitant with the enriched H3K27me3 levels, PGCs in the female reactivate their inactive X chromosome, which remains silenced in the surrounding somatic cells (see section 1.2.2) (Sugimoto & Abe 2007; Chuva de Sousa Lopes et al. 2008). By ~E10.0 global transcription is restored, as well as histone modifications coupled to permissive and active chromatin which were also transiently absent from chromatin in earlier PGCs (H3K4me2, H3K4me3 and H3K9ac) (Seki et al. 2007). Subsequently, at E11.5 when PGCs have arrived in the genital ridges, another genome wide reprogramming event has been reported to take place in the germ cells. At this time immunostaining results indicate that H3K27me3, H3K9me3, H1 histone linker, HP1 isoforms and numerous other histone modifications and histones variants disappear from PGC chromatin. Subsequently, they re-appear at E12.5 germ cells (Hajkova et al. 2008). However, further inspection of the chromatin status of E11.5 PGCs failed to confirm a number of these findings (Kagiwada et al. 2013), necessitating additional examination which eventually might advance our understanding on the overall germ cell reprogramming.

To date the functional importance of histone reprogramming in PGCs is not fully understood. In other epigenetic reprogramming events redundancy can ensure successful completion of a developmental process upon absence of standard histone modifications (for example during histone to protamine transition – see section 1.2.8). However, failure to reduce H3K9me2 or to subsequently increase H3K27me3 levels around E9.0 in PGCs, leads to their loss (Yamaji et al. 2008; Mansour et al. 2012). A potential role of the epigenetic reprogramming event in PGCs could be to provide a basis for epigenetic inheritance in the next generation, since promoters of many somatic developmental regulators are bivalently marked (and transcriptionally silenced) with H3K27me3 and H3K4me3 in E11.5 and E13.5 germ cells. The bivalency may contribute to prevent the expression of the somatic program in the germline, but at the same time keep it accessible for activation after fertilization (Sachs et al. 2013). It would be interesting to examine whether bivalency is established and detected in earlier stages of PGC development.

An additional epigenetic change that participates into the eradication of the somatic differentiation programme in PGCs targets the PGC methylome. Genome wide DNA demethylation takes place in two waves in PGCs (Seisenberger et al. 2012; Yamaguchi, Shen, et al. 2013; Hackett et al. 2013). During the first wave, that initiates approximately at E8.0-E8.5, DNA demethylation occurs in various regions, such as promoters and islands, genic and intergenic regions. At a later phase, at around E10.5, DNA demethylation targets CpG islands of the X chromosome in females as well as differentially methylated regions of imprinted genes (Seisenberger et al. 2012). Remarkably, PGCs are the only cells in the body in which the methylation marks of imprinted genes are reset, in order to allow new sex-dependent marks to be established in the emerging male and female germline. Methylation reaches the lowest levels at E13.5, with female germ cells appearing less methylated compared to male germ cells (Seisenberger et al. 2012; Guibert et al. 2012; Popp et al. 2010). However, not all methylation marks are erased during the global DNA demethylation wave. A number of genomic regions escape this process and retain their methylation signature as described in BOX1.

The mechanism by which DNA demethylation is accomplished in PGCs has been under debate for over 60 years and in general it was believed that DNA demethylation relied on active mechanisms. A number of observations pointed in that direction: 1) the methylation marks of some imprinted genes were reported to be erased at E11.5 when PGCs were considered to be arrested in the G2 phase of the cell cycle (Hajkova et al. 2002); 2) the replication cycle of PGCs was considered to be quite slow (Tam & Snow 1981) and 3) deficiency of components considered to be important for the DNA demethylation process (such as of Activation Induced Cytidine Deaminase, short known as AICD or AID) resulted in higher methylation levels in these mutated PGCs compared to wild type PGCs (Popp et al. 2010). However, as presented below, most of these points have now been refuted by results from more robust experiments, and passive demethylation appears to be the main mechanism involved.

When the TET pathway (thought to be involved in active DNA methylation, see section 2.1.1) was first discovered, this was then also studied in developing PGCs. Some studies indicated that TET proteins were expressed, concomitant with the formation of 5hmC in migratory PGCs (Hackett et al. 2013; Yamaguchi, Hong, et al. 2013; Yamaguchi, Shen, et al. 2013). Another group observed very low expression levels of solely *Tet1* in PGCs, while *Tet2* and *Tet3* were not detected at all (Kagiwada et al. 2013). Furthermore, although *Tet1/Tet2* double knock out PGCs completely lack global 5hmC as assessed by immunofluorescence, this 5hmC loss, was not accompanied by global increased levels of 5mC (Dawlaty et al. 2013). In addition, when assessing methylation levels specifically at regulatory regions of imprinted genes, hypermethylation was indeed recorded, but only in a fraction of *Tet1/Tet2* knock out embryos. In general, Dawlaty et al. (2013) observed that the "increased methylation levels" phenotype in regulatory regions of imprinted regions was variable among embryos of the same litter, and aberrant imprinting was not exclusively linked to lethality (Dawlaty et al. 2013). Together, these data have led to the now well accepted view that TET proteins affect DNA demethylation only at specific loci (review in Hill et al. 2014). Evidence supporting a much larger role for passive demethylation in PGCs came from the observation that components of the *de novo* or maintenance DNA methylation machineries, like DNMT3A/3B, DNMT1 and UHRF1, are either not expressed or depleted from PGC nuclei (Kurimoto et al. 2008; Kagiwada et al. 2013). In addition, re-analysis of the PGC cell cycle with BrdU pulse-chase experiments revealed that the proliferation of the germ cell precursors occurs frequent enough to support a passive DNA demethylation model (Kagiwada et al. 2013). In support of the passive demethylation scenario, not only genetic ablation of genes encoding the TET enzymes, but also of molecular components that are also thought to participate in the active DNA demethylation in PGCs, does not have such a dramatic effect on methylation levels, as someone would expect if only active demethylation pathways takes place. For example in *Aid* deficient embryos the increase in DNA methylation levels is only slight (Popp et al. 2010). A mathematical model that was built to recapitulate DNA methylation in mouse ESCs, which might be similar to what occurs in PGCs, also predicts that global DNA demethylation is driven by impaired DNA methylation maintenance (passive demethylation), and not by active DNA demethylation. However, TET-dependent demethylation was indeed confirmed with this mathematical model in a limited number of specific loci, including that of certain imprinted genes (von Meyenn et al. 2016).

All the above mentioned information comes from mouse studies. A lot of attention has lately turned to human, in order to specify whether analogous mechanisms occur in human developing germ cells. These studies revealed that, in the human germline, PGCs also undergo reprogramming, although there are some differences compared to the mouse. While in the mouse there is persistent enrichment of the repressive histone mark H3K27me3, compared to the surrounding soma, throughout germ cell development (Kagiwada et al. 2013), this histone modification, was undetectable by immunofluorescence analysis in hPGCs after week 9 of development. Conversely, H3K9me2 is globally depleted from mouse PGC nuclei shortly after these cells are specified (Seki et al. 2007), but is still detected in the human germ cell nuclei, albeit in lower levels compared to the surrounding somatic cells (Tang et al. 2015). Still, reactivation of the inactive X chromosome takes place both in mouse and human female PGCs (Gkountela et al. 2015; Guo et al. 2015).

Concerning the status of DNA methylation, detailed examination of the methylome by whole genome bisulfite sequence revealed that similar to the mouse, DNA demethylation takes place also in hPGCs. DNA methylation reprogramming targets promoters, transcription sites, intergenic regions and gene bodies (Tang et al. 2015). Most importantly, DNA demethylation targets imprints, highlighting the evolutionary conservation of epigenetic reprogramming as a whole taking place in the germline of mammals. The general DNA demethylation mechanism in hPGCs seems to include parallel operations of passive and active DNA demethylation pathways like mouse PGCs. TET1 and TET2 are enriched in hPGCs, and at the same time 5hmC is enriched in certain genomic areas (such as in germ cell gene promoters and imprinted genes), indicating the operation of active

DNA demethylation mechanisms (Gkountela et al. 2015; Guo et al. 2015; Tang et al. 2015). However, RNA-seq experiments failed to detect components that are thought to actively remove 5hmC from the DNA of hPGCs (e.g. AID) (Tang et al. 2015).

At the same time, despite detection of DNMT3A/3B, as well as of UHRF1 mRNA in the human germline, the protein levels examined by immunofluorescence are below detection in hPGCs (Tang et al. 2015), pointing to a passive dilution of 5hmC, since the *de novo* and maintenance methylation machineries are largely disabled.

BOX1: Escape from DNA demethylation

Despite the gradual loss of DNA methylation during mouse PGCs' reprogramming, certain regions of the genome resist DNA demethylation and remain methylated either fully or partially (Seisenberger et al. 2012; Guibert et al. 2012; Hackett et al. 2013). Classic examples of elements that behave in such manner are repetitive transposable elements like IAPs, ERV-LTR1, -ERVL, and -ERVK. Transposable elements are DNA sequences, which have the ability to mobilize and jump from one position in the genome to the next, thereby interrupting genes and leading to diseases. Therefore their expression must stay under tight control. An example of such control takes place in the germ line, where even in E13.5 germ cells, that have the lowest DNA methylation levels (Popp et al. 2010; Seisenberger et al. 2012) these elements do manage to retain their methylation signature.

DNA demethylation escapees also include single copy sequences that are widely distributed in the genome, including gene bodies, promoters, intergenic regions as well as regions located in close proximity to DNA demethylation resistant transponsable elements. In addition, retention of DNA methylation is also observed in pericentric satellite repeats and in subtelomeric regions (Guibert et al. 2012; Seisenberger et al. 2012; Hackett et al. 2013; Guo et al. 2015).

Intriguingly, all these DNA regions (transposons and not) that resist DNA demethylation may be vectors of epigenetic information across generations, leading to transgenerational inheritance, since they might influence activity of neighboring genes. How these elements resist DNA demethylation is largely unknown. A mechanism found recently to operate in PGCs involves H3K9me3 and/or H3K27me3 enrichment in these elements. Somehow, these repressive histone marks confer a level of protection against both active and passive DNA demethylation machineries. Deletion of *Setdb1*, the gene encoding H3K9me3 methyltransferase, resulted in loss of methylation and in de-repression of many retrotransposons. Other elements, however, remained silenced indicating the presence of alternative repressive pathways (Liu et al. 2014).

Like in the germline, early preimplantation embryos undergo a global DNA demethylation wave (reviewed in Marcho et al. 2015). However, in this case imprinted genes escape the demethylation process. Therefore early embryos and ESCs (derived from the ICM of the blastocyst) have been used to unravel escaping DNA demethylation mechanisms. Subsequently, the same mechanisms may also apply to the germ-line escapees.

Research in early embryos and ESCs revealed several factors participating in the process of protection of methylated DNA against demethylation, like the pluripotency factor STELLA in collaboration with H3K9me2, or the repressive TRIM28 complex. STELLA has been shown to protect 5mC from TET3-mediated conversion to 5hmC by binding to maternal chromatin containing H3K9me2 in mice (Nakamura et al. 2012). The TRIM28 complex includes heterochromatinisation components such as the H3K9me3 catalysing histone methyltrasnferase SETDB1, HP1 and the DNA methyltranferases DNMT1, DNMT3A/3B (Quenneville et al. 2011; Zuo et al. 2012). In addition, TRIM28 itself has been shown to associate with the KRAB zinc finder protein 57 (ZFP57) (Alexander et al. 2015; Li et al. 2008) and these proteins have been detected at imprinted loci and other regions, which contain the ZFP57 binding motif (TGCCGC) (Quenneville et al. 2011; Liu et al. 2012). It is evident, that the TRIM28/ZFP57 and co-factors complex plays a major role in controlling endogenous retroelements both in mouse (Rowe et al. 2010) and human stem cells (Turelli et al. 2014), in preimplantation embryos (Li et al. 2008; Alexander et al. 2015) as well as in other types of cells (Fasching et al. 2015); however, a direct role in maintaining retroelements methylated in the mouse germline has not been explored yet. In the human germline, binding motifs for the KRAB-TRIM28/ZFP57 repressive complex have been identified in retroelements that escape DNA demethylation (Tang et al. 2015), indicating that this complex may be used as a general repressor of different elements during reprogramming events taking place in the mammalian genome.

Interestingly, other types of repeat elements, like LINES, do follow the demethylation wave in the germline, but their demethylation is not necessarily coupled to transcription, which may have detrimental effects to the cells (Tang et al. 2015; Hackett et al. 2013; Seisenberger et al. 2012; Kim et al. 2014). The protein arginine methyltransferase 5 (PRMT5) has been found to repress transcription of such elements upon their demethylation during the reprogramming wave in PGCs (Kim et al. 2014). Specifically, PRMT5 catalyses formation of the repressive histone-mark H4/H2AR3me2, and ChIP experiments showed that this histone modification is enriched in transposons that become demethylated. In addition, at E11.5, PRMT5 exits the nucleus and then methylates the cytoplasmic PIWI proteins, which are major components of the piRNA-mediated *de novo* DNA methylation pathway of transposons (Kim et al. 2014; Berrens & Reik 2016). Therefore, PRMT5 seems to act in different ways in controlling transposable elements. Potentially, additional epigenetic controls may participate in their tight (post) transcriptional restraint.

1.2.6 Meiosis: activity and inactivity of sex chromosomes

When PGCs have completed the global wave of DNA methylation and overall reorganisation of their chromatin, they enter a quiescent stage in males that persists up to puberty. In contrast, all female PGCs enter meiotic prophase around E13.5 in mouse. During meiotic prophase, homologous chromosomes come in a very close proximity to pair and physically connect through a process termed synapsis. The pairing of the chromosomes is mediated by complex regulatory mechanisms involving specific telomere anchoring to the nuclear membrane, chromosome movement, and generation and repair of meiotic DNA double-strand breaks, whereby sequence similarity between parental homologs is used to ensure correct partner recognition. Concomitant with the progression of chromosome pairing and synapsis, homologs undergo meiotic recombination, so that genetic material of the parental genomes is shuffled and at the end of meiosis genetically unique haploid cells will arise.

In female meiosis, the sex chromosomes behave similar to the autosomes and as mentioned in 1.2.5, both X chromosomes are active in female oocytes (Sugimoto & Abe 2007; Chuva de Sousa Lopes et al. 2008). Meiosis then arrests at the end of prophase I, and is resumed at puberty, when a follicle has reached pre-ovulatory size, and the Follicle Stimulating Hormone (FSH) and Luteneizing Hormone (LH) surge initiate ovulation and trigger the oocyte to complete meiosis I. This is an asymmetrical division, generating a small polar body and a mature oocyte that is arrested at metaphase II. Upon fertilization, this second arrest is relieved and a second polar body forms.

Male meiosis initiates at puberty (Figure 5), and is re-initiated at regular time intervals from differentiated spermatogonia that develop from a spermatogonia stem cell pool during the rest of the adult life. The presence of the largely non-homologous X and Y chromosome challenges the chromosome pairing process in males: X and Y stably synapse only in a small region of homology, called the pseudoautosomal region (PAR) (Perry et al. 2001). The extensive asynapsis between the X and Y chromosomes is associated with their transcriptional inactivation (Monesi 1965) in a process called Meiotic Sex Chromosome Inactivation (MSCI). MSCI itself is a version of a more general silencing phenomenon known as Meiotic Silencing of Unsynapsed Chromatin (MSUC) (Baarends et al. 2005; Turner et al. 2005). Similar to the X and Y, when homologous autosomes do not manage to synapse during meiosis they also become transcriptionally silenced.

The molecular players involved in triggering MSCI and MSUC appear to be very similar. In both cases there is persistence of meiotic DNA DSBs, accumulation of proteins such as HORMAD1/2 that recognize unsynapsed regions (Wojtasz et al. 2009), and activation of the DNA damage response pathway, whereby ATR and BRCA1 will accumulate. This leads to the phosphorylation of γH2AX in a positive feedback loop (Turner et al. 2004; Mahadevaiah et al. 2008) causing gene silencing (Royo et al. 2013).

In striking contrast to MSCI though, MSUC can occur both in the female and male germline, is related to abnormal situations, and eventually leads to male and female infertility or reduced fertility due to germ cell arrest (reviewed in Turner 2015). MSCI, on the other hand, has evolved to be an absolute prerequisite for normal male meiosis, and if disrupted (e.g. upon induction of MSUC) male fertility is compromised (Lè Ne Royo et al. 2010). So despite the continuous presence of an obligatory unsynapsed chromosome pair (XY) during male meiosis, MSCI will never trigger germ cell arrest in normal situations.

Since transcription must be tightly restricted (BOX2) from the male sex chromosomes, the nuclear territory that the X and Y occupy (also known as XY or sex body) carries a number of heterochromatic features. Phosphorylation of γH2AX sets the basis for transcriptional inactivation. Subsequently, other chromatin alterations take place in the XY body. For example, there is enrichment of H3K9me2 (Greaves et al. 2006), H3K9me3 (Page et al. 2012), ubiquitinated H2A (Baarends et al. 2005), HP1β (Motzkus et al. 1999; Turner et al. 2001), HP1γ (Greaves et al. 2006), macroH2A variant (Hoyer-Fender et al. 2000) and the canonical H3 is substituted by the H3.3 variant (van der Heijden et al. 2007). In addition, histone modifications associated with transcriptional activity, such as H3K9ac, as well as (phosphorylated) RNA Polymerase II, are depleted from the XY body and in general this region is compartmentalized to the periphery of the nucleus (Page et al. 2012).

BOX2: Transcription from the X & Y during MSCI leads to arrest

MSCI has been linked to transcriptional dormancy of the X and Y chromosome in the male germ cells. This implies that, during MSCI, male germ cells are able to tolerate the absence of X and Y gene transcription. Interestingly though, X-linked genes important for meiosis and male fertility have been discovered to be expressed at the earliest stage of male germ cell development (spermatogonia), before meiosis commences and evolution came up with an additional mechanism, so that genes with important functions (e.g. housekeeping genes located on the X) will find alternative ways of expression during meiosis. In this case, a number of genes located on the X chromosome have been duplicated and integrated themselves via retrotransposition in autosomal positions, and around the time of MSCI they will be expressed and back up the function of the parental genes that are subjected to silencing via MSCI (Sin 2013). In addition, there appears to be a special mRNA stabilization mechanism that operates early during male and female meiotic prophase, in association with global transcriptional silencing during this phase (Abby et al. 2016). As autosomal gene transcription then re-initiates in pachytene, the sex chromosomes remain silent, and some transcripts might still be stabilized, although the observed overall reduction of sex-linked transcripts versus autosomal transcripts in purified spermatocytes nicely illustrates the global nature of MSCI (Turner et al. 2006). To provide a theory that could explain how this mechanism might have evolved, it was proposed that sex-linked gene mis-expression at the time of MSCI could be deleterious for male germ cells. In line with this argument, experiments with XYY male mice, and with transgenic mice expressing specific Y-linked genes from an autosome, provided compelling evidence in support of this hypothesis. In this case, the Y-chromosomes (or the autosomes carrying the Y-linked genes) perfectly synapse, escape MSCI, remain transcriptionally active, and the transcriptional activation of Y-linked genes leads to germ cell arrest (Royo et al. 2010).

Lastly, if MSUC is induced, due to an autosomal pairing problem in male germ cells, MSCI is incomplete. In this case, the mediators of MSCI are partially redistributed to the autosomal unsynapsed chromatin and therefore the MSCI process is impaired. The sex chromosomes are now transcriptionally active and the accumulation of toxic X and Y transcripts leads to germ cell arrest (Royo 2010). At the same time, MSUC itself is quite a germ cell stressful event and germ cells are not evolutionary adapted to cope with it, as they do with MSCI. Meiotic silencing in this situation will starve germ cells for a multitude of gene products related to the unsynapsed chromatin, and this may also contribute to germ cell arrest (Turner, 2015).

1.2.7 Silencing in post-meiotic haploid cells: Postmeiotic Sex Chromosome Repression (PSCR)

After completion of meiosis, diploid cells have given rise to four haploid spermatids that carry either an X or a Y chromosome. At this point, the XY body has dismantled and yH2AX and several proteins related to MSCI have been removed from the X and Y. Still, certain heterochromatic features are maintained in the sex chromosomes in the round spermatids, largely maintaining the transcriptionally silenced state of X and Y. The persistence of the X and Y in a silent postmeiotic state is referred to as post-meiotic sex chromosome repression (PSCR) (Namekawa et al. 2006).

Microarray analysis showed that 13% of the 676 genes examined on the X-chromosome are postmeiotically induced (87% silent genes). Interestingly, the majority of genes evading PMSC correspond to multi-copy genes, and their escape has been connected to their functional role in spermiogenesis (reviewed in Turner 2015). Knockdown experiments of such genes results in impaired sperm motility, numbers and reduced fertility (Mueller et al. 2008, Coquet et al. 2009). In addition, single copy genes have been reported to escape PSCR. These involve again genes both essential for fertility (e.g. *Akap4*) and genes that do not have a clear function in postmeiotic germ cell development (e.g. *Rnf8*, *Rnf12*) (Namekawa et al. 2006; Hu & Namekawa 2015).

Given that transcriptional silencing is highly maintained after MSCI, immunofluorescence studies revealed that solely the X (or the Y) among the rest of the chromosomes in round spermatids is marked by a more intense DAPI signal compared to the surrounding chromatin and is visible as a domain alongside the chromocenter. The chromocenter itself is also DAPI dense and consists of the pericentric heterochromatin of the autosomes present within the nucleus of round spermatids. As expected, histone modifications and proteins usually found in heterochromatin, such as H3K9me2/3, HP1β and HP1γ, also mark the sex chromosomes in round spermatids (Namekawa et al. 2006; Sin & Namekawa 2013). In addition, the histone variant H2A.Z is also enriched, and is thought to replace macroH2A (Greaves et al. 2006).

1.2.8 The histone-to-protamine transition: setting the paternal epigenome for the next generation

Despite the fact that the basic steps of meiosis are very similar between males and females, the mature gametes deriving from each sex are very different from each other, not only morphologically and structurally, but also epigenetically. The most striking difference between the two is that during the maturation process of the male haploid gametes, known as spermiogenesis (Figure 6), histones are replaced by other small basic proteins called protamines so that the genome of the sperm will be packaged and condensed in the most compact way. The packaging will facilitate the sperm to adapt a compact hydrodynamic shape needed for its journey along both male and female reproductive tracts, but also to protect its DNA from damage (Rathke et al. 2014).

The epigenetic transformation from histones to protamines occurs in three steps. In the first step, a number of canonical histones are replaced by testis specific histone variants.

The histone variants can incorporate at pre- and postmeiotic stages of spermatogenesis and both canonical histones and histone variants are present in the testis. The testis specific histones variants contribute to loosening of the chromatin structure and thus prepare the genome for the histone-to-protamine transition (Montellier et al. 2013). Alternatively, or in addition, testis specific histone variants may somehow guide the deposition of transition proteins (second step, see below) and protamines (Bao & Bedford 2016). Furthermore, in the testis, both canonical histones and histone variants can be post transcriptionally modified, and this type of regulation is also thought to contribute to the histone removal. For example, the ubiquitination of H2A and H2B has been proposed to be required for the hyperacetylation of H4 (H4K5, H4K8 and H4K16) (Lu et al. 2010), which subsequently promotes histone replacement and chromatin compaction (Hazzouri et al. 2000; Govin et al. 2006).

In the second step and just before the deposition of protamines, transition proteins briefly take the place of the majority of histones. In the mouse there are two transition proteins, TP1 and TP2. TP1 and TP2 can compensate for each other's loss, since the phenotypes of the single *Tp1* or *Tp2* knockout mouse models are quite similar and both are still able to produce offspring. In these single knockout models, transcription from the intact Tp gene was found to be upregulated (Yu et al. 2000; Zhao et al. 2001). In accordance with the functional compensation hypothesis, *Tp1* and *Tp2* double knockout mice are sterile, have abnormal sperm morphology, chromatin condensation is compromised and histones are retained during spermiogenesis (Zhao et al. 2004).

The third and last step that is required for full chromatin condensation in maturing spermatids is the deposition of protamines. With this step, the chromatin in the sperm nucleus will be 6-20 times more compact compared to a nucleus containing histone-based chromatin (Bao & Bedford 2016). The mouse genome encodes two types of protamines: PRM1 and PRM2. Similar to transition proteins, protamines are also small basic proteins. Interestingly, deletion of one allele of either *Prm1* or *Prm2* leads to haploinsufficiency accompanied by sterility; therefore single protamine gene knockout mice cannot be generated (Cho et al. 2001), demonstrating the essential role of these proteins in spermatogenesis.

At the end of mouse spermiogenesis, the vast majority of nucleosomes has been replaced by protamines. However, a small fraction (1%) of histones is retained in the mouse genome and in human this fraction is much higher (15%) (reviewed by Rathke et al. 2014). The presence of such histones and their epigenetic signature is of great interest since they may contribute to the regulation of developmental processes in the next generation(s). Therefore, many labs sought to determine their genomic position. One well-accepted genomic position where nucleosomes are retained is the centromere. Studies in

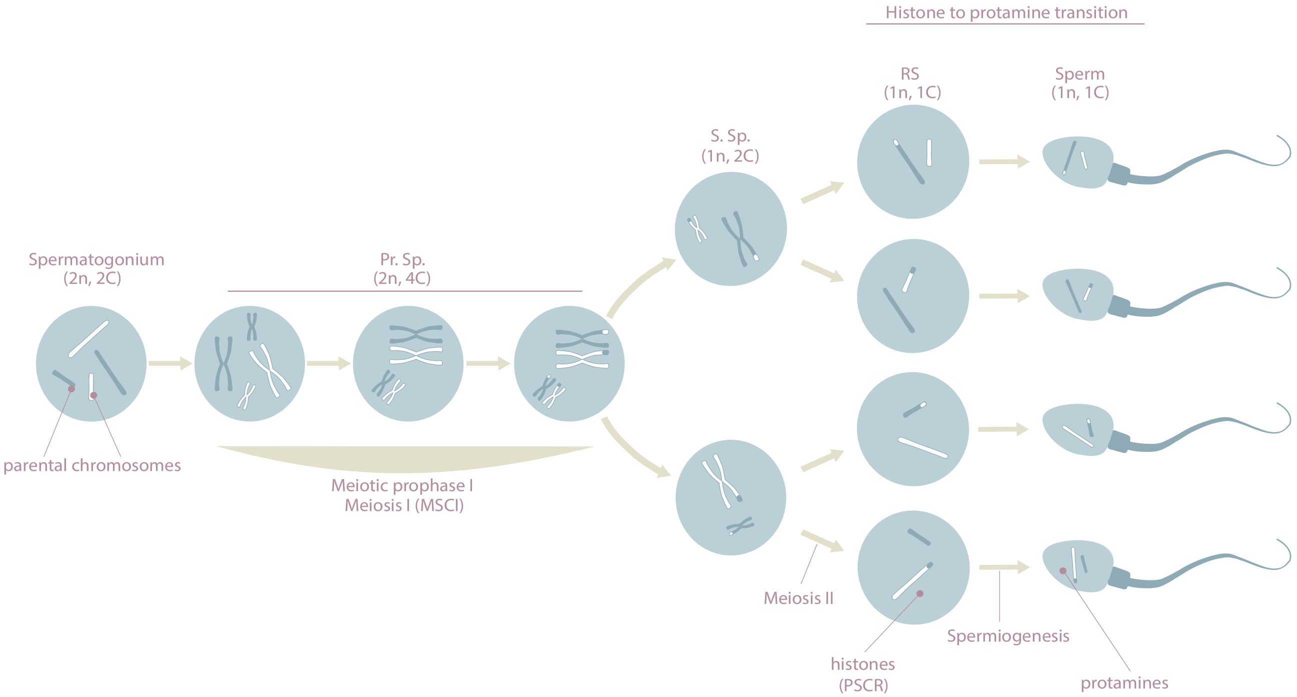
Histone to protamine transition
Spermatogonium
(2n, 2C)
Pr. Sp.
(2n, 4C)
S. Sp.
(1n, 2C)
RS
(1n, 1C)
Sperm
(1n, 1C)
parental chromosomes
Meiotic prophase I
Meiosis I (MSCI)
Meiosis II
histones
(PSCR)
Spermiogenesis
protamines

Figure 6: Mammalian spermatogenesis

Spermatogonia are diploid germ cells that carry one set of chromosomes from the mother (white chromosomes) and one from the father (dark green chromosomes). After replicating their DNA, a number of spermatogonia will enter Meiosis I (primary spermatocytes: Pr. Sp.), where homologues chromosomes will synapse and exchange genetic material during meiotic prophase I. During this period MSCI takes place in the sex chromosomes. The first meiotic division results in formation of haploid secondary spermatocytes (S. Sp.), which carry now a single homolog chromosome per pair. Secondary spermatocytes enter meiosis II, without replicating their DNA. Therefore, the second meiotic division will then generate haploid round spermatids (RS), where silencing of sex chromosomes still largely persists through PSCR. Round spermatids mature to spermatozoa through spermiogenesis, and during this process almost all histones will be replaced by protamines.

different organisms revealed that CENPH3 (also known as CENPA), a variant of histone H3 found on centromeres is not exchanged for protamines in a variety of species, including mammals, suggesting that the centromere identity must remain intact throughout all intense reprogramming processes that accompany developmental processes, and provide a centromere basis for early embryogenesis (Palmer et al. 1990; McKinley & Cheeseman 2015).

Apart from the clear retention of CENPH3, a number of studies, both in human and mouse sperm, support the notion that sperm histones are overrepresented in developmental gene promoters or exons and are barely found at repeat regions or introns (Hammoud et al. 2009; Hisano et al. 2013). Contrarily to this view, one recent publication indicated that nucleosome retention does not occur at gene promoters, but mostly in gene poor regions (Carone et al. 2014). At the same time, another publication indicated retention of sperm histones mostly at centromeric repeats and sites containing retrotransposons (Samans et al. 2014). Interestingly, re-analysis of the latter study by a different group (Royo et al. 2016), revealed that the bioinformatics strategy followed in their study was trivially performed; over-representation of nucleosomes at genomic repeats could not be detected upon re-examination of their data. The other discrepancies between the published studies may be caused by different experimental conditions in order to assess genomic position of nucleosome retention; enrichment at gene promoters could only be detected when high concentration micrococcal nuclease (MNase) was used.

Novel approaches may be needed to resolve this matter. However, whatever the exact location of the sperm histones is, experimental evidence suggests that these histones, also carrying specific modifications, may have a great impact on offspring development for more than one generation (Siklenka et al. 2015).

REFERENCES

Abby, E. et al., 2016. Implementation of meiosis prophase I programme requires a conserved retinoid-independent stabilizer of meiotic transcripts. Nature communications, 7, p.10324.

Abe, K. et al., 2011. Loss of heterochromatin protein 1 gamma reduces the number of primordial germ cells via impaired cell cycle progression in mice. Biology of reproduction, 85(5), pp.1013–24.

Adenot, P.G. et al., 1997. Differential H4 acetylation of paternal and maternal chromatin precedes DNA replication and differential transcriptional activity in pronuclei of 1-cell mouse embryos. Development (Cambridge, England), 124(22), pp.4615–25.

Alexander, K.A. et al., 2015. TRIM28 Controls Genomic Imprinting through Distinct Mechanisms during and after Early Genome-wide Reprogramming. Cell reports, 13(6), pp.1194–205.

Amouroux, R. et al., 2016. De novo DNA methylation drives 5hmC accumulation in mouse zygotes. Nature Cell Biology, 18(2), pp.225–233.

Aramaki, S. et al., 2013. A Mesodermal Factor, T, Specifies Mouse Germ Cell Fate by Directly Activating Germline Determinants. Developmental Cell, 27(5), pp.516–529.

Aucott, R. et al., 2008. HP1-beta is required for development of the cerebral neocortex and neuromuscular junctions. The Journal of cell biology, 183(4), pp.597–606.

Baarends, W.M. et al., 2005. Silencing of unpaired chromatin and histone H2A ubiquitination in mammalian meiosis. Molecular and cellular biology, 25(3), pp.1041–53.

Bannister, a J. et al., 2001. Selective recognition of methylated lysine 9 on histone H3 by the HP1 chromo domain. Nature, 410(6824), pp.120–124.

Bao, J. & Bedford, M.T., 2016. Epigenetic regulation of the histone-to-protamine transition during spermiogenesis. Reproduction (Cambridge, England), 151(5), pp.R55-70.

Barr, M.L. & Bertram, E.G., 1949. A morphological distinction between neurones of the male and female, and the behaviour of the nucleolar satellite during accelerated nucleoprotein synthesis. Nature, 163(4148), p.676.

Berrens, R. V & Reik, W., Prmt5: a guardian of the germline protects future generations.

Bertocchini, F. & Chuva de Sousa Lopes, S.M., 2016. Germline development in amniotes: A paradigm shift in primordial germ cell specification. BioEssays : news and reviews in molecular, cellular and developmental biology, 38(8), pp.791–800.

Bérubé, N.G., 2011. ATRX in chromatin assembly and genome architecture during development and disease. Biochemistry and cell biology = Biochimie et biologie cellulaire, 89(5), pp.435–44.

Bikoff, E.K. & Robertson, E.J., 2008. One PRDM is not enough for germ cell development. Nature genetics, 40(8), pp.934–5.

Burton, A. & Torres-Padilla, M.-E., 2010. Epigenetic reprogramming and development: a unique heterochromatin organization in the preimplantation mouse embryo. Briefings in functional genomics, 9(5–6), pp.444–54.

Cantú, A.V. & Laird, D.J., 2013. Wnt and Bmp Fit Germ Cells to a T. Developmental Cell, 27(5), pp.485–487.

Carone, B.R. et al., 2014. High-resolution mapping of chromatin packaging in mouse embryonic stem cells and sperm. Developmental cell, 30(1), pp.11–22.

Casanova, M. et al., 2013. Heterochromatin Reorganization during Early Mouse Development Requires a Single-Stranded Noncoding Transcript. Cell Reports, 4(6), pp.1156–1167.

Cerda, M.C. et al., 1999. Organisation of complex nuclear domains in somatic mouse cells. Biology of the cell / under the auspices of the European Cell Biology Organization, 91(1), pp.55–65. evidence of germ cell differentiation. Human reproduction (Oxford, England), 22(2), pp.567–77.

Chen, H.-F. et al., 2007. Derivation, characterization and differentiation of human embryonic stem cells: comparing serum-containing versus serum-free media and evidence of germ cell differentiation. Human reproduction (Oxford, England), 22(2), pp.567–77.

Chiquoine, A.D., 1954. The identification, origin, and migration of the primordial germ cells in the mouse embryo. The Anatomical Record, 118(2), pp.135–146.

Cho, C. et al., 2001. Haploinsufficiency of protamine-1 or -2 causes infertility in mice. Nature genetics, 28(may), pp.82–86.

Chuva de Sousa Lopes, S.M. et al., 2008. X chromosome activity in mouse XX primordial germ cells. PLoS genetics, 4(2), p.e30.

Clark, A.T. et al., 2004. Spontaneous differentiation of germ cells from human embryonic stem cells in vitro. Human Molecular Genetics, 13(7), pp.727–739.

Clemson, C.M. et al., 1996. XIST RNA paints the inactive X chromosome at interphase: evidence for a novel RNA involved in nuclear/chromosome structure. The Journal of cell biology, 132(3), pp.259–75.

Corbel, C. et al., 2013. Unusual chromatin status and organization of the inactive X chromosome in murine trophoblast giant cells. Development (Cambridge, England), 140(4), pp.861–72.

Di Croce, L. & Helin, K., 2013. Transcriptional regulation by Polycomb group proteins. Nature Structural & Molecular Biology, 20(10), pp.1147–1155.

Daujat, S. et al., 2009. H3K64 trimethylation marks heterochromatin and is dynamically remodeled during developmental reprogramming. Nature structural & molecular biology, 16(7), pp.777–81.

Dawlaty, M.M. et al., 2013. Combined deficiency of Tet1 and Tet2 causes epigenetic abnormalities but is compatible with postnatal development. Developmental cell, 24(3), pp.310–23.

Dawlaty, M.M. et al., 2014. Loss of Tet enzymes compromises proper differentiation of embryonic stem cells. Developmental cell, 29(1), pp.102–11.

Déjardin, J., 2015. Switching between Epigenetic States at Pericentromeric Heterochromatin. Trends in genetics : TIG, 31(11), pp.661–72.

Dinant, C. & Luijsterburg, M.S., 2009. The emerging role of HP1 in the DNA damage response. Molecular and cellular biology, 29(24), pp.6335–40.

Ehrlich, M. et al., 2008. ICF, an immunodeficiency syndrome: DNA methyltransferase 3B involvement, chromosome anomalies, and gene dysregulation. Autoimmunity, 41(4), pp.253–71.

Eickbush, T.H. & Moudrianakis, E.N., 1978. The histone core complex: an octamer assembled by two sets of protein-protein interactions. Biochemistry, 17(23), pp.4955–64.

Eissenberg, J.C. & Elgin, S.C., 2000. The HP1 protein family: getting a grip on chromatin. Current opinion in genetics & development, 10(2), pp.204–10.

Eymery, A. et al., 2009. A transcriptomic analysis of human centromeric and pericentric sequences in normal and tumor cells. Nucleic acids research, 37(19), pp.6340–54.

Fasching, L. et al., 2015. TRIM28 represses transcription of endogenous retroviruses in neural progenitor cells. Cell reports, 10(1), pp.20–8.

Feil, R., 2009. Epigenetic asymmetry in the zygote and mammalian development. The International journal of developmental biology, 53(2–3), pp.191–201.

Ferreira, A.R. et al., 2010. Allele-specific expression of the MAOA gene and X chromosome inactivation in in vitro produced bovine embryos. Molecular reproduction and development, 77(7), pp.615–21.

Fukuda, A. et al., 2015. Chromatin condensation of Xist genomic loci during oogenesis in mice. Development (Cambridge, England), 142(23), pp.4049–55.

Fukuda, A. et al., 2014. The role of maternal-specific H3K9me3 modification in establishing imprinted X-chromosome inactivation and embryogenesis in mice. Nature communications, 5, p.5464.

Fulka, H. & Aoki, F., 2016. Nucleolus Precursor Bodies and Ribosome Biogenesis in Early Mammalian Embryos: Old Theories and New Discoveries. Biology of reproduction, 94(6), p.143.

Garrick, D. et al., 2006. Loss of Atrx affects trophoblast development and the pattern of X-inactivation in extraembryonic tissues. PLoS genetics, 2(4), p.e58.

Ginsburg, M., Snow, M.H. & McLaren, A., 1990. Primordial germ cells in the mouse embryo during gastrulation. Development (Cambridge, England), 110(2), pp.521–8.

Gkountela, S. et al., 2015. DNA Demethylation Dynamics in the Human Prenatal Germline. Cell, 161(6), pp.1425–36.

Goldberg, A.D. et al., 2010. Distinct factors control histone variant H3.3 localization at specific genomic regions. Cell, 140(5), pp.678–91.

Gontan, C. et al., 2012. RNF12 initiates X-chromosome inactivation by targeting REX1 for degradation. Nature, 485(7398), pp.386–90.

Görisch, S.M. et al., 2005. Histone acetylation increases chromatin accessibility. Journal of cell science, 118(Pt 24), pp.5825–34.

Goto, T., Wright, E. & Monk, M., 1997. Paternal X-chromosome inactivation in human trophoblastic cells. Molecular human reproduction, 3(1), pp.77–80.

Govin, J. et al., 2006. Histone acetylation-mediated chromatin compaction during mouse spermatogenesis. Ernst Schering Research Foundation workshop, (57), pp.155–72.

Grabole, N. et al., 2013. Prdm14 promotes germline fate and naive pluripotency by repressing FGF signalling and DNA methylation. EMBO reports, 14(7), pp.629–37.

Greaves, I.K. et al., 2006. The X and Y Chromosomes Assemble into H2A.Z, Containing Facultative Heterochromatin, following Meiosis. Molecular and Cellular Biology, 26(14), pp.5394–5405.

Grewal, S.I.S. & Elgin, S.C.R., 2007. Transcription and RNA interference in the formation of heterochromatin. Nature, 447(7143), pp.399–406.

Grewal, S.I.S. & Moazed, D., 2003. Heterochromatin and epigenetic control of gene expression. Science (New York, N.Y.), 301(5634), pp.798–802.

Gu, T.-P. et al., 2011. The role of Tet3 DNA dioxygenase in epigenetic reprogramming by oocytes. Nature, 477(7366), pp.606–10.

Guenatri, M. et al., 2004. Mouse centric and pericentric satellite repeats form distinct functional heterochromatin. The Journal of cell biology, 166(4), pp.493–505.

Guibert, S., Forné, T. & Weber, M., 2012. Global profiling of DNA methylation erasure in mouse primordial germ cells. Genome research, pp.633–641.

Guo, F. et al., 2015. The Transcriptome and DNA Methylome Landscapes of Human Primordial Germ Cells. Cell, 161(6), pp.1437–52.

Hackett, J.A. et al., 2013. Germline DNA demethylation dynamics and imprint erasure through 5-hydroxymethylcytosine. Science (New York, N.Y.), 339(6118), pp.448–52.

Hadjantonakis, A.K. et al., 2001. An X-linked GFP transgene reveals unexpected paternal X-chromosome activity in trophoblastic giant cells of the mouse placenta. Genesis (New York, N.Y. : 2000), 29(3), pp.133–40.

Hajkova, P. et al., 2008. Chromatin dynamics during epigenetic reprogramming in the mouse germ line. Nature, 452(7189), pp.877–81.

Hajkova, P. et al., 2002. Epigenetic reprogramming in mouse primordial germ cells. Mechanisms of Development, 117, pp.15–23.

Hammoud, S., Liu, L. & Carrell, D.T., 2009. Protamine ratio and the level of histone retention in sperm selected from a density gradient preparation. Andrologia, 41(2), pp.88–94.

Hara, K. et al., 2009. Evidence for crucial role of hindgut expansion in directing proper migration of primordial germ cells in mouse early embryogenesis. Developmental biology, 330(2), pp.427–39.

Hata, K. et al., 2002. Dnmt3L cooperates with the Dnmt3 family of de novo DNA methyltransferases to establish maternal imprints in mice. Development (Cambridge, England), 129(8), pp.1983–93.

Hayashi-Takanaka, Y. et al., 2011. Tracking epigenetic histone modifications in single cells using Fab-based live endogenous modification labeling. Nucleic acids research, 39(15), pp.6475–88.

Hayashi, K. et al., 2012. Offspring from oocytes derived from in vitro primordial germ cell-like cells in mice. Science (New York, N.Y.), 338(6109), pp.971–5.

Hayashi, K. et al., 2011. Reconstitution of the Mouse Germ Cell Specification Pathway in Culture by Pluripotent Stem Cells. Cell, 146(4), pp.519–532.

HAZZOURI, M. et al., 2000. Regulated hyperacetylation of core histones during mouse spermatogenesis: involvement of histone-deacetylases. European Journal of Cell Biology, 79(12), pp.950–960.

van der Heijden, G.W. et al., 2005. Asymmetry in histone H3 variants and lysine methylation between paternal and maternal chromatin of the early mouse zygote. Mechanisms of development, 122(9), pp.1008–22.

van der Heijden, G.W. et al., 2007. Chromosome-wide nucleosome replacement and H3.3 incorporation during mammalian meiotic sex chromosome inactivation. Nature genetics, 39(2), pp.251–8.

Hill, P.W.S., Amouroux, R. & Hajkova, P., 2014. DNA demethylation, Tet proteins and 5-hydroxymethylcytosine in epigenetic reprogramming: an emerging complex story. Genomics, 104(5), pp.324–33.

Hirasawa, R. et al., 2008. Maternal and zygotic Dnmt1 are necessary and sufficient for the maintenance of DNA methylation imprints during preimplantation development. Genes & development, 22(12), pp.1607–16.

Hisano, M. et al., 2013. Genome-wide chromatin analysis in mature mouse and human spermatozoa. Nature protocols, 8(12), pp.2449–70.

Horáková, A.H. et al., 2010. SUV39h-independent association of HP1 beta with fibrillarin-positive nucleolar regions. Chromosoma, 119(3), pp.227–41.

Hoyer-Fender, S., Costanzi, C. & Pehrson, J.R., 2000. Histone macroH2A1.2 is concentrated in the XY-body by the early pachytene stage of spermatogenesis. Experimental cell research, 258(2), pp.254–60.

Hu, Y.-C. & Namekawa, S.H., 2015. Functional significance of the sex chromosomes during spermatogenesis. Reproduction (Cambridge, England), 149(6), pp.R265-77.

Inoue, A. et al., 2011. Generation and replication-dependent dilution of 5fC and 5caC during mouse preimplantation development. Cell research, 21(12), pp.1670–6.

Inoue, A. & Zhang, Y., 2011. Replication-dependent loss of 5-hydroxymethylcytosine in mouse preimplantation embryos. Science (New York, N.Y.), 334(6053), p.194.

Irie, N. et al., 2015. SOX17 is a critical specifier of human primordial germ cell fate. Cell, 160(1–2), pp.253–68.

Ito, S. et al., 2011. Tet proteins can convert 5-methylcytosine to 5-formylcytosine and 5-carboxylcytosine. Science (New York, N.Y.), 333(6047), pp.1300–3.

James, T.C. & Elgin, S.C.R., 1986. Identification of a Nonhistone Chromosomal Protein Associated with Heterochromatin in Drosophila melanogaster and Its Gene. MOLECULAR AND CELLULAR BIOLOGY, 6(11), pp.3862–3872.

Jolly, C. et al., 1997. HSF1 transcription factor concentrates in nuclear foci during heat shock: relationship with transcription sites. Journal of cell science, (23), pp.2935–41.

Jonkers, I. et al., 2009. RNF12 is an X-Encoded dose-dependent activator of X chromosome inactivation. Cell, 139(5), pp.999–1011.

Kagiwada, S. et al., 2013. Replication-coupled passive DNA demethylation for the erasure of genome imprints in mice. The EMBO journal, 32(3), pp.340–53.

Kay, G.F. et al., 1994. Imprinting and X chromosome counting mechanisms determine Xist expression in early mouse development. Cell, 77(5), pp.639–50.

Kim, S. et al., 2014. PRMT5 protects genomic integrity during global DNA demethylation in primordial germ cells and preimplantation embryos. Molecular cell, 56(4), pp.564–79.

Kohli, R.M. & Zhang, Y., 2013. TET enzymes, TDG and the dynamics of DNA demethylation. Nature, 502(7472), pp.472–479.

De Koning, L. et al., 2009. Heterochromatin protein 1alpha: a hallmark of cell proliferation relevant to clinical oncology. EMBO molecular medicine, 1(3), pp.178–91.

Kornberg, R.D., 1974. Chromatin structure: a repeating unit of histones and DNA. Science (New York, N.Y.), 184(4139), pp.868–71.

Kourmouli, N. et al., 2004. Heterochromatin and tri-methylated lysine 20 of histone H4 in animals. Journal of cell science, 117(Pt 12), pp.2491–501.

Kurimoto, K. et al., 2008. Complex genome-wide transcription dynamics orchestrated by Blimp1 for the specification of the germ cell lineage in mice. Genes & development, 22(12), pp.1617–35.

Kurimoto, K. & Saitou, M., 2015. Mechanism and Reconstitution In Vitro of Germ Cell Development in Mammals. Cold Spring Harbor symposia on quantitative biology, 80, pp.147–54.

De La Fuente, R., Baumann, C. & Viveiros, M.M., 2012. Chromatin structure and ATRX function in mouse oocytes. Results and problems in cell differentiation, 55, pp.45–68.

De La Fuente, R., Baumann, C. & Viveiros, M.M., 2011. Role of ATRX in chromatin structure and function: implications for chromosome instability and human disease. Reproduction (Cambridge, England), 142(2), pp.221–34.

Lachner, M. et al., 2001. Methylation of histone H3 lysine 9 creates a binding site for HP1 proteins. Nature, 410(6824), pp.116–120.

Lawson, K.A. et al., 1999. Bmp4 is required for the generation of primordial germ cells in the mouse embryo. Genes & Development, 13(4), pp.424–436.

Lawson, K.A. & Hage, W.J., 1994. Clonal analysis of the origin of primordial germ cells in the mouse. Ciba Foundation symposium, 182, pp.68-84-91.

Lè Ne Royo, H. et al., 2010. Report Evidence that Meiotic Sex Chromosome Inactivation Is Essential for Male Fertility. Current Biology, 20, pp.2117–2123.

Lechner, M.S. et al., 2005. The mammalian heterochromatin protein 1 binds diverse nuclear proteins through a common motif that targets the chromoshadow domain. Biochemical and biophysical research communications, 331(4), pp.929–37.

Lee, J.T., 2000. Disruption of imprinted X inactivation by parent-of-origin effects at Tsix. Cell, 103(1), pp.17–27.

Lee, J.T. & Lu, N., 1999. Targeted mutagenesis of Tsix leads to nonrandom X inactivation. Cell, 99(1), pp.47–57.

Lepikhov, K. & Walter, J., 2004. Differential dynamics of histone H3 methylation at positions K4 and K9 in the mouse zygote. BMC developmental biology, 4, p.12.

Lev Maor, G., Yearim, A. & Ast, G., 2015. The alternative role of DNA methylation in splicing regulation. Trends in genetics : TIG, 31(5), pp.274–80.

Li, X. et al., 2008. A maternal-zygotic effect gene, Zfp57, maintains both maternal and paternal imprints. Developmental cell, 15(4), pp.547–57.

Liu, H., Kim, J.-M. & Aoki, F., 2004. Regulation of histone H3 lysine 9 methylation in oocytes and early pre-implantation embryos. Development (Cambridge, England), 131(10), pp.2269–80.

Liu, S. et al., 2014. Setdb1 is required for germline development and silencing of H3K9me3-marked endogenous retroviruses in primordial germ cells. Genes & development, 28(18), pp.2041–55.

Liu, Y. et al., 2012. An atomic model of Zfp57 recognition of CpG methylation within a specific DNA sequence. Genes & development, 26(21), pp.2374–9.

Lomberk, G., Wallrath, L. & Urrutia, R., 2006. The Heterochromatin Protein 1 family. Genome biology, 7(7), p.228.

Lu, J. & Gilbert, D.M., 2007. Proliferation-dependent and cell cycle-regulated transcription of mouse pericentric heterochromatin. Journal of Cell Biology, 179(3), pp.411–421.

Lu, L.-Y. et al., 2010. RNF8-dependent histone modifications regulate nucleosome removal during spermatogenesis. Developmental cell, 18(3), pp.371–84.

Luger, K. et al., 1997. Crystal structure of the nucleosome core particle at 2.8 A resolution. Nature, 389(6648), pp.251–60.

Luikenhuis, S., Wutz, A. & Jaenisch, R., 2001. Antisense transcription through the Xist locus mediates Tsix function in embryonic stem cells. Molecular and cellular biology, 21(24), pp.8512–20.

Lyon, M.F., 1961. Gene action in the X-chromosome of the mouse (Mus musculus L.). Nature, 190, pp.372–3.

Magnúsdóttir, E. et al., 2013. A tripartite transcription factor network regulates primordial germ cell specification in mice. Nature cell biology, 15(8), pp.905–15.

Mahadevaiah, S.K. et al., 2008. Extensive meiotic asynapsis in mice antagonises meiotic silencing of unsynapsed chromatin and consequently disrupts meiotic sex chromosome inactivation. The Journal of cell biology, 182(2), pp.263–76.

Maison, C. et al., 2002. Higher-order structure in pericentric heterochromatin involves a distinct pattern of histone modification and an RNA component. Nature Genetics, 30(3), pp.329–334.

Maison, C. et al., 2011. SUMOylation promotes de novo targeting of HP1α to pericentric heterochromatin. Nature genetics, 43(3), pp.220–7.

Maison, C. et al., 2016. The methyltransferase Suv39h1 links the SUMO pathway to HP1α marking at pericentric heterochromatin. Nature communications, 7, p.12224.

Mak, W. et al., 2004. Reactivation of the paternal X chromosome in early mouse embryos. Science (New York, N.Y.), 303(5658), pp.666–9.

Mansour, A.A. et al., 2012. The H3K27 demethylase Utx regulates somatic and germ cell epigenetic reprogramming. Nature, 488(7411), pp.409–13.

Marahrens, Y. et al., 1997. Xist-deficient mice are defective in dosage compensation but not spermatogenesis. Genes & development, 11(2), pp.156–66.

Marcho, C., Cui, W. & Mager, J., 2015. Epigenetic dynamics during preimplantation development. Reproduction (Cambridge, England), 150(3), pp.R109-20.

Martens, J.H.A. et al., 2005. The profile of repeat-associated histone lysine methylation states in the mouse epigenome. The EMBO journal, 24(4), pp.800–12.

Martin, B.L. & Kimelman, D., 2010. Brachyury establishes the embryonic mesodermal progenitor niche. Genes & development, 24(24), pp.2778–83.

Martin, C. et al., 2006. Genome restructuring in mouse embryos during reprogramming and early development. Developmental biology, 292(2), pp.317–32.

Matsui, J., Goto, Y. & Takagi, N., 2001. Control of Xist expression for imprinted and random X chromosome inactivation in mice. Human molecular genetics, 10(13), pp.1393–401.

Mayer, W. et al., 2000. Demethylation of the zygotic paternal genome. Nature, 403(6769), pp.501–502.

Mayer, Robert, Alessandro Brero, Johann von Hase, Timm Schroeder, Thomas Cremer, Steffen Dietzel, M Schardin, et al. 2005. "Common Themes and Cell Type Specific Variations of Higher Order Chromatin Arrangements in the Mouse." BMC Cell Biology 6 (1). BioMed Central: 44. doi:10.1186/1471-2121-6-44.

McDowell, T.L. et al., 1999. Localization of a putative transcriptional regulator (ATRX) at pericentromeric heterochromatin and the short arms of acrocentric chromosomes. Proceedings of the National Academy of Sciences of the United States of America, 96(24), pp.13983–8.

McKinley, K.L. & Cheeseman, I.M., 2015. The molecular basis for centromere identity and function. Nature Reviews Molecular Cell Biology, 17(1), pp.16–29.

Merzouk, S. et al., 2014. Lineage-specific regulation of imprinted X inactivation in extraembryonic endoderm stem cells. Epigenetics & chromatin, 7, p.11.

Messerschmidt, D.M., 2016. A twist in zygotic reprogramming. Nature Cell Biology, 18(2), pp.139–140.

von Meyenn, F. et al., 2016. Impairment of DNA Methylation Maintenance Is the Main Cause of Global Demethylation in Naive Embryonic Stem Cells. Molecular cell, 62(6), p.983.

Minc, E., Courvalin, J.C. & Buendia, B., 2000. HP1gamma associates with euchromatin and heterochromatin in mammalian nuclei and chromosomes. Cytogenetics and cell genetics, 90(3–4), pp.279–84.

Molyneaux, K.A. et al., 2001. Time-lapse analysis of living mouse germ cell migration. Developmental biology, 240(2), pp.488–98.

Monesi, V., 1965. Differential rate of ribonucleic acid synthesis in the autosomes and sex chromosomes during male meiosis in the mouse. Chromosoma, 17(1).

Montellier, E. et al., 2013. Chromatin-to-nucleoprotamine transition is controlled by the histone H2B variant TH2B. Genes & development, 27(15), pp.1680–92.

Moreira de Mello, J.C. et al., 2010. Random X inactivation and extensive mosaicism in human placenta revealed by analysis of allele-specific gene expression along the X chromosome. PloS one, 5(6), p.e10947.

Motzkus, D., Singh, P.B. & Hoyer-Fender, S., 1999. M31, a murine homolog of Drosophila HP1, is concentrated in the XY body during spermatogenesis. Cytogenetic and Genome Research, 86(1), pp.83–88.

Mouse Genome Sequencing Consortium et al., 2002. Initial sequencing and comparative analysis of the mouse genome. Nature, 420(6915), pp.520–62.

Muchardt, C. et al., 2002. Coordinated methyl and RNA binding is required for heterochromatin localization of mammalian HP1alpha. EMBO reports, 3(10), pp.975–81.

Nakaki, F. et al., 2013. Induction of mouse germ-cell fate by transcription factors in vitro. Nature, 501(7466), pp.222–6.

Nakamura, T. et al., 2012. PGC7 binds histone H3K9me2 to protect against conversion of 5mC to 5hmC in early embryos. Nature, 486(7403), pp.415–9.

Namekawa, S.H. et al., 2006. Report Postmeiotic Sex Chromatin in the Male Germline of Mice. Current Biology, 16, pp.660–667.

Namekawa, S.H. et al., 2010. Two-step imprinted X inactivation: repeat versus genic silencing in the mouse. Molecular and cellular biology, 30(13), pp.3187–205.

Nesterova, T.B. et al., 2001. Loss of Xist imprinting in diploid parthenogenetic preimplantation embryos. Developmental biology, 235(2), pp.343–50.

Ng, J.-H. et al., 2013. In vivo epigenomic profiling of germ cells reveals germ cell molecular signatures. Developmental cell, 24(3), pp.324–33.

Ohinata, Y. et al., 2009. A signaling principle for the specification of the germ cell lineage in mice. Cell, 137(3), pp.571–84.

Ohinata, Y. et al., 2005. Blimp1 is a critical determinant of the germ cell lineage in mice. Nature, 436(7048), pp.207–13.

Ohno, S. & Hauschka, T.S., 1960. Allocycly of the X-chromosome in tumors and normal tissues. Cancer research, 20, pp.541–5.

Okamoto, I. et al., 2004. Epigenetic dynamics of imprinted X inactivation during early mouse development. Science (New York, N.Y.), 303(5658), pp.644–9.

Okamoto, I. et al., 2011. Eutherian mammals use diverse strategies to initiate X-chromosome inactivation during development. Nature, 472(7343), pp.370–4.

Okamoto, I. et al., 2005. Evidence for de novo imprinted X-chromosome inactivation independent of meiotic inactivation in mice. Nature, 438(7066), pp.369–73.

Okamoto, I., Tan, S. & Takagi, N., 2000. X-chromosome inactivation in XX androgenetic mouse embryos surviving implantation. Development (Cambridge, England), 127(19), pp.4137–45.

Ooi, S.K.T. et al., 2007. DNMT3L connects unmethylated lysine 4 of histone H3 to de novo methylation of DNA. Nature, 448(7154), pp.714–7.

Page, J. et al., 2012. Inactivation or non-reactivation: what accounts better for the silence of sex chromosomes during mammalian male meiosis? Chromosoma, 121(3), pp.307–26.

Palmer, D.K., O'Day, K. & Margolis, R.L., 1990. The centromere specific histone CENP-A is selectively retained in discrete foci in mammalian sperm nuclei. Chromosoma, 100(1), pp.32–36.

Patrat, C. et al., 2009. Dynamic changes in paternal X-chromosome activity during imprinted X-chromosome inactivation in mice. Proceedings of the National Academy of Sciences of the United States of America, 106(13), pp.5198–203.

Payer, B., 2016. Developmental regulation of X-chromosome inactivation. Seminars in cell & developmental biology, 56, pp.88–99.

Perry, J. et al., 2001. A short pseudoautosomal region in laboratory mice. Genome research, 11(11), pp.1826–32.

Peters, A.H.F.M. et al., 2001. Loss of the Suv39h Histone Methyltransferases Impairs Mammalian Heterochromatin and Genome Stability. Cell, 107(3), pp.323–337.

Peters, A.H.F.M. et al., 2003. Partitioning and plasticity of repressive histone methylation states in mammalian chromatin. Molecular cell, 12(6), pp.1577–89.

Petropoulos, S. et al., 2016. Single-Cell RNA-Seq Reveals Lineage and X Chromosome Dynamics in Human Preimplantation Embryos. Cell, 165(4), pp.1012–26.

Pinheiro, I. et al., 2012. Prdm3 and Prdm16 are H3K9me1 methyltransferases required for mammalian heterochromatin integrity. Cell, 150(5), pp.948–60.

Popp, C. et al., 2010. Genome-wide erasure of DNA methylation in mouse primordial germ cells is affected by AID deficiency. Nature, 463(7284), pp.1101–5.

Probst, A. V et al., 2010. A strand-specific burst in transcription of pericentric satellites is required for chromocenter formation and early mouse development. Developmental cell, 19(4), pp.625–38.

Puschendorf, M. et al., 2008. PRC1 and Suv39h specify parental asymmetry at constitutive heterochromatin in early mouse embryos. Nature genetics, 40(4), pp.411–20.

Quenneville, S. et al., 2011. In embryonic stem cells, ZFP57/KAP1 recognize a methylated hexanucleotide to affect chromatin and DNA methylation of imprinting control regions. Molecular cell, 44(3), pp.361–72.

Rathke, C. et al., 2014. Chromatin dynamics during spermiogenesis. Biochimica et biophysica acta, 1839(3), pp.155–68.

Richardson, B.E. & Lehmann, R., 2010. Mechanisms guiding primordial germ cell migration: strategies from different organisms. Nature reviews. Molecular cell biology, 11(1), pp.37–49.

Rizzi, N. et al., 2004. Transcriptional activation of a constitutive heterochromatic domain of the human genome in response to heat shock. Molecular biology of the cell, 15(2), pp.543–51.

Romeo, K. et al., 2015. The SENP7 SUMO-Protease Presents a Module of Two HP1 Interaction Motifs that Locks HP1 Protein at Pericentric Heterochromatin. Cell reports.

Rowe, H.M. et al., 2010. KAP1 controls endogenous retroviruses in embryonic stem cells. Nature, 463(7278), pp.237–40.

Royo, H. et al., 2013. ATR acts stage specifically to regulate multiple aspects of mammalian meiotic silencing. Genes & Development, 27(13), pp.1484–1494.

Royo, H., Stadler, M.B. & Peters, A.H.F.M., 2016. Alternative Computational Analysis Shows No Evidence for Nucleosome Enrichment at Repetitive Sequences in Mammalian Spermatozoa. Developmental cell, 37(1), pp.98–104.

Sachs, M. et al., 2013. Bivalent chromatin marks developmental regulatory genes in the mouse embryonic germline in vivo. Cell reports, 3(6), pp.1777–84.

Sado, T. et al., 2001. Regulation of imprinted X-chromosome inactivation in mice by Tsix. Development (Cambridge, England), 128(8), pp.1275–86.

Saitou, M. et al., 2016. Gametogenesis from Pluripotent Stem Cells. Cell Stem Cell, 18(6), pp.721–735.

Saitou, M. & Yamaji, M., 2012. Primordial germ cells in mice. Cold Spring Harbor perspectives in biology, 4(11), p.a008375.

Saksouk, N. et al., 2015. Constitutive heterochromatin formation and transcription in mammals. Epigenetics & Chromatin, 8(1), p.3.

Samans, B. et al., 2014. Uniformity of nucleosome preservation pattern in Mammalian sperm and its connection to repetitive DNA elements. Developmental cell, 30(1), pp.23–35.

Santenard, A. et al., 2010. Heterochromatin formation in the mouse embryo requires critical residues of the histone variant H3.3. Nature cell biology, 12(9), pp.853–62.

Santos, F. et al., 2002. Dynamic reprogramming of DNA methylation in the early mouse embryo. Developmental biology, 241(1), pp.172–82.

Santos, F. & Dean, W., 2004. Epigenetic reprogramming during early development in mammals. Reproduction (Cambridge, England), 127(6), pp.643–51.

Sarma K, Cifuentes-Rojas C, Ergun A, del Rosario A, Jeon Y, White F, Sadreyev R, Lee JT: ATRX Directs Binding of PRC2 to Xist RNA and Polycomb Targets. Cell 2014, 159:869–883.

Schotta, G. et al., 2008. A chromatin-wide transition to H4K20 monomethylation impairs genome integrity and programmed DNA rearrangements in the mouse. Genes & development, 22(15), pp.2048–61.

Schotta, G. et al., 2004. A silencing pathway to induce H3-K9 and H4-K20 trimethylation at constitutive heterochromatin. Genes & development, 18(11), pp.1251–62.

Seisenberger, S. et al., 2012. The dynamics of genome-wide DNA methylation reprogramming in mouse primordial germ cells. Molecular cell, 48(6), pp.849–62.

Seki, Y. et al., 2007. Cellular dynamics associated with the genome-wide epigenetic reprogramming in migrating primordial germ cells in mice. Development (Cambridge, England), 134(14), pp.2627–38.

Shen, L. et al., 2014. Tet3 and DNA Replication Mediate Demethylation of Both the Maternal and Paternal Genomes in Mouse Zygotes Cell Stem Cell Tet3 and DNA Replication Mediate Demethylation of Both the Maternal and Paternal Genomes in Mouse Zygotes. Cell Stem Cell, 15, pp.459–470.

Shin, J. et al., 2010. Maternal Rnf12/RLIM is required for imprinted X-chromosome inactivation in mice. Nature, 467(7318), pp.977–81.

Shumaker, D.K. et al., 2006. Mutant nuclear lamin A leads to progressive alterations of epigenetic control in premature aging. Proceedings of the National Academy of Sciences of the United States of America, 103(23), pp.8703–8.

Siklenka, K. et al., 2015. Disruption of histone methylation in developing sperm impairs offspring health transgenerationally. Science (New York, N.Y.), 350(6261), p.aab2006.

Sin, H.-S. & Namekawa, S.H., 2013. The great escape: Active genes on inactive sex chromosomes and their evolutionary implications. Epigenetics, 8(9), pp.887–92.

Skene, P.J. & Henikoff, S., 2013. Histone variants in pluripotency and disease. Development, 140(12).

Smothers, J.F. & Henikoff, S., 2000. The HP1 chromo shadow domain binds a consensus peptide pentamer. Current biology : CB, 10(1), pp.27–30.

Stavropoulos, N., Lu, N. & Lee, J.T., 2001. A functional role for Tsix transcription in blocking Xist RNA accumulation but not in X-chromosome choice. Proceedings of the National Academy of Sciences of the United States of America, 98(18), pp.10232–7.

Stein, P. et al., 1997. Stage-dependent redistributions of acetylated histones in nuclei of the early preimplantation mouse embryo. Molecular reproduction and development, 47(4), pp.421–9.

Sugimoto, M. & Abe, K., 2007. X chromosome reactivation initiates in nascent primordial germ cells in mice. PLoS genetics, 3(7), p.e116.

Sun, S. et al., 2015. Xist imprinting is promoted by the hemizygous (unpaired) state in the male germ line. Proceedings of the National Academy of Sciences of the United States of America, 112(47), pp.14415–22.

Surani, M.A., 2015. Human Germline: A New Research Frontier. Stem cell reports, 4(6), pp.955–60.

Tachibana, M. et al., 2012. X-chromosome inactivation in monkey embryos and pluripotent stem cells. Developmental biology, 371(2), pp.146–55.

Tada, T. et al., 2000. Imprint switching for non-random X-chromosome inactivation during mouse oocyte growth. Development (Cambridge, England), 127(14), pp.3101–5.

Takada, Y. et al., 2011. HP1γ links histone methylation marks to meiotic synapsis in mice. Development (Cambridge, England), 138(19), pp.4207–17.

Tam, P.P. & Snow, M.H., 1981. Proliferation and migration of primordial germ cells during compensatory growth in mouse embryos. Journal of embryology and experimental morphology, 64, pp.133–47.

Tam, P.P. & Zhou, S.X., 1996. The allocation of epiblast cells to ectodermal and germ-line lineages is influenced by the position of the cells in the gastrulating mouse embryo. Developmental biology, 178(1), pp.124–32.

Tanaka, A. et al., 2015. Fourteen babies born after round spermatid injection into human oocytes. Proceedings of the National Academy of Sciences of the United States of America, 112(47), pp.14629–34.

Tang, W.W.C. et al., 2015. A Unique Gene Regulatory Network Resets the Human Germline Epigenome for Development. Cell, 161(6), pp.1453–1467.

Tardat, M. et al., 2015. Cbx2 targets PRC1 to constitutive heterochromatin in mouse zygotes in a parent-of-origin-dependent manner. Molecular cell, 58(1), pp.157–71.

Terranova, R. et al., 2005. The reorganisation of constitutive heterochromatin in differentiating muscle requires HDAC activity. Experimental cell research, 310(2), pp.344–56.

Ting, D.T. et al., 2011. Aberrant overexpression of satellite repeats in pancreatic and other epithelial cancers. Science (New York, N.Y.), 331(6017), pp.593–6.

Torres-Padilla, M.-E. et al., 2006. Dynamic distribution of the replacement histone variant H3.3 in the mouse oocyte and preimplantation embryos. The International journal of developmental biology, 50(5), pp.455–61.

Trojer, P. & Reinberg, D., 2007. Facultative heterochromatin: is there a distinctive molecular signature? Molecular cell, 28(1), pp.1–13.

Turelli, P. et al., 2014. Interplay of TRIM28 and DNA methylation in controlling human endogenous retroelements. Genome research, 24(8), pp.1260–70.

Turner, J.M.A., 2015. Meiotic Silencing in Mammals. Annual review of genetics, 49, pp.395–412.

Turner, J.M.A. et al., 2006. Pachytene Asynapsis Drives Meiotic Sex Chromosome Inactivation and Leads to Substantial Postmeiotic Repression in Spermatids,

Turner, J.M.A. et al., 2004. Silencing of unsynapsed meiotic chromosomes in the mouse. Nature Genetics.

Turner, J.M.A. et al., 2005. Silencing of unsynapsed meiotic chromosomes in the mouse. Nature genetics, 37(1), pp.41–7.

Turner, J.M., Burgoyne, P.S. & Singh, P.B., 2001. M31 and macroH2A1.2 colocalise at the pseudoautosomal region during mouse meiosis. Journal of cell science, 114(Pt 18), pp.3367–75.

Vakoc, C.R. et al., 2005. Histone H3 lysine 9 methylation and HP1gamma are associated with transcription elongation through mammalian chromatin. Molecular cell, 19(3), pp.381–91.

Vincent, S.D. et al., 2005. The zinc finger transcriptional repressor Blimp1/Prdm1 is dispensable for early axis formation but is required for specification of primordial germ cells in the mouse. Development (Cambridge, England), 132(6), pp.1315–25.

Voon, H.P.J. et al., 2015. ATRX Plays a Key Role in Maintaining Silencing at Interstitial Heterochromatic Loci and Imprinted Genes. Cell reports, 11(3), pp.405–18.

Vourc'h, C. & Biamonti, G., 2011. Transcription of Satellite DNAs in Mammals. Progress in molecular and subcellular biology, 51, pp.95–118.

Wake, N., Takagi, N. & Sasaki, M., 1976. Non-random inactivation of X chromosome in the rat yolk sac. Nature, 262(5569), pp.580–1.

Wang, J. et al., 2001. Imprinted X inactivation maintained by a mouse Polycomb group gene. Nature Genetics, 28(4), pp.371–375.

Wang, X. et al., 2012. Random X inactivation in the mule and horse placenta. Genome research, 22(10), pp.1855–63.

Weber, S. et al., 2010. Critical function of

AP-2 gamma/TCFAP2C in mouse embryonic germ cell maintenance. Biology of reproduction, 82(1), pp.214–23.

van de Werken, C. et al., 2014. Paternal heterochromatin formation in human embryos is H3K9/HP1 directed and primed by sperm-derived histone modifications. Nature communications, 5, p.5868.

West, F.D. et al., 2010. KIT ligand and bone morphogenetic protein signaling enhances human embryonic stem cell to germ-like cell differentiation. Human reproduction (Oxford, England), 25(1), pp.168–78.

Wojtasz, L. et al., 2009. Mouse HORMAD1 and HORMAD2, two conserved meiotic chromosomal proteins, are depleted from synapsed chromosome axes with the help of TRIP13 AAA-ATPase. PLoS genetics, 5(10), p.e1000702.

Xue, F. et al., 2002. Aberrant patterns of X chromosome inactivation in bovine clones. Nature genetics, 31(2), pp.216–20.

Yamaguchi, S., Hong, K., et al., 2013. Dynamics of 5-methylcytosine and 5-hydroxymethylcytosine during germ cell reprogramming. Cell research, 23(3), pp.329–39.

Yamaguchi, S., Shen, L., et al., 2013. Role of Tet1 in erasure of genomic imprinting. Nature, 504(7480), pp.460–4.

Yamaji, M. et al., 2008. Critical function of Prdm14 for the establishment of the germ cell lineage in mice. Nature genetics, 40(8), pp.1016–22.

Ying, Y. et al., 2000. Requirement of Bmp8b for the generation of primordial germ cells in the mouse. Molecular endocrinology (Baltimore, Md.), 14(7), pp.1053–63.

Ying, Y. & Zhao, G.Q., 2001. Cooperation of endoderm-derived BMP2 and extraembryonic ectoderm-derived BMP4 in primordial germ cell generation in the mouse. Developmental biology, 232(2), pp.484–92.

Yu, Y.E. et al., 2000. Abnormal spermatogenesis and reduced fertility in transition nuclear protein 1-deficient mice. Proceedings of the National Academy of Sciences of the United States of America, 97(9), pp.4683–8.

Zhang, T., Cooper, S. & Brockdorff, N., 2015. The interplay of histone modifications - writers that read. EMBO reports, 16(11), pp.1467–81.

Zhao, M. et al., 2001. Targeted disruption of the transition protein 2 gene affects sperm chromatin structure and reduces fertility in mice. Molecular and cellular biology, 21(21), pp.7243–55.

Aim and scope of this thesis

During development, certain epigenetic signatures portray specific developmental processes. Each cell type in the body possesses a unique epigenome that will determine its proper gene expression and will ensure its specialized function. The field of epigenetics is continuously growing and with it our understanding that even environmental factors or nutrition can alter the epigenome of an individual. These potential epigenetic alterations may be then inherited from parent to future generations and lead to altered gene expression profiles.

In this thesis, I have focused on obtaining more insight onto epigenetic signatures and events that appear during early embryo development (pre- and post-implantation periods) or during differentiation of early embryo representatives (ESCs). By developing technical innovative approaches aimed at better detection of chromatin components and DNA, and at developing relevant models to study the molecular basis of XCI, I have aimed to contribute to insight in the regulation of PHC in primordial germ cells and in (imprinted) XCI in mouse and rat.

First, we have investigated the possible functional link between PSCR and iXCI in pre-implantation mouse female embryos using round spermatid injection (ROSI) into oocytes (**Chapter 2**). ROSI was used as a tool to investigate the possible impact of disturbance of the epigenome on early developmental processes, using iXCI as readout. ROSI technology has been shown to be able to generate several generations of mice, and it has been recently succesfully used in the clinic (Tanaka et al. 2015). Very little is known about possible epigenetic consequences of applying this technique, and our results warrant further research in that direction.

Another central point of this thesis concerns the epigenetic signature of PHC in early developing PGCs. Epigenetic reprogramming in PGCs has been mainly studied through immunofluorescence analysis. Interestingly, it has been reported that various histone modifications and readers, including those present on PHC, are transiently lost from E11.5 PGCs. They are then rapidly re-established one day later. This phenomenon resembles in some aspects the PHC signature of the paternal genome in the zygote. In **Chapter 3** we aimed to examine whether there is indeed a resemblance link between the PHC epigenetic signature of the paternal genome and of the developing PGCs. Taking into consideration that epitope availability can be compromised upon different conditions, we characterized in detail the epigenetic make up of PHC in developing PGCs using various preparation protocols.

In **Chapter 4** we aimed to characterize XCI in differentiating rat ESCs. In most XCI studies the mouse has been 'the model' species to study dosage compensation between males and females. Relevant studies in other rodent species were lacking. Despite the fact that different differentiation rat ESCs protocols are reported, these are not suitable to study XCI, since they make use of 2i inhibitors that block XCI from occuring. Therefore, we established a robust differentiation protocol in the absence of 2i inhibitors, to recapitulate and study the epigenetic phenomena accompanying XCI in the rat model. In addition, we aimed to unravel if the function of important XCI players is conserved between rodents.

Lastly, the establishment of robust and reproducible procedures is of great importance for both scientific and diagnostic purposes. Commonly, the detection of both RNA and DNA molecules in the same sample is laborious, long and technically challenging and many times the current procedures compromise the quality of the sample. Therefore in **Chapter 5**, we sought to establish a protocol for rapid, simultaneous and combined detection of RNA-DNA FISH signals in pre-implantation embryos.

In **Chapter 6** I discuss the findings presented in the research chapters and I provide insight on future experiments that may be pivotal in expanding our knowledge on these specific topics.

Chapter 2

ROUND SPERMATID INJECTION RESCUES LETHALITY OF A PATERNALLY INHERITED *XIST* DELETION IN MOUSE

Federica Federici[1#], **Aristea Magaraki[1#]**, Evelyne Wassenaar[1], Catherina JH van Veen-Buurman[2], Christine van de Werken[2], Esther B Baart[2], Joop SE Laven[2], J Anton Grootegoed[1], Joost Gribnau[1] and Willy M Baarends[1*]

Published in PLoS Genet
12:e1006358 (2016)

ROUND SPERMATID INJECTION RESCUES FEMALE LETHALITY OF A PATERNALLY INHERITED *XIST* DELETION IN MOUSE

Federica Federici[1#], Aristea Magaraki[1#], Evelyne Wassenaar[1], Catherina JH van Veen-Buurman[2], Christine van de Werken[2], Esther B Baart[2], Joop SE Laven[2], J Anton Grootegoed[1], Joost Gribnau[1] and Willy M Baarends[1*]

Author Affiliations:

[1]Department of Developmental Biology, Erasmus MC, University Medical Center, Rotterdam, The Netherlands

[2]Department of Obstetrics and Gynaecology, Erasmus MC, University Medical Center, Rotterdam, The Netherlands

[#]Both authors contributed equally to this work

[*]Corresponding author:
Dr. Willy M. Baarends
e-mail: w.baarends@erasmusmc.nl

Short title: Round spermatid injection rescues XpΔ*Xist* females

Abstract

In mouse female preimplantation embryos, the paternal X chromosome (Xp) is silenced by imprinted X chromosome inactivation (iXCI). This requires production of the noncoding *Xist* RNA in *cis*, from the Xp. The *Xist* locus on the maternally inherited X chromosome (Xm) is refractory to activation due to the presence of an imprint. Paternal inheritance of an *Xist* deletion (XpΔ*Xist*) is embryonic lethal to female embryos, due to iXCI abolishment. Here, we circumvented the histone-to-protamine and protamine-to-histone transitions of the paternal genome, by fertilization of oocytes via injection of round spermatids (ROSI). This did not affect initiation of XCI in wild type female embryos. Surprisingly, ROSI using Δ*Xist* round spermatids allowed survival of female embryos. This was accompanied by activation of the intact maternal *Xist* gene, initiated with delayed kinetics, around the morula stage, resulting in Xm silencing. Maternal *Xist* gene activation was not observed in ROSI-derived males. In addition, no *Xist* expression was detected in male and female morulas that developed from oocytes fertilized with mature Δ*Xist* sperm. Finally, the expression of the X-encoded XCI-activator RNF12 was enhanced in both male (wild type) and female (wild type as well as XpΔ*Xist*) ROSI derived embryos, compared to *in vivo* fertilized embryos. Thus, high RNF12 levels may contribute to the specific activation of maternal *Xist* in XpΔ*Xist* female ROSI embryos, but upregulation of additional Xp derived factors and/or the specific epigenetic constitution of the round spermatid-derived Xp are expected to be more critical. These results illustrate the profound impact of a dysregulated paternal epigenome on embryo development, and we propose that mouse ROSI can be used as a model to study the effects of intergenerational inheritance of epigenetic marks.

Author Summary

In sexual reproduction, maternal and paternal haploid sets of DNA are combined in one new diploid individual. However, not only DNA, but also epigenetic information, defined by DNA and histone modifications, is transferred to the zygote. Specific inactivation of the paternally inherited X chromosome (Xp) in the preimplantation female mouse embryo is required for embryo survival. This imprinted X chromosome inactivation (iXCI) is initiated by transcription of the *Xist* gene from Xp. In contrast, the maternal *Xist* gene is imprinted during oogenesis to remain silent. We have investigated the consequences of elimination of the histone-to-protamine and protamine-to-histone transitions on iXCI, by fertilization through injection of immature round spermatids into oocytes (ROSI). Interestingly, when the round spermatids used for ROSI carried an X chromosome with an *Xist* deletion (Δ*Xist*), we found that the *Xist* gene on the maternal X chromosome was activated, which rescued the female lethality of embryos that is invariably observed upon fertilization with mature Δ*Xist* spermatozoa. This striking result is best explained by deregulation of embryonic gene expression, in particular from Xp, when the paternal genome originates from round spermatids rather than spermatozoa. From this, we suggest that the use of round spermatids has unforeseen consequences for embryonic gene expression and its use in human assisted reproduction must be carefully considered.

Introduction

In mammals, as in all diploid organisms with a sexual reproduction cycle, the diploid zygote is formed upon fertilization by combination of the haploid maternal and paternal genomes. Sperm and egg each contribute a complete set of chromosomes, and in addition the gametes carry sex-specific epigenetic information that is important for correct execution of the early developmental gene expression program. A striking epigenetic difference between the paternal and maternal epigenomes is caused by the fact that the paternal chromatin undergoes two rounds of complete remodelling in the reproductive cycle. First, during the final post-meiotic phase of spermatogenesis, in elongating and condensing spermatids, the vast majority of histones is replaced by protamines, generating the compact sperm nucleus. Second, immediately following fertilization, the protamines are replaced by maternal histones. The maternally provided histones H3 and H4 on the paternal pronucleus are devoid of lysine di- and tri-methylation marks, which leads to clear global differences in heterochromatin organization between the paternal and maternal genomes that are maintained up to the 8-cell stage (Puschendorf et al. 2008; van der Heijden GW et al. 2005). In addition to a haploid set of autosomes, a spermatozoon contributes either an X or a Y chromosome to the zygote. The sex chromosomes are more drastically remodelled than the autosomes during spermatogenesis, because the heterologous X and Y chromosomes undergo meiotic sex chromosome inactivation (MSCI) in spermatocytes (reviewed by Turner 2007), which is associated with chromosome wide nucleosome exchange (van der Heijden et al. 2007). After meiosis, silencing of X- and Y-linked genes is largely maintained during spermatid differentiation through post-meiotic sex chromatin repression (PSCR) (Namekawa et al. 2006). Noteworthy, a number of X- and Y-linked genes, single and multi-copy, escape PSCR and become specifically reactivated (Namekawa et al. 2006; Mulugeta Achame et al. 2010; Hendriksen et al. 1995) until the global transcriptional silencing that accompanies the histone-to-protamine transition sets in, in condensing spermatids. Subsequently, after fertilization, the X chromosome of paternal origin (Xp) will always be inactivated in female pre-implantation embryos and this is maintained in the extra-embryonic tissues of post-implantation embryos. This imprinted X chromosome inactivation (iXCI) depends on expression and spreading *in cis* of the *Xist* noncoding RNA on the Xp (Okamoto et al. 2004). X-encoded RNF12 is a known and important XCI trans activator, acting through a dose-dependent mechanism in the activation of *Xist* transcription (Shin et al. 2010; Jonkers et al. 2009; Gontan et al. 2012). Maternal expression of RNF12 has been shown to be essential for iXCI, whereas deletion of the paternal copy is compatible with normal female embryo development and establishment if iXC (Shin et al. 2010). Thus, the inactive state established on the Xp by MSCI and PSCR in spermatogenesis is not directly transmitted to female pre-implantation embryos but has to be re-established. However, whether the epigenetic events associated with the presence of unsynapsed chromatin are involved in establishing a paternal imprint at the Xic is not fully clear. In one study, expression of the *Xist* transgene was observed in preimplantation embryos only when the transgene was inherited from the father, independently of hemi- or homozygosity, indicating that imprinting was normally established on the single copy *Xist* transgene (Okamoto et al. 2005). However, in a more recent study, correct imprinted expression was observed only when transgenic inserted *Xist* was transmitted from a hemizygous father (Sun et al. 2015). Here the transgene was present in multiple copies. Irrespective of the mechanistic background of the paternal Xic imprint, it is clear that paternal X-linked genes are transcriptionally active at the 2-cell stage and are then gradually inactivated de novo via *Xist* RNA-dependent silencing (Okamoto et al. 2005; Q. Deng et al. 2014). During iXCI *Xist* RNA spreading on the Xp triggers the recruitment of chromatin-modifying protein complexes, which in turn will establish repressive epigenetic marks on the Xp, rendering it transcriptionally inactive. At the blastocyst stage, while iXCI is stably maintained in extra-embryonic tissues, the Xp becomes reactivated in the epiblast followed by random XCI without a parent-of-origin bias (Mak et al. 2004). Paternal inheritance of a *Xist* deletion (Δ*Xist*) completely abolishes iXCI of the Xp (Marahrens et al. 1997), arrests development around E6.5, and results in reabsorption of mutant female embryos by E12.5 (Mugford et al. 2012). The strong bias towards Xp inactivation in iXCI is favoured by the presence of an imprinting mark on the X chromosome of maternal origin (Xm) that prevents it from expressing *Xist* (Tada et al. 2000; Fukuda et al. 2014). In addition, Xp may also be imprinted to become preferentially inactivated, as might be inferred from the recently reported effects from the pairing status of an *Xist* transgene during male meiotic prophase (Sun et al. 2015), although the nature of such an imprint remains elusive. It has been proposed that iXCI occurs as a two-step process (Namekawa et al. 2010). First, pre-inactivated intergenic repeat regions on the Xp may carry transgenerational epigenetic information from the paternal germline to the zygote, predisposing the Xp for iXCI independently of *Xist* (Namekawa et al. 2010). This might rely on the inheritance of sperm-derived nucleosomes and their associated modifications. Second, subsequent establishment of genic silencing strictly depends on *Xist* expression from the paternal allele (Namekawa et al. 2010). Alternatively, it has been suggested that the preferential inactivation of Xp may simply rely on early and robust activation of the paternal *Xist* gene (Heard et al. 2004). This may be facilitated, upon fertilization, by the protamine-to-histone transition, during which the protamine-based chromatin of the sperm acquires newly deposited histones lacking most heterochromatic marks. The transcriptionally permissive chromatin signature deposited on the haploid genome in the paternal pronucleus would then allow *Xist* expression from the paternal allele. Conclusive evidence for the contribution of the protamine-to-histone transition in the initiation of iXCI is lacking.

To test if the chromatin rearrangement in spermatids impacts on iXCI, we made use of mouse round spermatids to fertilize oocytes. When a round spermatid is injected into a mouse oocyte (ROSI), the paternal genome has a histone-based chromatin constitution, contrary to the protamine-packaged chromatin of spermatozoa. Hence, ROSI evades the protamine-to-histone replacement in the male pronucleus, but rather provides for a paternal genome with a spermatogenic histone-based chromatin composition. Here, by using ROSI as an experimental tool, and a method to visualize individual chromosomes in fixed early embryos, we could establish that the chromatin constitution of the X chromosome in round spermatids is maintained in ROSI-derived zygotes. Next, we observed that absence of genome wide paternal chromatin remodelling did not affect the timing of *Xist* expression in ROSI-derived female zygotes, on a wild type background. We then asked if the transcriptionally repressed state and the heterochromatin marks present on the X chromosome of round spermatids, because of MSCI and PSCR, might be sufficient to establish iXCI independently of *Xist*-mediated silencing. This was tested using round spermatids from male mice lacking a functional *Xist* gene (XpΔ*Xist*) for ROSI. Here, we would expect rescue of the early embryonic lethality of XpΔ*Xist* female embryos through maintenance of MSCI- and PSCR-mediated inactivation of Xp, which is *Xist*-independent. Our results showed that injection of XpΔ*Xist* round spermatids indeed prevents the female lethality, that is always observed upon fertilization with mature XpΔ*Xist* spermatozoa. Surprisingly, this rescue occurred through inactivation of the Xm and not by *Xist*-independent Xp silencing. In addition, we observed high levels of the XCI activator RNF12, in all ROSI derived embryos, independent of sex and genotype. These findings are discussed in the context of our current views on iXCI, and possible implications for transfer of dysregulated paternal epigenetic information to the embryo are described in relation to the clinical application of assisted reproductive technology.

Results and Discussion

Histones and associated epigenetic modifications are transmitted from round spermatids to ROSI-derived zygotes

To analyze the histone modification patterns of round spermatid-derived paternal chromatin in early embryos, and in particular the epigenetic profile of the Xp, we arrested ROSI-derived mouse embryos at the pro-metaphase stage of the first or second cleavage divisions (Avo Santos et al. 2011). This allows the visualization of epigenetic marks on individual chromosomes. As a control for staining specificity, zygotes obtained by intracytoplasmic sperm injection (ICSI), using epididymal spermatozoa, were subjected to the same experimental procedure.

Following the histone-to-protamine transition in spermatids, mouse epididymal spermatozoa contain approximately 1% of residual histones (Balhorn et al. 1977; van der Heijden et al. 2006). After sperm decondensation by heparin treatment and immunostaining for histone H3.1/2 and centromeres (with anti-centromere antibody, ACA), limited histone retention associated with pericentromeric regions was visible (Figure 1A, left panel), as previously shown (van der Heijden et al. 2006). After fertilization, when the protamine-to-histone transition has taken place, we did not detect any H3K9me3 at paternal prometaphase chromosomes of ICSI-derived zygotes (Figure 1A, right panel), while prometaphase chromosomes of maternal origin were strongly enriched for H3K9me3 at pericentromeric regions and displayed moderate H3K9me3 levels along the chromosome arms. These results are in accordance with results from previous studies on *in vivo* fertilized embryos, that showed epigenetic asymmetry between maternally and paternally inherited chromatin up to the third cleavage division (Puschendorf et al. 2008; van der Heijden et al. 2005; Arney et al. 2002; Santos et al. 2005).

In round spermatids, the X and Y chromosomes, as well as the constitutive pericentric heterochromatin clustered in the chromocenter, are enriched for H3K9me3 (Figure 1B, left panel), in accordance with previously published data (van der Heijden et al. 2007). In ROSI-derived zygotes at the first cleavage division, we detected persistence of H3K9me3 at the DAPI-dense heterochromatic chromosome ends of paternal origin and on the entire Xp (Figure 1B, right panel). This epigenetic profile mirrors the H3K9me3 pattern observed in round spermatids. ROSI-derived 2-cell stage female embryos that were arrested at the pro-metaphase of the second cleavage division displayed maintenance of a high enrichment for H3K9me3 in particular on one of the two X chromosomes (Figureure 1C), as confirmed by *Xist* DNA FISH (note that some residual H3K9me3 signal generates background staining after the FISH procedure Figureure 1C, right panel and enlargements). One blastomere (the lower one, in Figure 1C) showed DNA FISH staining also on the Xm, confirming that the embryo was indeed female.

The present results are in agreement with previous observations, that a substantial fraction of modified histones present in round spermatid chromatin is maintained in early pre-implantation embryos generated by ROSI (Kishigami et al. 2006). Here, we show that this concerns in particular the X chromosome, where the H3K9me3 chromatin signature covers the entire chromosome.

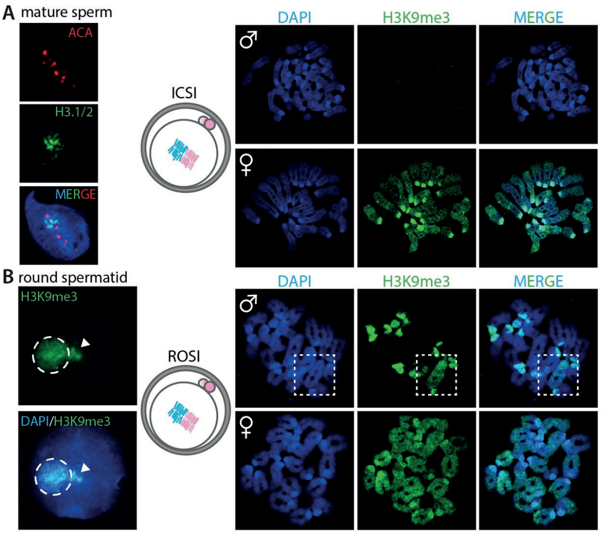

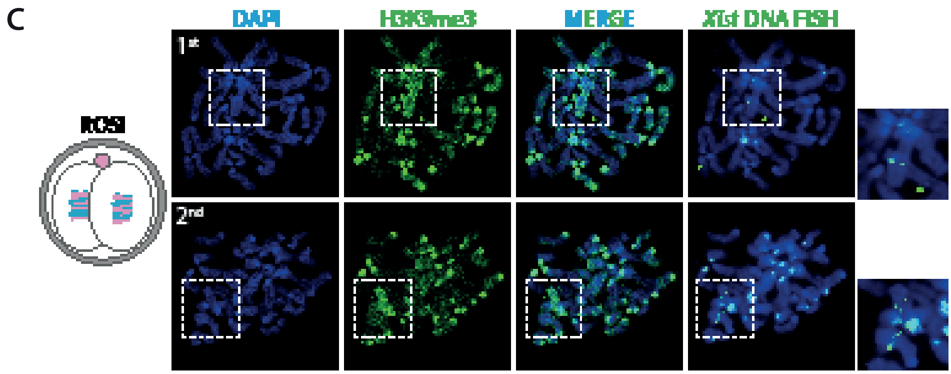

Figure 1: Chromatin remodeling in ROSI-derived embryos

A Left panel: Representative image of a decondensed nucleus of a mature mouse spermatozoon stained with H3.1/2 (green) and anti-centromere antibody (ACA) (red), to illustrate the limited presence of histones in association with pericentromeric chromatin in mature mouse sperm, as shown previously by others (van der Heijden et al. 2006). Right panels: Representative image of immunolocalization of H3K9me3 (green) in chromosome spreads of prometaphase-arrested mouse zygotes obtained by ICSI (as represented by the drawing, n=3 zygotes). The condensed chromosomes of paternal and maternal origin are cutouts from the whole zygote images (paternal chromosome set on top; maternal below). DNA is counterstained with DAPI (blue). **B** Left panel: Representative image of a nucleus of a mouse round spermatid immunostained for H3K9me3 (green), to illustrate the enrichment of H3K9me3 on the chomocenter (encircled) and adjacent sex chromosome (arrowhead) as described previously (van der Heijden et al. 2007). Right panels: Representative image of immunolocalization of H3K9me3 (green) in chromosome spreads of prometaphase-arrested zygotes obtained by ROSI (as represented by the drawing, n=20 zygotes). The condensed chromosomes of paternal and maternal origin are cutouts from the whole zygote images (paternal chromosome set on top; maternal below). The X chromosome is indicated by a white dashed square box, whose identity is inferred from the known enrichment of the round spermatid X chromosome for this marker (Nakamekawa et al. 2006). **C** Representative image of immunofluorescence analysis for H3K9me3 (green) on chromosome spreads of a representative prometaphase-arrested 2-cell stage embryo obtained by ROSI (as indicated by the drawing on the left, n=2). Each blastomere from the same embryo is cutout into separate images (1st blastomere on top; 2nd blastomere below). The X chromosome is indicated by a white dashed square box. *Xist* DNA FISH (left panel) was performed on the same chromosome spreads represented on the left. Square boxes on the right are blowups of each corresponding boxed area containing one X chromosome (1st blastomere, one X is not visible) or two X chromosomes (2nd blastomere).

Normal establishment of iXCI in ROSI-derived female zygotes

We then aimed to investigate if absent or limited remodeling of paternal chromatin in ROSI-derived female zygotes, and the heterochromatic epigenetic signature of the X chromosome specifically, might affect the timing of *Xist* expression and interfere with iXCI establishment. In ROSI-derived female embryos, *Xist* expression started normally at the 4-cell stage (Figure 2A), when clear *Xist* RNA FISH clouds are already visible, and these are further enhanced at the 8-cell stage (Figure 2B), similarly to what has been described for *in vivo* fertilized control embryos (Okamoto & Heard 2006). We cannot discriminate between the two parental X chromosomes in this experiment, but since we never observed *Xist* clouds,nor *Xist* mRNA expression above background in male wild type ROSI-derived morulas (see below), and since the timing of *Xist* expression is normal, we infer that it is the Xp that is inactivated. Thus, the data suggest that the protamine-to-histone transition does not play a major role in the activation of the paternal *Xist* gene. In addition, the enrichment of H3K9me3 along the X chromosome does not appear to interfere with *Xist* transcription. It therefore seems more likely that another type of imprint, or a different mechanism, controls preferential *Xist* expression from Xp.

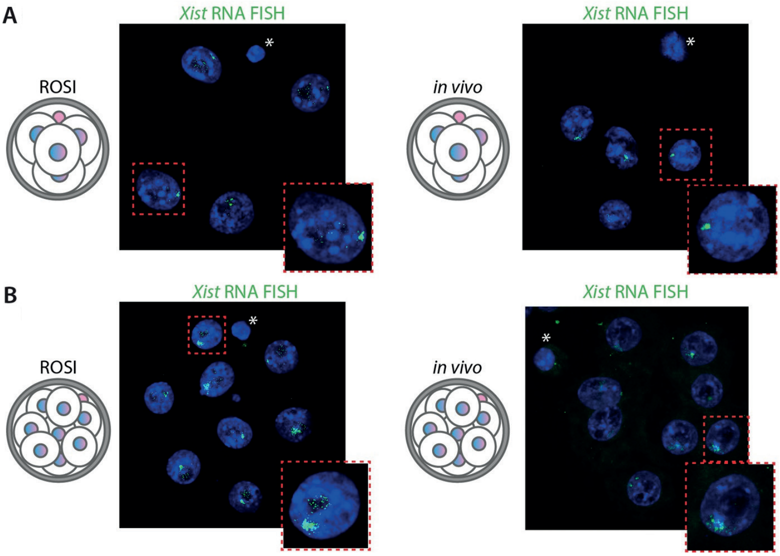

Figure 2: *Xist* expression in ROSI-derived embryos

A Representative images of *Xist* RNA FISH on a ROSI-derived 4-cell stage embryo on the left (n=5 ROSI embryos), and a 4-cell stage embryo derived by *in vivo* fertilization (n=4). Dashed red square boxes are blowups of each corresponding boxed area. **B** Representative image of *Xist* RNA FISH on a ROSI-derived 8-cell stage embryo on the left (n= 5 ROSI embryos), and an 8-cell stage embryo derived by *in vivo* fertilization. Dashed red square boxes are blowups of each corresponding boxed area.

Transmission of XpΔ*Xist* through round spermatids rescues female embryonic lethality

Female embryos inheriting an *Xist* deletion on the Xp can no longer be recovered by E12, because lack of imprinted inactivation of the Xp leads to embryonic lethality (Marahrens et al. 1997). We tested if transmission of an Xp carrying the *Xist* deletion through ROSI, instead of fertilization with mature sperm, might rescue the embryonic lethal phenotype. This experiment was based on the hypothesis that inheritance of an Xp that carries the transcriptionally silenced PSCR heterochromatic signature, might provide sufficient dosage compensation of X-linked genes in the absence of *Xist*, and thereby would allow female embryo survival. We performed ROSI with XpΔ*Xist* round spermatids from the C57BL/6 Δ*Xist* mouse line generated by Csankovszki et al. (1999). We also performed ICSI with XpΔ*Xist* mature sperm from the C57BL/6 mouse line. At E15, we obtained 17 pups after ROSI and 11 after ICSI (Table 1). This was approximately 10% of the number of 2-cell stage embryos that were transferred to pseudopregnant females, and 25% of the counted implantations, for both techniques. The sex of the embryos was determined by visual inspection of the isolated gonads and confirmed by genotyping PCR for all females and most males (Supplemental Figure S1A and S1B). The ICSI experiments yielded only males, as expected. In contrast, 5 out of the 17 E15 embryos generated by ROSI were female ($p<0.05$, chi square test). All male and female surviving embryos appeared normal in size and appearance and there was no overt difference between ICSI versus ROSI embryos, or between males and females. Interestingly, female embryos could not be generated when using XpΔ*Xist* spermatids from M. musculus castaneus (CAST/EiJ) males (Table 1, male sex assessed by the presence of testes). Male fertility parameters of CAST/EiJ mice differ significantly from those of C57BL/6 mice (Odet et al. 2015). Although CAST/EiJ males are normally fertile, this result indicates that there may be critical differences in gene expression between the two subspecies. At present we cannot point to any specific causal difference that would explain our failure to rescue on this background. For all our subsequent experiments we continued with C57BL/6 spermatids.

Table 1

	ICSI C57BL/6 (E15)	**ROSI C57BL/6 (E15)**	**ROSI C57BL/6 (P0)**	**ROSI CAST/EiJ (E15)**
# of independent experiments	4	4	2	3
# of 2-cell embryos transferred	104	163	64	156
# of pups	11	17	7	12
# of XY Males	11 (2,3,1,5)	12 (1,5,1,5)	5 (2,3)	12 (2,5,5)
# of XX Females	0	4 (0,1,1,2)	2 (0,2)	0
# of XO Females	0	1(1,0,0,0)	0	0

#; number, numbers in brackets indicates number of animals in each experiment

We genotyped all ROSI-derived female embryos, and found both a wild type *Xist* allele and a deleted *Xist* allele in embryonic and extraembryonic tissues of four of the female embryos, while one embryo was an XO female which had lost the mutated paternal X chromosome (Figure 3A). Next, we analysed the X chromosome to autosome ratio (X:A) for all embryos using quantitative PCR on genomic DNA, and observed the expected 1:1 ratio for the four XX embryos, and their placentas and isolated gonads (Figure 3B).

We then verified if ROSI-derived XpΔ*Xist* female embryos might develop to term. To this end, we collected pups in the morning after birth (P0). We obtained 7 live born pups (10% survival of 2-cell embryos that were transferred, Table 1), of which 5 were males and 2 were females. Sex was confirmed by PCR for *UbeX* and *UbeY* (Supplemental Figure S1C). The two XpΔ*Xist* females were comparable in size and body weight to the male wild type siblings (Figure 3C). Genotyping for the mutated and wild type *Xist* allele confirmed heterozygosity of these females (Figure 3C). Our recovery of embryos following ICSI or ROSI is relatively low, compared to previously published data (Yamauchi et al. 2015). Part of the low recovery yield from the ICSI can be explained by the lethality of females due to the paternal *Xist* deletion. For the ROSI experiments, the rescue that we observe appears to be only partial. This is based on a comparison between the male to female sex ratio of 2.83 observed when XpΔ*Xist* ROSI embryos and pups are taken together (n=23), and published sex ratios observed in 12 different published mouse ROSI experiments, involving comparable numbers of mice per experiment, whereby a mean male:female sex ratio of 0.93 ±0.48 was observed, with a maximum observed sex ratio of 2.33 (Supplemental Table S1).

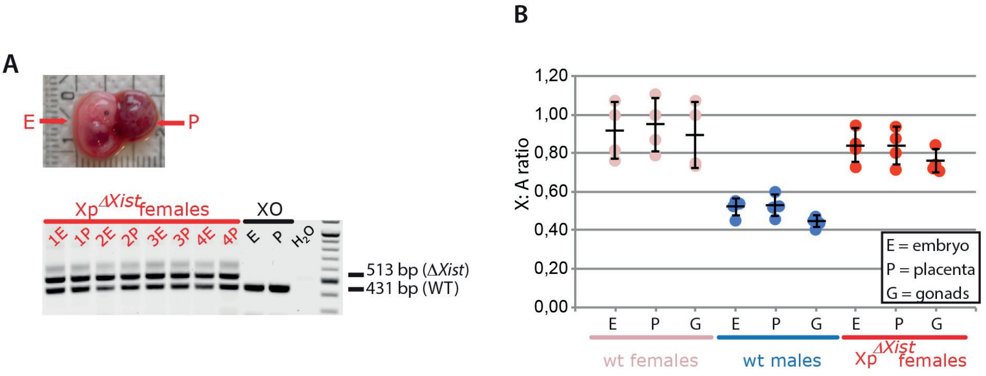

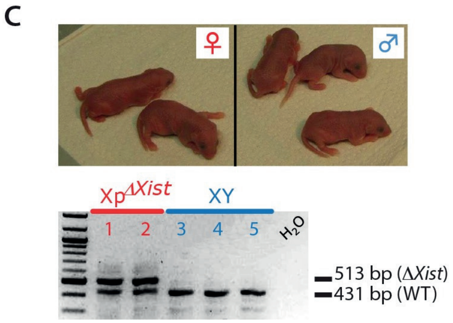

Figure 3: ROSI rescues female-specific lethality of a paternally inherited Xist deletion (XpΔ*Xist*)

A Representative E15 XpΔ*Xist* ROSI-derived female embryo (E) and attached placenta (P). Genotypes on DNA isolated from embryo and placenta of 4 ROSI-derived XpΔ*Xist* E15 female embryos and the single ROSI-derived XO embryo are shown on the right. Genotype was determined by the presence of a PCR product for the wt *Xist* allele (431bp band) and deleted allele (513 bp band). Water negative control and 100 bp marker were also loaded. **B** Bar graph showing X:A ratios determined for different tissues in E15 embryos as indicated below the X-axis. To determine the X:A ratios, qPCR on genomic DNA isolated from E15 embryos, placentas and gonads was performed for *Xist* (chromosome X) and Rex1 (chromosome 8). Results for each gene in each tissue were normalized to the values obtained in one reference wild type female. The X:A ratio was then determined for each individual tissue in 4 wild type females, 4 wild type males and in the 4 XpΔ*Xist* ROSI-derived female embryos. Results for each individual tissue are shown as dots, the average values (black horizontal line) and standard deviations (error bars) are also indicated. **C** Image of 5 newborn pups with normal appearance derived with ROSI using XpΔ*Xist* round spermatids (2 females on the left and 3 males on the right). Genotypes for the wt and deleted *Xist* alleles are shown below. As expected, both females were heterozygotes, while the males only had the wt *Xist* allele inherited from the mother.

ROSI with XpΔ*Xist* allows initiation of XCI on the maternal X chromosome

The unexpected survival of XpΔ*Xist* female embryos might be explained by maintenance of the PSCR state of the round spermatid-derived Xp, as we initially hypothesized. However, it cannot be excluded that survival of the embryos might be explained by inactivation of the wild type Xm, replacing iXCI of the mutant Xp. In order to distinguish between these different possibilities, we analyzed *Xist* expression levels by qPCR in three E15 control male and female placentas and in the ROSI-derived XpΔ*Xist* female placentas for which RNA samples were available. As expected, male placentas showed very low *Xist* expression, which most probably reflects expression from a very small number of maternal cells through decidua contamination (Figure 4A). Conversely, *Xist* expression was very high in wild type female placentas, in accordance with maintenance of stable iXCI of the Xp in this tissue, as is required for proper extraembyonic tissue development. Surprisingly, *Xist* RNA levels of ROSI-derived XpΔ*Xist* female placentas were comparable to those of wild type female placentas (Figure 4A). Since the paternal *Xist* allele was deleted, this expression is expected to be explained by robust transcription occurring from the wild type Xm. To investigate this further, we first checked *Xist* expression by RNA FISH on E15 placenta sections obtained from ROSI-derived XpΔ*Xist* female embryos (Figure 4B). By using the Reichert's membrane as reference for the embryonic side of the placenta, we verified that *Xist* RNA clouds were formed in the whole population of labyrinth cells of embryonic origin. Next, we performed a combined DNA/RNA FISH experiment, using two different probes; one recognizing both the wild type and mutant X chromosome, and the other recognizing only the wild type X chromosome. The results show that most cells display an *Xist* RNA cloud signal with both probes on the maternal wild type X, and that *Xist* RNA clouds are never observed on the paternal Δ*Xist* X chromosome (Figure 4C). Together, these results indicate that a switch from Xp inactivation to Xm inactivation has occurred in the XpΔ*Xist* female embryos that were obtained by ROSI. This is consistent with previous data showing that *Xist* mRNA is retained by the Xi of its origin (Jonkers et al. 2008).

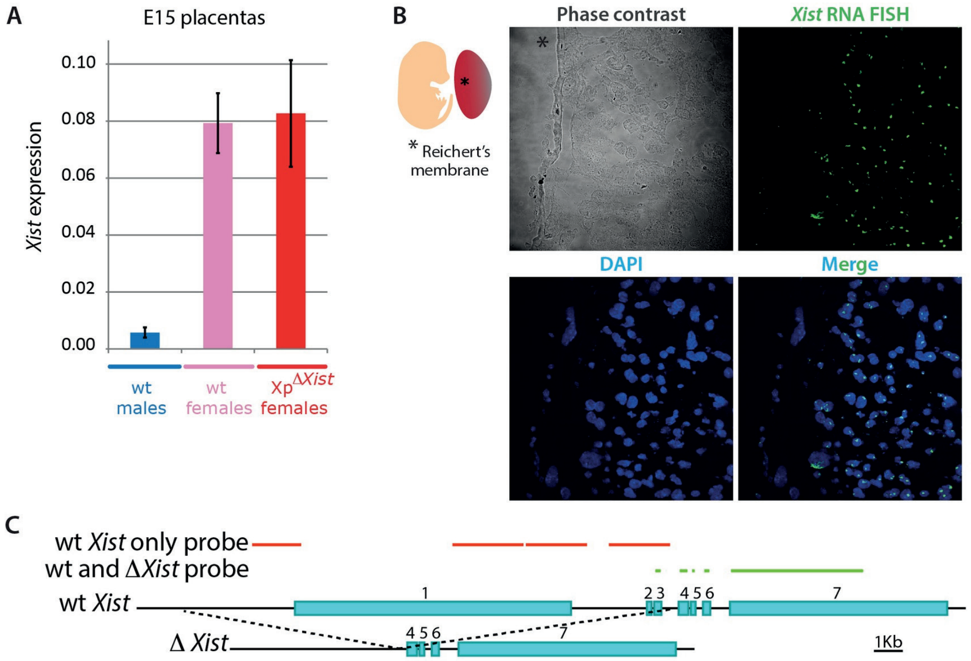

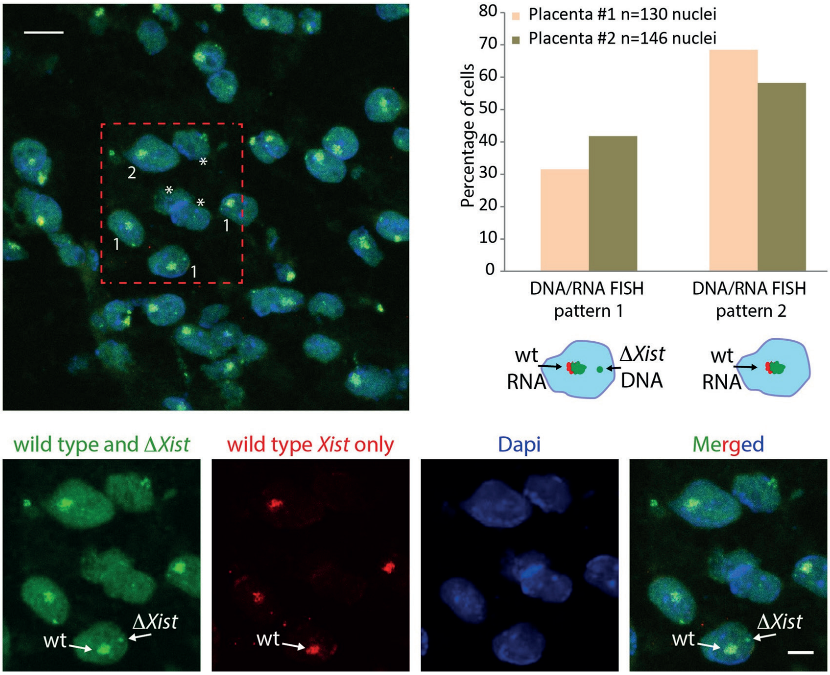

Figure 4: Δ*Xist* female survival is mediated by a shift to inactivation of the maternal X (Xm)
A Average *Xist* gene expression levels ± s.d. on RNA isolated from E15 placentas of 3 control males (light blue bars), 3 control females (pink bars) and 3 ROSI-derived XpΔ*Xist* females (red bars). The data were normalized to actin. **B** Representative image of the *Xist* RNA FISH (in green) on cryosections from a E15 ROSI-derived XpΔ*Xist* female placenta (n=2). From the phase contrast image on top (right), the Reichert's membrane on the embryonic side of the placenta can be visualized (marked by asterisk). DNA is counter-stained with DAPI. **C** Top: Schematic drawing of the RNA/DNA FISH probes used to detect the wild type (wt) *Xist* and the Δ*Xist* gene and/or RNA. Exon numbers are indicated. The green probe localizes to sequences present in both the wild type *Xist* and Δ*Xist* gene, whereas the red probe localizes to sequences that are only present in the wild type *Xist* gene (for further details see the Materials and Methods section). Left: representative merged image of the *Xist* RNA/DNA FISH using a probe recognizing the RNA produced by the wild type maternal allele and the DNA of both wild type *Xist* (signal is hidden under *Xist* RNA FISH cloud) and Δ*Xist* alleles (green), and a probe recognizing only the DNA of the wild type *Xist* allele (hidden under *Xist* RNA FISH cloud) and RNA produced by the wild type maternal X chromosome (red) on cryosections from a E15 ROSI-derived XpΔ*Xist* female placenta (n=2). DNA (Dapi) is shown in blue. Examples of nuclei are shown with an RNA FISH cloud signal with both probes, and a separate DNA FISH pinpoint in green (type 1), or with only an RNA FISH cloud signal with both probes (type 2). Cells lacking a cloud (some nuclear sections may not include the Xi) or with complicated staining patterns (due to the presence of polyploid cells, as was documented previously (Hu & Cross 2010) were not counted. Examples of such nuclei are indicated by asterisks. Scale bar represents 10 µm. Separate images of the nuclei in the boxed area are shown below, and the wild type and mutant chromosome are indicated with arrows for one nucleus. Scale bar represents 5 µm. Right: Quantification of type 1 and type 2 nuclei in two E15 ROSI-derived XpΔ*Xist* female placentas. Cells with a single green/red RNA FISH cloud and a separate red DNA FISH pinpoint were never observed.

Next, *Xist* mRNA expression was quantified through qRT-PCR on RNA isolated from morulas from normal fertilization with wild type and XpΔ*Xist* males, and from morulas generated by ROSI with XpΔ*Xist* round spermatids. We determined the sex of the embryos from the presence or absence of the Y-specific transcript *Eif2s3y*. As expected, *Xist* was present at very high levels in wild type female morulas, but absent from males. Also, none of the *in vivo* fertilized XpΔ*Xist* male and female morulas showed any *Xist* expression above background (Figure 5A). Interestingly, *Xist* levels were variable in ROSI-derived XpΔ*Xist* female morulas, and only one out of 11 analysed female embryos did not display any *Xist* expression. None of the wild type male morulas arising from these ROSI experiments with XpΔ*Xist* round spermatids showed *Xist* expression above background (Figure 5A). We further analysed the onset of Xm inactivation, and its variability. In wild type ROSI-derived female embryos, *Xist* clouds were prominent from the 4-cell stage onwards (Figure 1D & E, Figure 5B & C). This pattern was not significantly different from what was observed upon *in vivo* fertilization of wild type embryos. In contrast, none of the XpΔ*Xist*, 8-cell ROSI embryos that we analysed displayed *Xist* clouds in any of the cells (Figure 4B & C), but we did observe clear *Xist* RNA FISH clouds at the morula stage. The number of cells with an *Xist* cloud appeared somewhat more variable compared to what was observed in wild type female ROSI derived or *in vivo* fertilized morulas, and the average fraction of positive cells was lower, when compared to *in vivo* fertilized morulas, and on the border of significance for wild type ROSI derived females (Figure 5C). Thus, Xm *Xist* activation in the XpΔ*Xist* female preimplantation embryos is delayed compared to what is observed following ROSI or *in vivo* fertilization using wild type spermatids or sperm, respectively. The observed variation in the number of cells that have formed an *Xist* cloud at the morula stage, including two embryos with no *Xist* clouds (Figure 5C), is consistent with the variation in *Xist* level that we detected in the qRT-PCR experiments (Figure 5A). The lack of clouds in some embryos is also in accordance with the notion that we did not rescue all XpΔ*Xist* females by performing ROSI.

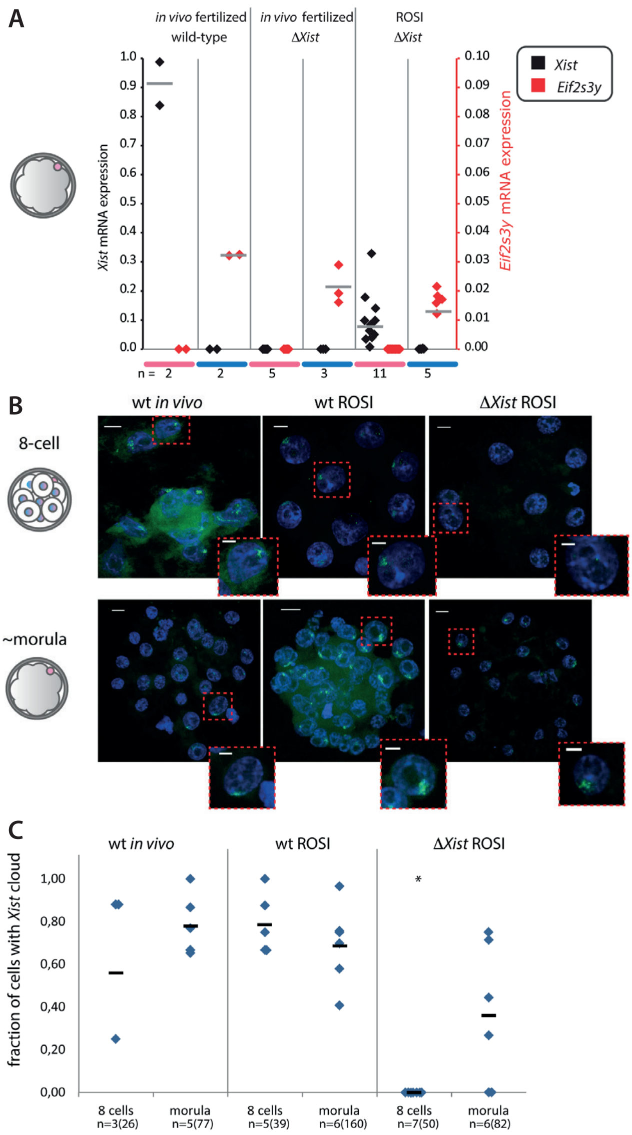

Figure 5: Maternal *Xist* expression in ROSI-derived XpΔ*Xist* females is variable and delayed compared to paternal *Xist* expression during iXCI

A Dot plot showing *Xist* (black) and *Eif2s3y* (red) mRNA expression levels for RNA isolated from individual *in vivo* fertilized wt and XpΔ*Xist* male (blue) and female (pink) mouse morulas, and from ROSI-derived XpΔ*Xist* male and female morulas. Expression levels were normalized to *Actin*. Grey lines indicate the average values, n values are indicated below the graph. **B** Representative images of *Xist* clouds in wild type *in vivo* fertilized female embryos, and wild type and XpΔ*Xist* ROSI-derived female embryos, analysed at the 8-cell and morula stages. Scale bars in whole embryo and single cell images represent 10, and 5 μm, respectively. **C** Quantification of *Xist* cloud formation in the embryo types described in B. Individual measurements are indicated, horizontal bars represent the average value. Asterisk indicates significantly different from the corresponding stage in wild type ROSI female embryos (P=0,00025). Numbers of analysed embryos are indicated at the bottom, and followed by total numbers of nuclei that could be scored (some nuclei were lost during procedures, and some embryos that were in the "8-cell" group contained 9 or 10 cells) in parenthesis.

Previous reports have shown that also in diploid parthenogenetic embryos one of the two maternal X chromosomes starts to express *Xist* around the morula stage (Kay et al. 1994; Nesterova et al. 2001). It was then suggested that this could occur because a repressive imprint on the Xm *Xist* allele, preventing its expression, is not retained throughout pre-implantation development. However, in a similar situation, when *in vivo* fertilized blastocysts disomic for Xm were analysed, Xm derived *Xist* clouds were hardly ever observed (Goto & Takagi 2000; Matsui et al. 2001). Thus, in this latter situation, the presence of a paternal genome most likely somehow helps to maintain the maternal imprint up to the blastocyst stage. Consistent with these findings, we also did not observe *Xist* expression above background levels in any of the XpΔ*Xist* female morulas obtained by natural mating (Figure 5A).

To further substantiate that the observed *Xist* clouds in the XpΔ*Xist* female morulas result in robust XCI, we investigated the immunolocalisation of H3K27me3 in female blastocysts derived from *in vivo* wild type fertilization in comparison to ROSI-derived XpΔ*Xist* female blastocysts. H3K27me3 is one of the earliest known histone modification that accompanies XCI, and is detectable as a domain covering the inactive Xp in wild type trophoblast cells (Plath 2003) and Figure 6A. We also observed such H3K27me3 domains in ROSI-derived XpΔ*Xist* female embryos, (Figure 6, B). These data are consistent with the occurrence of robust maternal XCI in trophoblast cells in ROSI-derived, XpΔ*Xist* female embryos. Still, not all cells may be able to activate *Xist* expression from Xm, and only if the fraction of cells that manage to do so is high enough, the embryo may be rescued.

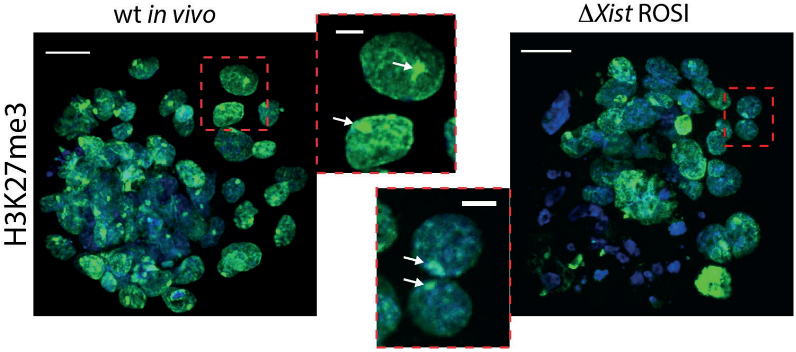

Figure 6: H3K27me3 marks the inactive Xm in ROSI-derived XpΔ*Xist* female blastocysts

H3K27me3 (green) marks the inactive Xp in wild type *in vivo* fertilized female blastocyst and the inactive Xm in ROSI-derived XpΔ*Xist* female blastocysts. DAPI is shown in blue. Size bars in whole embryo and single cell images represent 20, and 5 µm, respectively. H3K27me3 domain is indicated by arrows in the enlargements.

Recently, it was shown that expression of the X-linked XCI activator RNF12 is reduced in *in vitro* fertilized mouse embryos, and that this causes impaired iXCI, leading to skewed sex ratios of the offspring (Tan et al. 2016). In our ROSI model, we anticipated an opposite situation with high *Rnf12* expression, since *Rnf12* is one of the X-linked genes that becomes specifically reactivated in spermatids (Namekawa et al. 2006). If this status is maintained upon ROSI, then it may lead to higher RNF12 levels compared to what is observed following fertilization with mature sperm. We analysed RNF12 protein levels at the eight-cell stage, in wild type and XpΔ*Xist* ROSI derived, and *in vivo* fertilized female and male embryos. This time point was chosen because it is just prior to the initiation of *Xist* cloud formation in the XpΔ*Xist* female ROSI embryos. Interestingly, the overall RNF12 level was increased approximately three-fold in all ROSI-derived embryos compared to *in vivo* fertilized embryos (Figure 7A, B). However, no difference between male and female embryos was noted. In addition, RNF12 levels of all *in vivo* derived embryos, fertilized either by wild type or Δ*Xist* sperm, were similar (Figure 7A, B). This latter observation indicates that failure to inactivate the paternal X does not lead to a measurable significant increase in RNF12 levels using this type of semi-quantitative immunocytochemical analysis.

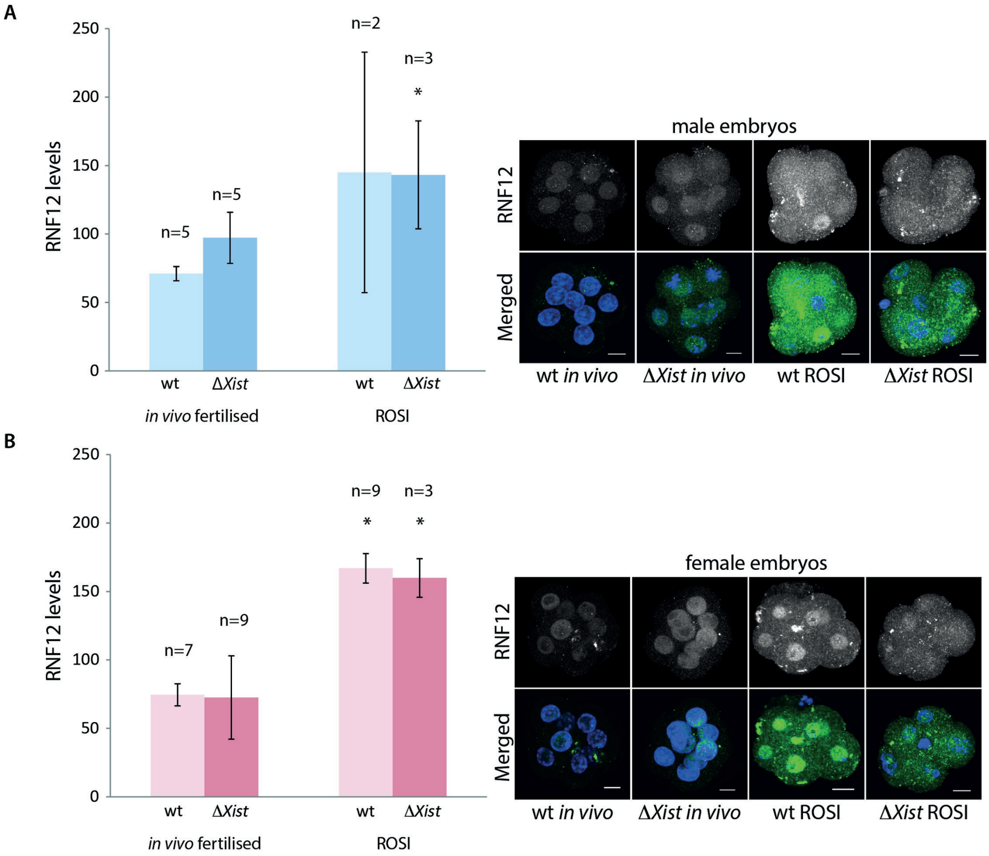

Figure 7: Enhanced expression of RNF12 in ROSI-derived compared to *in vivo* fertilized 8-cell embryos

A Quantification of RNF12 protein levels ± s.d. per male 8-cell embryo as measured from immunocytochemical staining using Image J (see Materials and Methods for details). Representative images of each analysed condition are shown on the right. Size bars represent 10 μm. Asterisk indicates significant difference (P=0,05) with *in vivo* wild type derived embryos. **B** As in **A**, for female embryos. Asterisk indicates significant difference (P≤0,05) with *in vivo* fertilized embryos. The following P values were obtained per comparison: wt *in vivo* versus wt ROSI derived embryos P=0,016, wt *in vivo* versus XpΔ*Xist* ROSI derived embryos P=0,0005, *in vivo* XpΔ*Xist* versus wt ROSI derived embryos P=0,0098 and *in vivo* XpΔ*Xist* versus XpΔ*Xist* ROSI derived embryos P=0,004.

RNF12 expression from the paternally inherited postmeiotically reactivated X chromosome by itself cannot easily explain our findings, since ROSI-derived males also display high RNF12 levels. Somehow, the injection of a round spermatid nucleus must either transfer a substantial amount of very stable RNF12 protein or mRNA, or other, autosomal spermatid-expressed genes ensure continuous *Rnf12* expression from the maternal X in males, and perhaps from both X chromosomes in females. It might be suggested that the observed enhanced RNF12 expression could contribute to the ability of XpΔ*Xist* embryos to overcome the maternal imprint on the Xic, and allow maternal XCI. However, other X-linked factors are most likely more critically involved in lowering the threshold for activation of the Xm *Xist* gene in the XpΔ*Xist* female embryos, because Xm inactivation was never observed in male ROSI embryos. Alternatively, or in addition, the chromatin structure of the paternal X chromosome, being heavily marked by silencing histone modifications, may titrate away factors that are important for maintenance of the inactive status of the maternal *Xist* gene.

In future experiments, comparative global gene expression analyses of ROSI derived and ICSI derived embryos might be used to identify novel XCI factors involved in both imprinted and random X chromosome inactivation. From this perspective, it will also be interesting to compare the gene expression profiles of purified round spermatids from C57BL/6 mice and CAST/EiJ mice, since we failed to rescue the lethality of paternal *Xist* deletion using ROSI on the latter genetic background. Microarray analyses of gene expression using total testis mRNAs of *M. musculus musculus* and *M. musculus castaneus* identified a relatively small number of differentially expressed spermatogenesis genes (Voolstra et al. 2007). In this dataset, expression of *Rnf12* was not significantly different between the *M. musculus* subspecies (Voolstra et al. 2007). Thus, we speculate that differences in regulation of expression of genes other than *Rnf12* may be critical for inducing maternal *Xist* expression in ROSI derived XpΔ*Xist* embryos on the C57BL/6 background only.

In the model in Figure 8, we schematically depict the differences between regulation of iXCI following *in vivo* fertilization, ROSI, or induction of parthenogenesis. When iXCI is initiated in wild type embryos carrying an Xp and an Xm (as opposed to two Xms in the parthenogenic situation), the Xp most likely is more responsive to XCI trans activator(s) such as RNF12 than the Xm. This differential response is related to an imprint of the *Xist* promoter on the Xm, which prevents *Xist* expression, and which is absent from the promoter on Xp (Fukuda et al. 2014). In addition, Xp may carry an (MSCI-dependent) imprint to facilitate *Xist* expression. At this stage, RNF12 expression is relatively high, due to the maternally provided store, and paternal *Xist* activation occurs independent of the X:A ratio. Transcription of the XCI activator(s) would reach the threshold for *Xist* expression from the Xp in all blastomeres by the 4-cell stage, but virtually never reach the threshold for activation of *Xist* expression from Xm. When the paternal copy of *Xist* is deleted, iXCI can not occur, and the maternal *Xist* gene remains repressed due to a paternal inhibitory effect that is missing in parthenogenetic embryos. ROSI somehow leads to elevated levels of RNF12 in morulas, but this by itself will not be enough to activate Xm in ROSI-derived males, consistent with earlier findings using *Rnf12* overexpression (Tan et al. 2016). Somehow, either the presence of two X chromosomes, or the specific epigenetic constitution of the Xp, contributes to efficient stimulation of *Xist* expression from Xm. Subsequent Xm silencing most likely allows rescue of XpΔ*Xist* females. In addition, prior to the establishment of *Xist* mediated Xm inactivation, the silencing epigenetic marks that are carried by the round spermatid-derived Xp may also contribute to a more optimal gene-expression balance. This may exert an additional positive effect on the fitness of the ROSI-derived XpΔ female embryos.

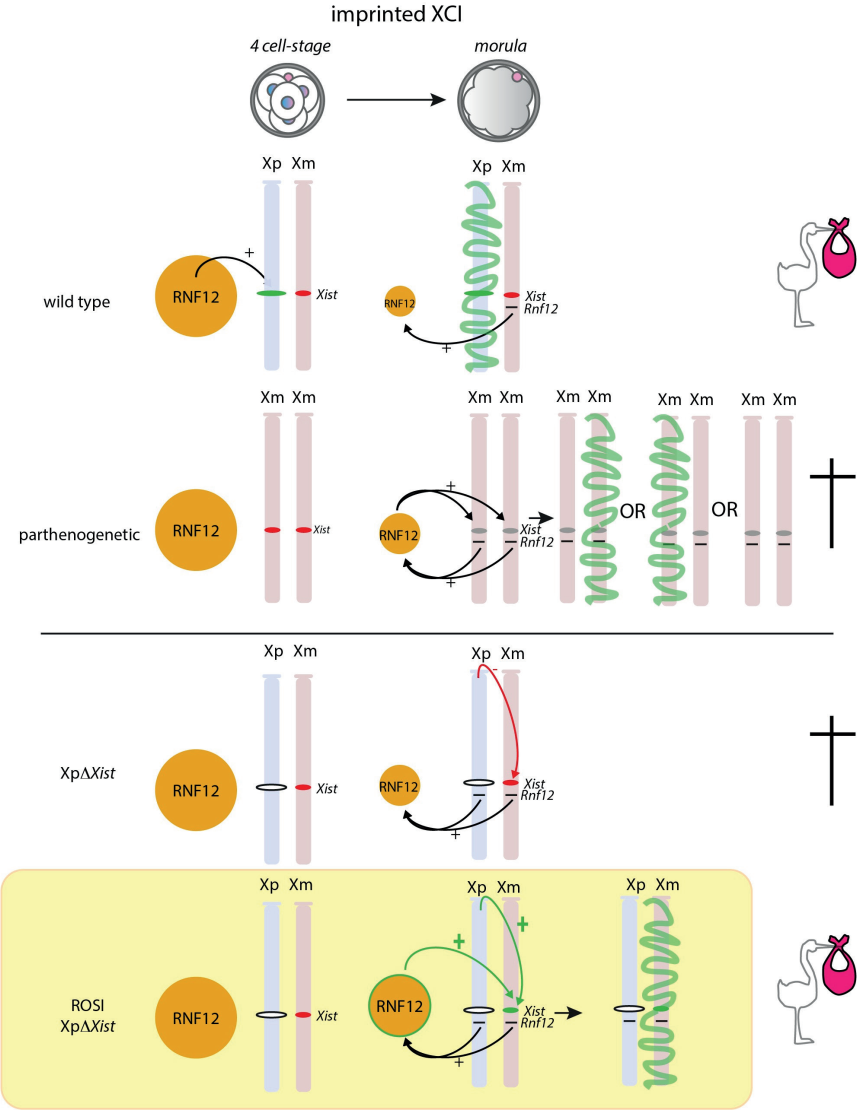
imprinted XCI
4 cell-stage
morula
Xp Xm
wild type
RNF12
Xist
Rnf12
+
Xm Xm
parthenogenetic
OR
XpΔXist
ROSI
XpΔXist

Figure 8: Schematic representation of critical factors during iXCI in wild type and parthenogenetic females, compared to XpΔ*Xist* females arising from *in vivo* fertilization or ROSI

Xp (blue) and Xm (pink) are schematically drawn, and the *Xist* and *Rnf12* loci are indicated where relevant. RNF12 protein levels are represented by the size of the orange circle. A green *Xist* locus indicates that it is primed for expression, whereas a red locus indicates that it is repressed. An open *Xist* locus represents the Δ*Xist* allele. During normal iXCI, that initiates around the four cell-stage, high maternally regulated RNF12 levels ensure *Xist* expression from Xp, establishing iXCI by the morula stage (green signal on Xp representing the *Xist* cloud). In parthenogenic embryos, the imprint on Xm is lost by the morula stage and *Xist* can be activated in a manner that appears to be regulated by dosage dependent XCI activators such as RNF12 (effect symbolized by two black arrows coming from the *Rnf12* loci), but this is inefficient. In contrast, when *Xist* is deleted from Xp, iXCI cannot be induced, most likely because the presence of a paternal genome helps to maintain repression of the maternal *Xist* gene (red arrow). Upon ROSI, round spermatid-specific epigenetic regulation (green arrow), possibly in combination with the double dosage of X chromosomes, allows activation of Xm by the morula stage. In addition, RNF12 levels are relatively high and may also aid in this process.

Taken together, the present experiments have demonstrated that ROSI allows activation of *Xist* transcription from the Xm in preimplantation mouse embryos in the absence of a paternal *Xist* gene. We propose that correct regulation of expression of X-linked trans activators of XCI from both the paternal and maternal X chromosome is of critical importance in iXCI in mouse.

In humans, X chromosome inactivation is initiated later than in mouse, and most likely is not imprinted (reviewed in (X. Deng et al. 2014). Still, our results do provide evidence that disturbances of the paternal epigenome impact on embryonic gene regulation, and this is relevant for considerations on human embryo quality. In humans, there is an increase in the histone:protamine ratio when sperm from male factor subfertility patients is compared with sperm from fertile men (Simon et al. 2014; Aoki et al. 2006). Also, when sperm is extracted from the testis and used for ICSI, it cannot be excluded that spermatids with an incomplete histone-to-protamine transition are selected for injection into oocytes, so that ICSI resembles ROSI. Furthermore, the birth of 14 ROSI-derived babies was recently described (Tanaka et al. 2015), making careful assessment of possible associated epigenetic risks more topical than ever.

Future clinical and basic animal research should go hand in hand to evaluate if there is a relation between embryo paternal epigenome quality and oocyte injection using spermatids or spermatozoa in which the histone-to-protamine transition has not been completed or is disturbed.

Materials and Methods

Ethics statement

For all experiments we aimed to reduce pain and stress as much as possible by housing animals in groups whenever possible, and using appropriate anesthetic agents during operation, followed by treatments to reduce pain. Animals more than one week old were killed using cervical dislocation. Embryos collected after day 13 of embryonic development, and pups younger than 1 week old were killed by decapitation and immediate collection of heads in liquid nitrogen. All animal experiments were approved by and were performed in strict accordance with the recommendations by the local animal experiments committee DEC-consult (approval numbers EMC2448 and EMC3200).

Animals

B6D2F1 mice (C57BL/6 × DBA/2) were used as oocyte donors. We used B10CBA females that were mated with vasectomized males as pseudopregnant surrogates for transfer of ICSI- and ROSI-derived two-cell stage embryos. C57Bl6 mice carrying an *Xist* deletion (Δ*Xist*) were those originally generated by Csankovszki and colleagues (1999), the allele was also crossed into a CAST/EiJ background for several generations, but round spermatids isolated form Δ*Xist* males with this background did not result in retrieval of viable female embryos. Control wild type C56BL/6 males were also used as spermatid and spermatozoa donors. To obtain embryos from *in vivo* fertilized oocytes, superovulated B6D2F1 females (see below for the superovulation protocol) were mated with wild type or Δ*Xist* males and zygotes were retrieved from the oviduct and cultured for different applications as described in the expanded view.

Microinsemination with round spermatids (ROSI)

ROSI was carried out as described previously [44] with minor modifications:

ROSI: Oocyte collection. Mature oocytes were collected from the oviducts of 6- to 16-wk-old B6D2F1 female mice (Harlan) that had been induced to superovulate with 5 IU pregnant mare's serum gonadrotopin (PMSG; Intervet), followed by 5 IU human chorionic gonadotropin (hCG; Intervet) 48 h later. Oocytes were collected from oviducts approximately 16 h after hCG injection and treated with 80 IU ml-1 hyaluronidase (Sigma) until the cumulus cells dispersed. The oocytes were then placed in G-1 PLUS medium (Vitrolife), covered with mineral oil (Sigma), and stored at 37°C (5% CO2:95% air). Before injection, oocytes were placed into Ca2+-free M16 containing 10 mM SrCl2 (Sigma) for 60 min. Oocytes were injected in MEMα medium (Life Technologies) supplemented per 500 ml with 2.5 g HEPES, 684 mg 50% sodium lactate solution, 55 mg sodium pyruvate, 70 mg

L-glutamin, 6% (v/v) fetal calf serum (pH set at 7.2).

ROSI: Spermatogenic cell suspension preparation. To collect round spermatids, seminiferous tubules of the testes from male mice were gently minced using two blunt ended curved forceps, and single cells were suspended in G-MOPS PLUS medium (Vitrolife).

ROSI: Microinsemination with round spermatids. ROSI was carried out at room temperature. The cover of a plastic dish was used as a microinjection chamber. A row of three 10 µl drops containing HEPES-buffered MEMα + supplements (for oocytes), 12% polyvinylpyrrolidone (PVP; Irvine scientific) in G-MOPS PLUS, and of the spermatogenic cell suspension, was placed on the bottom of the dish and covered with mineral oil. The dish was placed on the stage of an inverted microscope. The nuclei of the round spermatids were collected from the spermatogenic cell suspension drop by gentle pipetting using a 5 µm Piezo Drill Micropipette (Humangen) until the nuclei of the round spermatids had lost all cytoplasm and could then be collected, transferred to the clean PVP drop and subsequently used for microinjection. An oocyte was held to the holding pipette with the metaphase II spindle at either the 12 or the 6 o'clock position. The zona pellucida was breached by a laser applied pulse (XY clone, Hamilton Thorne) and the plasma membrane was subsequently penetrated by using a piezo-activated device (Burleigh). The spermatid nucleus was readily expelled into the ooplasm.

Injected oocytes were then transferred to G-1 PLUS medium and cultured for 24 and 96 h, to examine their development *in vitro*.

Microinsemination with mature spermatozoa (ICSI)

ICSI was carried out as described previously (Yoshida & Perry 2007).

Embryo culture and transfer

Injected oocytes were cultured for 24–30 h in G-1 PLUS medium until the two-cell stage. Thereafter, 10-15 two-cell embryos were transferred to each oviduct of surrogate females on day 1 of pseudopregnancy. Alternatively, embryos were cultured up to the 4-cell, 8-cell, or morula stage in G-1 PLUS medium and further processed for different applications as described below.

Chromosome spread preparations

Zygotes or two-cell embryos were incubated with colcemid (1.5 µg/ml) to arrest cells at prometaphase until pronuclei had disappeared. To obtain chromosome spreads, after zona pellucida removal with Acidic Tyrode's Solution (Sigma), arrested zygotes were incubated in hyposolution (25 % v/v FCS, 0.5 % w/v sodium citrate) for 5 min and subsequently transferred to a drop of fixative (1 % v/v paraformaldehyde, 0.2 % v/v Triton X-100, 0.1

mM dithiothreitol, pH 9.2) on a glass slide. After horizontal drying for 1 hour, the slides were washed with 0.08 % Photo-Flo (Kodak) and air dried. All slides were stored at −20 °C until further use.

Decondensation of mouse caput sperm

Decondensation of wild type mouse caput sperm was performed as described previously (van der Heijden et al. 2006).

Preparation of spread spermatid nuclei

Nuclei of wild type mouse spermatogenic cells were spread as previously described (Peters et al. 1997).

Immunofluorescence

For immunofluorescence stainings, the zona pellucida of the 8-cell embryos was removed with incubation in Acidic Tyrode's Solution (Sigma) at room temperature for 1 minute. Afterwards, embryos were washed in M2 medium, fixed in 4% PFA for 15 minutes at room temperature and then washed again in M2 medium. Subsequently, embryos and slides containing zygote or embryo chromosome spreads, decondensed sperm, or spread spermatid nuclei, were rinsed in PBS-phosphate-buffered saline PBS-T (PBS, 0.01% v/v Tween-20) and locked with blocking solution (PBS-T, 2% w/v bovine serum albumin (BSA fraction V), 5% v/v normal goat serum) for 30 minutes and incubated with primary antibodies at 4°C overnight. The following antibodies were used in this study: rabbit polyclonal against H3K9me3 (1:200, Abcam Ab8898-100), mouse monoclonal anti H3.1/2 (1:1000, gift from dr. P. de Boer, for validation see Godfried W van der Heijden et al. 2007), mouse monoclonal against RNF12 (1:50 Abnova), and human centromere autoantigen (ACA, 1:1000, Fitzgerald Industries, 90C-CS1058). After washing with PBS-T, slides were incubated with the appropriate secondary antibodies for 1 hour, washed with PBS-T and mounted with ProLong Gold mounting solution for DNA counterstaining. Images were obtained using a LSM700 confocal laser scanning microscope (Zeiss) and processed with Fiji and Adobe Photoshop CS3 software. Imaging of RNF12 stained embryos was performed using the same exposure time for each embryo. Quantification of total RNF12 levels per embryo was performed using Image J (Fiji) software. Subsequently, statistical significance was determined by Student's t test (*$P \leq 0.05$, significant).

RNA/DNA FISH on preimplantation embryos

Pre-implantation embryos were treated with Acidic Tyrode's Solution (Sigma) to remove the zona pellucida. The method for *Xist* RNA-FISH has been described (Barakat & Gribnau 2014), and we used a 5.5 Kb BglII cDNA fragment,covering exons 3-7 (in part) as a probe. For DNA FISH on chromosome spreads of prometaphase arrested embryos and on 8 cell embryos after RNA FISH or immunostaining (for sex determination), slides were denatured in 70% v/v formamide/2x SSC/10mM phosphate buffer for 5 minutes at 78^o C followed by dehydration in ice cold ethanol series (70%, 85% and 100%) 3 minutes each. Slides were left to dry for a few minutes at room temperature and then, the same *Xist* probe used for RNA FISH was applied on the slide. Detection was performed as for RNA FISH.

Placenta cryosections

Placentas were removed at E15. The tissues were snap frozen and stored at -80°C until use. For RNA FISH, 14 μm-thick frozen sections were made from frozen tissues on a cryostat and mounted on glass slides. Sections were briefly air-dried, extracted with 0.5% Triton X-100 in phosphate-buffered saline (PBS) on ice, fixed in 4% formaldehyde, 5% acetic acid for 18 min at room temperature, washed 3 times in PBS for 5 min each, dehydrated in 70-100% ethanol series and air-dried. Then the probes were applied. For DNA FISH the same procedure as described above for RNA/DNA FISH on preimplantation embryos' was followed. Both for RNA and DNA FISH, an additional *Xist* probe was used that is specific for the wild type X chromosome. This probe covers a 8.4 Kb fragment lying within the deleted area of the Δ*Xist*. It was generated by combination of PCR products obtained with the following primer sets: Fwprom CCCTCTGGAAGAGCAGTCAG and Rvprom GCCATAAGGCTTGGTGGTAG (~1,7Kb), Fw1 GCCAACCAATGAGACCACTT and Rv1 TGGCATGATGGAATTGAGAA (~2.5Kb), Fw2 CTACCCACCCCAGTACATGC and Rv2 TTGGCTCAGTGCTTATGGTG (~2.1Kb), Fw3 CAGTTGCCTTCTCCTTGCTC and Rv3 AGCTGTTAGTGCCGTCCAGT (~2.1Kb). The PCR conditions were: initial denaturation 94^o C for 5 min, followed by 35 cycles of 94^o C 30 sec, 55^o C 30 sec, 72^{o}C 3 min, and final extension at 72^o C for 5 min. PCR products were loaded on a 1% agarose gel, bands were extracted and DNA was isolated using NucleoSpin Extract II (Macherey Nagel) according to the manufacturer's protocol. Subsequently, the probe was made using the Biotin Nick translation mix (Roche diagnostics), according to the manufacturer's instructions.

Genotyping PCR

The primer pairs used to assess the genotype of the mice for the presence or absence of the *Xist* deletion, and to detect Ube1x and Ube1y have been previously described (*Xist* deletion: Gribnau et al. 2005, *Ube1x/y*: Chuma and Nakatsuji 2001). For *Sry* we used forward primer 5'GTGGTCCCGTGGTGAGAG3', and reversed primer 5'TTTTGTTGAGGCAACTGCAG3', generating a 250bp fragment. PCR conditions were as follows: Initial hold for 2 minutes at 98°C, followed by 35 cycles of 98°C for 10 seconds, 63°C for 15 seconds, and 72°C for 30 seconds, and finally 72°C for 5 minutes.

Quantitative PCR analyses

For quantitative RT–PCR (RT–qPCR) of single embryos, the Taqman® Cells-to-Ct Kit (Applied Biosystems) was used according to the manufacturer's protocol. All samples were analyzed in triplicate in a 10 µl final reaction volume using the BioRad CFX 384 Real-time System. The reaction mixture contained SYBR Green PCR Master Mix (Applied Biosystems), primers (for *Actin*, *Xist*, or *Eif2s3y*) and 2.5 µl of cDNA. The following primers were used: *Xist* for GGATCCTGCTTGAACTACTGC and *Xist* rev CAGGCAATCCTTCTTCTTGAG (Chureau et al. 2011), *Actin* for AACCCTAAGGCCAACCGTGAAAAG and rev CATGGCTGGGGTGTTGAAGGTCTC, *Eif2s3y* for CCAGGGACCAAAGGAAACTT and rev TAGCCTGGCTTTCTTTCACC (Vernet et al. 2014).

For copy number qPCR on genomic DNA, primers were designed for the X chromosome on the *Tsix* promoter region (for CCGAGATATCCACGCATCTT and rev AGCTGGCTATCACGCTCTTC) and for chromosome 12 on the *Rex1* allele (for GGTGCAAGAAGAAGCTGAGG and rev GTTTCGAGCTCTCCGTGAAG).

After an initial hold at 94°C for 2 minutes, reaction mixtures underwent 40 cycles of 30s at 94°C, 30s at 60°C, and 30s at 72°C. Results were expressed as Cycle threshold (Ct) values. Gene expression levels were normalized over *Actin* gene expression, according to the $2^{-\Delta CT}$ method (Livak & Schmittgen 2001). In order to be able to use a relative quantification approach to compare expression levels we ensured that the primer pairs have similar amplification efficiencies (E = 100 ± 10%).

Acknowledgements

The authors would like to acknowledge help of Bas de Hoon, Esther Sleddens-Linkels, Agnese Loda, dr. Catherine Dupont, dr. Kim Monkhorst, John Kong-a-San, dr. Alex Maas and Suzette de Groot (Erasmus MC, Rotterdam, The Netherlands).

REFERENCES

1. Puschendorf M, Terranova R, Boutsma E, Mao X, Isono K, et al. (2008) PRC1 and Suv39h specify parental asymmetry at constitutive heterochromatin in early mouse embryos. Nat Genet 40: 411-420.

2. van der Heijden GW, Dieker JW, Derijck AA, Muller S, Berden JH, et al. (2005) Asymmetry in histone H3 variants and lysine methylation between paternal and maternal chromatin of early mouse zygotes. Mech Dev 122: 1008.

3. Turner JM (2007) Meiotic sex chromosome inactivation. Development 134: 1823-1831.

4. van der Heijden GW, Derijck AA, Posfai E, Giele M, Pelczar P, et al. (2007) Chromosome-wide nucleosome replacement and H3.3 incorporation during mammalian meiotic sex chromosome inactivation. Nat Genet 39: 251-258.

5. Namekawa SH, Park PJ, Zhang LF, Shima JE, McCarrey JR, et al. (2006) Postmeiotic sex chromatin in the male germline of mice. Curr Biol 16: 660-667.

6. Hendriksen PJM, Hoogerbrugge JW, Themmen APN, Koken MHM, Hoeijmakers JHJ, et al. (1995) Postmeiotic transcription of X and Y chromosomal genes during spermatogenesis in the mouse. Dev Biol 170: 730-733.

7. Mulugeta Achame E, Wassenaar E, Hoogerbrugge JW, Sleddens-Linkels E, Ooms M, et al. (2010) The ubiquitin-conjugating enzyme HR6B is required for maintenance of X chromosome silencing in mouse spermatocytes and spermatids. BMC Genomics 11: 367.

8. Okamoto I, Otte AP, Allis CD, Reinberg D, Heard E (2004) Epigenetic dynamics of imprinted X inactivation during early mouse development. Science 303: 644-649.

9. Shin J, Bossenz M, Chung Y, Ma H, Byron M, et al. (2010) Maternal Rnf12/RLIM is required for imprinted X-chromosome inactivation in mice. Nature 467: 977-981.

10. Jonkers I, Barakat TS, Achame EM, Monkhorst K, Kenter A, et al. (2009) RNF12 is an X-Encoded dose-dependent activator of X chromosome inactivation. Cell 139: 999-1011.

11. Gontan C, Achame EM, Demmers J, Barakat TS, Rentmeester E, et al. (2012) RNF12 initiates X-chromosome inactivation by targeting REX1 for degradation. Nature 485: 386-390.

12. Okamoto I, Arnaud D, Le Baccon P, Otte AP, Disteche CM, et al. (2005) Evidence for de novo imprinted X-chromosome inactivation independent of meiotic inactivation in mice. Nature 438: 369-373.

13. Sun S, Payer B, Namekawa S, An JY, Press W, et al. (2015) Xist imprinting is promoted by the hemizygous (unpaired) state in the male germ line. Proc Natl Acad Sci U S A 112: 14415-14422.

14. Deng Q, Ramskold D, Reinius B, Sandberg R (2014) Single-cell RNA-seq reveals dynamic, random monoallelic gene expression in mammalian cells. Science 343: 193-196.

15. Mak W, Nesterova TB, de Napoles M, Appanah R, Yamanaka S, et al. (2004) Reactivation of the paternal X chromosome in early mouse embryos. Science 303: 666-669.

16. Marahrens Y, Panning B, Dausman J, Strauss W, Jaenisch R (1997) Xist-deficient mice are defective in dosage compensation but not spermatogenesis. Gen Dev 11: 156-166.

17. Mugford JW, Yee D, Magnuson T (2012) Failure of extra-embryonic progenitor maintenance in the absence of dosage compensation. Development 139: 2130-2138.

18. Tada T, Obata Y, Tada M, Goto Y, Nakatsuji N, et al. (2000) Imprint switching for non-random X-chromosome inactivation during mouse oocyte growth. Development 127: 3101-3105.

19. Fukuda A, Tomikawa J, Miura T, Hata K, Nakabayashi K, et al. (2014) The role of maternal-specific H3K9me3 modification in establishing

imprinted X-chromosome inactivation and embryogenesis in mice. Nat Commun 5: 5464.

20. Namekawa SH, Payer B, Huynh KD, Jaenisch R, Lee JT (2010) Two-step imprinted X-inactivation: Repeat vs genic silencing in the mouse. Mol Cell Biol.

21. Heard E, Chaumeil J, Masui O, Okamoto I (2004) Mammalian X-chromosome inactivation: an epigenetics paradigm. Cold Spring Harb Symp Quant Biol 69: 89-102.

22. Avo Santos M, van de Werken C, de Vries M, Jahr H, Vromans MJ, et al. (2011) A role for Aurora C in the chromosomal passenger complex during human preimplantation embryo development. Hum Reprod 26: 1868-1881.

23. Balhorn R, Gledhill BL, Wyrobek AJ (1977) Mouse sperm chromatin proteins: quantitative isolation and partial characterization. Biochemistry 16: 4074-4080.

24. van der Heijden GW, Derijck AA, Ramos L, Giele M, van der Vlag J, et al. (2006) Transmission of modified nucleosomes from the mouse male germline to the zygote and subsequent remodeling of paternal chromatin. Dev Biol 298: 458-469.

25. Arney KL, Bao S, Bannister AJ, Kouzarides T, Surani MA (2002) Histone methylation defines epigenetic asymmetry in the mouse zygote. Int J Dev Biol 46: 317-320.

26. Santos F, Peters AH, Otte AP, Reik W, Dean W (2005) Dynamic chromatin modifications characterise the first cell cycle in mouse embryos. Dev Biol 280: 225-236.

27. Kishigami S, Van Thuan N, Hikichi T, Ohta H, Wakayama S, et al. (2006) Epigenetic abnormalities of the mouse paternal zygotic genome associated with microinsemination of round spermatids. Dev Biol 289: 195-205.

28. Okamoto I, Heard E (2006) The dynamics of imprinted X inactivation during preimplantation development in mice. Cytogenet Genome Res 113: 318-324.

29. Csankovszki G, Panning B, Bates B, Pehrson JR, Jaenisch R (1999) Conditional deletion of Xist disrupts histone macroH2A localization but not maintenance of X inactivation. Nat Genet 22: 323-324.

30. Odet F, Pan W, Bell TA, Goodson SG, Stevans AM, et al. (2015) The Founder Strains of the Collaborative Cross Express a Complex Combination of Advantageous and Deleterious Traits for Male Reproduction. G3 (Bethesda) 5: 2671-2683.

31. Yamauchi Y, Riel JM, Ruthig V, Ward MA (2015) Mouse Y-Encoded Transcription Factor Zfy2 Is Essential for Sperm Formation and Function in Assisted Fertilization. PLoS Genet 11: e1005476.

32. Jonkers I, Monkhorst K, Rentmeester E, Grootegoed JA, Grosveld F, et al. (2008) Xist RNA is confined to the nuclear territory of the silenced X chromosome throughout the cell cycle. Mol Cell Biol 28: 5583-5594.

33. Nesterova TB, Barton SC, Surani MA, Brockdorff N (2001) Loss of Xist imprinting in diploid parthenogenetic preimplantation embryos. Dev Biol 235: 343-350.

34. Kay GF, Barton SC, Surani MA, Rastan S (1994) Imprinting and X chromosome counting mechanisms determine Xist expression in early mouse development. Cell 77: 639-650.

35. Goto Y, Takagi N (1999) Maternally inherited X chromosome is not inactivated in mouse blastocysts due to parental imprinting. Chromosome Res 7: 101-109.

36. Matsui J, Goto Y, Takagi N (2001) Control of Xist expression for imprinted and random X chromosome inactivation in mice. Hum Mol Genet 10: 1393-1401.

37. Plath K, Fang J, Mlynarczyk-Evans SK, Cao R, Worringer KA, et al. (2003) Role of histone H3 lysine 27 methylation in X inactivation. Science 300: 131-135.

38. Tan K, An L, Miao K, Ren L, Hou Z, et al. (2016) Impaired imprinted X chromosome

inactivation is responsible for the skewed sex ratio following in vitro fertilization. Proc Natl Acad Sci U S A 113: 3197-3202.

39. Voolstra C, Tautz D, Farbrother P, Eichinger L, Harr B (2007) Contrasting evolution of expression differences in the testis between species and subspecies of the house mouse. Genome Res 17: 42-49.

40. Deng X, Berletch JB, Nguyen DK, Disteche CM (2014) X chromosome regulation: diverse patterns in development, tissues and disease. Nat Rev Genet 15: 367-378.

41. Simon L, Liu L, Murphy K, Ge S, Hotaling J, et al. (2014) Comparative analysis of three sperm DNA damage assays and sperm nuclear protein content in couples undergoing assisted reproduction treatment. Hum Reprod 29: 904-917.

42. Aoki VW, Emery BR, Liu L, Carrell DT (2006) Protamine levels vary between individual sperm cells of infertile human males and correlate with viability and DNA integrity. J Androl 27: 890-898.

43. Tanaka A, Nagayoshi M, Takemoto Y, Tanaka I, Kusunoki H, et al. (2015) Fourteen babies born after round spermatid injection into human oocytes. Proc Natl Acad Sci U S A 112: 14629-14634.

44. Kimura Y, Yanagimachi R (1995) Mouse oocytes injected with testicular spermatozoa or round spermatids can develop into normal offspring. Development 121: 2397-2405.

45. Yoshida N, Perry AC (2007) Piezo-actuated mouse intracytoplasmic sperm injection (ICSI). Nat Protoc 2: 296-304.

46. Peters AH, Plug AW, van Vugt MJ, de Boer P (1997) A drying-down technique for the spreading of mammalian meiocytes from the male and female germline. Chromosome Res 5: 66-68.

47. Barakat TS, Gribnau J (2014) Combined DNA-RNA fluorescent in situ hybridization (FISH) to study X chromosome inactivation in differentiated female mouse embryonic stem cells. J Vis Exp.

48. Gribnau J, Luikenhuis S, Hochedlinger K, Monkhorst K, Jaenisch R (2005) X chromosome choice occurs independently of asynchronous replication timing. J Cell Biol 168: 365-373.

49. Chuma S, Nakatsuji N (2001) Autonomous transition into meiosis of mouse fetal germ cells in vitro and its inhibition by gp130-mediated signaling. Dev Biol 229: 468-479.

50. Chureau C, Chantalat S, Romito A, Galvani A, Duret L, et al. (2011) Ftx is a non-coding RNA which affects Xist expression and chromatin structure within the X-inactivation center region. Hum Mol Genet 20: 705-718.

51. Vernet N, Szot M, Mahadevaiah SK, Ellis PJ, Decarpentrie F, et al. (2014) The expression of Y-linked Zfy2 in XY mouse oocytes leads to frequent meiosis 2 defects, a high incidence of subsequent early cleavage stage arrest and infertility. Development 141: 855-866.

52. Livak KJ, Schmittgen TD (2001) Analysis of relative gene expression data using real-time quantitative PCR and the 2(-Delta Delta C(T)) Method. Methods 25: 402-408.

53. Hu D, Cross JC (2010) Development and function of trophoblast giant cells in the rodent placenta. Int J Dev Biol 54: 341-354.

Supporting Information:

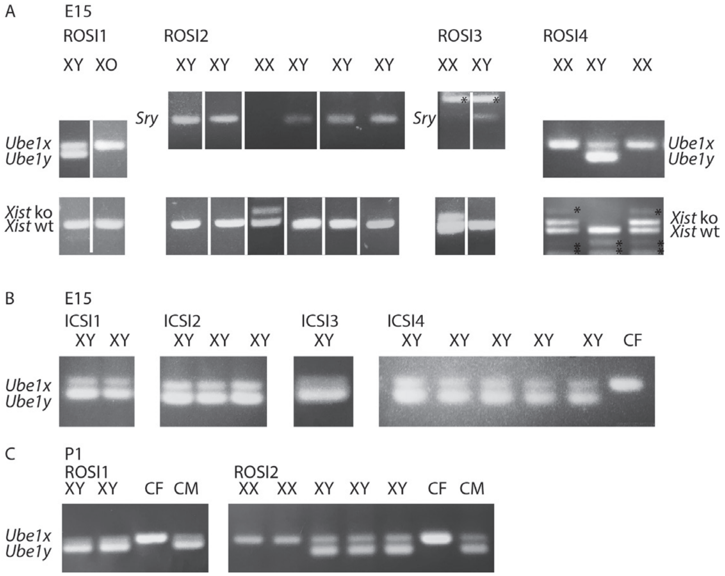
A
E15
ROSI1
ROSI2
ROSI3
ROSI4
XY XO
XY XY XX XY XY XY
XX XY
XX XY XX
Sry
Sry
Ube1x
Ube1y
Ube1x
Ube1y
Xist ko
Xist wt
Xist ko
Xist wt
*
B
E15
ICSI1
ICSI2
ICSI3
ICSI4
XY XY
XY XY XY
XY
XY XY XY XY XY CF
Ube1x
Ube1y
C
P1
ROSI1
ROSI2
XY XY CF CM
XX XX XY XY XY CF CM
Ube1x
Ube1y

S1 Figure: Genotyping of ROSI and ICSI embryos and pups

A DNA was isolated from E15 ROSI embryos and genotyped using primer sets amplifying either *Ube1x* and *Ube1y* or *Sry* (top). In addition, PCR was performed to detect the presence of *Xist* loci (wild type (wt) and knockout (ko)). All PCRs from XX female embryos should display a band for both alleles. One female was found to carry only a single X chromosome (20, X; XO). Results are grouped per experiment (1-4) in chronological order. In experiment 4, DNA was isolated for only 1 of the 5 males that were obtained. For the other four embryos, sex assignment was based solely on the presence of testes, since the results were congruent with the morphological assessment in all previous experiments. **B** DNA was isolated from E15 ICSI embryos and genotyped using primer sets amplifying either *Ube1x* and *Ube1y*. All embryos were male, a control female (CF) is shown for comparison. Results are grouped per experiment (1-4) in chronological order.
C DNA was isolated from P1 ROSI embryos and genotyped using primer sets amplifying *Ube1x* and *Ube1y* (CF; control female, CM; control male). Results are grouped per experiment (1-2) in chronological order.

S1 Table: Sex ratios reported in published mouse ROSI experiments

#: number; m: male; f: female

Author	system	# embryos	# pups	m	f	m /f	% survival	sex ratio
Kimura et al., 1995 [1]	wt ROSI	131	37	16	19	2	28,24%	0.84
Ogura et al., 1996 [2]	ICGN males ROSI	53	9	4	5		16,98%	0.80
Sasagawa and Yanagimachi. 1997 [3]	wt ROSI	46	11	4	7		23,91%	0.57
Sasagawa and Yanagimachi. 1997 [3]	Cryptorchid male ROSI	40	9	5	4		22,50%	1.25
Sasagawa and Yanagimachi. 1997 [3]	reversal Cryptorchid males 6w	41	9	4	5		21,95%	0.80
Sasagawa and Yanagimachi. 1997 [3]	reversal Cryptorchid males 14w	43	10	7	3		23,26%	2.33
Sasagawa et al., 1998 [6]	ROSI with spermatids from immature mice	148	29	13	16		19,59%	0.81
Sasagawa et al., 1998 [6]	wt ROSI	46	11	5	6		23,91%	0.83
Sasagawa et al., 1998b [7]	ROSI with Balb/c (hybrid sterile)	55	12	7	5		21,82%	1.40
Sasagawa et al., 1998b [7]	ROSI with B6D2F1 (hybrid fertile)	61	14	6	8		22,95%	0.75
Marh et al., 2003 [10]	wt ROSI	60	16	9	7		26,67%	1.29
Yanagimachi et al., 2004 [11]	ROSI wit *qk/qk* spermatids	96	18	8	10		18,75%	0.80
TOTALS		820	185	88	95	2	22,56%	0.93

References

1. Kimura Y, Yanagimachi R (1995) Mouse oocytes injected with testicular spermatozoa or round spermatids can develop into normal offspring. Development 121: 2397-2405.
2. Ogura A, Yamamoto Y, Suzuki O, Takano K, Wakayama T, et al. (1996) In vitro fertilization and microinsemination with round spermatids for propagation of nephrotic genes in mice. Theriogenology 45: 1141-1149.
3. Sasagawa I, Yanagimachi R (1997) Spermatids from mice after cryptorchid and reversal operations can initiate normal embryo development. JAndrol 18: 203-209.
4. Sasagawa I, Tomaru M, Adachi Y, Kubota Y, Nakada T (1997) Simultaneous injection of round spermatid nuclei from mice and hamster oscillogen can initiate the normal development of mouse embryos. J Urol 158: 2006-2008.
5. Suzuki K, Yanagida K, Yanagimachi R (1998) Comparison of the media for isolation and storage of round spermatid nuclei before intracytoplasmic injection. J Assist Reprod Genet 15: 154-157.
6. Sasagawa I, Tateno T, Adachi Y, Kubota Y, Nakada T (1998) Round spermatids from prepubertal mouse testis can develop into normal offspring. J Androl 19: 196-200.
7. Sasagawa I, Tateno T, Yazawa H, Ichiyanagi O, Ishigooka M, et al. (1998) Round spermatids from hybrid sterile mice can initiate normal embryo development. Hum Reprod 13: 3099-3102.
8. Sakurai A, Oda S, Kuwabara Y, Miyazaki S (1999) Fertilization, embryonic development, and offspring from mouse eggs injected with round spermatids combined with Ca2+ oscillation-inducing sperm factor. Mol Hum Reprod 5: 132-138.
9. Meng X, Akutsu H, Schoene K, Reifsteck C, Fox EP, et al. (2002) Transgene insertion induced dominant male sterility and rescue of male fertility using round spermatid injection. Biol Reprod 66: 726-734.
10. Marh J, Tres LL, Yamazaki Y, Yanagimachi R, Kierszenbaum AL (2003) Mouse round spermatids developed in vitro from preexisting spermatocytes can produce normal offspring by nuclear injection into in

vivo-developed mature oocytes. Biol Reprod 69: 169-176.
11. Yanagimachi R, Wakayama T, Kishikawa H, Fimia GM, Monaco L, et al. (2004) Production of fertile offspring from genetically infertile male mice. Proc Natl Acad Sci U S A 101: 1691-1695.

Chapter 3

SILENCING MARKERS ARE RETAINED ON PERICENTRIC HETEROCHROMATIN DURING MURINE PRIMORDIAL GERM CELL DEVELOPMENT

Aristea Magaraki[1], Godfried van der Heijden[2], Esther Sleddens-Linkels[1],
Antoine H. F. M. Peters[3,4], Joost Gribnau[1], Willy M. Baarends[1*#] and Maureen Eijpe[1#]

Submitted

SILENCING MARKERS ARE RETAINED ON PERICENTRIC HETEROCHROMATIN DURING MURINE PRIMORDIAL GERM CELL DEVELOPMENT

Aristea Magaraki[1], Godfried van der Heijden[2], Esther Sleddens-Linkels[1], Antoine H. F. M. Peters[3,4], Joost Gribnau[1], Willy M. Baarends[1*#] and Maureen Eijpe[1#]

Author Affiliations:
[1]Department of Developmental Biology, Erasmus MC, University Medical Center, Rotterdam, the Netherlands
[2]Division of Reproductive Medicine, Department of Obstetrics and Gynecology, Erasmus MC, Rotterdam, The Netherlands
[3]Friedrich Miescher Institute for Biomedical Research (FMI), Basel, Switzerland
[4]Faculty of Sciences, University of Basel, Basel, Switzerland

#These authors contributed equally to this work
*Corresponding author:
Dr. Willy M. Baarends
e-mail: w.baarends@erasmusmc.nl

Abstract

Background

In the nuclei of most mammalian cells, pericentric heterochromatin is characterized by DNA methylation, histone modifications such as H3K9me3 and H4K20me3, and specific binding proteins like heterochromatin binding protein 1 isoforms (HP1 isoforms). Maintenance of this specialized chromatin structure is of great importance for genome integrity and for the controlled repression of the repetitive elements within the pericentric DNA sequence. Here we have studied histone modifications at pericentric heterochromatin during primordial germ cell (PGC) development using different fixation conditions and fluorescent immunohistochemical and immunocytochemical protocols.

Results

We observed that pericentric heterochromatin marks, such as H3K9me3, H4K20me3, and HP1 isoforms, were retained on pericentric heterochromatin throughout PGC development. However, the observed immunostaining patterns varied, depending on the fixation method, explaining previous findings of a general loss of pericentric heterochromatic features in PGCs. Also, in contrast to the general clustering of multiple pericentric regions and associated centromeres in DAPI dense regions in somatic cells, the pericentric regions of PGCs were organized as individual entities. We also observed a transient enrichment of the chromatin remodeler ATRX in pericentric regions in E11.5 PGCs. We did not detect transcription of major satellite repeats in PGCs.

Conclusion

These results indicate that even though the structure and organization of PGCs' pericentric heterochromatin differs from that of the surrounding somatic cells at E11.5, this is not associated with major changes in known histone modifications, as previously reported, or with derepression of transcription from pericentromeres, but may involve a specific function of ATRX.

Keywords

pericentric heterochromatin; primordial germ cell, centromere; histone modifications; H3K9me3; H4K20me3; ATRX; HP1; immunochemistry; major satellites

Background

Chromatin is composed of DNA, histones, and other tightly associated proteins. Modifications of the DNA and of histones, directly or indirectly control the regulation of DNA related processes like transcription. Globally, the chromatin in a nucleus can be functionally divided in active and accessible euchromatin, and inactive and condensed heterochromatin. Heterochromatin exists in two forms: facultative and constitutive heterochromatin. Facultative heterochromatin is a flexible form of heterochromatin and can be found in various chromosomal regions, when gene-coding regions need to be repressed. Its size varies from gene clusters to an entire chromosome (the inactive X in female cells). Facultative heterochromatin is frequently marked by specific histone modifications such as H2AK119Ub and H3K27me3, mediated by the Polycomb Repressor Complexes (PRC) 1 and 2, respectively. Constitutive heterochromatin forms at specific regions of the genome, which are characterized by arrays of tandem DNA repeats: at the centromeres (minor satellite repeats), telomeres (telomeric repeats), and at pericentric regions (major satellite repeats). Here we focus on the pericentric heterochromatin. A known hallmark of this chromatin type is the lack of histone modifications that generally mark active chromatin, such as histone acetylation. Conversely, there is an accumulation of repressive histone marks such as H3K9me3 and H4K20me3 (Rea et al. 2000; Peters et al. 2001; Lehnertz et al. 2003; Schotta et al. 2004; Kourmouli et al. 2004). The presence of H3K9me3 results in recruitment of different heterochromatin protein (HP) isoforms that contribute to heterochromatin establishment and maintenance of this chromatin state (Bannister et al. 2001; Lachner et al. 2003). The basic unit of the major satellites in the mouse is an A/T rich ~230bp long monomer, which can be repeated many times, leading to regions of up to several megabases in size. In an interphase mouse nucleus, pericentric constitutive heterochromatin can be visualized as 4', 6 – diamidino – 2 – phenylindole (DAPI) dense regions, termed chromocenters, with each chromocenter consisting of multiple pericentric regions from different chromosomes. The periphery of each chromocenter contains the centromeres of the chromosomes as individual entities (Guenatri et al. 2004).

Maintenance of the heterochromatic nature of pericentric DNA is important for proper cell functions; failure impairs cell viability, induces chromosomal instabilities and increases the risk of tumorigenesis (Peters et al. 2001). Therefore, pericentric heterochromatin has for a long time been considered as an inert, highly condensed and inaccessible domain. In recent years, however, it has become clear that the biology of pericentric heterochromatin is more complicated. Emerging evidence indicates that some well controlled dynamical changes of pericentric heterochromatin structure may occur, which are associated in some cases with brief bursts of major satellite transcription. Transcription of major satellites has been shown to occur during canonical cell processes, e.g. during the normal cell cycle (Lu & Gilbert 2007; Boyarchuk et al. 2014), cell differentiation (Terranova et al. 2005; Govin et al. 2007) and during early (Puschendorf et al. 2008; Casanova et al. 2013), and late (Rudert et al. 1995) embryonic development. For example in pre-implantation mouse embryos, the paternal pericentric domains initially lack heterochomatin marks, such as H3K9me3 and HP1 proteins. This likely relates to the fact that the paternal genome enters the oocyte as a protamine packaged compact structure, largely devoid of nucleosomes.

After fertilization, the DNA rapidly decondenses as protamines are removed and replaced by maternal histones that lack pericentric heterochromatin histone modifications (Santos et al. 2005; Torres-Padilla et al. 2006; van der Heijden 2005). Concomitantly, active DNA demethylation occurs (Santos et al. 2002; Santos & Dean 2004). In contrast, maternal pericentric heterochromatin displays the typical somatic histone posttranslational modification marks. Interestingly, major satellites are transcribed (in forward direction) solely from the paternal pronucleus at the 2-cell stage, which might reflect the above-described specific epigenetic status of the paternal genome (Albert & Peters 2009). Then, a burst in transcription of the major satellites (in reversed direction) from both parental genomes facilitates the reorganization of pericentric heterochromatin from nuclear precursor bodies to the typical somatic like chromocenters in the developing embryo. This is completed by the 4- to 8-cell stage after which pericentric heterochromatin displays its specific H3K9me3 – HP1 chromatin state (Probst et al. 2010; Casanova et al. 2013).

Developing mouse primordial germ cells (PGCs) also undergo genome-wide epigenetic reprogramming, and this occurs between E8.0 and E13.5. It includes changes in histone modifications (e.g. global loss of H3K9me2 and H3K27me3 enrichment as assessed by immunofluorescence experiments), reactivation of the inactive X chromosome in the female embryos and global loss of DNA methylation, the last reaching its lowest levels at E13.5, both in male and female embryos (Hackett et al. 2012; Hill et al. 2014). Initiation of imprint erasure in PGCs takes place between E10.5 and E11.5 (Hajkova et al. 2002; Kagiwada et al. 2013) and concomitantly it has been reported that PGCs lose the DAPI-dense chromocenters (Hajkova et al. 2008). These events are accompanied by a transient apparent loss of H3K9me3, HP1 proteins, and other heterochromatin marks (Hajkova et al. 2008).

In this study we focus specifically on the pericentric heterochromatin in germ cells between E10.5 and E13.5 of mouse embryo development. Since we experienced difficulties to reproduce the previously reported transient loss of pericentric heterochromatin marks (Hajkova et al. 2008), we decided to revisit the possible loss and re-establishment of pericentric heterochromatin marks and of chromocenters during PGC development, by testing different preparation methods and fixation conditions. It is well known that different fixation and preparation methods may lead to variations in immunostaining results, and these should thus be interpreted with caution. In particular the inability to detect a protein does not always result from its absence, but could be caused, for example, by epitope masking. Using a method that is known as ”drying down” or “spreading” of (meiotic) nuclei (Peters et al. 1997) we observed persistence of H3K9me3, HP1 isoforms and H4K20me3 on pericentric heterochromatin of PGCs. Based on these results we conclude that the reported loss and re-establishment of pericentric heterochromatin signature (Hajkova et al. 2008) may reflect a structural change in pericentric heterochromatin, affecting epitope availability, rather than the actual loss of the markers.

In addition, we found ATRX, a chromatin remodeler known to associate with constitutive heterochromatin (McDowell et al. 1999; Baumann et al. 2008), to be highly enriched at pericentric heterochromatin in PGCs at E11.5 compared to the somatic cells of the same developmental stage. Lastly, immunofluorescent analysis of centromere and pericentromere (adjacent to the centromeres) staining showed that pericentromeres do not cluster together in the same fashion as in the surrounding somatic cells, and this may explain the weak DAPI staining of pericentric heterochromatin in developing PGCs. Still, consistent with the overall persistence of histone modifications and the enrichment of ATRX, no transcription of major satellite repeats was detected in isolated E11.5 PGCs. Together, our data indicate that although the pericentric heterochromatin in E11.5 mouse PGCs may exist as a less condensed structure compared to the chromocenters in somatic cells, this phenomenon is neither associated with a complete loss of heterochromatin hallmarks nor a burst in transcription of major satellite repeats.

Results

H3K9me3 remains present in pericentric heterochromatin throughout germ cell-development

In somatic mouse interphase nuclei, pericentromere clusters can be visualized as large blocks, which colocalise with the DAPI dense regions, the chromocenters (Guenatri et al. 2004). Among the global epigenetic changes that accompany mouse PGC development between E8.0 and E13.5, it has been reported that there is a transient loss of the chromocenters at E11.5, accompanied by loss of H3K9me3 (Hajkova et al. 2008). We wished to study this phenomenon further, and therefore we first re-analysed the reported dynamics of H3K9me3 (Hajkova et al. 2008) in PGCs of E10.5 to E13.5 mouse embryos. For this, we used a fluorescent immunohistochemical approach. Since fixation conditions may influence epitope availability, we fixed and embedded embryos using different protocols. OCT4 (E10.5 and E11.5) or TRA98 (E13.5) were used as germ cell markers. For H3K9me3 staining, we did not observe any robust and reproducible staining pattern using paraffin-embedded tissue sections. In contrast, cryosectioning of paraformaldehyde fixed samples did produce the typical pattern of H3K9me3 enrichment in heterochromatin areas of somatic cells. Interestingly, using two different fixation protocols, one involving fixation only prior to freezing and embedding (regular fixation), and another protocol that included a post-fixation step after sectioning (extended fixation, see Methods for details), two different staining patterns were observed. Using both methods, the pattern of H3K9me3 immunostaining in PGCs was similar to that of surrounding somatic cells at E10.5, despite the overall DAPI weak appearance of the PGCs' chromocenters (Figure 1, panel A and B). Using the regular fixation procedure, we observed an overall reduction of H3K9me3 signal solely from E11.5 germ cells, in accordance with previous observations (Hajkova et al. 2008) (Figure 1, panel A). In contrast, when using extended fixation, H3K9me3 signal was retained on the pericentric heterochromatin as the PGCs developed between E10.5 and E13.5 (Figure 1, panel B). As an alternative approach, and to further ensure epitope availability, we used a drying-down, alias meiotic spread method that is commonly used to study the localization of chromatin modifications and associated proteins in nuclei of meiotic prophase cells (Peters et al. 1997). It involves mixing of a cell suspension on a glass slide covered with a Triton-X100-containing fixative, followed by gradual drying, whereby the nuclei spread on glass. The spreading results in loss of most cytoplasmic and loosely DNA associated proteins, and flattening of the nuclear chromatin. Therefore, we will further refer to this type of preparation as nuclear spreads. We prepared slides containing nuclei from E10.5 and E11.5 gonadal regions and from E13.5 male and female gonads. Similar to the results obtained with the extended fixation protocol, H3K9me3 signal was retained in the pericentric heterochromatin of PGCs from E10.5 to E13.5 (Figure 1, panel C), indicating that there is no major loss of H3K9me3 from the pericentric regions in E11.5 PGCs. Lastly, in accordance with Kagiwada et al. (2013), we did not observe complete loss of the DAPI dense regions at any of the examined stages in all protocols tested, but the regions appeared less DAPI intense and at the same time smaller and less dense. This indicates that there may be some difference between the pericentric chromatin structure of PGCs and somatic cells. Importantly, our results indicate that previously reported absence of pericentric heterochromatin marks in E11.5 PGCs might be a consequence of the chosen experimental methodology.

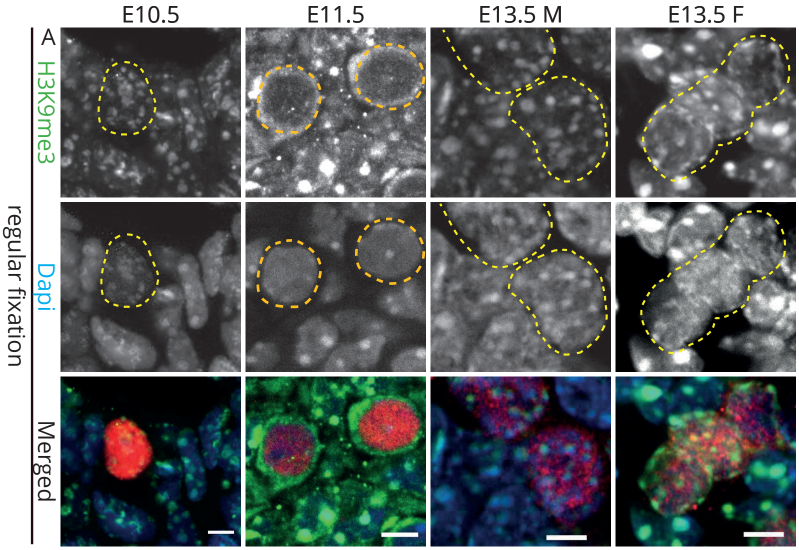

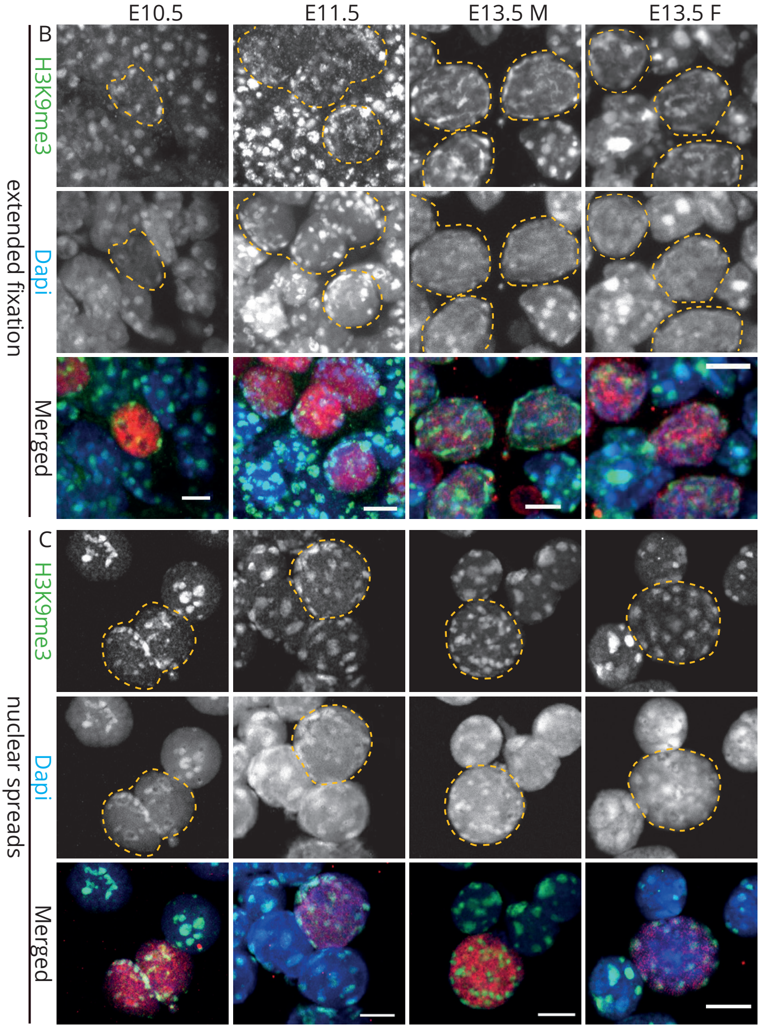

Figure 1: H3K9me3 persists on pericentric heterochromatin throughout germ cell development

A Immunofluorescent analysis of H3K9me3 (green) in cryosections of E10.5 and E11.5 trunks containing germ cells, and of E13.5 male and female gonads using the regular fixation protocol. H3K9me3 staining is present in DAPI (blue) dense regions of E10.5 PGCs and somatic cells. At E11.5 H3K9me3 transiently disappears from pericentric heterochromatin of E11.5 PGCs only. Thereafter, H3K9me3 returns in E13.5 DAPI dense regions. **B** Using extended fixation, H3K9me3 is retained in DAPI dense regions of PGCs and somatic cells in all embryonic stages examined. **C** Similar to **B**, H3K9me3 remains present in pericentric heterochromatin when nuclear spreads are used. E10.5 and E11.5 germ cells are marked with OCT4 (red), while E13.5 germ cells are marked with TRA98 (red). Using regular or extended fixation, two embryos or gonads were analysed per stage, and at least 20 PGC nuclei were recorded. Four or more embryo trunks or gonads were pooled for the nuclear spread preparations and at least 30 PGC nuclei were recorded. Representative germ cells are marked with yellow dashed circles. Scale bars represent 5μm in panels **A** and **B** (sections), and 10μm in panel **C** (nuclear spread).

HP1 isoforms are stably recruited to pericentric heterochromatin of developing germ cells

Specific histone modifications recruit certain proteins. Members of the Heterochromatin Protein 1 (HP1) protein family bind H3K9me3 and mark constitutive heterochromatin. In mammals, there are three different HP1 isoforms: HP1α, HP1β and HP1γ also known as CBX5, CBX3, and CBX1, respectively. We examined the localization of these three isoforms during PGC development. In the regular fixation protocol and using paraffin sections, HP1α immunostaining marked pericentric heterochromatin in E10.5 PGCs. Already at this stage, the signal for HP1α appeared lower in PGCs compared to surrounding somatic cells. Thereafter, HP1α was undetectable in developing germ cells (Additional file 1, panel A), which is in accordance with Haijkova et al., (2008). Using extended fixation conditions, HP1α signal appeared to be reduced (E10.5, E11.5 some PGCs, E13.5 female germ cells) or absent (E11.5 some PGCs, E13.5 male germ cells). It should be noted that in E13.5 male gonad sections, we could not reproducibly detect HP1α even in the surrounding somatic cells of sections, using either regular or extended fixation protocols (Additional file 1, panel A and B). This may be due to the different consistency of the male versus the female gonad at this age, causing differential and variable effects of the fixation protocols. When nuclear spreads from genital ridges or embryonic gonads were examined, HP1α immunostaining was readily detectable in DAPI dense regions of all cells, and appeared to be very similar in PGCs and surrounding somatic cells in all developmental stages examined (Figure 2, panel A).

Like HP1α, HP1β is also known to predominantly localize to heterochromatin. When we use our regular fixation protocol we observed accumulation of HP1β signal in DAPI dense regions of both somatic and germ cell nuclei at E10.5 and E11.5 stages. However, at E13.5, hardly any enrichment was observed in the DAPI dense regions of both in male and female germ cells (Additional file 2, panel A). Following extended fixation, HP1β signal was preserved on pericentric heterochromatin in all developmental germ cell stages examined (Additional file 2, panel B), similar to what was observed in nuclear spread preparations, where the levels of HP1β staining were comparable between germ and somatic cells at all stages examined (Figure 2, panel B).

The last HP1 isoform, HP1γ, is known to interact both with constitutive heterochromatin and euchromatin (Takada et al. 2011; Smallwood et al. 2012; Vakoc et al. 2005). Examination of HP1γ in nuclear spreads revealed a clear immunostaining signal for this HP1 isoform in DAPI dense regions in the nuclei of germ cells throughout development, with HP1γ levels appearing similar between the nuclei of the soma and the germline in E10.5 and E13.5 germ cells. HP1γ signal seemed more enriched at pericentric heterochromatic regions of E11.5 PGCs compared to those of the somatic cells (Figure 2, panel C). Comparable results were obtained upon regular or extended fixation in paraffin sections of E10.5, E11.5 genital ridges and of E13.5 female gonads. However, at the stage of E13.5 male development, detection of HP1γ in the surrounding somatic cells of paraffin sections, was difficult and variable, using either our regular or extended fixation protocol. This was similar to our HP1α results. We could detect accumulation of HP1γ in DAPI dense regions in some E13.5 male germ cells (Additional file 3, panel A and B, arrowhead), but not in all. Taken together, the observed localisation patterns of the HP1 isoforms during PGC development are consistent with the results obtained for H3K9me3, the histone modification that recruits the HP1 proteins. Therefore, HP1 isoforms remain on PHC of PGCs.

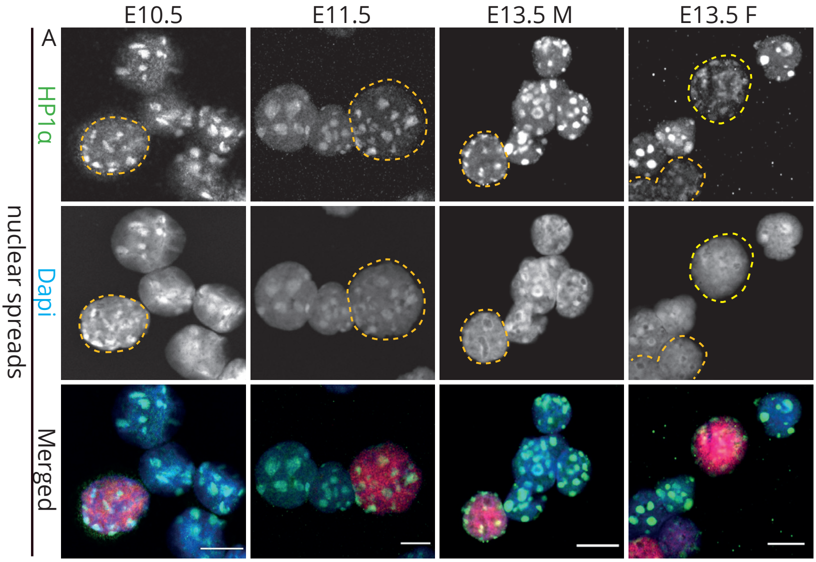

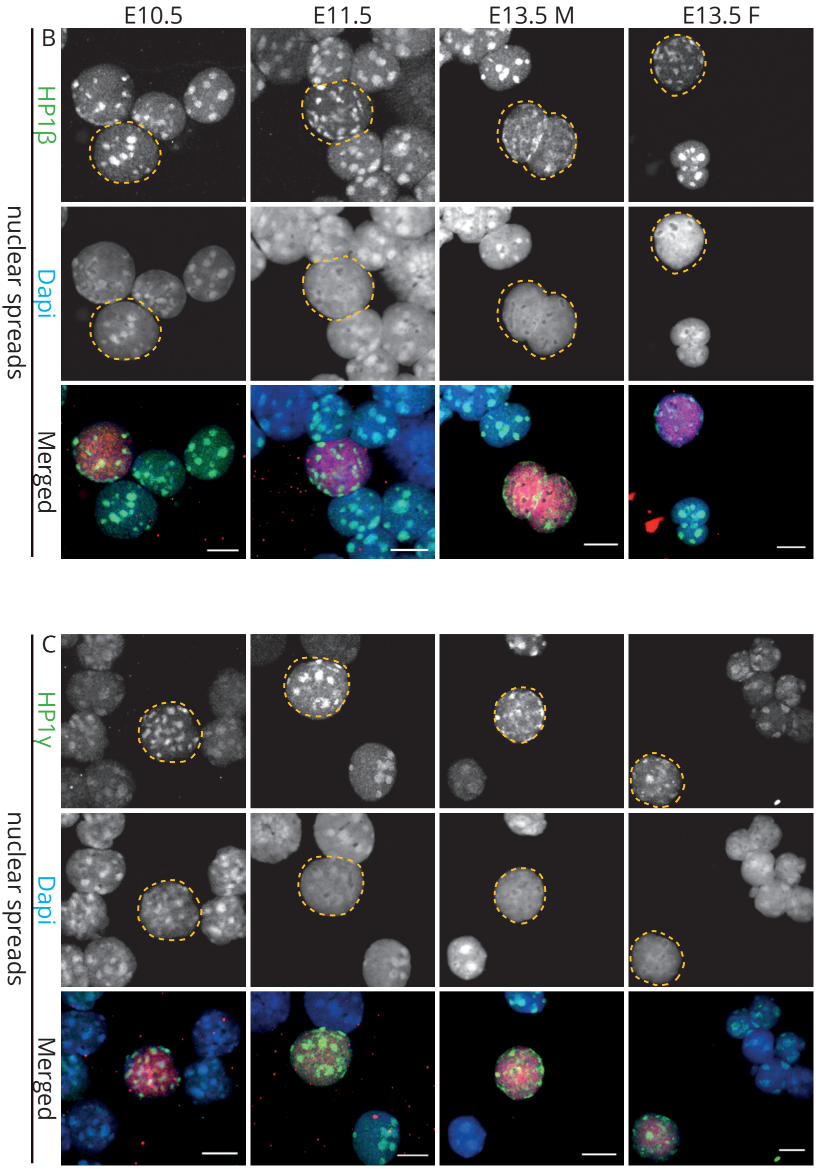
E10.5
E11.5
E13.5 M
E13.5 F
B
HP1β
Dapi
Merged
nuclear spreads
C
HP1γ
Dapi
Merged
nuclear spreads

Figure 2: HP1 isoforms are recruited to pericentric heterochromatin in E10.5 to E13.5 germ cells

A Nuclear spread preparations from E10.5, E11.5 embryos and from E13.5 male and female gonads were stained for HP1α (green). The pericentric heterochromatin of germ cells was always decorated with HP1α. **B** Similar to HP1α, HP1β (green) was always present in DAPI (blue) dense regions of germ cells in all stages examined. **C** The last HP1 isoform, HP1γ (green), is also stably recruited to pericentric heterochromatin of PGCs, in the three stages examined, but at E11.5 the levels of HP1γ seem higher at pericentric heterochromatin of PGCs compared to the somatic nuclei. E10.5 and E11.5 germ cells were identified by OCT4 (red), and E13.5 germ cells with TRA98 (red). For the spread preparations at least three embryos trunks or gonads were pooled and at least 30 PGC nuclei were recorded per stage for each HP1 isoform. Representative germ cells are marked with yellow dashed circles. Scale bars represent 10μm.

H4K20me3 is retained at pericentric heterochromatin of E11.5 PGCs

An additional histone mark that participates in the establishment of pericentric heterochromatin is H4K20me3 (Schotta et al. 2004; Kourmouli et al. 2004). This histone modification is mediated by the histone methyltransferase Suv4-20h2 in a Suv39h and HP1 dependent manner (Kourmouli et al. 2004). Suv39h is the enzyme responsible for establishing tri-methylation of H3K9 (Peters et al. 2001). Similar to H3K9me3, H4K20me3 is strongly enriched at DAPI dense regions (Kourmouli et al. 2004; Schotta et al. 2004). Again we performed comparative immunofluorescence in sections processed with regular and extended fixation, and in nuclear spreads. When using the regular fixation procedure on paraffin embedded embryo sections, H4K20me3 signal intensity appeared similar in developing PGCs and surrounding somatic cells at E10.5 (Figure 3, panel A). However, at E11.5 the immunostaining signal for this histone modification transiently disappeared from the DAPI dense chromocenters of the PGCs only, while it was strongly retained in the surrounding somatic cells (Figure 3, panel A). Two days later, at ~E13.5, H4K20me3 signal re-appeared, albeit at low levels compared to the surrounding soma and only in some TRA98 (red) positive cells, regardless of the embryo sex. When using the extended fixation protocol, H4K20me3 signal was retained throughout PGCs' development, but clearly reduced in the PGCs compared to the surrounding somatic cells at E11.5-E13.5 (Figure 3, panel B). Lastly, upon analysis of nuclear spread preparations, H4K20me3 signal was also retained on pericentric hererochromatin of PGCs in all stages examined. Here, the amount of signal for this histone modification also seemed to be somewhat reduced compared to that of the surrounding somatic cells at the two later stages (E11.5 & E13.5; Figure 3, panel C). Therefore, similar to H3K9me3, H4K20me3 did not transiently disappear from the DAPI dense regions of E11.5 PGCs. Nonetheless, its overall levels seemed to be reduced in the germ cells compared to the surrounding soma from that stage onwards. This indicates that a change in this modification accompanies the overall remodeling process of the chromatin in PGCs and contributes to the difference in epigenetic pericentric structure between germ cells and somatic cells.

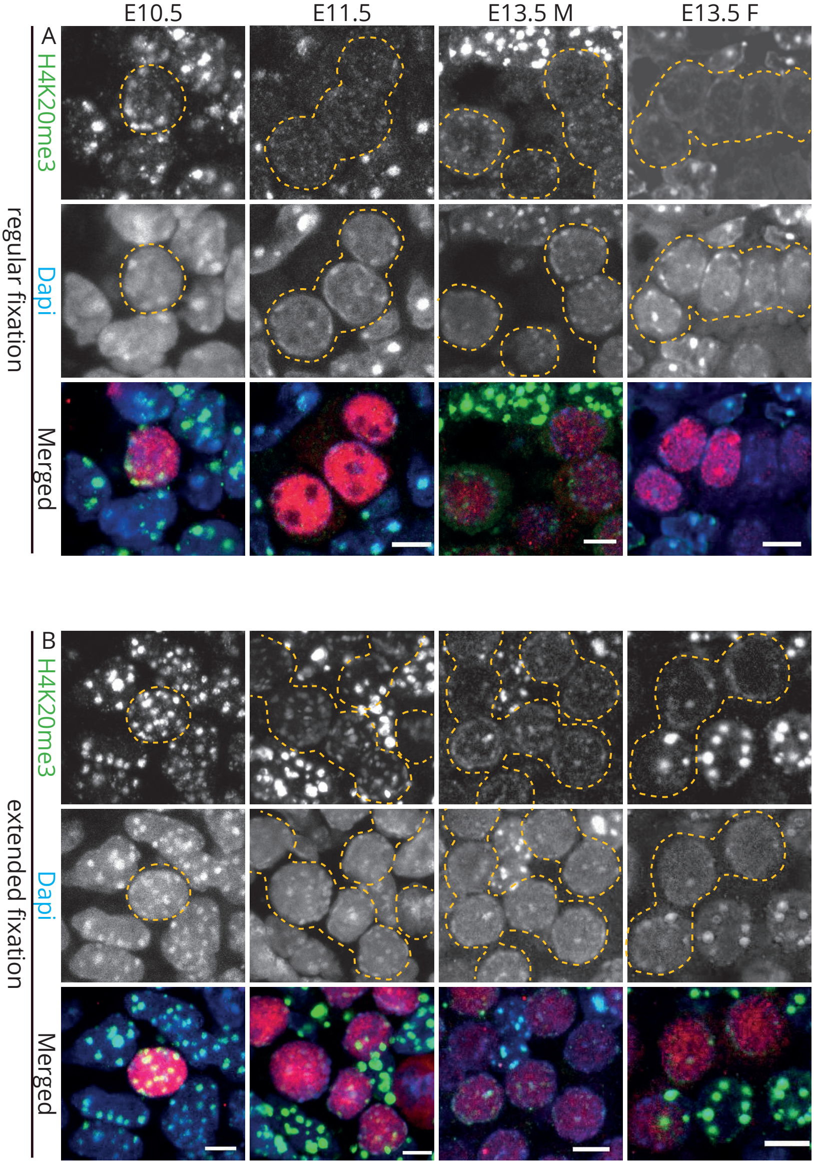
E10.5
E11.5
E13.5 M
E13.5 F
A
H4K20me3
Dapi
Merged
regular fixation
B
H4K20me3
Dapi
Merged
extended fixation

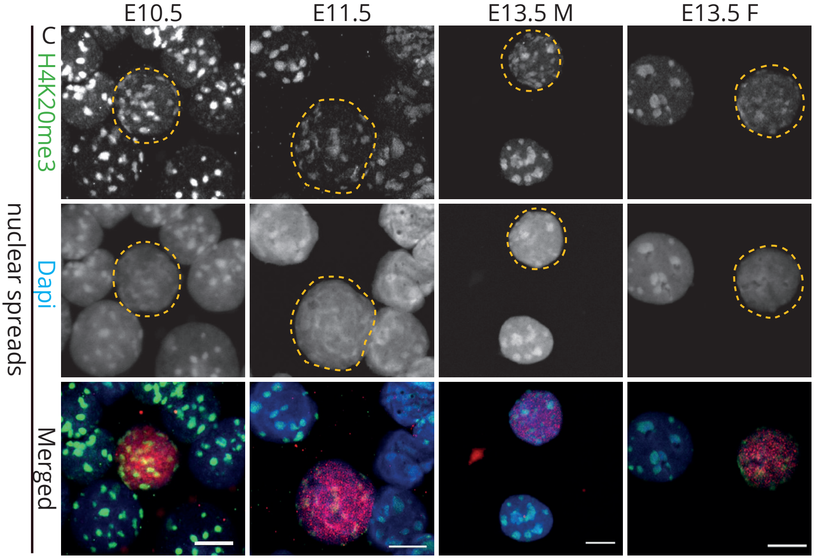

Figure 3: H4K20me3 is present in pericentric heterochromatin of developing germ cells

A Paraffin sections of E10.5 and E11.5 embryo trunks and of E13.5 male and female gonads were immunostained using anti-H4K20me3 (green) after applying the regular fixation protocol. At E10.5 H4K20me3 is present in pericentric heterochromatin of PGCs and surrounding soma. At E11.5, H4K20me3 is lost from DAPI (blue) dense regions of PGCs, while it is maintained in the somatic cells. At E13.5 H4K20me3 re-appears in some germ cells, but in substantially reduced levels compared to the surrounding gonadal somatic cells. **B** When applying the extended fixation protocol, H4K20me3 is retained at pericentric heterochromatin in PGC nuclei from E10.5 to E13.5. However, when compared to the H4K20me3 pattern in the surrounding somatic cells, the levels are somewhat reduced. **C** Similar to the extended fixation protocol, H4K20me3 enrichment at pericentric heterochromatin is retained in PGCs throughout germ cell development when analysed on nuclear spread preparations. From E11.5 onwards the levels of H4K20me3 seem to be reduced in PGCs compared to surrounding somatic cells. E10.5 and E11.5 germ cells were identified by OCT4 (red), and E13.5 germ cells with TRA98 (red). Using regular or extended fixation, two embryos or gonads were analysed per stage, and at least 20 PGC nuclei were recorded. Three or more embryo trunks or gonads were pooled for the nuclear spread preparations and at least 30 PGC nuclei were recorded. Representative germ cells are marked with yellow dashed circles. Scale bars represent 5μm in panels **A** and **B** (sections), and 10μm in panel **C** (nuclear spreads).

ATRX is enriched in pericentric heterochromatin of germ cells

The α-thalassemia mental retardation X-linked protein ATRX is a chromatin remodeler and a prominent marker of pericentric heterochromatin in somatic cells, in the mouse zygote and in neonatal spermatogonia (McDowell et al. 1999; Ishov et al. 2004; De La Fuente et al. 2015; Baumann et al. 2008). We explored the presence of ATRX in developing germ cells, only in nuclear spread preparations, since we observed that this protocol yielded the most reproducible results. At E10.5, the levels of ATRX in germ cells seemed to be similar to those of the somatic cells. Interestingly, in the germ cells of E11.5, ATRX immunostaining was increased in pericentric heterochromatin compared to that of the soma. At E13.5, ATRX levels were comparable to those of the gonadal somatic cells again (Figure 4, panel A). We did not observe any re-localisation of ATRX to the nuclear periphery in any of the E11.5 germ cells examined, in contrast to what was previously reported (Hajkova et al. 2008).

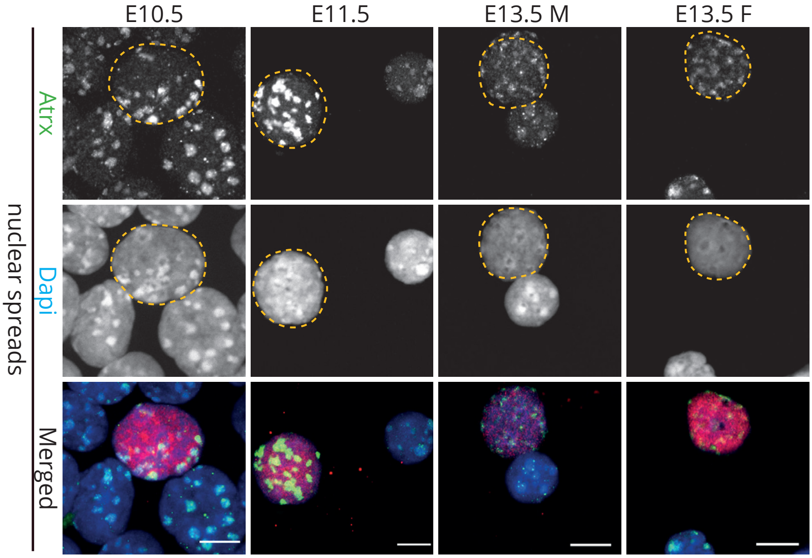

Figure 4: ATRX is enriched at pericentric heterochromatin of E11.5 PGCs

Analysis of ATRX (green) localisation patterns in nuclear spread preparations of E10.5 and E11.5 embryo trunks and E13.5 male and female gonads. ATRX is enriched at pericentric heterochromatin of germ and somatic cells in all stages examined. At E11.5, ATRX levels seem to be higher in PGCs compared to the surrounding somatic cells, while at E10.5 and E13.5 the levels of ATRX are comparable between germ cell and somatic nuclei. For the nuclear spread preparations at least three embryo trunks or gonads were pooled and at least 30 PGC nuclei were recorded. Representative germ cells are marked with yellow dashed circles. Scale bars represent 10μm.

Spatial organization of constitutive heterochromatin in germ cells

In order to examine the organisation of the chromocenters during germ cell development more globally, we stained nuclear spreads of all developmental stages examined within this study with CREST antisera, a marker of chromosome centromeres. Additionally, we used H4K20me3 to visualize the pericentric heterochromatin. In somatic cells the chromocenters consisted of more than one pericentric domain, as indicated by the multiple CREST signals within the DAPI dense (or H4K20me3 enriched) regions. This organisation reflects the clustering of groups of pericentromeres, which is a common hallmark of chromocenters (Guenatri et al. 2004). However, already at E10.5, we observed a large number of individual pericentric regions, containing only a single CREST signal, within the nucleus of germ cells (Figure 4, panel B, examples pointed with arrowheads). This observation may explain the size, number and intensity differences between the DAPI dense regions in germ cell versus somatic cell nuclei. This type of autonomous pericentromere organization persisted during subsequent stages of primordial germ cell development. Thus, we demonstrate that the organization of the chromocenters in E10.5-E13.5 PGCs is different compared to that of the somatic surrounding cells. A summary of all immunostaining results is presented in Table 1.

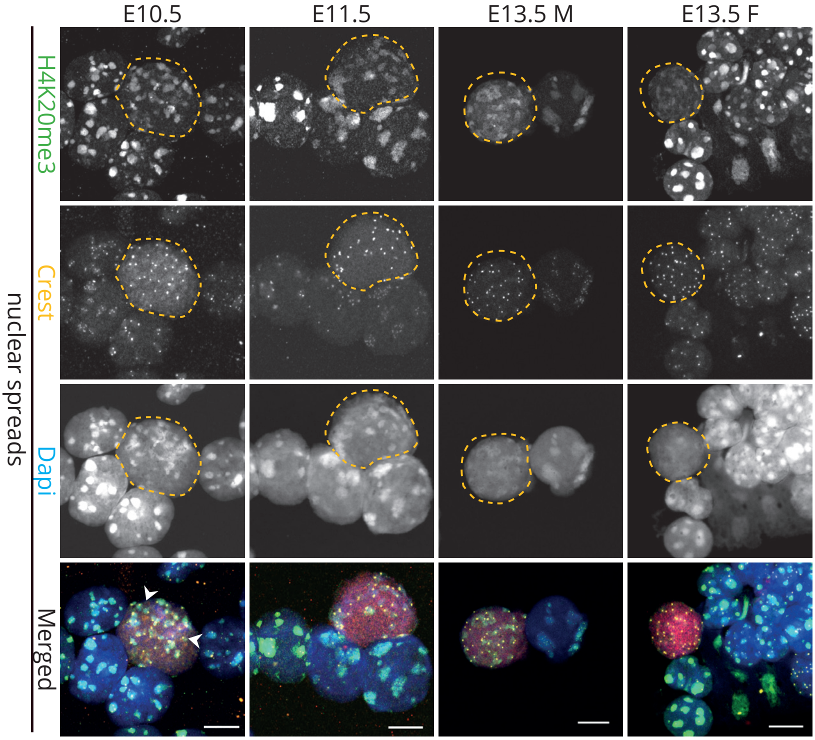

Figure 5: Chromocenters dissociate during germ cell development

Nuclear spread preparations were immunostained for CREST (yellow) and H4K20me3 (green). At E10.5, many small sized chromocenters (identified by DAPI (blue) and H4K20me3 enrichment) and their corresponding CREST signals can be observed in the PGCs. Examples of pericentric regions containining only a single CREST focus are indicated by arrowheads. This pattern of dispersed pericentric heterochromatin organisation in germ cells, as opposed to the clustering of pericentric heterochromatin regions and associated centromeres in somatic cells, is observed until E13.5. Germ cells were identified by the presence of OCT4 (red, E10.5 and E11.5), or TRA98 (red, E13.5). For the nuclear spread preparations at least three embryo trunks or gonads were pooled and at least 30 PGC nuclei were recorded. Representative germ cells are marked with yellow dashed circles. Scale bars represent 10µm.

Table 1: Summary of the immunosignals at pericentric heterochromatin of PGCs

	4% PFA (regular) paraffin	**4% PFA (extended) paraffin**	**4% PFA (regular) cryo**	**4% PFA (extended) cryo**	**1% PFA nuclear spreads**
H3K9me3	No signal	No signal	+E10.5 -E11.5 +E13.5♂ +E13.5♀	+E10.5 +E11.5 +E13.5♂ +E13.5♀	+E10.5 +E11.5 +E13.5♂ +E13.5♀
HP1α	+E10.5 -E11.5 -E13.5♂ -E13.5♀	+E10.5 *E11.5 -E13.5♂ +E13.5♀	n.d.	n.d.	+E10.5 +E11.5 +E13.5♂ +E13.5♀
HP1β	+E10.5 +E11.5 -E13.5♂ -E13.5♀	+E10.5 +E11.5 +E13.5♂ +E13.5♀	n.d.	n.d.	+E10.5 +E11.5 +E13.5♂ +E13.5♀
HP1γ	+E10.5 +E11.5 *E13.5♂ +E13.5♀	+E10.5 +E11.5 +E13.5♂ +E13.5♀	n.d.	n.d.	+E10.5 +E11.5 +E13.5♂ +E13.5♀
H4K20me3	+E10.5 -E11.5 *E13.5♂ *E13.5♀	+E10.5 +E11.5 +E13.5♂ +E13.5♀	n.d.	n.d.	+E10.5 +E11.5 +E13.5♂ +E13.5♀

The table displays whether a certain histone modification or chromatin binding protein at the pericentric heterochromatin is detected (+), not detected (-) or detected in some but not all (*) PGC nuclei at the embryonic stages indicated. Differences in the degree of enrichment between the pericentric heterochromatin of PGCs and somatic cells are not taken into account. n.d.: not determined

Major satellites are not transcribed in E11.5 murine PGCs

In order to examine if the altered organisation of the chromocenters during PGC development is associated with reduced transcriptional repression of major satellites, we FACS-sorted PGCs and somatic cells from developing gonads isolated from E11.5 embryos carrying a transgene encoding GFP under the control of the *Oct4* promoter. We isolated RNA and analysed expression of major satellite repeats. In addition, we analysed *Atrx*, *Oct4* and *Canx* gene expression. *Oct4* expression was detected only in the purified

GFP-positive germ cell fraction and was negligible in the GFP-negative somatic cells, confirming the success of our sorting strategy (Figure 6, A). We used *Canx* as a reference gene for our analysis, since it has been reported to have more stable expression compared to commonly used housekeeping genes, like *Actb* and *Gapdh*, between germ and somatic cells (van den Bergen et al. 2009). From the results of this analysis we conclude that although there is a enrichment of *Oct4* and *Atrx* mRNA in the E11.5 PGC fraction (Figure 6, A and B), in accordance with our immunocytochemical observations, no specific signal for major satellite RNA transcripts above the DNA contamination background (-RT) can be observed in both cell fractions (Figure 6, C). Reverse transcriptase controls (-RT) for the single-copy genes that were examined were always negative. To confirm the absence of major satellite transcription, we repeated the FACS-sorting experiment and included major satellite expressing NIH-3T3 cells as a positive control, this time using a slightly different protocol (see Methods). The results again indicate that there are no major satellite transcripts in the PGC or soma fraction, while they could be detected in NIH-3T3 cells (Additional file 4), as can be inferred from the ~5 cycles difference between Ct values of the +RT and – RT experiments.

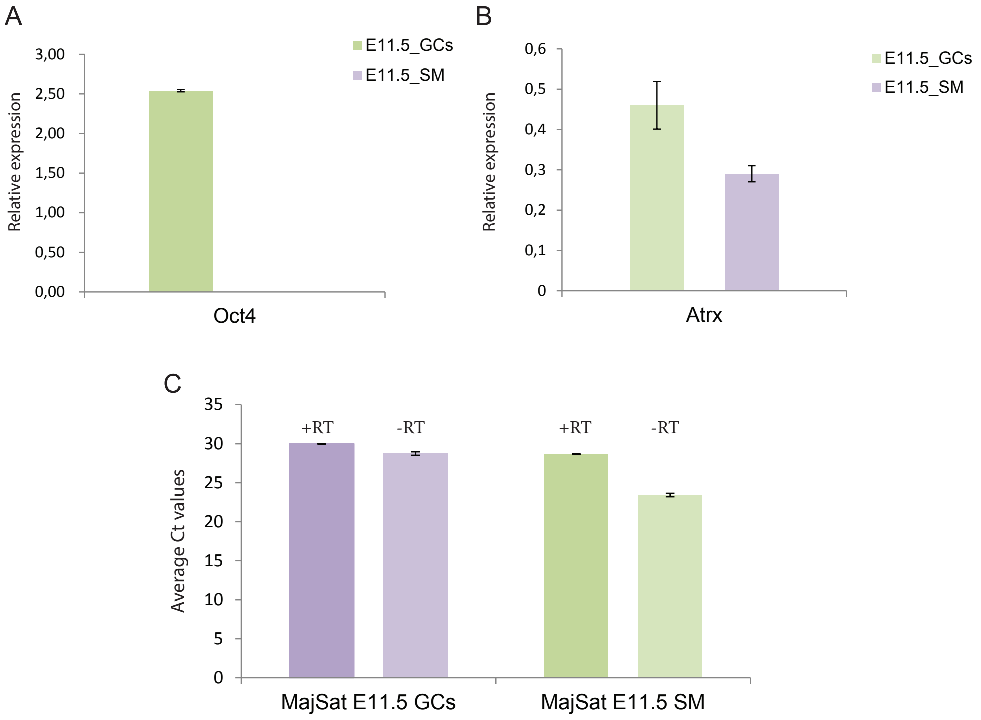

Figure 6: *Atrx* is more highly expressed in E11.5 PGCs compared to the soma, and no major satellite transcription is detected in either cell fraction

A Normalized expression values derived from qRT-PCR of E11.5 sorted OCT4-GFP positive (E11.5_GCs) and negative (E11.5_SM) cells, show that expression of *Oct4* and **B** *Atrx* is higher in PGCs compared to the soma. **C** Ct values aveage obtained after qRT-PCR of major satellites in OCT4-GFP positive (E11.5 GCs) and negative (E11.5 SM) cells shows that no transcription of major satellites above the background levels (lower Ct values in negative control (-RT)) could be detected in both E11.5 somatic and germ cells. E11.5_GCs and E11.5_SM correspond to the sorted PGC and somatic cell populations respectively. Error bars represent standard deviations within triplicates of one biological experiment.

Discussion

At the time of their specification, PGCs are epigenetically identical to the surrounding epiblast, and therefore primed towards a somatic fate [38, 39]. In order to activate their germ cell transcriptional network and at the same time repress their somatic fate, PGCs go through a series of extensive reprogramming events, which have been thoroughly characterized. The reprogramming encompasses DNA demethylation at several genomic loci, including the imprinted genes, but also involves changes in histone modifications (Hajkova et al. 2002; Seki et al. 2005; Seki et al. 2007; Kagiwada et al. 2013). An additional reprogramming cycle has been reported to take place specifically at E11.5, when many histone modifications are transiently lost, including those marking constitutive heterochromatin and its readers (Hajkova et al. 2008).

In our study, we carefully re-evaluated epigenetic remodeling targeting specifically constitutive heterochromatin from the period when PGCs enter the genital ridges (Molyneaux et al. 2001) -that is E10.5- until E13.5. At this time female germ cells enter meiosis, while male germ cells continue to be mitotically active until E15.5 (Yoshioka et al. 2009). Taking into account that epitope availability can be compromised under certain fixation conditions we decided to test different preparation and fixation protocols. Indeed, when using our regular fixation protocol in sections, we observed loss of constitutive heterochromatin marks such as H3K9me3, H4K20me3 and HP1α exclusively in the germ cell nuclei at E11.5. In striking contrast, upon extended fixation in sections, and in nuclear spread preparations, loss of these marks could not be reproduced. We obtained the most consistent results using nuclear spread preparations. This type of single cell methodology may in this case be superior to the former two, due to a better penetrance of the fixative and/or of the antibodies to the spread chromatin (Baarends et al. 2005; van der Heijden et al. 2005). In addition, loss of proteins that localise to the nucleoplasm and cytoplasm, and loss of proteins that are loosely associated with chromatin, may reduce the background signals, when histone modifications are studied. Previous studies used cytospin preparations to examine reprogramming taking place in germ cells (Hajkova et al. 2008). The discrepancy between our results using nuclear spreads and these results using whole fixed cells, may thus be attributed to higher background signals or reduced epitope accessibility in a more three-dimensional environment, whereby structural cellular and nuclear components such as membrane and matrix are still present. In support of our results, previous studies (Kagiwada et al. 2013) could also not reproduce chromatin changes of H1 linker histone or loss of H3K27me3 at E11.5 reported by Hajkova et al. (2008). This again illustrates that testing different experimental methodologies is important in order to correctly understand and characterize epigenetic phenomena during different developmental states. In addition, somite counting at these early stages of development is a prerequisite for consistent developmental staging of the different embryos examined, to reduce inter-individual variability, and thus improve reproducibility. From our findings it appears that neither H3K9me3 nor the HP1 proteins are lost from pericentric heterochromatin in PGCs between developmental stages E11.5 and E13.5 in mouse. H4K20me3 may be somewhat reduced between E11.5 and E13.5, but is also still enriched at pericentric sites compared to the surrounding euchromatin. In light of our observations, it would also be interesting to re-examine if H3K64me3, a newly identified histone modification marking constitutive heterochromatin, is truly absent from E12.0 to E13.5 germ cells as has been reported (Daujat et al. 2009). For this immunolocalization study, cryosections of embryo trunks and gonads were used, using a protocol very similar to our own regular fixation protocol (Daujat et al. 2009). As our results suggest, such a protocol may not be suitable for answering constitutive heterochromatin localization questions, since somehow epitopes may be masked.

Interestingly, our results show that ATRX, a chromatin remodeler and crucial factor for heterochromatin formation (McDowell et al. 1999; Sadic et al. 2015), is maintained on pericentric heterochromatin throughout germ cell development. In addition, ATRX is enhanced in these locations of E11.5 PGCs compared to the surrounding somatic cells. Importantly, ATRX has been reported to transcriptionally block expression of major satellites from the maternal genome in the mouse zygote (De La Fuente et al. 2015). At this stage, in the early zygote, the maternal pericentromeres are labelled with the classical somatic histone modifications, while these marks are absent from the paternal genome, where transcription of major satellites has been recorded (Puschendorf et al. 2008). In addition, studies in embryonic stem cells report that ATRX, together with the histone chaperone DAXX, safeguard the genome against expression of tandem repeats, even when DNA methylation levels are absent at those regions (He et al. 2015). Thus, in PGCs ATRX may also perform such a repressive function. It has been described that DNA methylation at pericentromeres is gradually replaced by 5-hydroxylmethylation and this DNA modification has also been suggested to mediate transcriptional repression from those repeats (Yamaguchi et al. 2013). Therefore, it is possible that more than one mechanism exists for silencing major satellite transcription in germ cells. In our study, we were unable to detect a burst in transcription of major satellites at E11.5 PGCs. Taking into account that the vital players of constitutive heterochromatin are continuously present and that ATRX is enriched at pericentric repeats of E11.5 PGCs, we dispute that expression of major satellite repeats takes place in these cells, in a fashion similar to what has been observed in the mouse pre-implantation embryos.

Nevertheless, analyses of the general distribution pattern of centromeres and adjacent pericentric heterochromatin revealed that there is a different organization of constitutive heterochromatin in germ cells compared to the surrounding somatic cells. Specifically, germ cells lack organization of their pericentromeres into chromocenters. This may be a natural consequence of germ cell development as they move from a somatic fate towards the more stem cell-like fate of a primordial germ cell and eventually towards the gonocyte. A similar phenomenon of a more dispersed constitutive heterochromatin has been described to take place upon reprogramming of mouse embryonic fibroblasts towards induced pluripotent stem cells, but also in the Nanog-positive cells of the inner cell mass of developing blastocysts (Fussner et al. 2011). In addition, DAPI rich regions appear to spread upon induction of embryonic stem cells towards 2-cell stage-like cells (Ishiuchi et al. 2015). Conversely, when cells differentiate, chromocenters appear to cluster. For example, when male germ cells reach their ultimate differentiated state in mouse adult testes, all chromocenters fuse into a single chromocenter in the nucleus of round, elongating and condensed spermatid (Govin et al. 2007). In addition, differentiation of myoblasts towards myocytes is also accompanied by centromere clustering and chromocenter formation, as well as further enrichment of H3K9me3 and H4K20me3. This differentiation is accompanied with transcriptional activation of major and minor satellite repeats (Terranova et al. 2005).

Conclusion

The present study reveals that pericentric heterochromatin organization in the embryonic PGC nucleus has changed dramatically from a clustered pattern into individual distribution, but retains the known hallmarks of heterochromatin are still present. In addition, ATRX, in combination with other mechanisms, may provide an extra level of protection against expression of major satellite transcripts. The observed changes in pericentric chromatin organization could be related to the transition of the germ cells from a somatic fate towards a stem cell-like one.

Methods

Collection of mouse embryos for immunofluorescence and immunocytochemistry

Female DBA2 mice were mated with C57BL/6 males to produce F1 fetuses. Mating was confirmed the next morning by the presence of a vaginal plug and recorded as E0.5. At E10.5, E11.5 and E13.5, embryos were dissected out of the uteri and were assessed for somite counting. We scored embryos with 34-36 somites as E10.5, 44-47 somites as E11.5. We could not determine with precision the somite number at E13.5 (60-62 somites), due to the advanced developmental stage of the embryo. Embryos were kept in ice cold PBS at all times, before any further processing.

Tissue processing for immunofluorescence and immunocytochemistry

After embryo isolation from the uteri, embryo regions containing the developing germ cells were dissected from E10.5 and E11.5 embryos. Gonads were isolated from the E13.5 embryos and the sex was determined by morphology. E10.5 and E11.5 gonadal regions were fixed in ice cold 4% PFA for 2 hours and 3 hours respectively, followed by consecutive washes in PBS. Gonads were fixed for 1.5 hours in ice cold 4% PFA. Tissues were then processed for O.C.T. or paraffin embedding using standard histology procedures. Cryo- and paraffin sections were 10μm and 5μm respectively.

For the regular and extended fixation, sections were fixed for an additional 10 minutes at room temperature or for 30 minutes at 37^o C, respectively, followed by brief PBS washes. The fixation step was performed after the O.C.T. or paraffin was removed from the sections.

Drying-down or nuclear spread preparations of germ cells

Embryo trunks containing the germ cells from E10.5, E11.5 and gonads from E13.5 embryos were dissected, pooled as indicated in figure legends, and incubated in 500μl TrypLE™ Express (ThermoFisher Scientific) for 6 minutes at 37o C. Dissociation was followed by two washes with 5% FBS in PBS. Spreads of nuclei for immunocytochemistry were obtained as described by Peters et al. (1997).

Immunohistochemistry and immunocytochemistry

Heat-mediated (900W in a microwave for 20 minutes) epitope retrieval in citrate buffer pH=6 was performed on paraffin sections. The following staining protocol was performed in all samples. Sections and nuclear spreads were blocked with 2% BSA, 5% donkey serum in PBS (blocking solution) for 30 minutes at room temperature, followed by primary antibody incubation, diluted in blocking solution, at 4° C overnight in a humid chamber. The next day, slides were washed in PBS (3x5 minutes) and blocked with secondary antibodies, diluted in blocking buffer, for 1 hour at room temperature, in a humid chamber. Slides were then washed in PBS (3x5 minutes) and mounted with ProLong® Gold Antifade Mountant with Dapi (ThermoFisher Scientific). Confocal imaging was performed on a Zeiss LSM700 microscope (Carl Zeiss, Jena). In this study the following primary antibodies were used: goat anti-OCT3/4 (N-19) by Santa Cruz (sc-8628) diluted 1:800 for sections and 1:50 for spread preparations, rabbit anti-OCT4 by Abcam (ab19857) diluted 1:250 for sections and 1:50 for spread preparations, rat anti-TRA98 by Abcam (ab82527, 1:500), rabbit anti-DDX4/MVH by Abcam (ab13840, 1:300), anti- rabbit H3K9me3 by Abcam (ab8898, 1:300), rabbit anti-H4K20me3 diluted 1:300 [49], goat anti-HP1α by Abcam (ab77256) diluted 1:200 for sections and 1:400 for spread preparations, mouse anti-HP1β by Abcam (ab10478, 1:200), rabbit anti-HP1γ by Abcam (ab10480, 1:200) and rabbit anti-ATRX (H-300) by Santa Cruz (sc-15408) 1:250, human anti- CREST (CS-1058) by Cortex Biochem 1:1000. The following Alexa Fluor secondary antibodies were used: donkey anti-goat 555/488, donkey anti-rat 555, donkey anti-mouse 488 and donkey anti-rabbit 488 by ThermoFisher Scientific. All the Alexa Fluor 555 antibodies were used at a dilution of 1:400, while the Alexa Fluor 488 antibodies were diluted 1:250. To detect CREST we used donkey anti-human 488 DyLight 488 (SA5-10126) by ThermoFisher Scientific at a 1:250 dilution.

FACS sorting

Female DBA2 mice were mated with OCT4-GOF18/GFP C57BL/6 males to produce F1 fetuses carrying the OCT4-GFP transgene [50]. Staging of the embryos and dissociation of the tissue was performed as described above (**Drying-down or nuclear spread preparations of germ cells section**). Equal numbers of PGCs and somatic cells were isolated using the SORP-FACSAria II flow cytometer (BD).

qRT-PCR

For quantitative RT-PCR (RT-qPCR) cells were collected by centrifugation after FACs sorting, RNA was isolated and cDNA was made using Cells-to-cdna II kit (Thermo Fisher Scientific; AM1722) according to the manufacturer's instructions. All samples were analysed in a triplicate in a 15μl final reaction volume using the BioRad CFX 384 Real-time System. An alternative method was used to generate data of Additional file 4. Here, RNA isolation was performed with Trizol. Subsequently, RNA samples were treated with Turbo DNAse (Thermo Fisher Scientific; AM1970) and cDNA was made with Superscript III (Thermo Fisher Scientific; AM1970) and cDNA was made with Superscript III (Thermo

Fisher Scientific; 18080-044) according to manufacturer's instructions. Each reaction contained SYBR Green PCR Master Mix (4309155; Thermo Fisher Scientific), primers to a final concentration of 0,2μM and 1μl of cDNA. The following primers were used: *Oct4* Fw CCCCAATGCCGTGAAGTTG and Rv TCAGCAGCTTGGCAAACTGTT, major satellites Fw GGCGAGAAAACTGAAAATCACG and Rv AGGTCCTTCAGTGTGCATTTC [50], *Canx* Fw CCACATAGGAGGTCTGACAGC and Rv CACCACCAGCATTCCAAAA [35], *Atrx* Fw GAGCTTGACGTGAAACGAAGAG and Rv TTGTTGCTGTTGCTGCTGAG.

After an initial hold at 94^{o} C for 4 minutes, reaction mixtures underwent 40 cycles of 30 seconds at 94^{o} C, 30 seconds at 60^{o} C and 30 seconds at 72^{o} C. Gene expression levels were normalized over *Canx* expression according to the $2^{-\Delta Ct}$ method. For the major satellites, the Ct values were compared.

List of abbreviations

4', 6 – diamidino – 2 – phenylindole (DAPI)
Heterochromatin Protein 1 (HP1)
Primordial Germ Cell (PGC)
Polycomb Repressor Complexes 1 and 2 (PRC1 and PRC2)

Declarations

Ethics approval and consent to participate: All animal experiments were approved by the animal experiments committee DEC-Consult.

Consent for publication: not applicable

Availability of data and material: not applicable

Competing interests: The authors declare that they have no competing interest

Funding: This work was supported by a NWO-VIDI grant 917.10.367 to ME

Authors' contributions: AM and ME conceived the work and designed the experiments, GvdH, JG, AHFMP and WMB contributed to the design of the experiments, AM and ESL acquired and analysed the data, AM, ME, and WMB interpreted the data, AM and WMB wrote the draft of the manuscript, GvdH, JG, AHFMP, and ME critically revised the manuscript. All authors are accountable for all aspects of the work and have approved the manuscript.

Acknowledgements: We thank Dr. Sarra Merzouk for scientific discussions.

REFERENCES

Albert, M. & Peters, A.H.F.M., 2009. Genetic and epigenetic control of early mouse development. Current opinion in genetics & development, 19(2), pp.113–21.

Baarends, W.M. et al., 2005. Silencing of unpaired chromatin and histone H2A ubiquitination in mammalian meiosis. Molecular and cellular biology, 25(3), pp.1041–53.

Bannister, a J. et al., 2001. Selective recognition of methylated lysine 9 on histone H3 by the HP1 chromo domain. Nature, 410(6824), pp.120–124.

Baumann, C. et al., 2008. Association of ATRX with pericentric heterochromatin and the Y chromosome of neonatal mouse spermatogonia. BMC molecular biology, 9, p.29.

van den Bergen, J.A. et al., 2009. Normalizing gene expression levels in mouse fetal germ cells. Biology of reproduction, 81(2), pp.362–70.

Boyarchuk, E. et al., 2014. Pericentric heterochromatin state during the cell cycle controls the histone variant composition of centromeres. Journal of cell science, (June), pp.3347–3359.

Casanova, M. et al., 2013. Heterochromatin Reorganization during Early Mouse Development Requires a Single-Stranded Noncoding Transcript. Cell Reports, 4(6), pp.1156–1167.

Daujat, S. et al., 2009. H3K64 trimethylation marks heterochromatin and is dynamically remodeled during developmental reprogramming. Nature structural & molecular biology, 16(7), pp.777–81.

Frescas, D. et al., 2008. KDM2A represses transcription of centromeric satellite repeats and maintains the heterochromatic state. Cell cycle (Georgetown, Tex.), 7(22), pp.3539–47.

Fussner, E. et al., 2011. Constitutive heterochromatin reorganization during somatic cell reprogramming. The EMBO journal, 30(9), pp.1778–89.

Govin, J. et al., 2007. Pericentric heterochromatin reprogramming by new histone variants during mouse spermiogenesis. Journal of Cell Biology, 176(3), pp.283–294.

Guenatri, M. et al., 2004. Mouse centric and pericentric satellite repeats form distinct functional heterochromatin. The Journal of cell biology, 166(4), pp.493–505.

Hackett, J.A., Zylicz, J.J. & Surani, M.A., 2012. Parallel mechanisms of epigenetic reprogramming in the germline. Trends in genetics : TIG, 28(4), pp.164–74.

Hajkova, P. et al., 2008. Chromatin dynamics during epigenetic reprogramming in the mouse germ line. Nature, 452(7189), pp.877–81.

Hajkova, P. et al., 2002. Epigenetic reprogramming in mouse primordial germ cells. Mechanisms of Development, 117, pp.15–23.

He, Q. et al., 2015. The Daxx/Atrx Complex Protects Tandem Repetitive Elements during DNA Hypomethylation by Promoting H3K9 Trimethylation. Cell stem cell, 17(3), pp.273–86.

van der Heijden, G.W. et al., 2005. Asymmetry in histone H3 variants and lysine methylation between paternal and maternal chromatin of the early mouse zygote. Mechanisms of development, 122(9), pp.1008–22.

Hill, P.W.S., Amouroux, R. & Hajkova, P., 2014. DNA demethylation, Tet proteins and 5-hydroxymethylcytosine in epigenetic reprogramming: an emerging complex story. Genomics, 104(5), pp.324–33.

Ishiuchi T, Enriquez-Gasca R, Mizutani E, Bošković A, Ziegler-Birling C, Rodriguez-Terrones D, Wakayama T, Vaquerizas JM, Torres-Padilla M-E: Early embryonic-like cells are induced by downregulating replication-dependent chromatin assembly. Nat Struct Mol Biol 2015, 22:662–671.

Ishov, A.M., Vladimirova, O. V & Maul, G.G., 2004.

Heterochromatin and ND10 are cell-cycle regulated and phosphorylation-dependent alternate nuclear sites of the transcription repressor Daxx and SWI/SNF protein ATRX. Journal of cell science, 117(Pt 17), pp.3807–20.

Kagiwada, S. et al., 2013. Replication-coupled passive DNA demethylation for the erasure of genome imprints in mice. The EMBO journal, 32(3), pp.340–53.

Kourmouli, N. et al., 2004. Heterochromatin and tri-methylated lysine 20 of histone H4 in animals. Journal of cell science, 117(Pt 12), pp.2491–501.

De La Fuente, R., Baumann, C. & Viveiros, M.M., 2015. ATRX contributes to epigenetic asymmetry and silencing of major satellite transcripts in the maternal genome of the mouse embryo. Development (Cambridge, England), (April), pp.1806–1817.

Lachner, M., O'Sullivan, R.J. & Jenuwein, T., 2003. An epigenetic road map for histone lysine methylation. Journal of cell science, 116(Pt 11), pp.2117–24.

Lehnertz, B. et al., 2003. Suv39h-mediated histone H3 lysine 9 methylation directs DNA methylation to major satellite repeats at pericentric heterochromatin. Current biology : CB, 13(14), pp.1192–200.

Lu, J. & Gilbert, D.M., 2007. Proliferation-dependent and cell cycle-regulated transcription of mouse pericentric heterochromatin. Journal of Cell Biology, 179(3), pp.411–421.

Maze, I. et al., 2011. Cocaine dynamically regulates heterochromatin and repetitive element unsilencing in nucleus accumbens. Proceedings of the National Academy of Sciences of the United States of America, 108(7), pp.3035–40.

McDowell, T.L. et al., 1999. Localization of a putative transcriptional regulator (ATRX) at pericentromeric heterochromatin and the short arms of acrocentric chromosomes. Proceedings of the National Academy of Sciences of the United States of America, 96(24), pp.13983–13988.

Molyneaux, K.A. et al., 2001. Time-lapse analysis of living mouse germ cell migration. Developmental biology, 240(2), pp.488–98.

Ohinata, Y. et al., 2009. A signaling principle for the specification of the germ cell lineage in mice. Cell, 137(3), pp.571–84.

Peters, A.H. et al., 1997. A drying-down technique for the spreading of mammalian meiocytes from the male and female germline. Chromosome research : an international journal on the molecular, supramolecular and evolutionary aspects of chromosome biology, 5(1), pp.66–8.

Peters, A.H.F.M. et al., 2001. Loss of the Suv39h Histone Methyltransferases Impairs Mammalian Heterochromatin and Genome Stability. Cell, 107(3), pp.323–337.

Peters, A.H.F.M. et al., 2003. Partitioning and plasticity of repressive histone methylation states in mammalian chromatin. Molecular cell, 12(6), pp.1577–89.

Probst, A.V. et al., 2010. A Strand-Specific Burst in Transcription of Pericentric Satellites Is Required for Chromocenter Formation and Early Mouse Development. Developmental Cell, 19(4), pp.625–638.

Puschendorf, M. et al., 2008. PRC1 and Suv39h specify parental asymmetry at constitutive heterochromatin in early mouse embryos. Nature genetics, 40(4), pp.411–20.

Rea, S. et al., 2000. Regulation of chromatin structure by site-specific histone H3 methyltransferases. Nature, 406(6796), pp.593–9.

Rudert, F. et al., 1995. Transcripts from opposite strands of gamma satellite DNA are differentially expressed during mouse development. Mammalian genome : official journal of the International Mammalian Genome Society, 6(2), pp.76–83.

Sadic, D. et al., 2015. Atrx promotes heterochromatin formation at retrotransposons. EMBO reports, 16(7), pp.836–50.

Santos, F. et al., 2005. Dynamic chromatin modifications characterise the first cell cycle in mouse embryos. Developmental Biology, 280(1), pp.225–236.

Santos, F. et al., 2002. Dynamic reprogramming of DNA methylation in the early mouse embryo. Developmental biology, 241(1), pp.172–82.

Santos, F. & Dean, W., 2004. Epigenetic reprogramming during early development in mammals. Reproduction (Cambridge, England), 127(6), pp.643–51.

Schotta, G. et al., 2004. A silencing pathway to induce H3-K9 and H4-K20 trimethylation at constitutive heterochromatin. Genes & development, 18(11), pp.1251–62.

Seki, Y. et al., 2007. Cellular dynamics associated with the genome-wide epigenetic reprogramming in migrating primordial germ cells in mice. Development (Cambridge, England), 134(14), pp.2627–38.

Seki, Y. et al., 2005. Extensive and orderly reprogramming of genome-wide chromatin modifications associated with specification and early development of germ cells in mice. Developmental biology, 278(2), pp.440–58.

Smallwood, A. et al., 2012. CBX3 regulates efficient RNA processing genome-wide. Genome research, 22(8), pp.1426–36.

Takada, Y. et al., 2011. HP1γ links histone methylation marks to meiotic synapsis in mice. Development (Cambridge, England), 138(19), pp.4207–17.

Terranova, R. et al., 2005. The reorganisation of constitutive heterochromatin in differentiating muscle requires HDAC activity. Experimental cell research, 310(2), pp.344–56.

Torres-Padilla, M.-E. et al., 2006. Dynamic distribution of the replacement histone variant H3.3 in the mouse oocyte and preimplantation embryos. The International journal of developmental biology, 50(5), pp.455–61.

Vakoc, C.R. et al., 2005. Histone H3 lysine 9 methylation and HP1gamma are associated with transcription elongation through mammalian chromatin. Molecular cell, 19(3), pp.381–91.

Yamaguchi, S. et al., 2013. Dynamics of 5-methylcytosine and 5-hydroxymethylcytosine during germ cell reprogramming. Cell research, 23(3), pp.329–39.

Yoshimizu, T. et al., 1999. Germline-specific expression of the Oct-4/green fluorescent protein (GFP) transgene in mice. Development, Growth and Differentiation, 41(6), pp.675–684.

Yoshioka, H., McCarrey, J.R. & Yamazaki, Y., 2009. Dynamic nuclear organization of constitutive heterochromatin during fetal male germ cell development in mice. Biology of reproduction, 80(4), pp.804–12.

Additional Files:

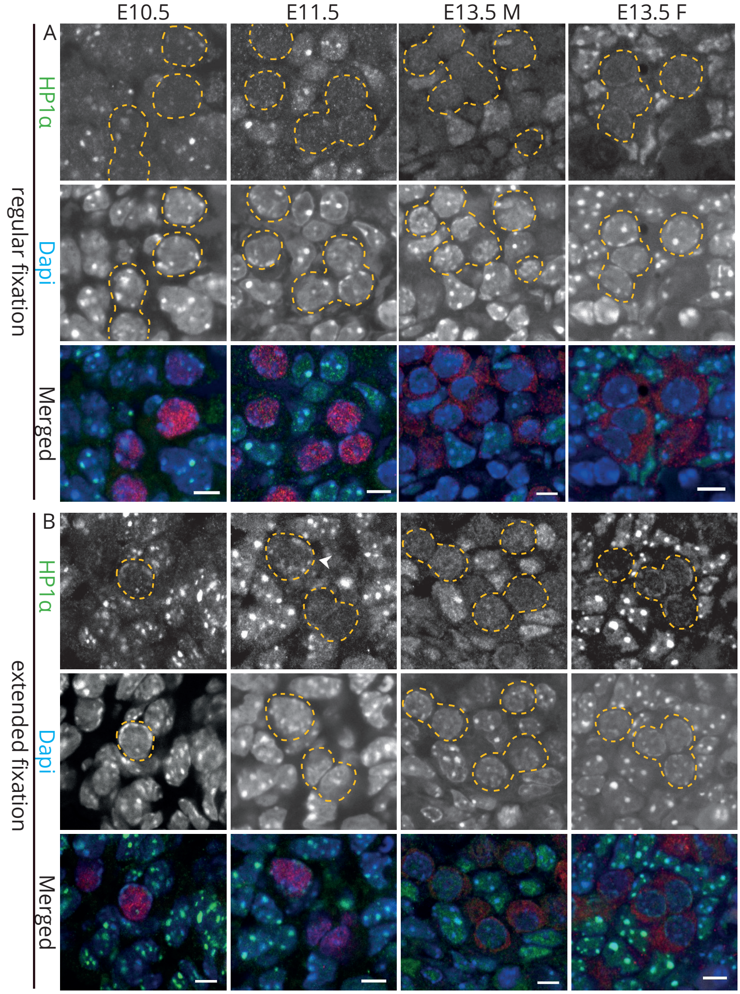

Additional file 1: Immunofluorescent analysis of HP1α in paraffin sections using the regular and extended fixation protocols

A In E10.5 embryos HP1α (green) is enriched at pericentric heterochromatin, but its levels are lower in PGCs compared to somatic cells. From E11.5 onwards, HP1α signal is depleted from DAPI (blue) dense regions in PGCs. **B** Results were similar to **A** when using extended fixation conditions. However, at E11.5 some PGCs could be detected with some signal of HP1α still present at the percentric heterochromatin (marked by arrowhead). Note that in E13.5 male gonads HP1α could not be reproducibly detected in somatic cells, both in **A** and **B**. For each stage two embryos were analysed per fixation protocol and at least 20 nuclei were recorded. E10.5 and E11.5 PGCs were marked with OCT4 (red). E13.5 male and female germ cells were identified by the presence of DDX4/MVH (red). Representative images are shown with germ cells highlighted by dashed yellow circles and scale bars represent 5µm.

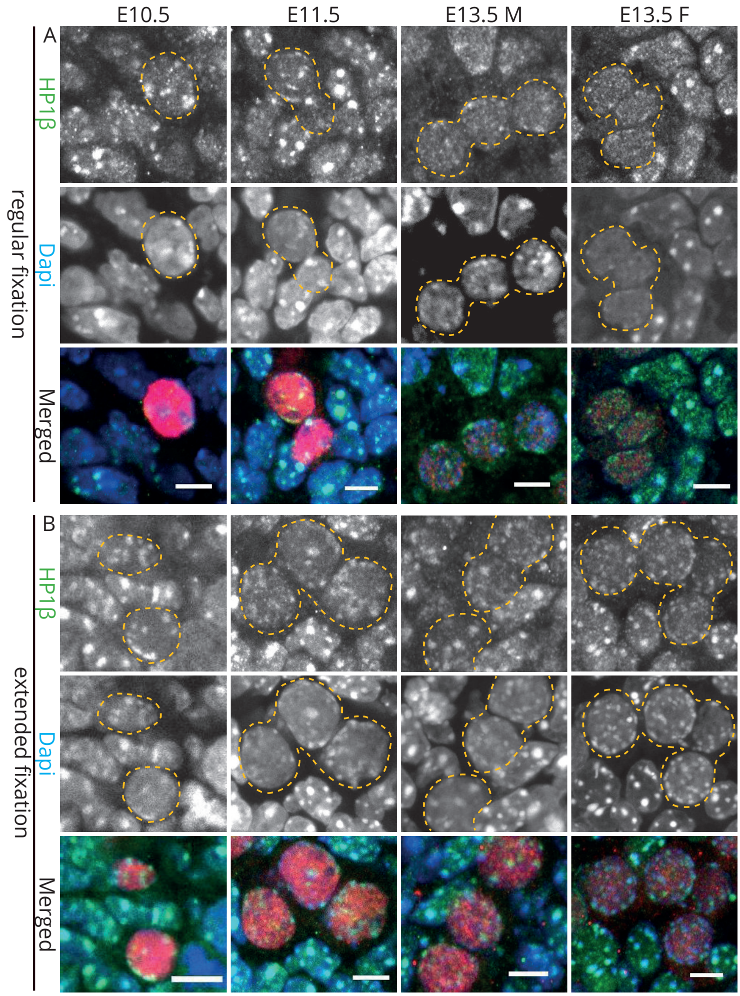

Additional file 2: Immunofluorescent analysis of HP1β in paraffin sections using the regular and extended fixation protocols

A Using the regular fixation protocol, HP1β signal is enriched at DAPI (blue) dense regions of E10.5 and E11.5 PGCs and somatic cells. HP1β is then substantially reduced in E13.5 female and male germ cells. **B** With the extended fixation protocol, HP1β is retained in pericentric heterochromatin of PGCs throughout development. For each stage two embryos were analysed per fixation protocol and at least 20 nuclei were recorded. E10.5 and E11.5 PGCs were marked with OCT4 (red). E13.5 male and female germ cells were identified by the presence of TRA98 (red). Representative images are shown with germ cells highlighted by dashed yellow circles and scale bars represent 5μm.

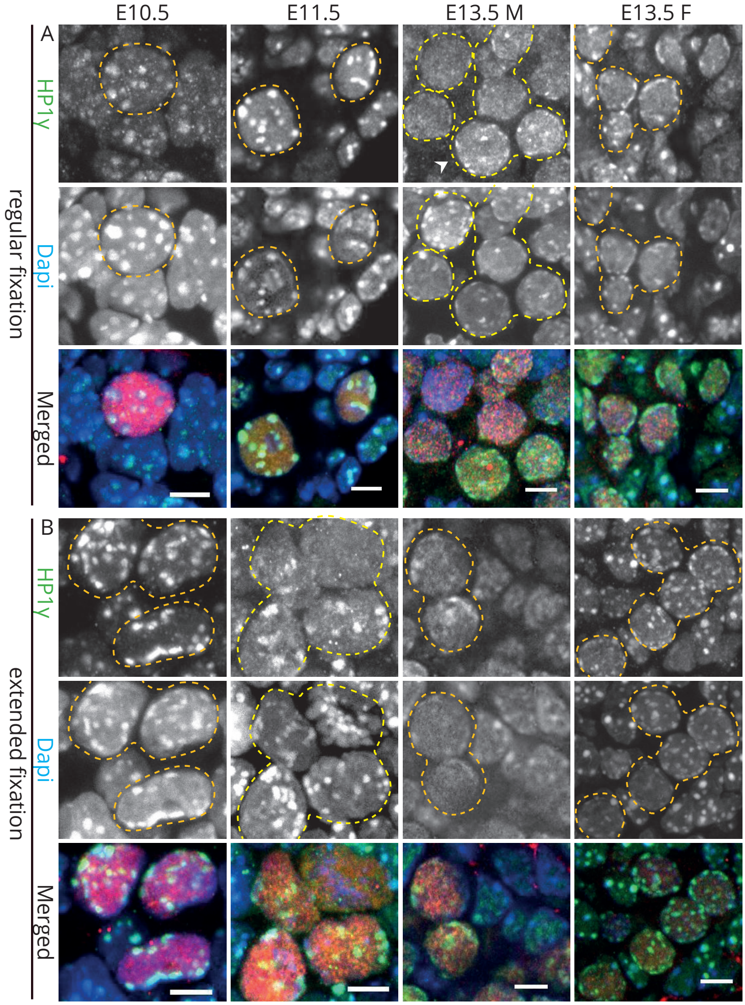

Additional file 3: Immunofluorescent analysis of HP1γ in paraffin sections using the regular and extended fixation protocols

A HP1γ (green) signal is enriched at DAPI (blue) dense regions of E10.5 and E11.5 PGCs and somatic cells using the regular fixation protocol. Thereafter, at E13.5, HP1γ could not be detected in male germ cells, while it was still present in E13.5 female germ cell nuclei. **B** Upon application of the extended fixation protocol, enrichment of HP1γ signal was observed in pericentric heterochromatin of E10.5 and E11.5 PGCs. Similar to **A**, HP1γ could not be detected at pericentric heterochromatin of male E13.5 germ cells, while it was still present in E13.5 female germ cells. Note that in both protocols (**A** and **B**) HP1γ could not reproducibly be detected in pericentric heterochromatin of E13.5 somatic cells. For each stage two embryos were analysed per fixation protocol and at least 20 PGC nuclei were recorded. E10.5 and E11.5 PGCs were marked with OCT4 (red). E13.5 male and female germ cells were identified by the presence of TRA98 (red). Representative images are shown with germ cells highlighted by dashed yellow circles and scale bars represent 5μm.

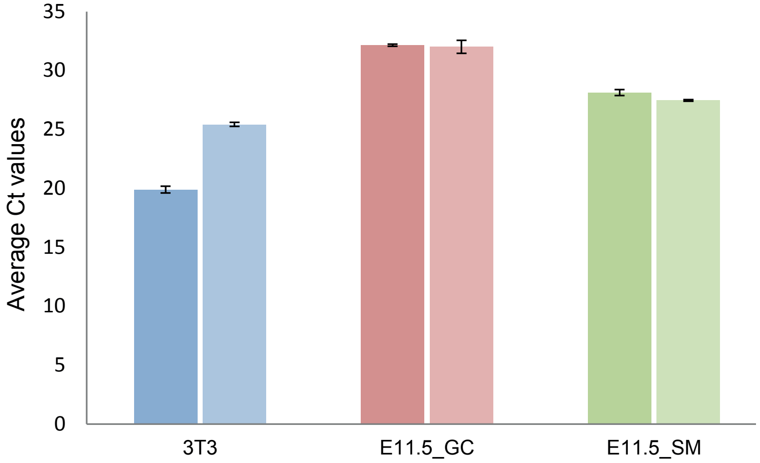

Additional file 4: Expression of major satellites in NIH-3T3 cells and in sorted E11.5 PGCs and somatic cells

Results from qRT-PCR (shown as Ct values) for major satellites in E11.5 sorted GFP positive (PGCs) and negative (soma) cells after Trizol RNA isolation and Turbo DNAse treatment shows that expression of major satellites could not be detected above background (-RT) in both sorted populations. In contrast, mouse NIH-3T3 cells show expression of these transcripts above background levels, as previously described (Frescas D et al., 2008). The average Ct values are plotted for each cell type in +RT and – RT samples. Error bars indicate standard deviation within triplicate samples of one biological experiment.

Chapter 4

GENERATION OF A NOVEL *IN VITRO* DIFFERENTIATION STRATEGY TO STUDY THE DYNAMICS OF X CHROMOSOME INACTIVATION IN RAT

Aristea Magaraki[#1], Agnese Loda[#1], Cristina Gontan Pardo[1], Stephen Meek[2],
Willy M. Baarends, Tom Burdon[2] and Joost Gribnau[1*]

Manuscript in preparation

GENERATION OF A NOVEL *IN VITRO* DIFFERENTIATION STRATEGY TO STUDY THE DYNAMICS OF X CHROMOSOME INACTIVATION IN RAT

Aristea Magaraki[#1], Agnese Loda[#1], Cristina Gontan Pardo[1], Stephen Meek[2], Willy M. Baarends, Tom Burdon[2] and Joost Gribnau[1*]

Author affiliations:
[1]Department of Developmental Biology, Erasmus University Medical Center, Wytemaweg 80, 3015 CN Rotterdam, The Netherlands
[2]The Roslin Institute and R(D)VS, University of Edinburgh, Easter Bush, Midlothian, EH25 9RG, Scotland
[#]These authors contributed equally to this work
[*]Corresponding author
Joost Gribnau
email: j.gribnau@erasmusmc.nl

Abstract

X chromosome inactivation (XCI) is a developmentally regulated process and its accomplishment relies on several mechanisms including antisense transcription, non-coding RNA-mediated silencing, and recruitment of chromatin remodelling complexes. *In vitro* modelling of XCI provides a powerful tool to study the dynamics of this process by genetically modifying key regulatory players. Importantly, *in vitro* strategies are based on differentiation of pluripotent stem cells into functional cell types and overcome the need to use early developing embryos, thus increasing the number of species in which XCI can be investigated. However, to date, robust XCI *in vitro* has been exclusively achieved upon differentiation of mouse pluripotent cells. Here, we established a novel monolayer differentiation protocol for rat ES cells to study XCI. We show that efficient XCI initiation can only be achieved upon complete withdrawal of MEK and GSK3 inhibitors upon differentiation. We also show that in differentiating rat female cells, *Xist* RNA starts accumulating *in cis* on the X chromosome around day 2 of differentiation, and the accumulation is rapidly followed by H3K27me3 enrichment on the inactive X (Xi). Finally, we demonstrate that the critical roles of RNF12 and REX1 in mediating XCI in the mouse, are also well conserved in rats. Our work provides the basis to investigate the mechanisms directing the XCI process in a model organism different from the mouse.

Introduction

In mammals, X chromosome inactivation (XCI) ensures the dosage compensation of sex chromosomal genes between females (XX) and males (XY) (Gendrel & Heard 2014; van Bemmel et al. 2016). The process of XCI occurs early upon female embryonic development and is mediated by a multitude of epigenetic mechanisms that result in the complete transcriptional inactivation of one entire X chromosome within the nucleus of every female somatic cell. In eutherians, initiation of XCI is mediated by long non-coding RNAs, with the non-coding gene *Xist* being the major player of XCI in placental mammals (Grant et al. 2012; Marahrens et al. 1997; Penny et al. 1996; Borsani et al. 1991; Brockdorff et al. 1991). During XCI, *Xist* RNA spreads *in cis* along the entire length of the X chromosome and triggers chromosome-wide silencing of X-linked genes. Although most likely functionally similar, the molecular mechanisms by which *Xist* and *Rsx* (a large, repeat-rich RNA, that similar to *Xist* is transcribed from and coats the inactive X chromosome in marsupial Monodelphis domestica (Grant et al. 2012)) induce transcriptional inactivation remain largely unknown. The study of XCI relies both on *in vivo* and *in vitro* models that allow genetic manipulation of the factors involved, and the vast majority of our current knowledge has been achieved by using the mouse as a model organism. *In vivo* studies have shown that XCI starts around the 4-8 cell stage of female mouse embryonic development and is initially imprinted (iXCI), resulting in exclusive inactivation of the paternal X chromosome (Xp) (Huynh & Lee 2003; Mak et al. 2004; Okamoto et al. 2004; Patrat et al. 2009). Later on in development, at the blastocyst stage (~E4.5), the Xp becomes reactivated in the inner cell mass (ICM) of the embryo, whereas iXCI is maintained in the extra-embryonic lineages (Mak et al. 2004; Okamoto et al. 2004). Reactivation of Xp in the ICM is then followed by random inactivation (rXCI) of either the paternal or maternal X chromosome in cells of the developing epiblast. *In vitro*, mouse embryonic stem cells (mESCs) have been extensively used to model rXCI. In fact, undifferentiated mESCs carry two active X chromosomes and faithfully mimic the pluripotent environment of the ICM, whereas their differentiation results in random inactivation of one of the two X chromosomes. Mouse ESC-based *in vitro* studies have led to the discovery of the long non-coding gene *Tsix*, which is transcribed antisense to *Xist* and represents the major repressor of *Xist* upregulation at the onset of XCI in the mouse (Lee & Lu 1999; Navarro et al. 2006; Sado et al. 2005; Ohhata et al. 2008). XCI is tightly linked to loss of the pluripotent state (Wutz & Jaenisch 2000; Schulz et al. 2014) and several pluripotency factors including NANOG, SOX2, OCT4, REX1 and PRDM14 have been described to function as XCI-inhibitors either by directly inhibiting *Xist* expression or by enhancing *Tsix* upregulation (Ma et al. 2011; Navarro et al. 2008; Navarro et al. 2010; Payer et al. 2013). Activation of XCI is mediated at least in part by the X-linked E3 ubiquitin ligase RNF12 that mediates degradation of REX1 in a dose-dependent manner (Jonkers et al. 2009; Gontan et al. 2012). Interestingly, the study of XCI in female pre-implantation embryos from different species suggested that the epigenetic processes that mediate XCI might be more heterogeneous than expected. Similar to mouse, iXCI occurs in the extra-embryonic lineages of rat and cow (Wake et al. 1976; Dindot 2004; Xue et al. 2002), but in other species such as human, monkey, horse, pig and rabbit, only rXCI has been exclusively observed in both embryonic and extra-embryonic tissues (Okamoto et al. 2011; Moreira de Mello et al. 2010). Comparative analysis of *Xist* RNA expression dynamics and X-linked gene silencing between rabbit and human pre-implantation embryos confirmed substantial diversity in the timing and regulation of XCI initiation among mammals, with cells of the human ICM showing two active X chromosomes regardless of *Xist* RNA coating (Okamoto et al. 2011, Petropoulos et al. 2016). In addition, the overall *Xist* gene structure appears to be conserved in all placental mammals, but the *Xist* sequence evolved rapidly and differs considerably between species (Chureau et al. 2002; Duret 2006; Nesterova et al. 2001; Elisaphenko et al. 2008). Finally, *Tsix* antisense transcription through the *Xist* promoter has not been found in human (Migeon et al. 2001; Migeon et al. 2002) but appears to be conserved in rodents (Shevchenko et al. 2011). Interestingly, differentiation of mouse-rat allodiploid ES cells leads to specific primary inactivation of the mouse X chromosome (Li et al. 2016). This mouse allele-biased expression of *Xist* has been proposed to result from the higher expression of *Tsix* from the rat allele, interfering with expression of *Xist* in *cis* (Li et al. 2016). Clearly, the development of novel *in vitro* systems derived from different species is necessary to reach a comprehensive understanding of the XCI process. However, although the induced pluripotent stem cells (iPSCs) technology has allowed the generation of several ES cell-like lines from different species (Takahashi & Yamanaka 2006; Watanabe et al. 2007; Friedrich Ben-Nun et al. 2011), both the characterization of the X chromosomes status and the generation of *in vitro* differentiation protocols that recapitulate XCI have proven to be challenging (Tchieu et al. 2010; Mekhoubad et al. 2012; Pasque & Plath 2015). In this context, rat ES cells (rESCs) only recently became well characterized (Meek et al. 2014; Meek et al. 2013; Meek et al. 2010; Buehr et al. 2008; Li et al. 2008; Masaki Kawamata & Ochiya 2010a; M. Kawamata & Ochiya 2010b; Hirabayashi et al. 2009; Men et al. 2012), and the establishment of the novel CRISPR/Cas9 system for genome editing rapidly enhanced the generation of genetically modified rat models potentially facilitating genetic studies on XCI in rESCs (Shao et al. 2014; Guan et al. 2014). Therefore, we set out to generate a robust *in vitro* system that could faithfully mimic the dynamics of XCI in rat. By developing a monolayer differentiation protocol for rESCs similar to the one recently reported by Vaskova and colleagues (Vaskova et al. 2015), we were able to follow several aspects of XCI regulation in rat. Similar to mouse, we were able to observe (I) *Xist* up-regulation at an early stage of rESCs differentiation followed by (II) transcriptional inactivation of X-linked genes and (III) H3K27me3 accumulation on the inactive X chromosome (Xi). In addition, (IV) overexpression experiments in rESCs confirmed that the REX1-RNF12 axis of *Xist* regulation is conserved between rat and mouse. Thus, we have established the technical basis to study the dynamics of XCI in a different system from the mouse and shown that specific aspects of XCI are conserved in rodents.

Results

In vitro neuronal differentiation of rESCs

In vitro differentiation of mESCs towards different functional cell types including neurons, cardiomyocytes, hepatocytes and pancreatic cells can be efficiently achieved by several established protocols (Schroeder et al. 2009). Usually, differentiation strategies are based on the formation of embryoid bodies (EB) followed by growth-factor-mediated induction of early progenitor cells to differentiate into their respective lineages. Despite of the growing list of differentiation protocols for mESCs, differentiation of rESC is extremely difficult to achieve *in vitro*. To date, only two strategies have been described in which rESCs were triggered to differentiate into either cardiomyocytes or neuronal precursors. In these differentiation protocols MEK and GSK3β inhibitors (generally known as 2i), that are commonly used for ESC culture, are always present in low concentrations in the differentiation media (Cao et al. 2011; Peng et al. 2013). Normally, when for example mouse ESCs are induced to differentiate, these inhibitors are removed from the culture medium, but in the case of the rat ESCs, such an immediate removal rapidly leads to massive cell death. Only later in the rESC differentiation protocol (day 3) the two inhibitors are completely removed. We initially set out to assess rat XCI after inducing rESCs differentiation according to the already established protocols. Several rESCs derived from different rat inbred strains were differentiated, including three pure Lewis lines (LEW) (A4p20, A9p20, A10p20), and two lines of a mixed background of dark agouti (DA) and Sprague-Dawley (SD) (135-7, 141-6). In all cases, we were never able to observe either *Xist* up-regulation or its associated X-linked gene silencing, although both female and male rat cells appeared to be morphologically differentiated.

XCI is closely linked to loss of pluripotency, and the presence of an inactive X chromosome is a powerful readout for cell differentiation. We reasoned that the lack of XCI features upon differentiation could rely on the differentiation culture conditions we applied. As already mentioned above, in both experimental published strategies, rESC differentiation is never achieved without complete withdrawal of the MEK and GSK3 inhibitors. Inhibiting both the MAPK and Gsk3β pathways is necessary for the maintenance of the homogeneous pluripotent ground state of rESCs (Buehr et al. 2008). However, since *Xist* regulation and function are strictly linked to cell differentiation, stabilizing the pluripotent state results in tight repression of *Xist* expression (Schulz et al. 2014; Navarro et al. 2008;

2010; Payer et al. 2013). Therefore, we hypothesized that the supplement of MEK and GSK3 inhibitors at the onset of rESCs differentiation might interfere with *Xist* up-regulation, thus preventing XCI initiation. To test our hypothesis, we implemented the neuronal differentiation protocol initially described by Peng and colleagues (Peng et al. 2013) as follows: (I) we completely eliminated the presence of both 2i factors starting from day 1 of neuronal differentiation, (II) we increased the concentration of ROCK (rho-associated protein kinase) inhibitor, which has been shown to prevent dissociation-induced apoptosis in cultured human ES cells (Ishizaki et al., 2000; Watanabe et al., 2007) and finally, (III) we started rESCs differentiation with a greater number of cells. Using these modified conditions, we were able to maintain viable differentiating male and female rESCs in the absence of 2i (Figure 1A). Importantly, qPCR analysis of both pluripotency and differentiation marker expression levels at different time points upon differentiation confirmed efficient downregulation of the pluripotency factors *Esrrb*, *Prdm14* and *Rex1*, and parallel up-regulation of the neuronal precursor marker *Nestin* (Figure 1B). Interestingly, we also observed massive cell death of female rESCs compared to male cells around day 3 of differentiation, suggesting that impairment of XCI initiation might have an impact on cell survival. Cell death was not observed when the already published protocols (2i factors present throughout differentiation) were used.

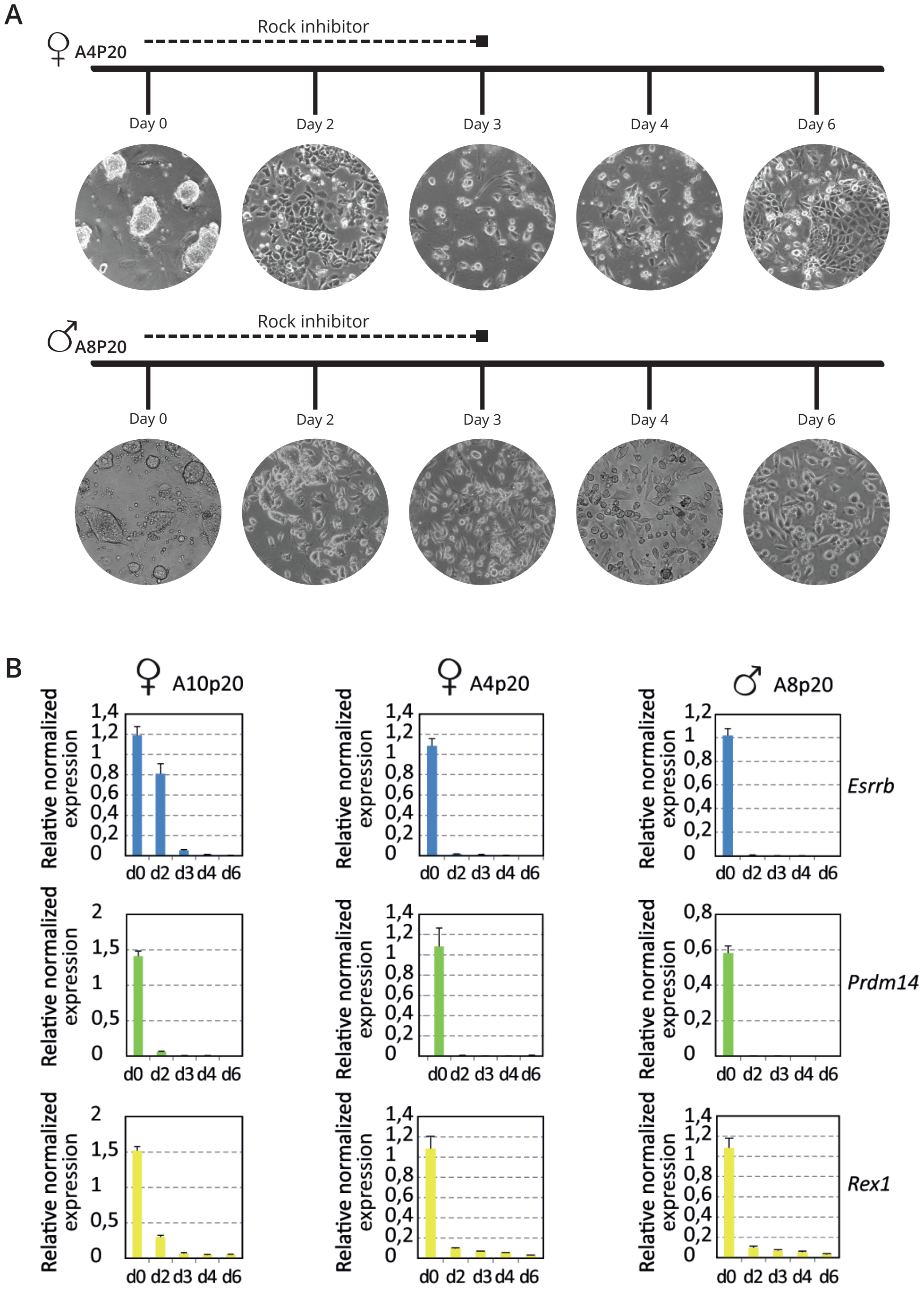
A
♀ A4P20
Rock inhibitor
Day 0
Day 2
Day 3
Day 4
Day 6
♂ A8P20
Rock inhibitor
Day 0
Day 2
Day 3
Day 4
Day 6
B
♀ A10p20
♀ A4p20
♂ A8p20
Relative normalized expression
1,4
1,2
1
0,8
0,6
0,4
0,2
0
2
1,5
0,5
d0 d2 d3 d4 d6
Esrrb
Prdm14
Rex1

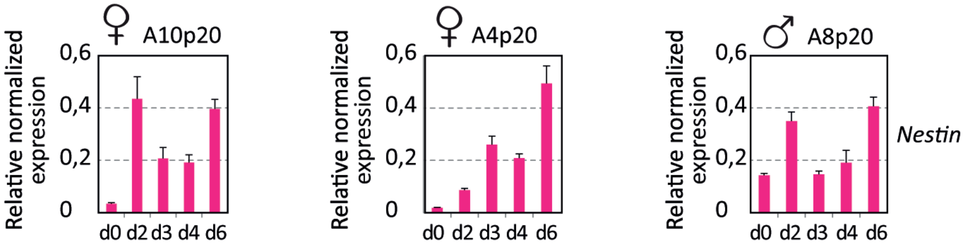

Figure 1: Neuronal differentiation of rESCs

A Schematic representation of our neuronal differentiation strategy. Brightfield images of female (A4p20, top) and male (A8p20, bottom) rESCs at several time points upon differentiation are shown. **B** qRT-PCR analysis of *Esrrb*, *Prdm14*, *Rex1* (pluripotency factors) and *Nestin* (neuronal differentiation marker) expression levels normalised to *Actin* in female (A10p20, A4p20) and male (A8p20) differentiating rESCs at different time points after initiation of differentiation as indicated. Error bars represent standard deviation of three technical experiments.

Female rESCs undergo XCI upon *in vitro* neuronal differentiation

We then addressed the question of whether differentiating rESCs without the supplement of 2i factors would facilitate XCI to occur. To this end, four independent female rESC lines were differentiated and the *Xist* RNA expression level was assessed by qRT-PCR analysis at different time points upon neuronal differentiation. Importantly, in order to assess the sex-specific regulation of *Xist* RNA, one male rESC line was also included into our analysis. As in mouse, *Xist* upregulation occurs exclusively in female rat cells between day 2 and day 4 of differentiation (Figure 2A). In parallel, we also assessed *Tsix* expression levels and contrary to what is observed in mouse, where expression of *Xist* and *Tsix* is anti-correlated (Loos et al. 2016), *Tsix* appears to be efficiently downregulated upon differentiation in only two out of four female rESC lines. Moreover, male rESCs showed persistent *Tsix* expression throughout differentiation, although the expression levels decreased around day 2 (Figure 2A). These observations suggest that the interplay between *Tsix* and *Xist* regulation at the onset of XCI might differ slightly between mouse and rat.

Next, we addressed the dynamics of *Xist* expression by performing *Xist* RNA FISH analysis at different time points upon neuronal differentiation. In undifferentiated rESCs, *Xist* RNA pinpoint signals were observed within the nuclei of both female and male cells (Figure 2B). However, since the *Xist* RNA FISH probe can hybridize to either *Xist* or *Tsix* RNA, the pinpoint signal might represent *Tsix* expression instead of *Xist*. Around day 2 of neuronal differentiation, *Xist* RNA starts to accumulate exclusively on a single X chromosome within female nuclei, whereas *Xist* RNA accumulation was never observed in differentiating male rESCs (Figure 2B). Importantly, upon differentiation of A10p20 and A4p20 rESC female lines, 60% of the nuclei showed a *Xist* RNA-coated X chromosome at day 6 of differentiation (Figure 2C). Taken together, these observations show that neuronal differentiation of rESCs in absence of 2i inhibitors allows *Xist* RNA to be upregulated and to spread *in cis* from a single X chromosome in female cells.

In addition, we determined at which time point upon neuronal differentiation *Xist*-mediated silencing of X-linked genes is established. In mouse, the gene silencing-associated H3K27me3 histone modification represents one of the earliest histone marks that accumulates on the Xi during XCI (Chaumeil et al. 2006; Silva et al. 2003; Plath et al. 2003). Therefore, in order to determine whether the formation of *Xist* clouds was followed by further downstream events normally associated with robust XCI, we monitored enrichment of H3K27me3 by immunofluorescence analysis upon differentiation of both male and female rESCs. In undifferentiated rESCs, no H3K27me3 domains were observed in neither male nor female cells (Figure 3A). However, starting from day 2 of differentiation and in line with female-specific upregulation of *Xist* RNA, H3K27me3 starts to accumulate into specific nuclear domains within female cells. By day 6, more that 60% of the female nuclei show one H3K27me3 domain, thus confirming that XCI is efficiently initiated upon female rESCs differentiation (Figure 3A). Finally, to precisely assess the dynamics of X-linked gene silencing, we followed the *Xist*-mediated inactivation of the X-linked gene *Pgk1* in conjunction with *Xist* RNA cloud formation by two-colour RNA-FISH analysis at different time points upon rESCs differentiation. While the single copy of *Pgk1* in male cells remains actively transcribed throughout differentiation, the transcriptional inactivation of one copy of *Pgk1* in female cells starts around day 2 of differentiation (Figure 3C). However, robust *Pgk1* inactivation in up to 70% of the female nuclei is only reached around day 6 of differentiation (Figure 3C).

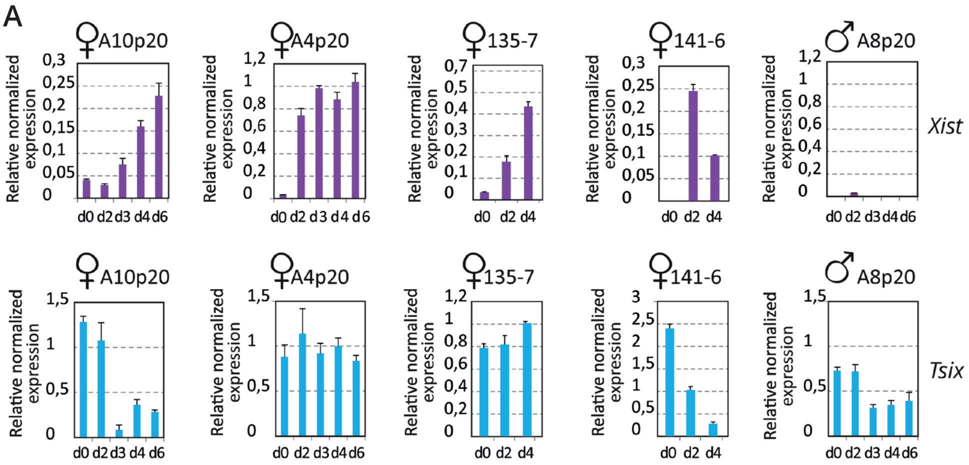

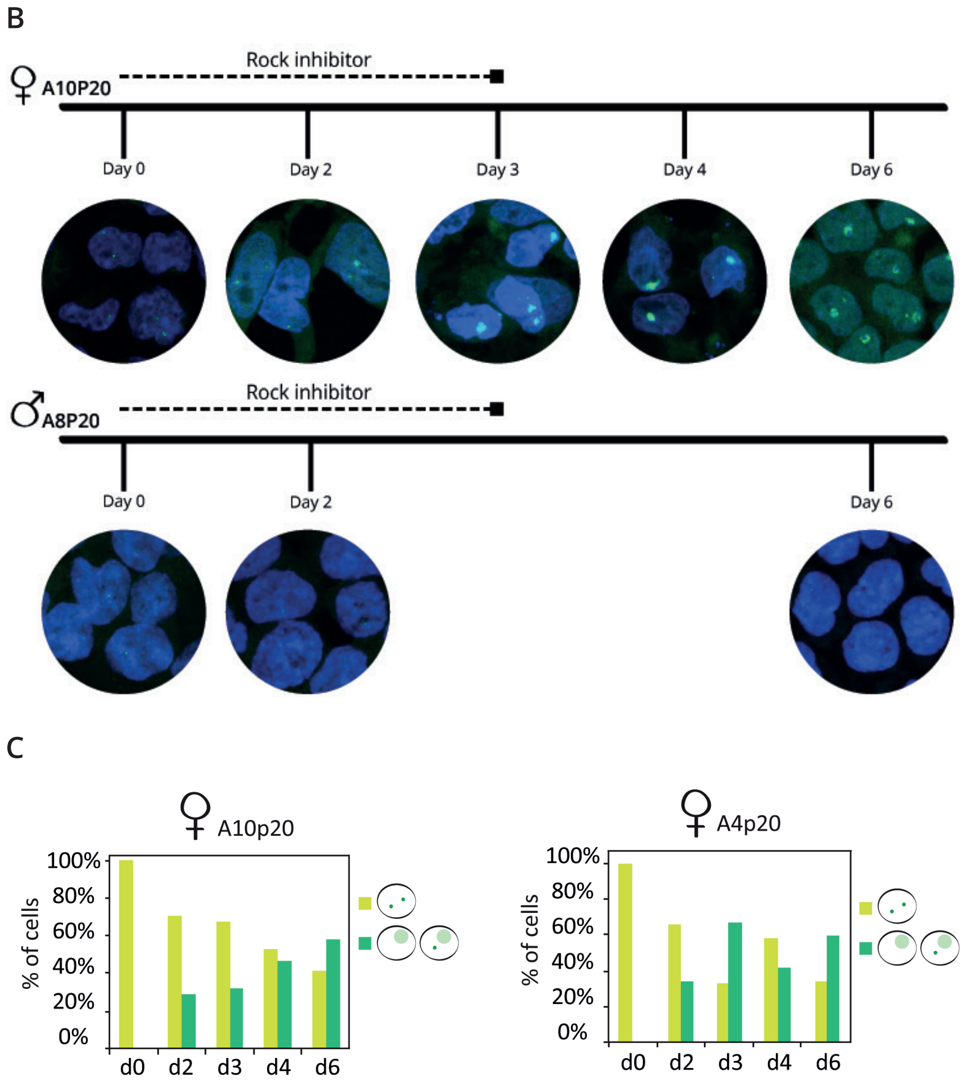
B
Rock inhibitor
♀ A10P20
Day 0
Day 2
Day 3
Day 4
Day 6
Rock inhibitor
♂ A8P20
Day 0
Day 2
Day 6
C
♀ A10p20
% of cells
100%
80%
60%
40%
20%
0%
d0
d2
d3
d4
d6
♀ A4p20
% of cells
100%
80%
60%
40%
20%
0%
d0
d2
d3
d4
d6

Figure 2: Monoallelic upregulation of *Xist* RNA upon female rESCs differentiation

A *Xist* and *Tsix* qRT-PCR expression analysis in female (A10p20, A4p20, 135-7, 141-6) and male (A8p20) differentiating rESCs. Expression levels of *Xist* and *Tsix* at different time points upon neuronal differentiation are shown. Error bars represent standard deviation of three technical experiments. **B** Representative images of *Xist* RNA FISH (green) analysis upon differentiation of female (A10p20) and male (A8p20) rESCs. DNA is stained with DAPI (blue). *Xist* RNA FISH was performed in two independent female cell lines (A10P20 and A4p20) and one male (A8P20). **C** Quantification of relative number of *Xist* RNA signals (pinpoints or clouds in patterns as indicated to the right of the graphs) in A10p20 and A4p20 female rESCs at day 0, 2, 3, 4 and 6 upon neuronal differentiation. *Xist* clouds were never observed in male nuclei. 150 nuclei were counted for each differentiation time point per female cell line.

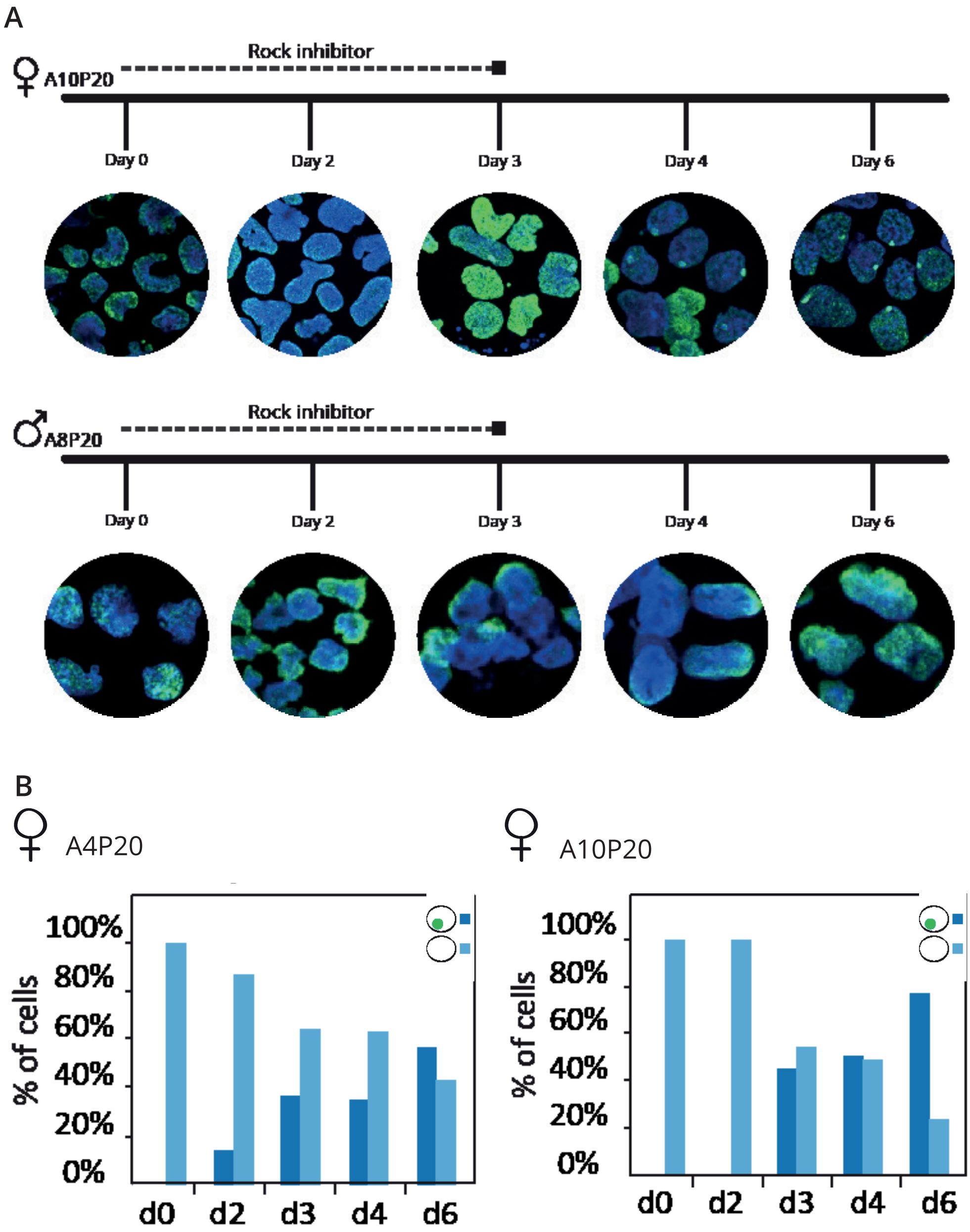
A
Rock inhibitor
♀ A10P20
Day 0
Day 2
Day 3
Day 4
Day 6
Rock inhibitor
♂ A8P20
Day 0
Day 2
Day 3
Day 4
Day 6
B
♀ A4P20
% of cells
100%
80%
60%
40%
20%
0%
d0
d2
d3
d4
d6
♀ A10P20
% of cells
100%
80%
60%
40%
20%
0%
d0
d2
d3
d4
d6

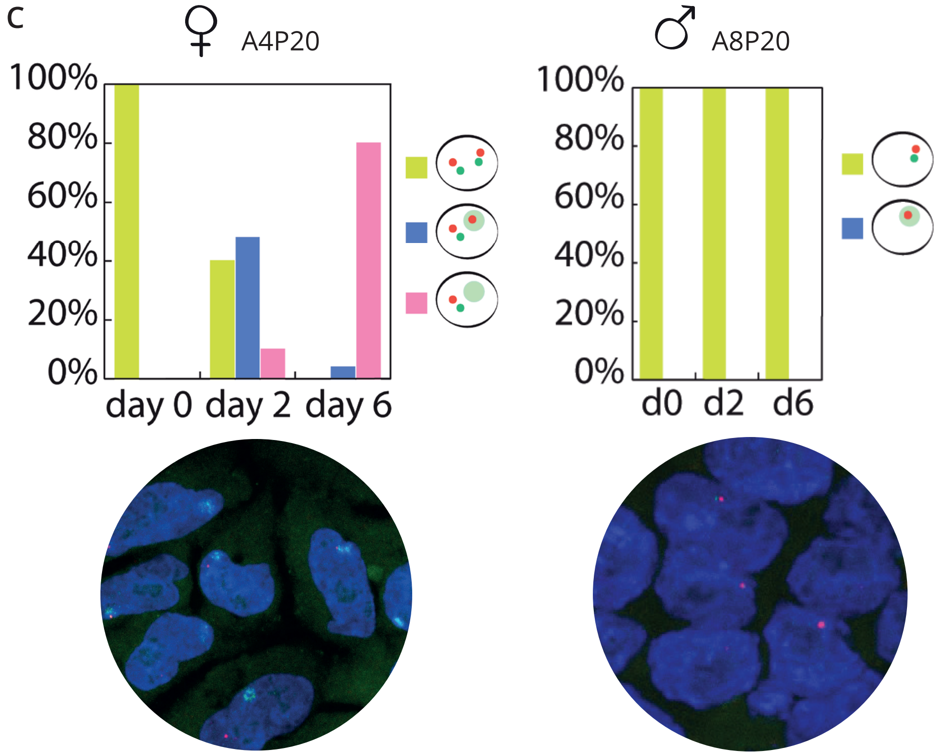

Day 6
Xist Pgk1

Day 6
Xist Pgk1

Figure 3: *Xist*-mediated silencing of X-linked genes

A Representative images of H3K27me3 (green) immunofluorescence analysis in female (A10p20) and male (A8p20) rESC at different time points upon neuronal differentiation. DNA is stained with DAPI (blue). Staining against H3K27me3 was performed in two independent female cell lines (A10P20 and A4p20) and one male (A8P20). **B** Quantification of relative number of cells carrying a H3K27me3 domain at day 0, 2, 3, 4 and 6 of neuronal differentiation. Data of A10p20 and A4p20 female rESC lines are shown. H3K27me3 domains were never noticed in male nuclei (A8P20). 150 nuclei were counted for each depicted differentiation time point. **C** *Xist* (green)/*Pgk1* (red) two-colour RNA-FISH quantitative analysis at different time points upon neuronal differentiation of female (A10p20) and male (A8p20) rESCs. The relative number of cells showing either biallelic or monoallelic *Pgk1* expression is quantified, together with the relative number of cells carrying *Xist* pinpoints or clouds signals in patterns as indicated to the right of the graphs. DNA is stained with DAPI (blue). Representative images of both female and male D6 differentiating rat cells are shown. 100 nuclei were counted for each depicted differentiation time point in each female and male cell line.

Overexpression of RNF12 and REX1 in undifferentiated rESCs modulates *Xist* expression

The X-linked E3 ubiquitin ligase RNF12 has been previously shown to activate *Xist* transcription at the onset of XCI (Barakat et al. 2011; Jonkers et al. 2009). Importantly, the pluripotency factor REX1 has been identified as a key target of RFN12, and dose-dependent degradation of REX1 by RNF12 has been proposed to act as an important mechanism directing the initiation of XCI upon differentiation of female mESCs (Gontan et al. 2012). Since the RNF12-REX1 axis represents an important pathway for XCI to occur in mouse, we asked whether these factors play similar roles in rat XCI. To this end, we transiently overexpressed the mouse RNF12 (mRNF12) and REX1 (mREX1) proteins in rESCs, and determined the impact of overexpression on *Xist* RNA regulation. According to the mouse data, we expected REX1 overexpression to result in the inhibition of *Xist* transcription whereas overexpressing RNF12 would lead to *Xist* up-regulation (Barakat et al. 2011; Gontan et al. 2012). *Xist* RNA expression levels were determined by qRT-PCR analysis, and the experiment was performed in two independent female rESC lines and a single male rESC line (Figure 4). Overexpression of mRNF12 consistently resulted in upregulation of *Xist* RNA in both male and female rESCs, thus confirming RNF12 to act as major trans-acting activator of XCI in both mouse and rat (Figure 4A and B right graph). Interestingly, overexpressing mREX1 in rESCs did not lead to a clear inhibition of *Xist* RNA transcription (Figure 4A). This observation might be explained by the fact that *Xist* RNA repression in undifferentiated mESCs is already maximal, and established not only by REX1, but also by other pluripotency factors (Navarro et al. 2008; 2010; Payer et al. 2013). However, it can not be excluded that the lack of effect could be caused by the fact that we used the mouse protein, which may not function optimally in a rat ESC environment.

Although the critical catalytic ring finger domain of RNF12 shows 100% of amino acid sequence identity between mouse and rat, the important zinc finger domains, determining DNA binding specificity, of REX1 are less well conserved (Figure 4C). Indeed, overexpression of rat REX1 (rREX1) in undifferentiated rESCs resulted in downregulation of *Xist* RNA in both female and male cells (Figure 4B).

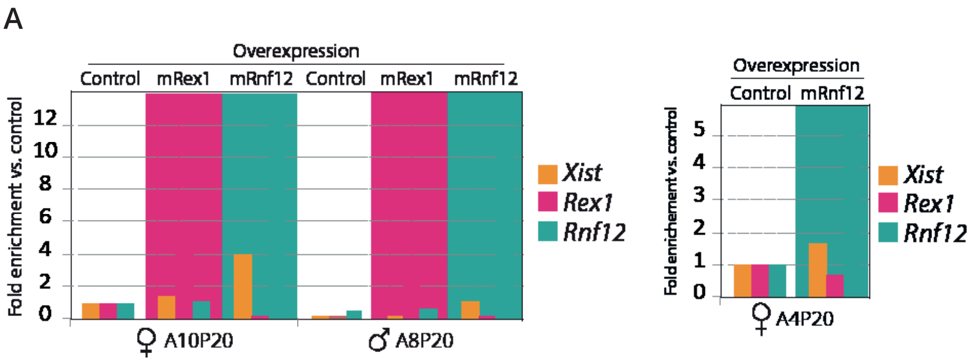

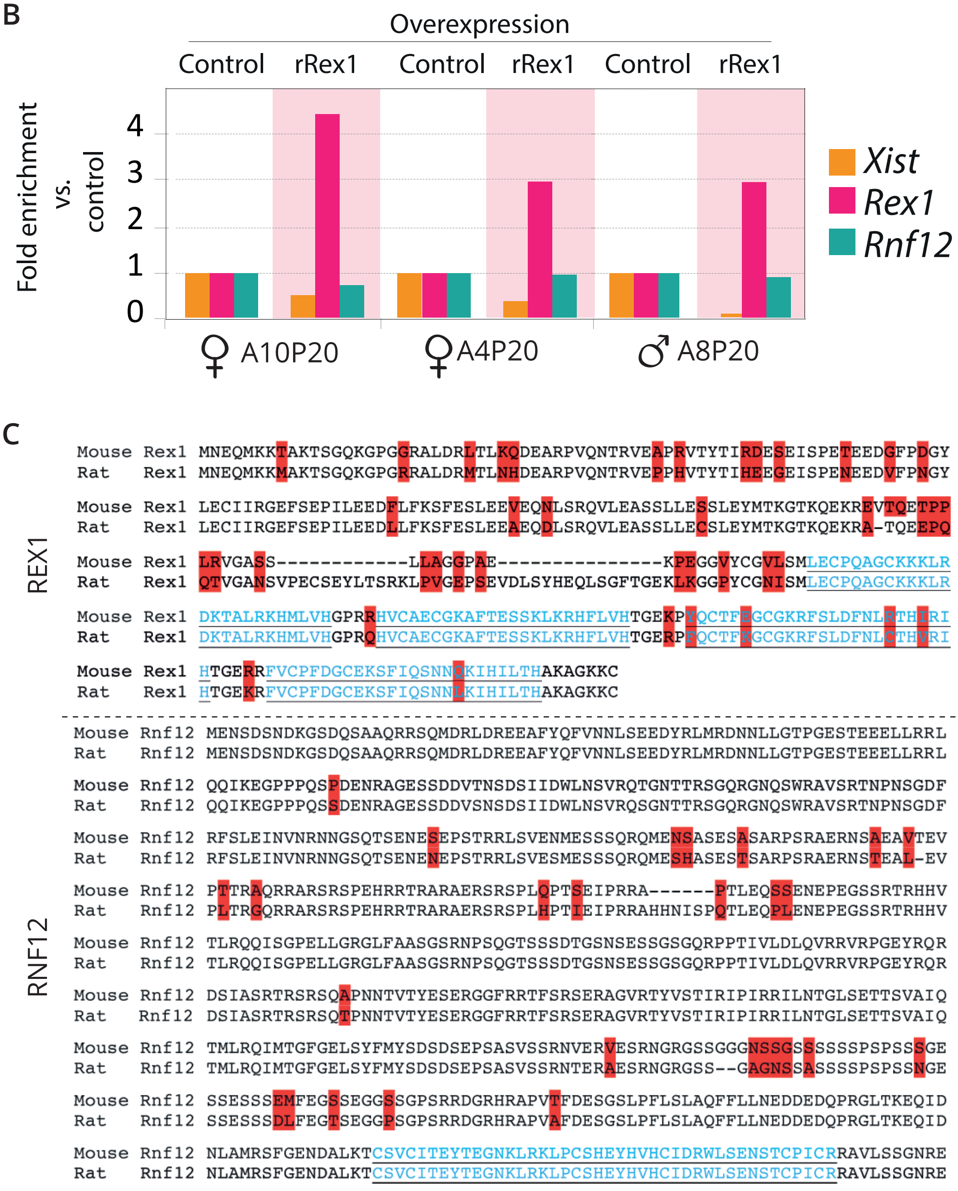

```
Mouse Rex1 MNEQMKKTAKTSGQKGPGGRALDRLTLKQDEARPVQNTRVEAPRVTYTIRDESEISPETEEDGFPDGY
Rat   Rex1 MNEQMKKMAKTSGQKGPGRRALDRMTLNHDEARPVQNTRVEPPHVTYTIHEEGEISPENEEDVFPNGY

Mouse Rex1 LECIIRGEFSEPILEEDFLFKSFESLEEVEQNLSRQVLEASSLLESSLEYMTKGTKQEKREVTQETPP
Rat   Rex1 LECIIRGEFSEPILEEDLLFKSFESLEEAEQDLSRQVLEASSLLECSLEYMTKGTKQEKRA-TQEEPQ

Mouse Rex1 LRVGASS------------LLAGGPAE---------------KPEGGVYCGVLSMLECPQAGCKKKLR
Rat   Rex1 QTVGANSVPECSEYLTSRKLPVGEPSEVDLSYHEQLSGFTGEKLKGGPYCGNISMLECPQAGCKKKLR

Mouse Rex1 DKTALRKHMLVHGPRRHVCAECGKAFTESSKLKRHFLVHTGEKPYQCTFEGCGKRFSLDFNLRTHIRI
Rat   Rex1 DKTALRKHMLVHGPRQHVCAECGKAFTESSKLKRHFLVHTGERPFQCTFKGCGKRFSLDFNLCTHVRI

Mouse Rex1 HTGERRFVCPFDGCEKSFIQSNNQKIHILTHAKAGKKC
Rat   Rex1 HTGEKRFVCPFDGCEKSFIQSNNLKIHILTHAKAGKKC
---------------------------------------------------------------------------
Mouse Rnf12 MENSDSNDKGSDQSAAQRRSQMDRLDREEAFYQFVNNLSEEDYRLMRDNNLLGTPGESTEEELLRRL
Rat   Rnf12 MENSDSNDKGSDQSAAQRRSQMDRLDREEAFYQFVNNLSEEDYRLMRDNNLLGTPGESTEEELLRRL

Mouse Rnf12 QQIKEGPPPQSPDENRAGESSDDVTNSDSIIDWLNSVRQTGNTTRSGQRGNQSWRAVSRTNPNSGDF
Rat   Rnf12 QQIKEGPPPQSSDENRAGESSDDVSNSDSIIDWLNSVRQSGNTTRSGQRGNQSWRAVSRTNPNSGDF

Mouse Rnf12 RFSLEINVNRNNGSQTSENESEPSTRRLSVENMESSSQRQMENSASESASARPSRAERNSAEAVTEV
Rat   Rnf12 RFSLEINVNRNNGSQTSENENEPSTRRLSVESMESSSQRQMESHASESTSARPSRAERNSTEAL-EV

Mouse Rnf12 PTTRAQRRARSRSPEHRRTRARAERSRSPLQPTSEIPRRA------PTLEQSSENEPEGSSRTRHHV
Rat   Rnf12 PLTRGQRRARSRSPEHRRTRARAERSRSPLHPTIEIPRRAHHNISPQTLEQPLENEPEGSSRTRHHV

Mouse Rnf12 TLRQQISGPELLGRGLFAASGSRNPSQGTSSSDTGSNSESSGSGQRPPTIVLDLQVRRVRPGEYRQR
Rat   Rnf12 TLRQQISGPELLGRGLFAASGSRNPSQGTSSSDTGSNSESSGSGQRPPTIVLDLQVRRVRPGEYRQR

Mouse Rnf12 DSIASRTRSRSQAPNNTVTYESERGGFRRTFSRSERAGVRTYVSTIRIPIRRILNTGLSETTSVAIQ
Rat   Rnf12 DSIASRTRSRSQTPNNTVTYESERGGFRRTFSRSERAGVRTYVSTIRIPIRRILNTGLSETTSVAIQ

Mouse Rnf12 TMLRQIMTGFGELSYFMYSDSDSEPSASVSSRNVERVESRNGRGSSGGGNSSGSSSSSPSPSSSGE
Rat   Rnf12 TMLRQIMTGFGELSYFMYSDSDSEPSASVSSRNTERAESRNGRGSS--GAGNSSASSSSPSPSSNGE

Mouse Rnf12 SSESSSEMFEGSSEGGSSGPSRRDGRHRAPVTFDESGSLPFLSLAQFFLLNEDDEDQPRGLTKEQID
Rat   Rnf12 SSESSSDLFEGTSEGGPSGPSRRDGRHRAPVAFDESGSLPFLSLAQFFLLNEDDEDQPRGLTKEQID

Mouse Rnf12 NLAMRSFGENDALKTCSVCITEYTEGNKLRKLPCSHEYHVHCIDRWLSENSTCPICRRAVLSSGNRE
Rat   Rnf12 NLAMRSFGENDALKTCSVCITEYTEGNKLRKLPCSHEYHVHCIDRWLSENSTCPICRRAVLSSGNRE
```

Figure 4: RNF12 and REX1 overexpression in rESCs

A qRT-PCR analysis of *Xist*, *Rex1* and *Rnf12* expression levels after overexpression of mREX1 and mRNF12 proteins. In the A4P20 female cell line only the mRNF12 (and not the mREX1) was overexpressed. **B** qRT-PCR analysis of *Xist*, *Rex1* and *Rnf12* expression levels after overexpression rREX1 protein in undifferentiated female (A10p20 and A4P20) and male (A10p20) rESCs. **C** Amino acid sequences alignment of mouse and rat REX1 and RNF12. Highlighted in red are the not conserved amino acids. In blue, the four zinc fingers domains of REX1 protein and the RING finger domain of RNF12.

Discussion

Our knowledge concerning the regulation of XCI in developing rat embryos is limited and relies on conservation of the key regulators *Xist* and *Tsix* between mouse and rat and a few studies in which, similar to mouse, iXCI has been proposed to occur in early rat embryonic development (Wake et al. 1976; Nesterova et al. 2001; Chureau et al. 2002; Elisaphenko et al. 2008; Duret et al. 2006). Studying the XCI process in rESCs offers the opportunity to explore species-specific epigenetic features and will generally help to reach a more comprehensive understanding of the XCI process in mammals. Although rESCs *in vitro* differentiation protocols have been previously established (Cao et al. 2011; Peng et al. 2013), the potential difference between female and male differentiation capacity and efficiency has never been taken into account, and the transcriptional status of the X chromosomes has never been characterized. Here, we did not observe any of the XCI-related epigenetic features of rESCs during differentiation according to the previously established protocols, and we therefore set up a novel monolayer *in vitro* differentiation strategy that efficiently recapitulates the XCI process in rat cells. Importantly, the key feature that allowed us to achieve robust initiation of XCI is the complete absence of 2i inhibitors throughout the entire differentiation protocol. In the meantime, Vaskova and colleagues reported a similar strategy to trigger XCI upon differentiation of pluripotent rat cells (Vaskova et al. 2015). As in our protocol, withdrawing 2i factors from the differentiating culture medium resulted in efficient *Xist* up-regulation, thus confirming that inhibition of the MAPK and Gsk3β pathways upon *in vitro* differentiation of rESCs prevents XCI. We next exploited our *in vitro* system to assess the dynamics of XCI in differentiating rESCs. As in mESCs, both X chromosomes are active in undifferentiated rESCs and *Xist* RNA monoallelic upregulation starts to occur around day 2 of neuronal differentiation. Interestingly, the downregulation of *Tsix* expression at the onset of rat XCI appeared to be heterogeneous compared to what we observed in mESCs (Loos 2016). However, since allele-specific analysis of *Tsix* expression levels cannot be assessed in our rESCs system, whether the observed *Tsix* expression is derived from the active or the inactive chromosome remains an open question and will need to be addressed in hybrid cell lines.

In addition, we showed that transcriptional inactivation of X-linked genes directly follows *Xist* RNA accumulation on one of the two X chromosomes. In fact, the exclusive enrichment of H3K27me3 loci in female nuclei starts around day 3 of neuronal differentiation, and *Xist*-mediated silencing of X-linked gene *Pgk1* occurs with dymanics similar to H3K27me3 acummulation. Finally, by overexpressing the XCI key regulators RNF12 and REX1 in undifferentiated rESCs, we have confirmed the conservation of their critical function in directing *Xist* expression. Importantly, we show that overexpression of mRNF12 protein in rESCs efficiently recapitulates RNF12 function, whereas in the case of REX1 only the overexpression of the rREX1 homologue results in *Xist* RNA downregulation in rESCs. In line with this observation, the DNA-binding domains of REX1 proteins from different species show an average of 11-20 amino acid differences (Kim et al. 2007) thus confirming that the degree of protein conservation between mouse and rat REX1 homologues may explain our results. In contrast, RNF12 is highly conserved among mammals (Bach et al. 1999), and the observed up-regulation of rat *Xist* upon mRNF12 overexpression confirms what we previously observed upon overexpression of human RNF12 in mESCs (Jonkers et al. 2009). In conclusion, we were able to set up a robust *in vitro* system to study the regulation of XCI in differentiating rESCs and our results suggest that the main steps of XCI in our rat *in vitro* system are highly similar to those of mouse XCI. The generation of hybrid F1 polymorphic rESCs and utilisation of the recently developed CRISPR/Cas9 technology for genomic editing will increase the use of rat as a model organism in basic epigenetic and biomedical research.

Experimental procedures

Cell culture and DNA transfection

rESCs were derived as previously described (Meek et al. 2010) and subsequently maintained in N2B27 medium supplemented with 3μM CHIR99021 (Stemgent), 1μM PD0325901 and 1000U/ml mouse LIF on mouse embryonic (MEF) feeders.

For the monolayer differentiation culture plates were coated with 100μg/ml laminin (Sigma-Aldrich) for at least 4 hours at 37^{o} C, followed by three PBS washes. Single rESCs were plated at a density of 10^5/cm^2 for the female cell lines and 2x10^4/cm^2 for the male cell lines in N2B27 supplemented with 10μM of ROCK inhibitor (Sigma-Aldrich) for the first three days. Thereafter, the ROCK inhibitor was eliminated the culture medium. Medium was refreshed daily.

For the overexpression experiments, the m*Rex1*, r*Rex1* and m*Rnf12* coding sequences were subcloned into pCAG-Flag, a CAG-driven expression vector containing a Flag-tag. Undifferentiated rESCs, maintained as described above, were transfected using lipofectamine 2000 (Invitrogen) according to the manufacturer's instructions, followed by 48 hours of puromycin selection.

Probe preparation and Fluorescent in Situ Hybridization (FISH)

For preparing probes detecting *Xist* and *Pgk1* mRNAs, BACs harboring these genes were labelled as a whole, with digoxigenin and biotin respectively, by nick translation (11745816910 and 11745824910, Roche diagnostics) following the manufacturer's instructions.

For RNA-FISH at different time points of neuronal differentiation, cells were grown on glass coverslips and then fixed with 3% PFA for 10 minutes on ice, followed by three washes in PBS. Next, cells were permeabilised with 0.5% Triton and washed again three times in PBS. Cytoplasm was removed by treating the cells with 0.025% pepsin in 0.01N HCL for 3 minutes at 37^o C. Subsequently, cells were dehydrated with sequential ethanol washes (70%, 85% and 100% 2 minutes each) and air-dried. Finally, probes were applied on the samples overnight at 37^o C in a 50% Formamide/2XSSC humid chamber. The next day, slides were washed two times, 5 minutes each, in 50% Formamide/2xSSC pH=7.4 at 37^o C, followed by two washes, 5 minutes each. in 2xSSC at 37^o C and cells were blocked for 30 minutes at room temperature with TSBSA (2 mg/ml bovine serum albumin in 0.1 M Tris and 0.15 M NaCl) in a humid chamber at room temperature. Detection was performed by incubation with anti-digoxigenin FITC (Boehringer, 1:250) and streptavidin alexa fluor 555 (Thermofisher Scientific, 1:400) in TSBSA for 30 minutes at room temperature. Slides were then washed two times, 5 minutes each with TS (0.1 M Tris, 0.15 M NaCl) and mounted with ProLong® Gold Antifade Mountant with Dapi (ThermoFisher Scientific). Imaging was performed on a Zeiss LSM700 microscope (Carl Zeiss, Jena).

Expression analysis

Cells were lysed by direct addition of 500 µl of TRIZOL and total RNA was extracted according to the manufacturer's instructions (Invitrogen). To remove genomic DNA contamination, samples were treated 15 minutes at 37°C with DNaseI (Invitrogen). Next, 1 µg of RNA was reverse transcribed by Superscript II reverse transcriptase with random hexamers (Invitrogen). For quantitative PCR (qPCR) gene expression levels were quantified using 2x SYBR Green PCR Master Mix (Applied Biosystems) in a CFX384 Real-Time machine (Bio-Rad) with primers listed is Table S1. Expression levels were normalized to *Actin b* using the $2^{-\Delta Ct}$ method (Livak & Schmittgen 2001).

Immunocytochemistry

For immunofluorescence analysis on different time points of neuronal differentiation, cells were grown on glass coverslips and then fixed with 3% PFA for 10 minutes at room temperature followed by three washes in PBS (3x5'). Thereafter, cells were permeabilised with 0.5% Triton, washed with PBS (3x5') and blocked with 2% BSA, 5% donkey serum in PBS (blocking solution) for 30 minutes at room temperature. This was followed by rabbit anti-H3K27me3 (Diagenode, 1:500) incubation, diluted in blocking solution, at 4^o C overnight in a humid chamber. The next day, slides were washed in PBS (3x5') and blocked with donkey anti-rabbit alexa fluor 488 (ThermoFischer Scientific, 1:250) secondary antibody, diluted in blocking solution for 1 hour at room temperature in a humid chamber. Slides were then washed in PBS (3x5’) and mounted with ProLong® Gold Antifade Mountant with Dapi (ThermoFisher Scientific). Confocal imaging was performed on a Zeiss LSM700 microscope (Carl Zeiss, Jena).

REFERENCES

van Bemmel, J.G., Mira-Bontenbal, H. & Gribnau, J., 2016. Cis- and trans-regulation in X inactivation. Chromosoma, 125(1), pp.41–50.

Borsani, G. et al., 1991. Characterization of a murine gene expressed from the inactive X chromosome. Nature, 351(6324), pp.325–329.

Brockdorff, N. et al., 1991. Conservation of position and exclusive expression of mouse *Xist* from the inactive X chromosome. Nature, 351(6324), pp.329–331.

Buehr, M. et al., 2008. Capture of Authentic Embryonic Stem Cells from Rat Blastocysts. Cell, 135(7), pp.1287–1298.

Chureau, C. et al., 2002. Comparative sequence analysis of the X-inactivation center region in mouse, human, and bovine. Genome research, 12(6), pp.894–908.

Dindot, S. V., 2004. Epigenetic and Genomic Imprinting Analysis in Nuclear Transfer Derived Bos gaurus/Bos taurus Hybrid Fetuses. Biology of Reproduction, 71(2), pp.470–478.

Duret, L., 2006. The *Xist* RNA Gene Evolved in Eutherians by Pseudogenization of a Protein-Coding Gene. Science, 312(5780), pp.1653–1655.

Elisaphenko, E.A. et al., 2008. A Dual Origin of the *Xist* Gene from a Protein-Coding Gene and a Set of Transposable Elements S. Gadagkar, ed. PLoS ONE, 3(6), p.e2521.

Friedrich Ben-Nun, I. et al., 2011. Induced pluripotent stem cells from highly endangered species. Nature Methods, 8(10), pp.829–831.

Gendrel, A.-V. & Heard, E., 2014. Noncoding RNAs and Epigenetic Mechanisms During X-Chromosome Inactivation. Annual Review of Cell and Developmental Biology, 30(1), pp.561–580.

Gontan, C. et al., 2012. RNF12 initiates X-chromosome inactivation by targeting REX1 for degradation. Nature, 485(7398), pp.386–90.

Grant, J. et al., 2012. Rsx is a metatherian RNA with *Xist*-like properties in X-chromosome inactivation. Nature, 487(7406), pp.254–258.

Guan, Y. et al., 2014. Generation of Site-Specific Mutations in the Rat Genome Via CRISPR/Cas9. In pp. 297–317.

Hirabayashi, M. et al., 2009. Establishment of rat embryonic stem cell lines that can participate in germline chimerae at high efficiency. Molecular Reproduction and Development, p.n/a-n/a.

Huynh, K.D. & Lee, J.T., 2003. Inheritance of a pre-inactivated paternal X chromosome in early mouse embryos. Nature, 426(6968), pp.857–862.

Jonkers, I. et al., 2009. RNF12 is an X-Encoded dose-dependent activator of X chromosome inactivation. Cell, 139(5), pp.999–1011.

Kawamata, M. & Ochiya, T., 2010. Establishment of Embryonic Stem Cells from Rat Blastocysts. In pp. 169–177.

Kawamata, M. & Ochiya, T., 2010. Generation of genetically modified rats from embryonic stem cells. Proceedings of the National Academy of Sciences, 107(32), pp.14223–14228.

Lee, J.T. & Lu, N., 1999. Targeted mutagenesis of *Tsix* leads to nonrandom X inactivation. Cell, 99(1), pp.47–57.

Li, P. et al., 2008. Germline Competent Embryonic Stem Cells Derived from Rat Blastocysts. Cell, 135(7), pp.1299–1310.

Li, X. et al., 2016. Generation and Application of Mouse-Rat Allodiploid Embryonic Stem Cells. Cell, 164(1–2), pp.279–292.

Livak KJ, Schmittgen TD (2001) Analysis of relative gene expression data using real-time quantitative PCR and the 2(-Delta Delta C(T)) Method. Methods 25: 402-408.

Ma, Z. et al., 2011. Sequence-specific regulator Prdm14 safeguards mouse ESCs from entering extraembryonic endoderm fates. Nature Structural & Molecular Biology, 18(2), pp.120–127.

Mak, W. et al., 2004. Reactivation of the paternal X chromosome in early mouse embryos. Science (New York, N.Y.), 303(5658), pp.666–9.

Marahrens, Y. et al., 1997. *Xist*-deficient mice are defective in dosage compensation but not spermatogenesis. Genes & development, 11(2), pp.156–66.

Meek, S. et al., 2010. Efficient Gene Targeting by Homologous Recombination in Rat Embryonic Stem Cells D. S. Milstone, ed. PLoS ONE, 5(12), p.e14225.

Meek, S. et al., 2013. Tuning of β-catenin activity is required to stabilize self-renewal of rat embryonic stem cells. STEM CELLS, 31(10), pp.2104–2115.

Meek, S., Sutherland, L. & Burdon, T., 2014. Tuning Differentiation Signals for Efficient Propagation and In Vitro Validation of Rat Embryonic Stem Cell Cultures. In pp. 73–85.

Mekhoubad, S. et al., 2012. Erosion of Dosage Compensation Impacts Human iPSC Disease Modeling. Cell Stem Cell, 10(5), pp.595–609.

Men, H., Bauer, B.A. & Bryda, E.C., 2012. Germline Transmission of a Novel Rat Embryonic Stem Cell Line Derived from Transgenic Rats. Stem Cells and Development, 21(14), pp.2606–2612.

Migeon, B.R. et al., 2001. Identification of *TSIX*, Encoding an RNA Antisense to Human *XIST*, Reveals Differences from its Murine Counterpart: Implications for X Inactivation. The American Journal of Human Genetics, 69(5), pp.951–960.

Migeon, B.R. et al., 2002. Species Differences in *TSIX*/*Tsix* Reveal the Roles of These Genes in X-Chromosome Inactivation. The American Journal of Human Genetics, 71(2), pp.286–293.

Moreira de Mello, J.C. et al., 2010. Random X inactivation and extensive mosaicism in human placenta revealed by analysis of allele-specific gene expression along the X chromosome. PloS one, 5(6), p.e10947.

Navarro, P. et al., 2010. Molecular coupling of *Tsix* regulation and pluripotency. Nature, 468(7322), pp.457–460.

Navarro, P. et al., 2008. Molecular Coupling of *Xist* Regulation and Pluripotency. Science, 321(5896), pp.1693–1695.

Navarro, P. et al., 2006. *Tsix*-mediated epigenetic switch of a CTCF-flanked region of the *Xist* promoter determines the *Xist* transcription program. Genes & Development, 20(20), pp.2787–2792.

Nesterova, T.B. et al., 2001. Characterization of the Genomic *Xist* Locus in Rodents Reveals Conservation of Overall Gene Structure and Tandem Repeats but Rapid Evolution of Unique Sequence. Genome Research, 11(5), pp.833–849.

Ohhata, T. et al., 2008. Crucial role of antisense transcription across the *Xist* promoter in *Tsix*-mediated *Xist* chromatin modification. Development (Cambridge, England), 135(2), pp.227–35.

Okamoto, I. et al., 2004. Epigenetic dynamics of imprinted X inactivation during early mouse development. Science (New York, N.Y.), 303(5658), pp.644–9.

Okamoto, I. et al., 2011. Eutherian mammals use diverse strategies to initiate X-chromosome inactivation during development. Nature, 472(7343), pp.370–4.

Pasque, V. & Plath, K., 2015. X chromosome reactivation in reprogramming and in development. Current opinion in cell biology, 37, pp.75–83.

Patrat, C. et al., 2009. Dynamic changes in paternal X-chromosome activity during imprinted X-chromosome inactivation in mice. Proceedings of the National Academy of Sciences of the United States of America, 106(13), pp.5198–203.

Payer, B. et al., 2013. *Tsix* RNA and the Germline Factor, PRDM14, Link X Reactivation and Stem Cell Reprogramming. Molecular Cell, 52(6), pp.805–818.

Peng X, Gao H, Wang Y, Yang B, Liu T, Sun Y, Jin H, Jiang L, Li L, Wu M, Qian Q: Conversion of rat embryonic stem cells into neural precursors in chemical-defined medium. Biochem Biophys Res Commun 2013, 431:783–787.

Penny, G.D. et al., 1996. Requirement for *Xist* in X chromosome inactivation. Nature, 379(6561), pp.131–137.

Sado, T., Hoki, Y. & Sasaki, H., 2005. *Tsix* Silences *Xist* through Modification of Chromatin Structure. Developmental Cell, 9(1), pp.159–165.

Schulz, E.G. et al., 2014. The Two Active X Chromosomes in Female ESCs Block Exit from the Pluripotent State by Modulating the ESC Signaling Network. Cell Stem Cell, 14(2), pp.203–216.

Shao, Y. et al., 2014. CRISPR/Cas-mediated genome editing in the rat via direct injection of one-cell embryos. Nature protocols, 9(10), pp.2493–512.

Shevchenko, A.I. et al., 2011. Variability of Sequence Surrounding the *Xist* Gene in Rodents Suggests Taxon-Specific Regulation of X Chromosome Inactivation B. P. Chadwick, ed. PLoS ONE, 6(8), p.e22771.

Takahashi, K. & Yamanaka, S., 2006. Induction of Pluripotent Stem Cells from Mouse Embryonic and Adult Fibroblast Cultures by Defined Factors. Cell, 126(4), pp.663–676.

Tchieu, J. et al., 2010. Female Human iPSCs Retain an Inactive X Chromosome. Cell Stem Cell, 7(3), pp.329–342.

Vaskova, E.A. et al., 2015. Transcriptome Characteristics and X-Chromosome Inactivation Status in Cultured Rat Pluripotent Stem Cells. Stem Cells and Development, 24(24), pp.2912–2924.

Wake, N., Takagi, N. & Sasaki, M., 1976. Non-random inactivation of X chromosome in the rat yolk sac. Nature, 262(5569), pp.580–1.

Watanabe, K. et al., 2007. A ROCK inhibitor permits survival of dissociated human embryonic stem cells. Nature Biotechnology, 25(6), pp.681–686.

Wutz, A. & Jaenisch, R., 2000. A shift from reversible to irreversible X inactivation is triggered during ES cell differentiation. Molecular cell, 5(4), pp.695–705.

Xue, F. et al., 2002. Aberrant patterns of X chromosome inactivation in bovine clones. Nature genetics, 31(2), pp.216–20.

Supplementary Table 1

SEQUENCE	DESCRIPTION
TGCCTGGATTTAGAGGAG	Forward primer *Xist* expression
CTCCACCTAGGGATCGTCAA	Reverse primer *Xist* expression
GTATCCACAGCCCCGATG	Forward primer *Tsix* expression
ACCTCGGATACCTGCGTTT	Reverse primer Tsix expression
TAGCCCTGATTCTTCTAGCA	Forward primer *Nanog* expression
TTTGCTGCAACGGCACATAA	Reverse primer *Nanog* expression
GGCGTTCTTCAAGAGAACCA	Forward primer *Esrrb* expression
CCCACTTTGAGGCATTTCAT	Reverse primer *Esrrb* expression
AGGAACTGCGCTTCGTTCT	Forward primer *Prdm14* expression
GGCATCACCAAAAGCTGTCT	Reverse primer *Prdm14* expression
AAATCATGACGAGGCAAGGC	Forward primer *Rex1* expression
TGAGTTCGCTCCAACAGTCT	Reverse primer *Rex1* expression
CTCTGCTGGAGGCTGAGAAC	Forward primer *Nestin* expression
TGGTATCCCAAGGAAATTCG	Reverse primer *Nestin* expression
GCTGGCCTTAGAGACCACAG	Forward primer *Actin* expression
AAGCAATTCAGCAACACCAA	Reverse primer *Actin* expression

List of primers used in this study

Chapter 5

A ROBUST PROTOCOL FOR SIMULTANEOUS DNA-RNA FISH IN MOUSE PRE-IMPLANTATION EMBRYOS

Aristea Magaraki, Agnese Loda, Joost Gribnau and Willy M. Baarends

Invited manuscript (Springer Protocols)

A ROBUST PROTOCOL FOR SIMULTANEOUS DNA-RNA FISH IN MOUSE PRE-IMPLANTATION EMBRYOS

Aristea Magaraki[1], Agnese Loda[1], Joost Gribnau[1] and Willy M. Baarends*[1]

Author Affiliations:
[1]Department of Developmental Biology, Erasmus University Medical Center, Wytemaweg 80, 3015 CN Rotterdam, The Netherlands

*Corresponding author:
Dr. Willy M. Baarends
e-mail: w.baarends@erasmusmc.nl

Abstract

Fluorescence in situ hybridization (FISH) is a powerful cytogenetic technique that allows the visualization and quantification of RNA and DNA molecules in different cellular contexts. In general, FISH applications help to advance research, cytogenetics and diagnostics. DNA FISH can be applied, for example, for gene mapping and for detecting genetic aberrations. RNA FISH provides information about gene expression. However, in cases where RNA and DNA molecules need to be detected in the same sample, the result is often compromised by the fact that the tissue sample is damaged due to the multitude of processing steps that are required for each application. In addition, the sequential application of RNA and DNA FISH protocols on the same sample is very time consuming. Here we describe a brief protocol that enables the combined and simultaneous detection of the non-coding *Xist* RNA, abundantly present in female cells, and centromeric DNA of chromosome 6 in mouse pre-implantation embryos. In addition, we describe how to generate indirect-labeled probes starting from BACs. This protocol may be potentially applied to any combination of RNA and DNA detection.

Key words

RNA and DNA FISH, combination of RNA and DNA FISH Fluorescent in situ hybridization (FISH), mouse pre-implantation embryos, *Xist* FISH, X chromosome inactivation, long non-coding RNA FISH, DNA FISH

1 Introduction

Fluorescence in situ hybridization is a macromolecule detection technology that is based on the ability of a single stranded DNA (probe) to anneal to complementary DNA (DNA FISH) or to RNA (RNA FISH). In general, this technology is applied for many different purposes in molecular research and diagnostics. Importantly, FISH not only provides visualization of the subcellular localization of nucleic acids, but it can also be used for quantification purposes. For example, the development of very sensitive RNA FISH protocols using multi-color probes, has allowed the analysis of spatio-temporal patterns of endogenous gene expression in the same environment (Raj et al. 2008; reviewed in Kwon 2013). The probes used for FISH can be directly or indirectly labeled using different protocols, such as the nick translation method. When probes are directly labeled, a fluorophore is directly associated with the DNA probe, while in the case of indirectly labeled probes a non-fluorescent molecule is covalently attached to the probe. Thereafter, detection is accomplished by incubating the specimen with appropriate fluorophore-labeled antibodies or specific binding molecules. The unlabeled molecule is typically a hapten, such as digoxigenin or biotin. Digoxigenin is derived from the plant steroid hormone digoxin, found in the plants Digitalis sp (Hart & Basu 2009). Biotin, on the other hand, is a small protein (vitamin B7) that is also present in all mammalian cells, but is more abundant in certain tissues, such as brain and liver (Said 2012).

The advantage of using indirect labeled probes lies in the fact that the antibodies or molecules (such as avidin or streptavidin when biotinylated probes are generated) that are used to detect the hybridized probe can carry multiple fluorophores. Therefore, this methodology has the potential to generate a more intense fluorescent signal, compared to directly labeled probes, and this can be of critical importance when the genomic area to be detected is small in size. On the other hand, using an indirect labeling method requires a detection reaction that will always generate some background signal. Additional background signal may be also generated by non-specific binding of the probe itself. This disadvantage applies particularly to biotin-labeled probes, since biotin is a biological molecule present in mammalian cells and binding of, for example fluorescent-tagged avidin, to endogenous biotin can cause a high background signal. Background issues may not constitute a significant problem when nascent RNA transcripts, directly transcribing from the corresponding chromosome itself, need to be detected. In this case, the cytoplasm of the specimen can be completely digested by enzymes, such as pepsin, which are routinely used in immunohistochemistry, RNA and DNA FISH procedures. In addition, digestion of structural and soluble protein components of the cytoplasm would also allow better penetration of the probe and the fluorophore-conjugated antibodies or molecules (e.g.

avidin) into the nucleus, which will result in enhanced nuclear signal. In general, despite the fact that indirect labeled probes produce more background compared to direct labeled ones, robust and clear signals can be produced when the probe and sample preparation are well monitored, the target genes or transcripts are efficiently exposed, and at the same time the morphology and integrity of the sample are well maintained. Lastly, the indirect labeling procedure is cheaper compared to direct labeling.

A transcript frequently and commonly studied in the X chromosome inactivation field is *Xist*. Female cells carry two copies of all X-linked genes, and males only have a single copy of all these genes (>1000). This generates a dosage problem in X-linked gene expression between the two sexes that needs to be equalized. In mammals, the X-linked gene dosage problem is solved by inactivation of one of the two X chromosomes in all female somatic nuclei by a mechanism termed X chromosome inactivation (XCI). When XCI is initiated, *Xist* becomes highly expressed only from the future inactive X chromosome, covers this X *in cis* and becomes detectable as a cloud in the nucleus using RNA FISH (Clemson et al. 1996). This is then followed by addition of a repertoire of repressive histone modifications to ensure the faithful establishment of X silencing (Okamoto et al. 2004; Brockdorff & Turner 2015; Wutz 2011). In mouse preimplantation embryos, XCI is imprinted. Around the four-cell stage, imprinted XCI (iXCI) is initiated always targeting the paternal X chromosome in female mouse embryos (Marahrens et al. 1997; Okamoto et al. 2004; Mak et al. 2004). While iXCI is maintained in the extraembryonic cell lineage, it is eventually reversed in the inner cell mass of the blastocyst that will give rise to the embryo proper (Okamoto et al. 2004; Mak et al. 2004). XCI is then re-initiated in a random fashion in the developing embryo, where either the paternal or the maternal X chromosome becomes inactive (Takagi et al. 1982).

Over the years, accumulating evidence suggests that the position of a gene within the nucleus environment can influence its transcriptional activity (revied in Takizawa et al. 2008). To study such relationships between gene nuclear spatial positioning and activity, numerous DNA-RNA FISH protocols have been developed (Chaumeil et al. 2008; Namekawa & Lee 2011). Nonetheless, despite the excellent detection of the nucleic acids in these protocols, RNA and DNA FISH are performed sequentially, rather than simultaneously. Due to the sensitivity of RNA transcripts to degradation by traces of RNAse or by the harsh conditions routinely applied during DNA FISH, RNA FISH is usually performed first. It is then followed by DNA FISH.

Here we have developed a robust and reproducible DNA-RNA FISH protocol, where RNA and DNA molecule detection is performed simultaneously, and without compromising the sample's quality. We have incorporated a 0.2N HCl incubation step in our protocol, which we found to be an absolute prerequisite for the successful detection of DNA targets. Treatment of formalin-fixed tissue samples with HCL is a standard step in DNA FISH, and it is thought to help to deproteinize the sample and reverse formaldehyde fixation (Bartlett 2004; Sommerlad et al. 2002). In particular, the basic histones may be extracted, allowing better access to DNA. The stripping of the proteins during DNA-RNA FISH may be very essential, especially if proteins mask the DNA targets and at the same time extremely harsh conditions (e.g. long denaturation times in high temperatures) cannot be applied if RNA molecules are to be detected. In addition, we applied two different denaturation steps, which also enhanced the DNA FISH signal, since omitting one of the two, compromised the DNA FISH signal. Usually, when RNA FISH protocols are followed, HCl treatment and denaturation steps are not applied, while they are typically found in DNA FISH protocols. Incorporation and adjustment of these two steps in our combined protocol did not influence detection of RNA transcripts. We set up our protocol in mouse pre-implantation embryos where we detected *Xist* transcripts and centromeric regions of chromosome 6. Therefore this protocol may be used to study different aspects XCI in the early embryo. At the same time it may be likely adapted and applied to other systems, such as on differentiating embryonic stem cells, frozen tissue sections and differentiated cultured cells (e.g. fibroblasts), where both nascent RNA transcripts (*Xist* or others) and genomic positions need to be detected. In the future, it would be important to determine whether this protocol can be applied successfully in detecting coding mRNAs together with DNA targets. Such an application may provide important information on how different genomic loci interact with each other, and at the same time how such interactions influence gene activity at the single cell level and in different cellular developmental and differentiation contexts.

2 Materials

2.1 Generating probes from BACs

2.1.1 BAC culture and isolation

1. BAC containing the genomic region to be detected
2. Agar (A1296, Sigma-Aldrich)
3. Sterile toothpicks
4. Antibiotics for bacterial selection
5. LB broth (L3022, Sigma-Aldrich)
6. 10cm petri dishes (90032TS, Thermo Fisher Scientific)
7. BAC DNA isolation kit (740414, Macherey Nagel)
8. Pyrex 500ml bottles (B5420-500, Corning®)
9. Inoculating loop (8388-500EA, Sigma-Aldrich)

10. Sterile, RNAse free H_2O
11. Glycerol (G9012, Sigma-Aldrich)
12. Erlenmeyer flasks (N3231, Sigma-Aldrich)
13. Centrifuge (Model Allegra® X-15R, Beckman Coulter)
14. Centrifuge bottles for bacterial cultures (for Allegra® X-15R Item number 356855, Beckman Coulter)
15. Incubator shaker (Model Innova® 43, Incubator Shaker Series)
16. 15ml and 50ml falcon tubes (14-959-53A and 14-432-22, Thermo Fisher Scientific)
17. Heating-drying oven (Model UT 6060, Thermo Fisher Scientific Heraeus)

2.1.2 Probe preparation, purification and precipitation

1. Sterile, RNAse free water
2. Eppendorf tubes (30120086, Eppendorf)
3. Absolute ethanol (32221, Sigma-Aldrich)
4. Eppendorf (refrigerated) centrifuge (Model 5417R and Model 5810R, Eppendorf)
5. NaAc 3M pH 5.5 (S7670, Sigma-Aldrich)
6. Digoxigenin (11745816910, Roche Diagnostics) and Biotin nick translation kit (11745824910, Roche Diagnostics)
7. 0.5M EDTA pH 8.0 (E9884, Sigma-Aldrich)
8. Mouse Cot-1 DNA (18440016, Thermo Fisher Scientific)
9. UltraPure™ Salmon Sperm DNA Solution (15632011, Thermo Fisher Scientific)
10. Yeast tRNA (15401011, Thermo Fisher Scientific)
11. Sephadex G-50 (17004101, GE Healthcare Life Sciences)
12. Syringes, 1ml (300013, BD Plastipak)
13. Medical cotton
14. 2% agarose gel
15. 100bp DNA ladder (N3231, NEB)
16. Eppendorf™ ThermoStat Plus Interchangeable Block Heater (Model 22670565, Eppendorf)
17. Tube centrifuge (Model 5810R, Eppendorf)
18. 15ml falcon tubes (14-959-53A, Thermo Fisher Scientific)

2.2 Slide pre-preparation for embryo deposition

1. 50x Denhardt’s solution: 1% BSA (BU-102, Jena Bioscience), 1% Ficoll (46326 Fluka), 1% Polyvinylpyrrolidone (PVP-360, Sigma-Aldrich) in sterile H_2O, filter sterilized, aliquoted and stored in -20^{o} C. Use to make 3xDenhardt/3x SSC.
2. 20x SSC: 3M NaCl (S9888, Sigma-Aldrich), 0,3M sodium citrate tribasic dehydrate

(C8532, Sigma-Aldrich) in sterile RNAse free H_2O, pH 7.2-7.4. Use to make 3xDenhardt/3x SSC

3. 1M HCl (100317, Merck Millipore)
4. Sterile, RNAse free water
5. Absolute ethanol (32221, Sigma-Aldrich)
6. Acetic acid (33209, Sigma Aldrich)
7. Diamond pen (6120300, Marienfeld-Superior)
8. Slides superfrost (10143560W90, Thermo Fisher Scientific)
9. Slide rack
10. 50ml falcon tubes (14-432-22, Thermo Fisher Scientific)

2.3 Embryo donors' preparation, embryo isolation & culture

1. 6-8 week old female mice and 8 weeks or older male mice
2. Pregnant Mare Serum Gonadotrophin (PMSG) (REG NL 1396, MSD Animal Health; Intervet)
3. Human Chorionic Gonadotropin (hCG) (REG NL 1249, MSD Animal Health; Intervet)
4. 1ml syringe with 26G needle (300013, BD Plastipak with 305111, BD Worldwide)
5. Embryo-tested bovine testes hyaluronidase (H-4272, Sigma)
6. M2 medium (M7167, Sigma)
7. M16 (M7292, Sigma)
8. Mineral Oil tested for embryo culture (M8410, Sigma)
9. Forceps, watchmaker's #5, two pairs (HB105, Meekers Medical)
10. Glass capillaries (1,5 OD x 1,17 ID x 150L, GC150T-10, Harvard Apparatus)
11. The STRIPPER BP Stainless Steel Slimline embryo-handling micropipetter (MXL3-STR-BP-SW, ORIGIO) with silicone bulb (MXL3-BUBL, ORIGIO)
12. Stereomicroscope, SZH10 Olympus
13. Humidified CO_2 (5% v/v in air) incubator (MCO-17AIC, Sanyo)
14. 60x15 mm IVF one well dish tested for embryotoxicity (353653, Falcon)
15. 60x15 mm IVF round dish tested for embryotoxicity (353652, Falcon)

2.4 DNA-RNA FISH Day 1

2.4.1 Probe preparation for DNA-RNA FISH procedure

1. 50+ hybridization solution: 50% Formamide (3272350000, Acros organics), 2x SSC (use 20x SSC provided in 2.2), 50mM phosphate buffer pH 7.0 (use 1M phosphate buffer: 6,9g NaH_2PO_4-H_2O (S9638, Sigma-Adlrich), 7,1g Na_2PO_4 (255793, Sigma-Aldrich) in 50ml of sterile, RNAse free H_2O, pH 7.0), 10% dextrane sulfate pH 7 (31403, Fluka)
2. Mouse Cot-1 DNA (18440016, Thermo Fisher Scientific)

3. Eppendorf™ ThermoStat Plus Interchangeable Block Heater (Model 22670565, Eppendorf)
4. 15ml and 50ml falcon tubes (14-959-53A and 14-432-22, Thermo Fisher Scientific)

2.4.2 Sample preparation for DNA-RNA FISH and DNA-RNA FISH procedure (Day 1)

1. 10cm cell culture dishes or petri dishes (CLS430167, Sigma-Aldrich or 90032TS, Thermo Fisher Scientific)
2. Acidic Tyrode's Solution (T1788, Sigma-Aldrich)
16. M2 and M16 (M7167, Sigma and M7292, Sigma)
17. Glass capillaries (1,5 OD x 1,17 ID x 150L, GC150T-10, Harvard Apparatus)
18. The STRIPPER BP Stainless Steel Slimline embryo-handling micropipetter (MXL3-STR-BP-SW, ORIGIO) with silicone bulb (MXL3-BUBL, ORIGIO)
19. Embryo transfer glass pipette: Glass capillaries were pulled on a flame to smoothly produce a tube with an internal diameter slightly larger than the diameter of the zygotes (200-300 μm) and a narrow shaft approximately 1-2 cm long. The edge of the shaft was smoothened by rapidly flaming it (adapted from Sarvari et al. 2013).
20. Denhartd's coated slides (see 2.2 and 3.2)
21. Fixing solution: 3% PFA (50-980-487, Electron Microscopy Sciences) supplemented with 0,5% Triton X-100 (T8787, Sigma-Aldrich) in PBS
22. Post fixing solution: 3% PFA in sterile, RNAse free H_2O
23. Cell culture grade PBS (D8537, Sigma-Aldrich)
24. 0.2N HCl in sterile, RNAse free H_2O
25. 70%, 85% (diluted in sterile, RNAse free H2O) and 100% ethanol
26. 0.02% pepsin (P7000, Sigma-Aldrich) in 0.01N HCl
27. 50% Formamide (3272350000, Acros organics)/2xSSC pH 7.2-7.5 (prepare from 20xSSC **section 2.2**) in sterile, RNAse free H_2O
28. Denaturation buffer: 70% Formamide /2x SSC/10 mM phosphate buffer in sterile, RNAse free H_2O (see 2.4.1) pH 7.0
29. Slide chamber

2.4.3 DNA-RNA FISH procedure (Day 2)

1. FA/2xSSC washing solution: 50% Formamide (3272350000, Acros organics)/2xSSC pH 7.2-7.5 (prepare from 20xSSC section **2.2**) in sterile, RNAse free H_2O
2. Detection antibodies: Anti-Digoxigenin-Fluorescein, Fab fragments conjugated with FITC (11207741910, Roche, 1:250), streptavidin Alexa Fluor® 555 conjugate (S-21381, Thermo Fisher Scientific 1:400)
3. Vanadyl Ribosyl Complex ((VRC) S1402S, New England Biolabs)

4. 10x saline solution: 1.5M NaCl (S9888, Sigma-Aldrich) in sterile, RNAse free H_2O
5. Blocking solution: 500 µl 10x saline, 250 µl 2 M Tris base (T1503, Sigma-Aldrich), 1 ml 100x BSA (B9001S, New England Biolabs), 3.25 ml sterile, RNAse free H2O
6. Tris-saline washing solution (TS): 100 ml 10x saline, 50 ml 2M Tris, in 1 L of sterile, RNAse free water.
7. ProLong® Gold Antifade Mountant with DAPI (P36931, Thermo Fisher Scientific).

3 Methods

3.1 Generating probes from BACs

There are several ways to prepare a DNA probe, in order to detect RNA or DNA molecules. In the following lines we provide a detailed description on how to generate indirect labeled probes using BACs as a template. The same procedure applies for probes to be used for DNA or RNA FISH. In general, it is extremely important to use RNAse free water in all steps, such as DEPC treated water or commercial RNAse free H_2O. Autoclaved H_2O is not sufficient and it will compromise the RNA FISH signal.

3.1.1 BAC culture and isolation (adapted from Wood 1983)

1. Identify and order the BAC containing the area of interest, where the DNA FISH probe will hybridize. Here we used a BAC containing the centromeric region of chromosome 6. For the RNA FISH probe, identify a BAC containing the gene of interest. The RNA FISH probe will hybridise to the gene's nascent RNA, directly transcribing from the corresponding chromosome. Here we use a BAC containing the *Xist* gene (Note 1). We routinely acquire BAC clones from http://dna.brc.riken.jp/en/NBRPB6Nbacen.html.
2. BAC clones are supplied in agar. Prepare a stock of LB broth (according to the manufacture's instructions) containing the appropriate bacterial resistance antibiotic (provided with the specification sheet of the BAC).
3. Dip a sterile toothpick in the BAC-agar and transfer it in 10ml of LB broth. Grow overnight at 37° C shaking.
4. To prepare LB-agar solution, add 17.5 gr of agar in 500ml of LB in a pyrex 500ml bottle. Autoclave the bottle with the content. Allow the LB-agar to cool down and add the appropriate antibiotic. Distribute the content in petri dishes (approximately 20ml per petri dish). Let the petri dishes with the LB-agar stand at room temperature overnight (the LB-agar solidifies after a couple of hours) and then store them at 4° C for three months.
5. The next day, dip an inoculating loop into the liquid culture from step 3 and make a wave-shaped line on a 37° C pre-warmed LB agar plate (Figure 1) containing the appropriate antibiotic.

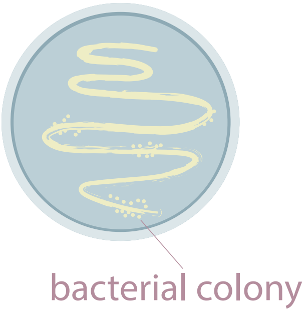

Figure 1: Plating bacteria on a LB-agar plate (containing the appropriate antibiotic)

Make a wave shaped line with the inoculating loop containing the bacteria, and culture overnight at 37° C. The next day pick up an individual colony and culture it further.

6. Grow overnight at 37° C.
7. Pick an individual colony with a sterile toothpick (Figure 1) and transfer it in a 15ml falcon tube with 5ml of LB containing the appropriate antibiotic. Culture overnight at 37° C shaking.
8. Create a frozen stock of the expanded bacterial colony containing the BAC, by mixing 500µl of the culture of step 7 with 500µl of 100% glycerol. Store at -80° C.
9. Expand the culture further by transferring the remaining bacterial culture in 500ml LB broth containing the appropriate antibiotic. Grow overnight at 37° C, shaking.
10. Collect the culture in a centrifuge bottle and centrifuge at 4000 rpm for 30’ at 4° C.
11. Discard the supernatant and isolate BAC DNA using a BAC DNA isolation kit (Note 2). Alternatively the pellet can be stored at -20° C or -80° C and the BAC DNA can be isolated later.
12. Re-suspend in 150µl of sterile H_2O and store at 4° C.

3.1.2 Probe preparation, purification and precipitation

Take approximately 1.5µg of BAC DNA. We routinely use 5µl of the DNA suspension from 3.1.1 BAC culture and isolation step 12.

1.Prepare four tubes with 1.5µg BAC DNA. Prepare two tubes with the nick translation reaction mixture from each labeling kit (Digoxigenin or Biotin labeled) according to the manufacturer’s instructions. One replica from each kit is used to monitor the size of the probe fragments (step 3).
2. After the incubation time indicated by the manufacturer of the kit, stop the reactions temporarily by placing them on ice, and prepare a 2% gel.
3. Take 3µl of the replicas (both from the Digoxigenin and Biotin labeled mixtures) and denature at 95° C for 5’. Add H_2O and loading solution to generate a total volume of 20µl (test probe). Place on ice for a few minutes.

4. Load the 20µl of each test probe on the 2% gel with a 100bp ladder as a size control and run the gel until the bands of the marker are clearly separated.

5. Inspect the size of the probes. The size of the majority probe fragments should range between 100bp to 500bp, as shown in Figure 2.

6. If the probe size is appropriate, the nick translation reaction in all tubes should be permanently stopped by supplementing it with 0.5M EDTA and heating it to 65° C for 10 minutes in a thermoblock. If the probe size is not as expected refer to Note 3.

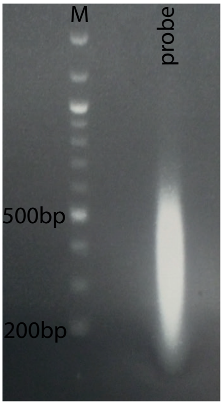

Figure 2: Probe size after nick translation

The majority of the probe fragments should be between 100bp and 500bp as shown in the figure (Note 4).

7. The two tubes containing the reactions (one containing a complete reaction mixture, and the other containing the remainder after removing some probe for the size inspection) from each kit can now be combined. Add sterile water up to 60µl and place on ice.

8. In order to purify the probes, prepare two 'home-made' sephadex G50 columns as follows: add medical cotton into an empty 1ml syringe (discard the plunger) up to the 150-200µl mark (Figure 3). Place the syringe into an empty 15ml tube, load the sephadex G50 beads and centrifuge 1 minute at 1800 rpm. Discard the flow through and repeat the loading of the sephadex beads until they fill approximately 80-90% of the syringe volume.

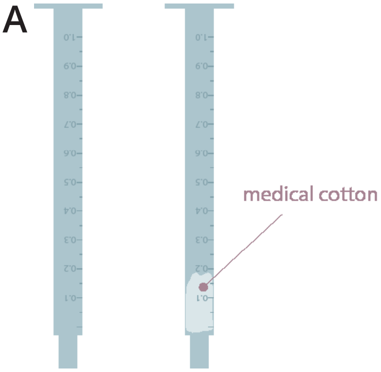

Figure 3: Home-made sephadex G50 column

A Discard the syringe's plunger and **B** place medical cotton at the tip of the syringe until it reaches ~200µl. The syringe is now ready to be loaded with the sephadex G-50 beads.

9. Transfer the column into a new 15ml tube and load the probe (60µl) without touching the beads. Centrifuge 2 minutes at 1800rpm. The flow through contains the probe.
10. Transfer each of the two probes into an eppendorf tube and precipitate the DNA by adding 10µl of 10mg/ml tRNA, 20µl of 1mg/ml mouse cot-1 DNA, 10µl of 10mg/ml salmon sperm DNA, 50µl of 3M NaAc pH 5.6 (Note 5) and 350µl of 100% ethanol. Mix well and store in -20^o C for 20 minutes (Note 6).
11. Centrifuge for 30 minutes at max speed at 4^o C. A pellet should be visible. Discard the supernatant and wash the pellet with 500µl 70% ethanol. Centrifuge 5' at max speed at 4^o C. Discard the 70% ethanol and repeat the 70% ethanol-washing step.
12. Allow the pellet to dry at 37^o C for a few minutes. Inspect that the ethanol is fully evaporated. When the pellet is dry dissolve the pellet in 50µl of 50+ hybridization solution at 37^o C until it is completely dissociated. The probe is now ready and can be stored at -20^o C for several years (Note 7).

3.2 Slide pre-preparation for embryo deposition (adapted from Veuskens et al. 1993)

To prepare the slides, wear talc free gloves and touch only the edges of the slides.

1. Place slides in racks and soak them in 1M HCl for 30 minutes.
2. Rinse briefly two times in sterile, RNAse free H_2O.
3. Soak in absolute ethanol for 30 minutes and air-dry the slides.
4. Place them in 3x Denhardt's/3x SSC in sterile RNAse free H_2O at 65^o C overnight.
5. Dip briefly in sterile RNAse free H_2O.
6. Place the slides in Ethanol:Glacial acetic acid 3:1 for 20 minutes at room temperature.
7. Air dry. Make a mark line on the back of the slide and close to the edge of the slide using the diamond pen, as shown in Figure 4.
8. Store at 4^o C up to 6 months.

3.3 Superovulation, plugging, embryo isolation & culture

In order to obtain a relatively large number of embryos per female donor we routinely super-ovulate the female donor mice. We use DBA2 females and C57B/6 males.

1. Inject the females (26G needle, intraperitoneal (IP)) with 5UI of PMSG.
2. Approximately 48 hours later inject the females with 5IU of hCG (26G needle, IP) and place the male in the same cage.
3. The next day (approximately 16 hours post-hCG injection), females should be inspected for the presence of a vaginal plug. If a plug is present, then embryos at embryonic day

0.5 (E0.5) are expected to be present in the oviduct.

4. Sacrifice the females, collect the oviducts and place each oviduct in a ~100µl drop of M2 medium in a 60x15 mm IVF round dish.
5. Working under the stereomicroscope, hold the oviduct wall with one pair of forceps and tear the evidently plugged ampulla containing the fertilised oocytes (zygotes). The zygotes are still in complex with the cumulus cells and after tearing they should emerge from the oviduct as a single mass. Discard the oviducts and keep the zygote-cumulus cell masses in the M2 medium drop.
6. After the zygote-cumulus cell masses isolation has been completed move them by using a glass capillary (not pulled in the flame) attached to the hand pipette in a 60x15 mm IVF one well dish containing M2 medium supplemented with 300µg/ml bovine testis hyaluronidase.
7. Allow the masses to stay in the solution for approximately 1 minute – inspect them carefully - and gently pipette up and down with the same glass capillary to release the zygotes from the cumulus cells (Note 8).
8. After the zygotes have detached from the cumulus cells, remove them with a transfer pipette (pulled in the flame) and place them in a 60x15 mm IVF one-well dish with fresh M2 medium (without hyaluronidase).
9. Transfer the zygotes to a 50µl drop of pre-equilibrated M16 medium under mineral oil in a 60x15 mm IVF round dish (place the plate 10 minutes before use in the incubator). Then distribute 5 zygotes per 20µl drop of pre-equilibrated M16 medium under mineral oil in a 60x15 mm IVF round dish (Note 9).
10. Examine the embryos after 2 or 3 days for the presence of blastocysts.

3.4 DNA-RNA FISH

3.4.1 Probe preparation for DNA-RNA FISH procedure (Day 1)

1. Start preparing the DNA and RNA FISH probes before you start step 12 of 3.4.2 DNA-RNA FISH procedure.
2. Place 13,5µl of hybridization solution 50+ in an eppendorf tube and add 1µl of each probe (total volume 16µl, approximately 60-100ng per DNA FISH or RNA FISH probe) and 0.5µl of cot-1 DNA (1mg/ml). Mix well and denature the probes at 99^{o} C for 6 minutes.
3. Incubate 45 minutes at 37^{o} C on a thermoblock to allow Cot-1 DNA to hybridize to repeat sequences that are present in the probe.
4. Place on ice until the sample is ready.

3.4.2 Sample preparation for DNA-RNA FISH and DNA-RNA FISH procedure (Day 1)

1. Take the lid of a 10cm cell culture dish and make 20μl drops of the following solutions: 2 drops of M2, 2 drop of Acidic Tyrode's (AT) solution, 3 drops of M2. All solutions should be at room temperature.
2. Place all the embryos to be processed in the M2 medium to wash away the M16 (Note 10).
3. Transfer 10 embryos at a time in the first AT drop to wash away the M2 media and then in the second AT drop to remove the zona pellucida. Incubate for a few seconds in AT, and when the zona pellucida starts to dissociate, transfer the embryos into the next M2 drop.
4. Pipette the embryos gently up and down with the transfer pipette until the zona pellucida is completely removed.
5. Transfer the embryos in the 2 subsequent M2 drops for additional washes.
6. Transfer one embryo at a time on a Denhardt's coated slide, next to the line that was drawn with the diamond pen as depicted in Figure 4. Carefully remove all the transferred media with the transfer pipette.
7. Repeat step 5, for all the remaining embryos (Note 11).
8. Allow the embryos to dry well on the slide for 30 minutes at room temperature.

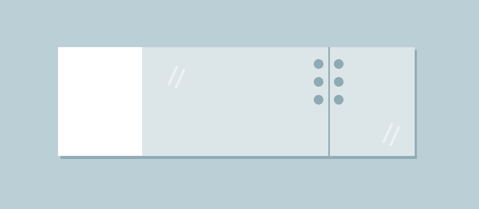

Figure 4: Slide preparation and embryo deposition

Carve a line on the backside and close to the end of the slide with the use of a diamond pen (green-blue line). Place the embryos adjacent to the line (green-blue circles). The line can be used later (upon imaging) as a reference to locate the embryos.

9. Fix the embryos by placing the slide ice cold 3% PFA/0.5% Triton in PBS on ice for 10 minutes.
10. Wash the embryos with ice-cold PBS 2 times on ice, 2 minutes each.
11. The protocol can be paused here, by washing the slide with ice cold 70% ethanol on ice, 2 times each. After the second time place the slide in 70% ethanol and store in -20^{o} C up to several months. Otherwise proceed to step 12.
12. If the embryos have been stored in 70% ethanol, rehydrate them by washing them 2

times, 2 minutes each with ice cold sterile, RNAse free H_2O.

13. Place the slide with the embryos in 37° C pre-warmed 0.02% pepsin/0.01N HCl in sterile, RNAse free H_2O for 1,5 minutes.

14. Dilute the pepsin by quickly transferring the specimen in ice cold sterile, RNAse free H_2O (Note 12).

15. Post-fix in ice cold 3% PFA in ice cold sterile, RNAse free H_2O for 5’ on ice.

16. Wash 3 times 2 minutes each in ice cold sterile, RNAse free H_2O.

17. Place the slide with the embryos in ice cold 0.2N HCl in ice cold sterile, RNAse free H_2O on ice for 12 minutes.

18. Wash 3 times 2 minutes each with ice cold sterile, RNAse free H_2O.

19. Place the slide with the embryos at 65° C on a hot plate (Note 13). Apply 50µl of denaturation buffer on the slide next to the embryos. Place a coverslip to spread the denaturation buffer on the embryos and incubate 5 minutes (Note 14) (This is the first denaturation step).

20. Remove the coverslip with one move by tapping the slide in the edge of a lab chemical container in the fume hood and place the slide quickly in -20° C pre-chilled 70% ethanol for 3 minutes.

21. Continue the sample dehydration with subsequent washes with pre-chilled 85% and 100% ethanol (-20° C) for 3 minutes each.

22. Allow the embryos to dry for 10 minutes at room temperature.

23. Apply the probe mixture (containing both the labeled DNA and RNA FISH probes) on the embryos and cover it with a coverslip. Place the slide at 78° C on a hot plate for 4 minutes (This is the second denaturation step, note 15).

Place the slide in a humid chamber with 50% formamide/2x SSC pH 7.2-7.5 at 37° C for 18 hours.

3.4.3 DNA-RNA FISH procedure (Day 2)

1. Wash the slide in pre-warmed FA/2xSSC at 37° C two times, for 5 minutes each.
2. Wash the slide in pre-warmed 2xSSC at 37° C two times, for 5 minutes each.
3. Wash the slide in 2xSSC for a few seconds at room temperature.
4. Block with blocking solution supplemented with 2mM VRC for 10 minutes at room temperature.
5. Incubate with the anti-DIG FITC (1:250) and streptavidin Alexa Fluor® 555 conjugate (1:400) diluted in blocking solution, supplemented with 2mM VRC, for 45 minutes at room temperature.
6. Wash two times in TS washing solution.
7. Mount in Prolong Antifade supplemented with Hoechst.

8. Proceed for imaging. We routinely use a Zeiss LSM700 microscope (Carl Zeiss, Jena).
9. A representative image is presented in Figure 5.

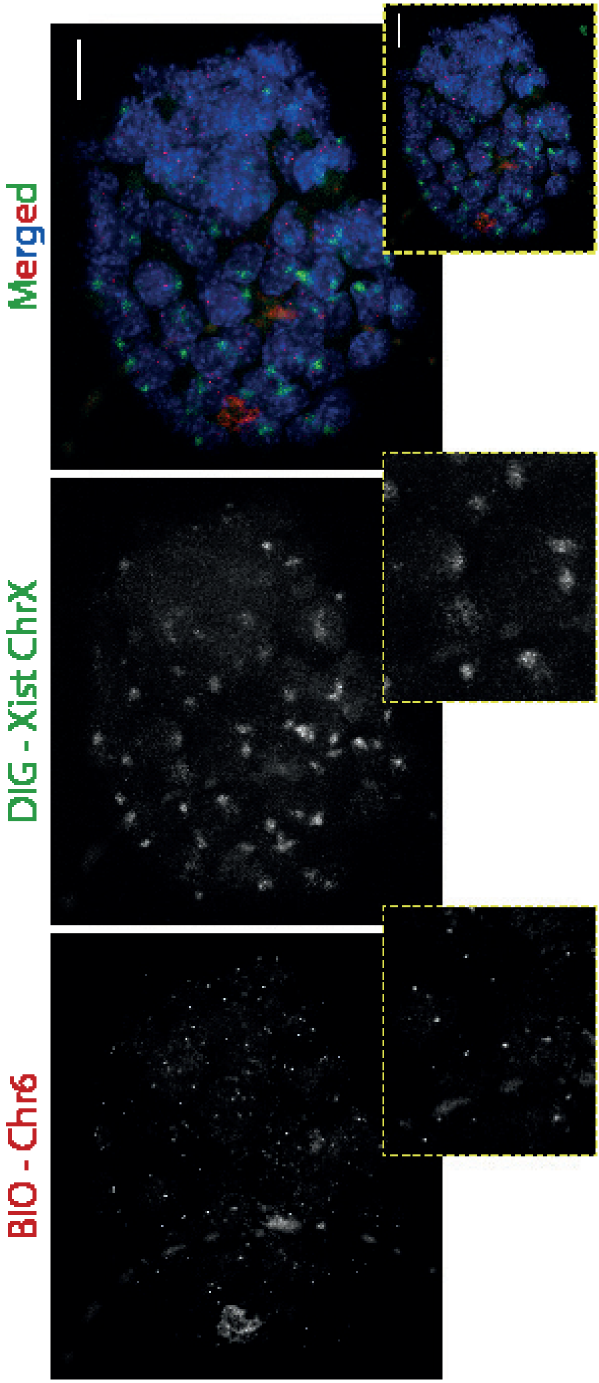

Figure 5: DNA-RNA FISH in pre-implantation embryos

Representative image of simultaneous detection of *Xist* (green) and chromosome 6 (red) in mouse pre-implantation embryos, by DNA-RNA FISH. Cell representatives are shown in the blown up panels. Scale bars represent 15 µm in the whole embryo and 5 µm in the cropped nuclei.

4 Notes

1. Note 1: For a strong DNA FISH signal, the corresponding probe should hybridise to at least 6Kb of the target DNA. In addition, no transcription should take place from the chosen genomic region, in order to avoid detection of nascent RNA. Using BACs containing centromeric and telomeric regions may provide suitable substrates for generating such probes.
2. Note 2: When isolating the BAC DNA that will be used for detecting nascent RNA, avoid using the RNAse that is provided by the kit, during the DNA isolation procedure. Remnants of RNAse after the BAC DNA isolation may compromise the RNA FISH results.
3. Note 3: If the majority of the probe fragments are larger than 500bp the nick translation reaction should be continued for another 30’ and the probe size should be re-evaluated. If the majority of the probe fragments are smaller than 100bp, the probe might not be optimal, and the nick translation may need to be repeated from the beginning, with a shorter incubation time. In general, the final evaluation step of the labeling capacity of a probe is the DNA or RNA FISH experiment itself.
4. Note 4: At times, the intensity of probe fragment bands on the gel may not be as high as in Figure 2. If the probe smear is not visible at all, the concentration of the probe might be too low. In this case, a pilot RNA or DNA experiment should be conducted in order to validate the probe quality. If signal is not detected, prepare the probe from the beginning with more BAC substrate.
5. Note 5: The pH of the NaAC should be adjusted with glacial acetic acid and not by HCl.
6. Note 6: The incubation in -20^{o} C can be extended to longer periods e.g. days.
7. Note 7: It is convenient to prepare Digoxigenin and Biotin-labeled probes for both the DNA FISH and RNA FISH probes, so that different combinations can be tested.
8. Note 8: The zygotes should not be mechanically forced-squeezed since this can result to apoptosis.
9. Note 9: The use of embryo toxicity certified plastic-ware is essential for optimal embryo development. Non-certified plastics, especially during the culture period, can greatly compromise the embryo development.
10. Note 10: If there are more embryos that still need to be cultured to reach the blastocyst stage, transfer the dish back to the incubator. Inspect the embryos a few hours later and process them accordingly.
11. Note 11: We routinely put 16 embryos on one slide. If there are more embryos present, replica slides can be made for future use.
12. Note 12: The incubation time with pepsin is very critical. Longer incubation time with

pepsin will result in the complete degeneration of the specimen. The specimens can be examined under the microscope to ensure that sufficient cytoplasm removal took place. Endogenous biotin in cells can cause a significant problem with the use of biotin-labeled probes, especially when cytoplasmic pepsin digestion is not sufficient. In such case, continue incubating with pepsin for additional 20-second intervals until cytoplasmic extraction is sufficient.

13. Note 13: The drying of the specimen does not create a significant background problem. For enhancing the DNA signal, aging of the specimen can be performed at 65^o C for 1 hour, before applying the denaturation solution for the first denaturation step.

14. Note 14: After applying the denaturation solution in the first denaturation step the timing of the incubation at 65^o C is extremely critical. Long incubation times result in complete disintegration of the nucleus.

16. Note 15: We noticed that by adding a second denaturation step with the probe mix improves the intensity of the DNA FISH signal compared to using only the first or the second denaturation step. The time of the second denaturation step is as critical as the first. Long incubation time results in complete disintegration of the nucleus.

In general when this protocol is tested on other types of material e.g. earlier stages of embryo development, embryonic stem cells, differentiating stem cells, differentiated cells, frozen tissue sections or others, critical parameters may need to be adapted empirically and accordingly. These parameters include: the percentage of pepsin and pepsin incubation time to efficiently remove cytoplasm, the HCl incubation time (the 0.2N HCl concentration should suffice), and the incubation time of the two denaturation steps at 65^o C and 78^o C.

REFERENCES

Bartlett, J.M.S., 2004. Fluorescence in situ hybridization: technical overview. Methods in molecular medicine, 97, pp.77–87.

Brockdorff, N. & Turner, B.M., 2015. Dosage Compensation in Mammals. Cold Spring Harbor Perspectives in Biology, 7(3), p.a019406.

Chaumeil, J. et al., 2008. Combined Immunofluorescence, RNA Fluorescent In Situ Hybridization, and DNA Fluorescent In Situ Hybridization to Study Chromatin Changes, Transcriptional Activity, Nuclear Organization, and X-Chromosome Inactivation. In pp. 297–308.

Clemson, C.M. et al., 1996. *Xist* RNA paints the inactive X chromosome at interphase: evidence for a novel RNA involved in nuclear/chromosome structure. The Journal of cell biology, 132(3), pp.259–75.

Hart, S.M. & Basu, C., 2009. Optimization of a digoxigenin-based immunoassay system for gene detection in Arabidopsis thaliana. Journal of biomolecular techniques : JBT, 20(2), pp.96–100.

Kwon, S., 2013. Single-molecule fluorescence in situ hybridization: quantitative imaging of single RNA molecules. BMB reports, 46(2), pp.65–72.

Mak, W. et al., 2004. Reactivation of the paternal X chromosome in early mouse embryos. Science (New York, N.Y.), 303(5658), pp.666–9.

Marahrens, Y. et al., 1997. Xist-deficient mice are defective in dosage compensation but not spermatogenesis. Genes & development, 11(2), pp.156–66.

Namekawa, S.H. & Lee, J.T., 2011. Detection of nascent RNA, single-copy DNA and protein localization by immunoFISH in mouse germ cells and preimplantation embryos. Nature Protocols, 6(3), pp.270–284.

Okamoto, I. et al., 2004. Epigenetic dynamics of imprinted X inactivation during early mouse development. Science (New York, N.Y.), 303(5658), pp.644–9.

Raj, A. et al., 2008. Imaging individual mRNA molecules using multiple singly labeled probes. Nature Methods, 5(10), pp.877–879.

Said, H.M., 2012. Biotin: biochemical, physiological and clinical aspects. Sub-cellular biochemistry, 56, pp.1–19.

Sarvari, A. et al., 2013. A technique for facile and precise transfer of mouse embryos. Avicenna journal of medical biotechnology, 5(1), pp.62–5.

Sommerlad, C. et al., 2002. FISH Technology B. W. Rautenstrauss & T. Liehr, eds., Berlin, Heidelberg: Springer Berlin Heidelberg.

Takagi, N., Sugawara, O. & Sasaki, M., 1982. Regional and temporal changes in the pattern of X-chromosome replication during the early post-implantation development of the female mouse. Chromosoma, 85(2), pp.275–86.

Takizawa, T., Meaburn, K.J. & Misteli, T., 2008. The Meaning of Gene Positioning. Cell, 135(1), pp.9–13.

Veuskens, J., Hinnisdaels, S. & Mouras, A., 1993. In situ hybridization to plant metaphase chromosomes: radioactive and non-radioactive detection of repetitive and low copy number genes. In Plant Tissue Culture Manual. Dordrecht: Springer Netherlands, pp. 723–737.

Wood, E., 1983. Molecular Cloning. A Laboratory Manual. Biochemical Education, 11(2).

Wutz, A., 2011. Gene silencing in X-chromosome inactivation: advances in understanding facultative heterochromatin formation. Nature Reviews Genetics, 12(8), pp.542–553.

Chapter 6

GENERAL DISCUSSION

General Discussion

Over the last decade, research attention concerning the regulation of gene expression has shifted from analyzing short regulatory DNA sequences towards analyses of larger domains, within the context of chromatin. More specifically, there is a general focus on the various mechanisms that mediate different layers of DNA and chromatin, and on the miscellaneous factors and chemical modifications that participate and regulate these processes. A common feature of regulatory modifications, set either on the DNA (e.g. methylation) or on its associated histones, is that they do not alter the DNA code. In addition, the effect that these modifications exert, for example gene silencing or activation, can be heritable during cell divisions. Together, all these modifications comprise the epigenome. With its multitude of roles in different kinds of processes, such as in development and cell differentiation, but also in health and disease, studying the epigenome has become a hot scientific topic (epigenetics). However, although we now appreciate that there are several extra layers of complexity added to the concept of gene regulation and have accepted the importance of the epigenome, we are still far from understanding all of its regulatory and functional aspects.

In contrast to the DNA code, the epigenetic signature can be plastic so that cellular identities can dynamically change. For example during germ cell development, epigenetic reprogramming will erase all the epigenetic makeup that was acquired during early post-implantation development (Hackett et al. 2012; Hill et al. 2014). This overall epigenetic reprogramming facilitates the formation of epigenetic marks that will eventually allow totipotency to be transferred to the zygote (Condic 2014). However, certain genomic regions such as centromeric and pericentromeric chromatin, may need to keep their epigenetic signature throughout many differentiation and/or reprogramming processes, since failure to do so would possibly result in genomic instability (Peters et al. 2001).

Epigenetic dynamics and plasticity is also evident during the process of X chromosome inactivation (XCI) in the early female mouse embryo. Around the 4-cell stage, the active paternal X chromosome undergoes imprinted XCI (iXCI) (Marahrens et al. 1997; Okamoto et al. 2004). Subsequently, the inactive state is reversed only in the inner cell mass (ICM) of the blastocyst, which gives rise to the embryo-proper. This reactivation of the inactive X chromosome is then again followed by another round of inactivation. However, at this time, it occurs through a process that involves a random choice of either the maternal or the paternal X chromosome in the tissues of the developing embryo (Takagi et al. 1982). The majority of our knowledge about the mechanisms leading to iXCI in early pre-implantation development in mammals comes from the mouse, and whether this imprinted phenomenon is a peculiarity of the mouse itself or whether it extends to other rodents has not been investigated.

Interestingly, a dynamic process of sex chromosome inactivation also takes place during another developmental process: spermatogenesis. This form of sex chromosome inactivation takes place through a process that is different from the typical XCI, it targets both the X and Y chromosome and has been termed Meiotic Sex Chromosome Inactivation (MSCI) (Turner 2015). This global silencing of the sex chromosomes largely persists post-meiotically during the haploid round spermatid stage (Post-meiotic Sex Chromosome Repression (PSCR)) (Satoshi H Namekawa et al. 2006). In contrast to XCI, the silencing of the X chromosome in the testis is not driven by gene dosage differences between the X and Y, but by the almost complete lack of homologous interactions with the Y chromosome, as discussed in **Chapter 1**. However, in spite of the overall temporal and mechanistic differences between these two different forms of X inactivation, a common feature is represented by the presence of genes escaping the X chromosome wide silencing process in both cases (reviewed in Sin & Namekawa 2013 and Peeters et al. 2014).

Although epigenetic signatures may be dynamic in nature in some situations, they can be stably transferred to the next generation. For example, during spermatogenesis, the majority, but not all of the histones are replaced by protamines. Certain developmentally important loci remain rich for nucleosomes during the overall histone-to-protamine transition and are transferred to the oocytes upon fertilization (reviewed in Rathke et al. 2014). In this new environment they are involved in regulating gene expression in the early embryo. Surprisingly, the effects of those histones can sometimes be observed in subsequent generations, a phenomenon known as transgenerational epigenetic inheritance (Siklenka et al. 2015).

In this thesis we investigated different aspects of epigenome regulation through specific developmental processes. Specifically, we investigated whether the epigenetic profile of a round spermatid can alter normal regulation of iXCI when used for fertilization of oocytes, through round spermatid injection (ROSI) (**Chapter 2**). We examined in detail the epigenetic signature of pericentric heterochromatin throughout germ cell development (**Chapter 3**). We also characterised XCI dynamics upon differentiation of rat embryonic stem cells (rESCs) and assessed if XCI mechanisms are conserved between the mouse and the rat (**Chapter 4**). Lastly, we set up a robust and reproducible protocol for simultaneous detection of DNA/RNA molecules (DNA/RNA FISH) (**Chapter 5**).

In the following paragraphs I critically discuss the information obtained from our studies. In addition, I will provide suggestions for future research directions, in line with experimental restrictions but also possibilities when studying low abundance-cells, such as PGCs or early embryos. Further experimentation on the chapters presented in this thesis will help in understanding questions that have arisen during the course of my work, but also will facilitate obtaining a better overview of the examined epigenetic phenomena described in this thesis.

PSCR and iXCI: the epigenome of the father matters

In the female mouse preimplantation embryo the paternal X chromosome (Xp) is preferentially inactivated over the maternal X chromosome (Xm) through iXCI. A longstanding question in the field of XCI relates to the mechanism by which this favored inactivation of the Xp takes place. While it has become apparent that the compact maternal *Xist* genomic locus does not allow *Xist* expression from the Xm (Fukuda et al. 2015), the predisposition of Xp for iXCI is still under debate (**Chapter 1**, Sun et al. 2015; Okamoto et al. 2005).

Regardless of the mechanistic preference for Xp inactivation during the early steps of preimplantation development, one important, but yet unexplored question in the iXCI field lies in the contribution of the protamine-to-histone transition of the paternal genome in the initiation of iXCI. In **Chapter 2** we examined whether injection of a round spermatid, which already carries a largely inactive X chromosome due to PSCR, into mouse oocytes by round spermatid injection (ROSI) is sufficient to establish iXCI. In order to examine our hypothesis, we made use of round spermatids deficient for *Xist* (XpΔ*Xist*). The use of such spermatids excludes Xp*Xist* expression and thus its contribution to Xp silencing during iXCI. It is also well known that female XpΔ*Xist* embryos derived by natural mating die in utero due to failure of iXCI establishment in their extra-embryonic tissues (Marahrens et al. 1997). Therefore, by using a round spermatid, which already carries an inactive Xp enriched for silencing marks such as H3K9me3, we hypothesized that we would rescue the embryonic lethality caused by the lack of a functional paternal *Xist* allele, and thus lack of iXCI.

Indeed, by performing ROSI we were able to rescue the embryonic lethality and for the first time obtain live born female pups carrying an XpΔ*Xist* allele. Surprisingly though, RNA/DNA FISH analysis of E15.0 female placentas revealed that rescuing was not achieved by *Xist* independent silencing of the Xp as we expected; but rather by *Xist* dependent silencing of Xm, which compensated for iXCI. Interestingly, this rescue was only obtained with C57B/6 XpΔ*Xist* round spermatids. When ROSI was performed with CAST/EiJ XpΔ*Xist* round spermatids, the XpΔ*Xist* female embryonic lethality could not be rescued. These results suggest differential expression of proteins and/or RNAs in the round spermatids of these two mouse subspecies. Comparative global gene expression analysis in C57B/6 and CAST/EiJ round spermatids, but also from ROSI and ICSI embryos derived from those spermatids, may thus lead to the identification of novel *Xist* regulators.

In order to examine our finding further we performed immunofluorescence analysis for RNF12, an important XCI trans-activator (Jonkers et al. 2009; Shin et al. 2010), in embryos derived by ROSI and ICSI or natural mating (wild type and XpΔ*Xist*), since it is known to escape PSCR (Satoshi H. Namekawa et al. 2006). Despite the significantly increased levels of RNF12 in all ROSI derived embryos compared to the ones derived by ICSI or natural mating, the protein levels were similar in both embryo sexes. Since ROSI derived male embryos never showed any *Xist* cloud formation, the immunofluorescence data did not provide strong evidence for the critical participation of the enhanced levels of RNF12 in the rescuing. Nonetheless, the importance of RNF12 in iXCI has been previously demonstrated (Shin et al. 2010; Fukuda et al. 2016). We speculate that other X-linked factors may facilitate silencing of Xm perhaps also requiring enhanced levels of RNF12. Together with *Rnf12*, a number of other genes escape PSCR and their contribution to XCI needs to be evaluated. Again, comparative analysis of RNA-seq data from ROSI and ICSI derived embryos, but also from round spermatids, may be of great value in identifying such factors/ genes, which may be key players in both imprinted and random XCI.

Valuable information about the possible contribution of paternal RNF12 to Xm inactivation upon ROSI could be studied by performing ROSI experiments with round spermatids that are deficient for both *Xist* and *Rnf12*. In addition, such an experiment would provide insight into the possible role of RNF12 in the maintenance of XCI in these ROSI derived female embryos (XpΔ*Xist*/Δ*Rnf12*/Xm). The forced *Xist* expression from the Xm and the subsequent inactivation of the Xm in these ROSI female embryos would render the embryos fully deficient for *Rnf12* expression. It would then be interesting to determine whether the Xm can be maintained and propagated in the inactive form in the complete absence of RNF12 and whether viable female mice can be born. Inconveniently though, full knock out *Rnf12* and *Xist* male mice cannot be generated, since females carrying the simultaneous deletion for *Rnf12* and *Xist* the same X chromosome are not viable and cannot be generated by homologous recombination in trans heterozygous females (see table 1).

Table 1 Phenotype of mice carrying a deletion for *Rnf12* or *Xist*

Rnf12 (Shin et al. 2010)		*Xist* (Marahrens et al. 1997)	
$Xm^{Rnf12-}Y$	viable	$Xm^{Xist-}Y$	viable
$Xm^{Rnf12-}Xp^{Rnf12+}$	lethal	$Xm^{Xist-}Xp^{Xist+}$	viable
$Xm^{Rnf12+}Xp^{Rnf12-}$	viable	$Xm^{Xist+}Xp^{Xist-}$	lethal

Complementary to the above described approach, ROSI using Δ*Xist* spermatids and oocytes from *Rnf12* heterozygote females could also provide insight in the mechanisms of rXCI and iXCI. In this scenario when a female embryo inherits the *Rnf12* knockout allele from the mother, this mutated Xm (Xm*Xist*Δ*Rnf12*) might become inactivated in the extra-embryonic tissue. Again, Xp inactivation cannot occur in this case due to the *Xist* deletion on the paternal X (Xp*Rnf12*Δ*Xist*). Therefore, similar to our ROSI experiment, the genotype (Xp*Rnf12*Δ*Xist*Xm*Xist*Δ*Rnf12*) that is normally lethal in females generated via normal fertilization, might also be rescued upon ROSI.

In addition to altered regulation of expression of XCI activators or repressors due to the ROSI procedure, the epigenetic status of the paternal genome, and especially that of the Xp might also somehow contribute to the rescue of embryonic lethality of XpΔ*Xist* embryos. During natural fertilization, the sperm's protamines are rapidly replaced by unmodified histones provided by the oocyte rendering the paternal genome transcriptionally permissive. By performing ROSI we transfer a paternal genome carrying a largely inactive X chromosome to the oocyte. It might be suggested that the paternal X chromosome, in its globally silenced configuration in the oocyte, competes with the Xm*Xist* locus for factors that normally keep this gene silenced. It would be interesting to examine the epigenetic profile of the maternal *Xist* locus from ROSI derived embryos by ChIP-Seq and compare it to embryos derived by ICSI or natural mating. However, in spite of the development of an extremely sensitive ChIP protocol (Brind'Amour et al. 2015), that was also recently applied for mapping the genome wide distribution of H3K4me3 and H3K27me3 in pre-implantation embryos (Liu et al. 2016), this technology may not be easily applied to ROSI derived embryos yet. In general the recovery of embryos after ROSI is lower compared to that of ICSI and this novel ChIP-seq protocol requires at least 500 cells. Therefore, this current methodology might still be challenging when locus specific epigenetic signatures need to be analysed in ROSI derived embryos. Additionally, comparative DNA FISH experiments on the *Xist* locus may also provide valuable information about the compaction state of this region in ROSI and ICSI derived embryos. Furthermore, comparative immunofluorescence experiments on various histone modifications in ROSI and ICSI derived embryos will provide valuable information about the global epigenetic similarities and differences between these two embryo types. Subsequently, it may be possible to deduce to what extent changes in chromatin structure contribute to the ability of the ROSI derived embryos to initiate *Xist* expression from the Xm.

Lastly, ROSI-derived embryos may represent an interesting model to investigate inter- and trans- generational inheritance in general, especially since ROSI technology has been applied to human assisted reproduction (Tanaka et al. 2015). The histone to protamine transition taking place during spermiogenesis may be considered as an extra step of epigenetic resetting, as potentially acquired epimutations can be erased through this maturation step, by exchanging histones by protamines. In addition, accumulating evidence suggests that histone retention in certain loci in sperm affects gene regulation and development of the early embryo in the mouse (Hammoud et al. 2009; Erkek et al. 2013; Hisano et al. 2013; Siklenka et al. 2015). It would be of interest to examine if and to what extent the expression profile of ROSI embryos is altered compared to those derived by natural fertilization, but also whether the offspring of such individuals present any type of phenotypic or behavioral abnormalities. In addition, in light of the recent utilization of ROSI in human, investigating potential consequences of this technology, using animal models is more urgent than ever.

Primordial Germ Cells: is everything reprogrammed?

Primordial germ cells (PGCs), the precursors of the sperm and oocyte, represent a cell lineage with the unique ability to give rise to a new organism. The germ cell lineage is specified early in development by inductive signals emerging from the extra-embryonic ectoderm upon the epiblast, which gives rise to the embryo (Lawson & Hage 1994; Tam & Zhou 1996).

As already discussed in **Chapter 1**, PGCs undergo extensive reprogramming, which includes genome wide DNA de-methylation, chromatin remodeling and erasure of genomic imprints. The latter process is unique to PGCs. Gender specific imprints will be re-established later in PGC development so that monoallelic expression of imprinted genes can take place in a parent of origin specific manner in the next generation.

Epigenetic reprogramming in PGCs has been thoroughly investigated. The changes in localization and levels of several histone post-translational modifications and their readers during this process have been mainly analyzed by immunofluorescence procedures. Using cytospin preparations, Hajkova and colleagues reported that E11.5 gonadal PGCs, among others, are devoid of histone modifications and markers related to pericentric constitutive heterochromatin (PCH). The identity of PHC is then rapidly re-established within 24 hours (Hajkova et al. 2008).

In **Chapter 3** we sought to re-examine the epigenetics of PCH in PGCs by using different fixation and cell preparation methodologies. Our results indicate that PHC identity is maintained throughout germ cell development. We also showed that depending on the method of fixation and further processing of the material the results varied, and the original observations by others could also be reproduced under certain conditions. The data we obtained illustrated nicely the necessity of evaluating results with different experimental approaches in order to construct valid conclusions. This is particularly important in immunohistochemistry of chromatin components, where clear-cut negative control experiments to check for antibody specificity are not always an option due to lack of proper (conditional) knockout models, and epitope availability rather than the presence or absence of a protein or protein modification, may determine the result obtained. It appears that in nuclear spread preparations, epitope availability of certain epigenetic markers is less variable than in section or cytospin preparations. However, in case of a lack of signal for a certain protein, it should be taken into account that if this protein is only loosely associated with chromatin, it might be lost during the preparation of the samples (Eijpe et al. 2000).

Now that our studies have revealed that all known components of PHC are still detectable between E11.5 and E13.5 in PGCs, it might be suggested that this chromatin region escapes from any large epigenetic reorganisation event during the overall reprogramming in PGCs. However, we did observe clear changes in the clustering of PHC of different chromosomes into chromocenters already at E10.5 when compared to the surrounding somatic cells. Specifically, immunofluorescence analysis of centromere (CREST–centromeric marker) and pericentromere (H4K20me3-pericentromeric marker) localization revealed that the majority of the chromocenters dissociate and PHC regions appear as independent entities within the PGC nuclei. However, this was not the case for the surrounding somatic cells, where PHC from different chromosomes remained clustered in chromocenters in all the developmental stages we examined. Whether this dynamic alteration of chromocenter clustering in PGCs also reflects a less compact chromatin structure in PHC regions compared to that of the somatic cells remains to be established. In a pilot experiment, we visualized major satellite DNA in E11.5 PGCs and somatic cells by DNA FISH (data not shown). However, relative size comparison of the regions that were positive for the FISH signal did not reveal any obvious compaction differences of the PHC areas between PGCs and somatic cell nuclei. A possible explanation for this result might be that the compaction difference in PHC between E11.5 PGCs and somatic cells might be too small for detecting small changes in chromatin compaction by a DNA FISH approach. An alternative and more sensitive methodology for studying chromatin composition questions would be chromatin immunoprecipitation (ChIP) analysis. However, such a methodology would require a substantial amount of chromatin substrate, which is not available in low abundant cell populations, such as in PGCs. Interestingly though, the recent development of ChIP protocols applied with small cell populations (~100 cells) may provide valuable quantitative data for compaction mediators in PHC regions in PGCs and somatic cells from various developmental stages (Cao et al. 2015; Brind'Amour et al. 2015). Lastly, the functional significance of this alteration in PHC organisation is not known, although it could be expected to reflect some aspect of the differentiation process of PGCs towards the mature gametes. In male spermatogonial stem cells the clustering of centromeres in chromocenters, like in PGCs, is also lost. This loss of clustering results in the localization of centromeres to the periphery of the nucleus. In addition, staining of these nuclei against H3K9me3 shows that this histone modification localises in the nuclear periphery of the SSCs (Shirakawa et al. 2013) (Figure 1). If the reorganisation of clustering in early PGCs is the start for the specific organisation in spermatogonial stem cells still needs to be determined.

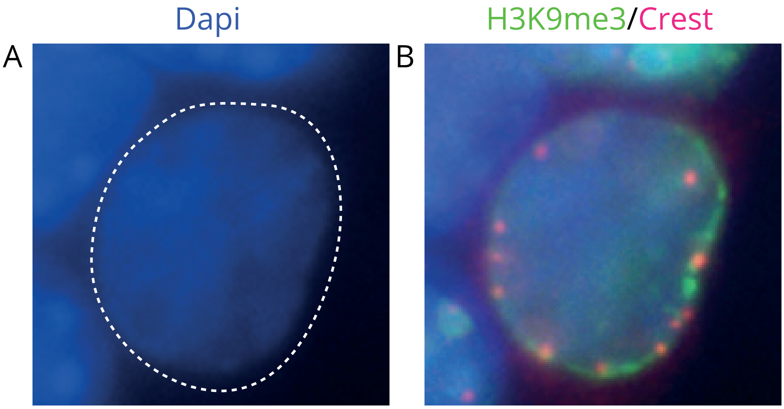

Figure 1: PHC and centromeres of spermatogonial stem cells (SSCs) localize to the periphery of SSC nucleus

A DAPI staining reveals the absence of DAPI dense chromocenters from the SSC nucleus. **B** Analysis of H3K9me3 (green) reveals that PHC localizes to the periphery on the SSC nucleus. Centromeres (red) also localize as individual entities to the periphery of the nucleus, as visualized by CREST, a centromere marker.

Our present data indicate that whatever change may occur in the organization of PHC in PGCs compared to that of the somatic cells in the mouse, the overall repression of transcription from these regions appears to be maintained. This is because our real-time RT-PCR experiments did not provide any evidence for the presence of transcripts derived from the major satellite repeats.

In this context, it is interesting that we identified ATRX as a highly enriched component of PHC of E11.5 PGCs. At lower levels, it could also be detected at PHC of somatic cells and PGCs at other stages of development. A number of studies have reported that ATRX contributes to silencing of tandem repeats such as those of PHC in certain biological contexts: I) in the maternal pronucleus during early pre-implantation development, where expression of major satellites takes place solely from the paternal pronucleus (De La Fuente et al. 2015), II) in heterochromatic repeats found throughout the genome in ESCs (Voon et al. 2015; He et al. 2015) and III) in PHC of neonatal spermatogonia, where DNA methylation is lacking from those regions as determined by 5mC immunofluorescence, as well as on the Y chromosome of both neonatal spermatogonia and mouse embryonic fibroblasts (Baumann et al. 2008). It is tempting to speculate that the enrichment of ATRX on PHC of E11.5 PGCs contributes to the silencing of the repetitive DNA regions during germ cell reprogramming. PRMT5 is an arginine methyltransferase that localizes throughout the germ cell's nucleus from ~E8.5 onwards (Ancelin et al. 2006). This enzyme catalyses symmetric dimethylation of arginine 3 of the histones H2A and H3, forming a repressive epigenetic mark that blocks expression of transposable elements (Kim et al. 2014). Whether it inhibits expression of major satellites was not reported, but curiously, at E11.5 it relocates from the nucleus to the PGCs' cytoplasm (Kim et al. 2014; Ancelin et al. 2006). From this, it might be suggested that ATRX then takes over this function and ensures maintenance of transcriptional silencing from PHC regions, and also from transposable elements. Interestingly, Liu et al. (2014) combined ChIP and expression data from E13.5 wild type, Setdb1 heterozygotic and knockout germ cells, and showed that the SETDB1-H3K9me3 pathway acts as an important guardian against transcriptional activation of repetitive elements in E13.5 germ cells (Liu et al. 2014). It would be interesting to examine if this pathway also contributes to PHC transcriptional regulation during PGC development.

To conclude, our results indicate that histone modification reprogramming during PGCs' development does not target PHC regions in these cells. Instead, PHC retains its "canonical" epigenetic identity and potential changes in chromatin compaction in those regions are not accompanied by expression of major satellites. Now that multiple players and pathways have been identified to participate in the organization and regulation of PHC in somatic cells and in embryonic stem cells (ESCs) (He et al. 2015; Rapkin et al. 2015; Voon et al. 2015; Goldberg et al. 2010; Sadic et al. 2015) functional studies should address whether similar mechanisms operate in PGCs.

Aspects of XCI are conserved between mouse and rat

Sex chromosomes differentiate females from males, with mammalian females having two X sex chromosomes, while males carry one X and one Y chromosome. This implies that females have twice as many X-linked genes compared to males, and if these genes were to be transcribed and translated into protein there would be a disequilibrium that would disrupt the fine-tuned development of the body. Nature has ensured a solution for this issue: mammalian female cells inactivate one of their X chromosomes through the process of X chromosome inactivation (XCI), which results into a striking epigenetic and functional asymmetry between the two X chromosomes.

Most of our knowledge concerning the mechanisms of XCI regulation comes from mouse.

Identification of polymorphisms in different mouse strains has allowed the separate analysis of paternal and maternal X-linked genes, and thereby formed an important tool in the study of XCI, and particularly that of iXCI, during early stages of embryonic development. Conveniently, cell culture differentiation protocols of mouse embryonic stem cells largely recapitulating the process of random XCI have facilitated the research into this topic, and helped to shed light on many mechanistic aspects of the process. However, accumulating evidence suggests that there are significant differences in the biology of XCI during the pre-implantation period in several eutherian species (Wang et al. 2012; Okamoto et al. 2011; Petropoulos et al. 2016; Ferreira et al. 2010). This has necessitated the need for establishment of additional non-mouse models to study XCI.

In **Chapter 4** we developed a novel monolayer differentiation protocol, using as starting material rat embryonic stem cells (rESCs). Our protocol can be used to characterize the dynamics of rat XCI *in vitro* as well as to determine decisive players of the process. Importantly, it can be used for the evaluation of possibly conserved XCI features between the mouse and the rat, especially since the latter is gaining more and more ground in the study and modeling of human diseases (Iannaccone & Jacob 2009). We determined that XCI during differentiation of rESCs takes place with similar dynamics as observed during mESC differentiation. Additionally, overexpression experiments of RNF12 and REX1 revealed that the function of these proteins in the XCI process is conserved between rat and mouse. However, *in vivo* experiments in rat pre- and post-implantation embryos and placentas would be essential not only to fully elucidate differences and similarities on XCI between the two species, but also to validate our *in vitro* findings. The application of genome editing technologies recently applied in the rat (Chapman et al. 2015; Shao et al. 2014; Tesson et al. 2016; Tachibana et al. 2012), would be a valuable tool in designing the rat models that would be required for such *in vivo* experiments.

In general, it has to be noted that in spite of the fact that *in vitro* systems using ESCs or induced pluripotent stem cells (iPSCs) have greatly advanced our knowledge and our understanding on the molecular mechanisms of XCI, they do not always faithfully reflect the physiological process of *in vivo* X chromosome inactivation. For example, contrarily to the mouse ESCs and iPSCs, where pluripotency is accompanied by the presence of two active X chromosomes, faithfully recapitulating the *in vivo* ESCs of the mouse blastocyst, human ESCs and iPSCs have a much more variable X-inactivation/reactivation status. Specifically, different female human ESCs cell lines, derived by different protocols, have been reported to either carry one inactive X or two active X chromosomes (reviewed in Pasque & Plath 2015). Intriguingly, human embryo single cell RNA-sequencing revealed that *XIST* expression takes place from both X chromosomes in female pre-implantation embryos. More surprisingly, this study indicated that X chromosome dosage compensation in the preimplantation embryo is accomplished by reducing the expression of both X chromosomes, in contrast to the complete silencing of one selected X chromosome that occurs later in human development, but also in the mouse (Petropoulos et al. 2016). Whether the current hESCs derivation protocols result in the establishment of cell lines corresponding to late, early or to a very transient developmental stage of human embryo development needs to be determined.

All in all, despite that the use of *in vitro* systems has greatly advanced our knowledge about XCI inactivation, the use of *in vivo* models to study XCI is also extremely important, since it provides a more complete overview on the regulation of XCI.

General conclusions

In general, research studies using small populations of cells, like PGCs, early preimplantation embryos, hematopoietic stem cells and others, have always been technically challenging. The inability to conduct biochemical studies with such confined cell populations prompted researchers to mainly use immunofluorescence technologies, in order to gain insight about the molecular identity of those cells. Nevertheless, the urge to gain more in-depth knowledge on such cell populations' identity has led to the development of highly sensitive technologies, where accurate results can be obtained in just microscopic reactions. One example, is the RNA-seq technology complemented with microfluidics, which enables the analysis of a set of transcripts in single cells by quantitative PCR in nanolitre volumes, allowing for truly quantitative information of gene expression to be extracted (Burton & Torres-Padilla 2014). More interestingly though, even burdensome for small populations experiments such as ChIP-seq, can also be conducted with the use of microfluidics (Rotem et al. 2015). The application of such technologies to PGCs or early pre-implantation embryos would provide an enormous body of information on several molecular processes taking place in these cells, but also on their epigenetic profile, even on the single gene level.

In addition to the developments that geared towards improved sensitivity and quality of quantitative measurements in very small cell populations, other developments involve setting up *in vitro* models. These models would allow expansion of such cell populations followed by more standard, and perhaps still more robust, analyses methods. This is of particular importance in the absence of *in vivo* models to study certain developmental processes. Still, despite the fact that *in vitro* models have greatly contributed to the knowledge that we have acquired so far, they do not always recapitulate what is happening *in vivo*. Therefore, *in vitro* observations should always be confirmed *in vivo* and if differences are observed between the two, then these differences should assist in designing improved *in vitro* strategies. This is of great importance especially since good *in* *vitro* models can be extremely powerful in rendering breakthroughs that are important for both basic science and in the design of treatments for human diseases.

REFERENCES

Ancelin, K. et al., 2006. Blimp1 associates with Prmt5 and directs histone arginine methylation in mouse germ cells. Nature cell biology, 8(6), pp.623–30.

Baumann, C. et al., 2008. Association of ATRX with pericentric heterochromatin and the Y chromosome of neonatal mouse spermatogonia. BMC molecular biology, 9, p.29.

Brind'Amour, J. et al., 2015. An ultra-low-input native ChIP-seq protocol for genome-wide profiling of rare cell populations. Nature communications, 6, p.6033.

Burton, A. & Torres-Padilla, M.-E., 2014. Chromatin dynamics in the regulation of cell fate allocation during early embryogenesis. Nature Reviews Molecular Cell Biology, 15(11), pp.723–735.

Cao, Z. et al., 2015. A microfluidic device for epigenomic profiling using 100 cells. Nature methods, 12(10), pp.959–62.

Chapman, K.M. et al., 2015. Targeted Germline Modifications in Rats Using CRISPR/Cas9 and Spermatogonial Stem Cells. Cell reports, 10(11), pp.1828–35.

Condic, M.L., 2014. Totipotency: what it is and what it is not. Stem cells and development, 23(8), pp.796–812.

Eijpe, M. et al., 2000. Localisation of RAD50 and MRE11 in spermatocyte nuclei of mouse and rat. Chromosoma, 109(1–2), pp.123–132.

Erkek, S. et al., 2013. Molecular determinants of nucleosome retention at CpG-rich sequences in mouse spermatozoa. Nature structural & molecular biology, 20(7), pp.868–75.

Ferreira, A.R. et al., 2010. Allele-specific expression of the MAOA gene and X chromosome inactivation in in vitro produced bovine embryos. Molecular reproduction and development, 77(7), pp.615–21.

Fukuda, A. et al., 2015. Chromatin condensation of Xist genomic loci during oogenesis in mice. Development (Cambridge, England), 142(23), pp.4049–55.

Fukuda A, Mitani A, Miyashita T, Sado T, Umezawa A, Akutsu H Maintenance of Xist Imprinting Depends on Chromatin Condensation State and Rnf12 Dosage in Mice. PLOS Genet 2016, 12:e1006375.

Goldberg, A.D. et al., 2010. Distinct factors control histone variant H3.3 localization at specific genomic regions. Cell, 140(5), pp.678–91.

Hackett, J.A. et al., 2012. Promoter DNA methylation couples genome-defence mechanisms to epigenetic reprogramming in the mouse germline. Development (Cambridge, England), 139(19), pp.3623–32.

Hajkova, P. et al., 2008. Chromatin dynamics during epigenetic reprogramming in the mouse germ line. Nature, 452(7189), pp.877–81.

Hammoud, S., Liu, L. & Carrell, D.T., 2009. Protamine ratio and the level of histone retention in sperm selected from a density gradient preparation. Andrologia, 41(2), pp.88–94.

He, Q. et al., 2015. The Daxx/Atrx Complex Protects Tandem Repetitive Elements during DNA Hypomethylation by Promoting H3K9 Trimethylation. Cell stem cell, 17(3), pp.273–86.

Hill, P.W.S., Amouroux, R. & Hajkova, P., 2014. DNA demethylation, Tet proteins and 5-hydroxymethylcytosine in epigenetic reprogramming: an emerging complex story. Genomics, 104(5), pp.324–33.

Hisano, M. et al., 2013. Genome-wide chromatin analysis in mature mouse and human spermatozoa. Nature protocols, 8(12), pp.2449–70.

Iannaccone, P.M. & Jacob, H.J., 2009. Rats! Disease models & mechanisms, 2(5–6), pp.206–10.

Jonkers, I. et al., 2009. RNF12 is an X-Encoded dose-dependent activator of X chromosome inactivation. Cell, 139(5), pp.999–1011.

Kim, S. et al., 2014. PRMT5 protects genomic integrity during global DNA demethylation in primordial germ cells and preimplantation embryos. Molecular cell, 56(4), pp.564–79.

De La Fuente, R., Baumann, C. & Viveiros, M.M., 2015. ATRX contributes to epigenetic asymmetry and silencing of major satellite transcripts in the maternal genome of the mouse embryo. Development (Cambridge, England), (April), pp.1806–1817.

Lawson, K.A. & Hage, W.J., 1994. Clonal analysis of the origin of primordial germ cells in the mouse. Ciba Foundation symposium, 182, pp.68-84-91.

Liu, S. et al., 2014. Setdb1 is required for germline development and silencing of H3K9me3-marked endogenous retroviruses in primordial germ cells. Genes & development, 28(18), pp.2041–55.

Liu, X. et al., 2016. Distinct features of H3K4me3 and H3K27me3 chromatin domains in pre-implantation embryos. Nature, 537(7621), pp.558–562.

Marahrens, Y. et al., 1997. Xist-deficient mice are defective in dosage compensation but not spermatogenesis. Genes & development, 11(2), pp.156–66.

Namekawa, S.H. et al., 2006. Postmeiotic Sex Chromatin in the Male Germline of Mice,

Namekawa, S.H. et al., 2006. Report Postmeiotic Sex Chromatin in the Male Germline of Mice. Current Biology, 16, pp.660–667.

Okamoto, I. et al., 2004. Epigenetic dynamics of imprinted X inactivation during early mouse development. Science (New York, N.Y.), 303(5658), pp.644–9.

Okamoto, I. et al., 2011. Eutherian mammals use diverse strategies to initiate X-chromosome inactivation during development. Nature, 472(7343), pp.370–4.

Okamoto, I. et al., 2005. Evidence for de novo imprinted X-chromosome inactivation independent of meiotic inactivation in mice. Nature, 438(7066), pp.369–73.

Pasque, V. & Plath, K., 2015. X chromosome reactivation in reprogramming and in development. Current opinion in cell biology, 37, pp.75–83.

Peeters, S.B., Cotton, A.M. & Brown, C.J., 2014. Variable escape from X-chromosome inactivation: identifying factors that tip the scales towards expression. BioEssays : news and reviews in molecular, cellular and developmental biology, 36(8), pp.746–56.

Peters, A.H.F.M. et al., 2001. Loss of the Suv39h Histone Methyltransferases Impairs Mammalian Heterochromatin and Genome Stability. Cell, 107(3), pp.323–337.

Petropoulos, S. et al., 2016. Single-Cell RNA-Seq Reveals Lineage and X Chromosome Dynamics in Human Preimplantation Embryos. Cell, 165(4), pp.1012–1026.

Rapkin, L.M. et al., 2015. The histone chaperone DAXX maintains the structural organization of heterochromatin domains. Epigenetics & Chromatin, 8(1), p.44.

Rathke, C. et al., 2014. Chromatin dynamics during spermiogenesis. Biochimica et biophysica acta, 1839(3), pp.155–68.

Rotem, A. et al., 2015. Single-cell ChIP-seq reveals cell subpopulations defined by chromatin state. Nature Biotechnology, 33(11), pp.1165–1172.

Sadic, D. et al., 2015. Atrx promotes heterochromatin formation at retrotransposons. EMBO reports, 16(7), pp.836–50.

Shao, Y. et al., 2014. CRISPR/Cas-mediated genome editing in the rat via direct injection of one-cell embryos. Nature protocols, 9(10), pp.2493–512.

Shin, J. et al., 2010. Maternal Rnf12/RLIM is required for imprinted X-chromosome inactivation in mice. Nature, 467(7318), pp.977–81.

Shirakawa, T. et al., 2013. An epigenetic switch is crucial for spermatogonia to exit the undifferentiated state toward a Kit-positive identity. Development (Cambridge, England), 140(17), pp.3565–76.

Siklenka, K. et al., 2015. Disruption of histone methylation in developing sperm impairs offspring health transgenerationally. Science (New York, N.Y.), 350(6261), p.aab2006.

Sin, H.-S. & Namekawa, S.H., 2013. The great escape: Active genes on inactive sex chromosomes and their evolutionary implications. Epigenetics, 8(9), pp.887–92.

Sun, S. et al., 2015. Xist imprinting is promoted by the hemizygous (unpaired) state in the male germ line. Proceedings of the National Academy of Sciences of the United States of America, 112(47), pp.14415–22.

Tachibana, M. et al., 2012. X-chromosome inactivation in monkey embryos and pluripotent stem cells. Developmental biology, 371(2), pp.146–55.

Takagi, N., Sugawara, O. & Sasaki, M., 1982. Regional and temporal changes in the pattern of X-chromosome replication during the early post-implantation development of the female mouse. Chromosoma, 85(2), pp.275–86.

Tam, P.P. & Zhou, S.X., 1996. The allocation of epiblast cells to ectodermal and germ-line lineages is influenced by the position of the cells in the gastrulating mouse embryo. Developmental biology, 178(1), pp.124–32.

Tanaka, A. et al., 2015. Fourteen babies born after round spermatid injection into human oocytes. Proceedings of the National Academy of Sciences of the United States of America, 112(47), pp.14629–34.

Tesson, L. et al., 2016. Genome Editing in Rats Using TALE Nucleases. Methods in molecular biology (Clifton, N.J.), 1338, pp.245–59.

Turner, J.M.A., 2015. Meiotic Silencing in Mammals. Annual review of genetics, 49, pp.395–412.

Voon, H.P.J. et al., 2015. ATRX Plays a Key Role in Maintaining Silencing at Interstitial Heterochromatic Loci and Imprinted Genes. Cell reports, 11(3), pp.405–18.

Wang, X. et al., 2012. Random X inactivation in the mule and horse placenta. Genome research, 22(10), pp.1855–63.

Addendum

SUMMARY
SAMENVATTING
ABBREVIATION LIST
CURRICULUM VITAE
LIST OF PUBLICATIONS
PHD PORTFOLIO
ACKNOWLEDGEMENTS

SUMMARY

During the course of mammalian life the epigenome of each cell in the body responds to intra- and extracellular stimuli and it adapts and shapes its features (e.g. histone modifications, DNA methylation) accordingly. This is in contrast to the genome sequence, which mostly remains constant throughout life and it is almost identical in every cell of the body. Nevertheless, the coordinated functions of the genome and the epigenome will guide the unique gene expression program of each cell type, which will eventually define its functional identity during development.

In this thesis I focused on several major epigenetic reorganization events that take place during early preimplantation rodent (mouse and rat) development and also during the course of gametogenesis.

One of the epigenetic changes that occur in the early life of the mouse concerns solely the female mouse preimplantation embryo and involves regulation of the activity of its two X chromosomes. Following fertilization, the presence of a single X chromosome in the male embryo and of two X chromosomes in the female embryo generates a X-linked gene dosage imbalance. To establish a balance between X and autosomal gene expression, and to compensate for the X-linked gene expression dosage difference between the sexes, the female embryo silences one of its two X chromosomes through a process known as X chromosome inactivation (XCI). In murine preimplantation stages, it is always the paternal X chromosome (Xp) that is silenced and therefore this is an imprinted XCI (iXCI) mechanism. XCI is initiated by *Xist*, a long non-coding RNA that is transcribed from the future inactive X chromosome and covers that chromosome *in cis*. Interestingly enough, iXCI is not conserved in all mammalian species. For example, in human preimplantation embryos *XIST* upregulation takes place at the blastocyst stage from both parental X chromosomes and X-linked dosage compensation between the two sexes is achieved by lowering expression levels of the X-linked genes in females from both X chromosomes at the same time, rather than shutting down completely one X chromosome. This finding indicates that iXCI may be a feature of the mouse pre-implantation embryo solely and underscores the necessity of characterizing XCI in other rodent species.

As the mouse embryo develops, iXCI is reversed in the inner cell mass (ICM) of the blastocyst around embryonic day 4.5 (E4.5). This X reactivation is then again followed by XCI at approximately E5.5 in the epiblast cells. This time though, XCI is random, meaning that both parental X chromosomes have equal chances to get inactivated. The epiblast cells will give rise to the embryo proper. Once one X chromosome gets silenced in an epiblast cell de novo, its silenced state will be clonally propagated in the subsequent divisions.

At around E6.5 of mouse embryo development, the formation of the germline initiates in the dorsal epiblast through signalling emerging from the proximal extra-embryonic ectoderm. At this point the emerging primordial germ cells (PGCs) hold the same epigenetic signature and gene expression profile as the surrounding epiblast cells, which are destined to become somatic in nature. While developing further, genome wide reprogramming takes place in PGCs. This includes global alterations in histone modifications e.g. loss of H3K9me2, enrichment of H3K27me3 and global loss of DNA methylation, including also DNA methylation marking imprinted genes. All these alterations will lead to silencing of the somatic gene expression program, and to the activation of a germline one. However, during this reprogramming wave, the pericentromeres may need to retain their main epigenetic characteristics, especially since loss of histone modifications on these regions is linked to genetic aberrations. The inactive X chromosome does not escape from the genome wide epigenetic resetting in the germline and it is reactivated in the female PGCs. At around E13.5-E14.5, female PGCs enter meiosis, where both X chromosomes within the developing oocyte remain active. In addition, during oogenesis the X chromosome acquires an imprint, which will ensure that the maternal X chromosome will remain active during early mouse preimplantation development.

In male E13.5-E14.5 embryos, the PGCs enter mitotic arrest. Mitosis is resumed shortly after birth and male germ cells initiate spermatogenesis. As in females, male germ cells also enter meiosis, where homologous chromosomes pair and exchange genetic information to eventually produce genetically unique haploid gametes. The pairing of the X and Y sex chromosomes is challenging since the sex chromosomes are highly non-homologous and only synapse in a small homologous region called pseudoautosomal region (PAR). The extensive asynapsis between the X and Y chromosomes is associated with their transcriptional inactivation in a process called Meiotic Sex Chromosome Inactivation (MSCI). This transcriptional inactivation largely persists (although some genes are reactivated) one stage later, in the haploid round spermatids and is now termed as Post-meiotic Sex Chromosome Repression (PSCR). Later on, during spermiogenesis, the vast majority of histones in the developing sperm is replaced by protamines, that will facilitate the further compaction of the sperm genome into the small sperm nucleus.

Following fertilization, the protamines are removed and replaced with unmodified histones provided by the oocyte. Current evidence suggests, that the Xp *Xist* gene becomes active at the 2-cell stage, concomitant with zygotic genome activation (ZGA). However, the possibility that certain epigenetic marks related to MSCI and PSCR persist on the sperm genome, and may have an impact on iXCI after fertilisation, cannot be excluded.

All the above-mentioned reprogramming events must be tightly coordinated and controlled, since defects in the cascade of steps comprising these events is linked to embryonic lethality or infertility. In this thesis I have focused on characterising and understanding epigenetic phenomena taking place during early rodent preimplantation and PGC development.

Therefore, in **Chapter 1** I provide a detailed theoretical overview of the epigenetic phenomena examined in this thesis.

In **Chapter 2**, we sought to examine the impact of the paternal epigenome on mouse iXCI. For this purpose, we made use of the round spermatid injection (ROSI) technology, and we injected round spermatids deficient for *Xist* (XpΔ*Xist*) and which already carry a largely transcriptionally inactive X chromosome (due to PSCR), enriched with silencing histone marks such as H3K9me3. We speculated that by bypassing the histone-to-protamine and protamine-to-histone transitions through ROSI and by injecting an already pre-inactivated Xp we might be able to establish Xp inactivation, in the absence of a functional paternal *Xist*. At the same time we hypothesized that we would rescue female embryonic lethality that is normally observed when sperm lacking functional *Xist* is used for fertilisation. Indeed, by performing ROSI with Δ*Xist* round spermatids we were able to rescue the embryonic lethality of Xp*Xist*Xm female embryos. Surprisingly though, RNA-DNA FISH experiments for the maternal wild type and the paternal mutated *Xist* gene and RNA revealed that the rescue was not mediated by an *Xist* independent inactivation of Xp, but rather by inactivating the maternal X chromosome (Xm) through maternally provided *Xist* mediated silencing. Initiation of Xm inactivation in XpΔ*Xist*Xm ROSI derived female embryos takes place later (~morula stage) compared to Xp inactivation in wild type embryos derived either by natural mating or by injecting wild type round spermatids (~4-cell stage), and silencing marks (H3K27me3) are established in the blastocyst rather than during the morula stage. We found that an XCI trans-activator named RNF12 is present in high levels in male and female embryos, when performing ROSI. However, since we never observed *Xist* expression in male embryos following ROSI, we speculate that additional still unknown factors act together with RNF12 to mediate to silencing of Xm, in the presence of XpΔ*Xist*. This then eventually allows survival of these female embryos. Interestingly, rescuing was not achieved when CAS/EiJ spermatids were used instead of C57BL6, indicating that critical factors contributing to the rescuing may not be (sufficiently) expressed in the CAS/EiJ round spermatids. Overall, our data suggest that the correct regulation of expression of X-linked trans-activators of XCI from possibly both X chromosomes is of critical importance in the establishment of XCI in mouse. Future experimentation may provide evidence on the identity of such XCI trans-activators.

Going one step later in development, in **Chapter 3** we focused on the epigenetic signature of pericentric heterochromatin during PGC development. In this study, we used different fixation and sample preparation methods to carefully examine the epigenetic state of pericentric heterochromatin during PGC development. Our results indicated that pericentric heterochromatin maintains its epigenetic marks throughout PGC development. However, we did notice that under a certain condition the original observations by others - that pericentric heterochromatin loses its epigenetic identity at E11.5 mouse embryo development - could also be reproduced. The data we obtained nicely illustrated the necessity of evaluating results of different experimental approaches in order to reach valid conclusions. In addition, analysis by immunofluorescence with specific markers of pericentromeric clustering (chromocenter formation) revealed that pericentromeres did not cluster together in a similar fashion as in the surrounding somatic cells, but they mainly remained as individual entities within the E10.5-E13.5 PGC nuclei. This individualisation was not accompanied by transcriptional activation of pericentric transcripts (major satellites), and might reflect alterations in the organisation and structure of PGC pericentromeres. Lastly, we observed higher accumulation of the chromatin remodeller ATRX on the pericentromeres of E11.5 PGCs compared to the surrounding soma of the same developmental stage. In the future it would be interesting to examine what is the exact function of the elevated ATRX accumulation in the pericentromeres of E11.5 PGCs, and when the dissociation of the chromocenters initiates in the germline.

In **Chapter 4** we established a robust *in vitro* differentiation strategy in order to examine XCI in rat differentiating stem cells (ESCs). Studying XCI in a species other than the mouse may provide valuable information about the conserved aspects of iXCI in rodents. This is particularly important, especially since iXCI does not seem to be conserved in all mammalian species e.g. human. With the use of our *in vitro* strategy, we were able to demonstrate that the process of XCI in the female rat cell lines initiates at ~ day 2 of differentiation by accumulation of *Xist* transcripts on one of the two X chromosomes. X-linked gene silencing through H3K27me3 enrichment on the same X chromosome also rapidly follows the *Xist* accumulation. Importantly, by overexpressing factors known to be decisive for XCI in mouse (REX1 and RNF12), in rESCs we observed that certain XCI regulation aspects (REX1-RNF12 axis) are indeed conserved between mouse and rat.

In **Chapter 5** we established a powerful and rapid DNA-RNA FISH protocol, which enables the simultaneous detection of DNA and RNA molecules in mouse pre-implantation embryos, without compromising the sample's quality. This was achieved by incorporating and adapting steps used in DNA FISH such as sample incubation in HCl solution in our RNA FISH protocol common. The use of our DNA-RNA FISH protocol may be a valuable tool not only in basic science, for example when studying different XCI aspects in the early embryo, but also in diagnostics, since it could be potentially adapted and applied to any other type of material (e.g. cultured cells, patient tissue samples) where both nascent RNA transcripts (*Xist* or others) and genomic positions need to be detected.

To conclude, in **Chapter 6** I have discussed the results obtained during the course of my Ph.D. study in light of the current knowledge concerning the epigenetic phenomena presented and studied in this thesis. Finally, I provide suggestions for future research directions, in line with experimental restrictions but also possibilities when studying low abundance-cells, such as PGCs or early embryos, that will facilitate obtaining a better overview of the examined epigenetic phenomena described here.

Samenvatting

Tijdens het leven van zoogdieren reageert het epigenoom van elke lichaamscel op intra- en extracellulaire stimuli en adapteert en vormt zich daarnaar (door middel van bijvoorbeeld histon modificaties en DNA methylatie). Dit in tegenstelling tot het genoom zelf, wat vrijwel onveranderd blijft tijdens het leven en nagenoeg identiek is in elke lichaamscel.

Desalniettemin, resulteren de onderling gecoördineerde functies van het genoom en het epigenoom in genexpressie patronen die specifiek zijn voor elk cel type. Hierdoor wordt uiteindelijk de functionele identiteit gedefinieerd tijdens de ontwikkeling. In dit proefschrift focus ik op verschillende belangrijke grootschalige veranderingen in het epigenoom die plaatsvinden in het pre-implantatie embryo en tijdens gametogenese bij knaagdieren (muis en rat). Een van de epigenetische veranderingen die plaatsvinden in de vroege ontwikkeling van de muis is specifiek voor vrouwelijke pre-implantatie embryo's en betreft de regulatie van de activiteit van de twee X chromosomen. Na bevruchting is er een gendosering verschil tussen mannelijke embryo's die over één X chromosoom per cel beschikt en de vrouwelijke embryo's die over 2 exemplaren beschikken.

Om gen expressie van de X chromosomen en de autosomale chromosomen in evenwicht te brengen en om de verschillen in dosering van X chromosoom gelinkte genexpressie tussen de seksen te compenseren, inactiveert het vrouwelijke embryo één van de X chromosomen door middel van een proces dat bekend staat als X chromosoom inactivatie (XCI). In de pre-implantatie stadia bij de muis is het altijd het paternale X chromosoom (Xp) dat geinactiveerd wordt. Daarom is dit een geïmprint XCI (iXCI) mechanisme. XCI wordt geïnitieerd door *Xist*, een lang, niet coderend RNA dat wordt afgeschreven van het toekomstige inactieve X chromosoom en het chromosoom bedekt *in cis*. Interessant is dat iXCI niet geconserveerd is in alle zoogdier soorten. Bijvoorbeeld, in humane pre-implantatie embryo's vindt verhoogde expressie van *XIST* plaats van beide X chromosomen. Dosering van expressie van de X chromosomen wordt bij de mens tot stand gebracht door verlaging van expressie niveaus van de X-chromosoom gelinkte genen voor beide chromosomen in het blastocysten stadium, niet door het volledig inactiveren van één heel chromosoom. Deze vinding geeft aan dat iXCI een eigenschap kan zijn specifiek voor muis pre-implantatie embryo's en geeft het belang aan voor beschrijving van XCI in andere knaagdier soorten.

Tijdens de verdere ontwikkeling van de muis wordt iXCI ongedaan gemaakt in de embryoblast van de blastocyst rond dag 4.5 van de embryonale ontwikkeling (E4.5). Deze reactivatie van het X chromosoom wordt wederom gevolgd door XCI rondom dag E5.5 in de epiblast cellen. Echter, in dit stadium vindt XCI willekeurig plaats, wat betekent dat beide ouderlijke chromosomen een evenredige kans hebben om geïnactiveerd te worden. De epiblast cellen vormen later het eigenlijke embryo. Zodra een van de twee X chromosomen geïnactiveerd wordt in een epiblast cel, dan zal deze de novo geïnactiveerde staat clonaal gepropageerd worden tijdens de volgende celdelingen.

De formatie van de kiembaan wordt rond dag E6.5 dorsaal in de epiblast geïnitieerd door signalen komend uit het proximale embryologische ectoderm. In dit stadium hebben de primordiale kiemcellen (PKCs) dezelfde epigenetische opmaak en gen expressie als de naburige epiblast cellen, welke voorbestemd zijn het toekomstige soma te worden. Tijdens de verdere ontwikkeling, vindt herprogrammering van het gehele genoom plaats in PKCs. Dit gaat gepaard met veranderingen in histon modificaties, bijvoorbeeld verlies van H3K9me2, verrijking van H3K27me3 en verlies van DNA methylatie, inclusief DNA methylatie markering van geïmprinte genen. Al deze veranderingen leiden tot het inactiveren van het gen expressie patroon specifiek voor somatische cellen en de vorming van een gen expressie patroon specifiek voor kiemcellen.

De pericentromeren zouden wel eens uitgezonderd kunnen zijn van deze herprogrammering, in het bijzonder omdat verlies van histon modificaties in deze regionen gelinked zijn aan genetische afwijkingen. Het inactieve X chromosoom wordt niet uitgezonderd van de epigenetische herprogrammering in de kiembaan en wordt gereactiveerd in vrouwelijks PKCs. Rondom dag 13.5-14.5 van de embryonale ontwikkeling beginnen vrouwelijke PKCs aan de meiose, tijdens welke beide X chromosomen transcriptioneel actief zijn. Daarnaast krijgt het X chromosoom tijdens de oögenese een imprint die ervoor zorgt dat het maternale X chromosoom actief blijft tijdens de pre-implantatie stadia van de muis. In mannelijke embryo's raken de PKCs op dit embryonale tijdstip mitotisch gearresteerd. De mitotische delingen worden vervolgd kort na geboorte en de mannelijke kiemcellen initiëren spermatogenese. Net als in de vrouwelijke sekse, doorlopen mannelijke kiemcellen meiose. Hierin worden homologe chromosomen gepaard gepositioneerd en waarna dan genetische informatie uitgeruild wordt, om zo uiteindelijk genetisch unieke haploïde gameten te vormen. Het paren van de X en Y chromosomen is een uitdaging omdat de sex chromosomen grotendeels niet homoloog zijn. Een kleine homoloog domein, genaamd de pseudoautosomale regio (PAR) is de enige plek waar synapsis plaats vindt. Het grotendeels ontbreken van synapsis is geassocieerd met hun transcriptionele inactivatie in een proces genaamd Meiotische Sex Chromosoom Inactivatie (MSCI). Deze transcriptionele inactivatie wordt grotendeels gehandhaafd (met de uitzondering van enkele genen) tijdens het daaropvolgende stadium in de spermiogenese. Daar wordt dit fenomeen dan Postmeiotische Sex Chromosoom Repressie (PSCR) genoemd. Tijdens de spermiogenese wordt in de elongerende spermatide het merendeel van de histonen verwijderd en vervangen door protamines. Deze zullen de verdere compactie van de nucleus van de zaadcel faciliteren.

Gelijk na de bevruchting worden de protamines verwijderd en vervangen door ongemodificeerde maternale histonen. Inzichten van nu suggereren dat het *Xist* gen gelegen op het paternale X chromosoom actief wordt in het 2-cellig embryo, tegelijkertijd met de activatie van het embryonale genoom. Toch blijft het mogelijk dat bepaalde epigenetische markeringen gerelateerd aan MSCI en PSCR aanwezig blijven in het zaadcel genoom en een mogelijke invloed hebben op het proces van iXCI na bevruchting.

Alle hierboven genoemde herprogrammering gebeurtenissen moeten zorgvuldig gecoördineerd en gecontroleerd worden. Defecten in deze processen zijn gelinkt aan embryonale sterfte of infertiliteit.

In dit proefschrift heb ik gefocust op het beschrijven en begrijpen van epigenetische fenomenen die plaats vinden in de vroege, pre-implantatie stadia en PKC ontwikkeling bij knaagdieren.

Hiertoe geef ik in **Hoofdstuk 1** een gedetailleerd theoretisch overzicht van de epigenetische fenomenen die aan bod komen in dit proefschrift.

In **Hoofdstuk 2** hebben we geprobeerd de impact van het paternale epigenoom te bepalen op iXCI in de muis, We hebben gebruik gemaakt van ROnde Spermatide Injecties (ROSI) waarbij ronde spermatiden in oocyten worden geïnjecteerd. We hebben spermatiden geïnjecteerd waarbij het *Xist* gen ontbrak (XpΔ*Xist*) en die al een grotendeels door PSCR transcriptioneel geïnactiveerd X chromosoom dragen, wat verrijkt is met inactieve markering zoals H3K9me3. We speculeren dat door het overslaan van de histon-naar-protamine transitie en het injecteren van een al geïnactiveerd Xp we in staat zijn om Xp inactivatie te bewerkstelligen in de afwezigheid van een functioneel paternal *Xist* gen. Tegelijkertijd was onze hypothese dat we sterfte die in vrouwelijke embryo's optreedt wanneer deze zijn bevrucht met zaadcellen waarin het *Xist* gen ontbreekt zouden kunnen voorkomen.

Inderdaad waren we in staat om de sterfte van vrouwelijke embryo's te voorkomen door Δ*Xist* ronde spermatiden te injecteren. Verrassend was onze observatie, met RNA-DNA FISH experimenten voor het maternale normale *Xist* allel en het paternale gemuteerde *Xist* gen en RNA, dat dit niet werd voorkomen door een *Xist* onafhankelijke inactivatie van het Xp maar door inactivatie van het maternale X chromosoom (Xm) door maternaal geleverd, *Xist* gemedieerde inactivatie.

Initiatie van de inactivatie van Xm in de met ROSI tot stand gebrachte XpΔ*Xist*Xm vrouwelijke embryo's vindt later plaats (~morula stadium) dan Xp inactivatie in normale embryo's die op de normale manier of met ROSI tot stand zijn gebracht (~4 cellig stadium), en inactieve histon modificaties verschijnen in het blastocyste stadium in plaats van in het morula stadium.

We hebben gevonden dat een XCI trans-activeerder genaamd RNF12 in hoge niveaus aanwezig is in mannelijke en vrouwelijke embryo's wanneer er ROSI wordt uigevoerd. Maar omdat er door ons nooit *XIST* expressie is waargenomen in mannelijke embryo's na ROSI, speculeren we dat additionele nog onbekende factoren samen werken met RNF12 om inactivatie van Xm in de aanwezigheid van XpΔ*Xist* te medieëren. Dit zorgt er dan uiteindelijk voor dat deze vrouwelijke embryo's overleven. Interessant is ook dat vrouwelijke embryo's niet gered konden worden als CAS/EiJ spermatiden in plaats van C57BL6 gebruikt werden. Dit suggereert dat kritische factoren die bijdragen aan de overleving van deze embryo's niet (voldoende) tot expressie komen in ronde CAS/EiJ spermatiden. Alles bij elkaar genomen laat onze data zien dat correcte regulatie van expressie van X gelinkte trans activatoren van XCI, mogelijkerwijs van beide X chromosomen, zeer belangrijk is voor de uitvoer van XCI in de muis. Toekomstige experimenten kunnen mogelijk deze XCI transactivatoren identificeren.

In **Hoofdstuk 3** hebben we gekeken naar een proces wat later in de embryonale ontwikkeling plaatsvindt: de epigenetische opmaak van het pericentrische heterochromatine tijdens PKC ontwikkeling. In dit onderzoek hebben we verschillende fixatie en prepareer protocollen toegepast om zorgvuldig de epigenetische opmaak van het pericentrische heterochromatine tijdens PKC ontwikkeling in kaart te brengen. Onze resultaten laten zien dat pericentrisch heterochromatine zijn epigenetische markering behoud tijdens het proces van differentiatie. De observatie van anderen, dat pericentrisch heterochromatine zijn epigenetische opmaak verliest op embryonale dag 11.5, konden we ook reproduceren door specifieke fixatie en prepareer omstandigheden. Deze data laat goed zien hoe noodzakelijk het is om verschillende experimentele methoden te evalueren om tot de juiste conclusies te komen. Daarnaast heeft analyse door middel van immunofluorescentie met specifieke makers van pericentrische clustering (chromocenter formatie) laten zien dat pericentromeren niet clusteren op de manier waarin dit gebeurd in somatische cellen maar veelal individueel aanwezig bleven in de PKC nucleus. Deze individualisering ging niet samen met transcriptionele activatie van pericentrische transcripten, en dit is wellicht een teken van en verandering in de organisatie en structuur van pericentromeren in PKCs. Als laatste hebben we ook een verhoogde aanwezigheid van de chromatine hervormer ATRX op de pericentromeren van PKCs op embryonale dag 11.5 waargenomen in vergelijking met de daarom liggende somatische cellen. Verder onderzoek zal moeten uitwijzen wat de exacte functie is van deze verhoogde ATRX niveaus en wanneer de dissociaties van chromocentra in de kiembaan geïnitieerd wordt.

In hoofdstuk 4 hebben we een robuuste *in vitro* differentiatie strategie voor embryonale stam cellen van de rat (rESCs) ontwikkeld voor het bestuderen van XCI in deze knaagdier soort. Het bestuderen van XCI in een soort ander dan de muis kan waardevolle inzichten geven over geconserveerde aspecten van iXCI in knaagdieren. Dit is in het bijzonder van belang omdat iXCI niet geconserveerd lijkt te zijn in alle zoogdieren (bijvoorbeeld de mens). Door middel van onze *in vitro* strategie zijn we er in geslaagd te demonstreren dat het proces van XCI in vrouwelijke rat cellen op ~dag 2 geïnitieerd wordt door accumulatie van *Xist* transcripten op een van de twee X chromosomen. Inactivatie van X gelinkte genen door verrijking van H3K27me3 op hetzelfde X chromosoom volgt ook snel op *Xist* accumulatie. Belangrijk is dat het tot over expressie brengen van factoren die een essentiële functie hebben in XCI in de muis (REX1 en RNF12), in rESCs dezelfde regulatoire effecten hebben en dat de REX1-RNF12 as inderdaad geconserveerd is in zowel de muis en de rat.

In **Hoofdstuk 5** presenteren we een krachtig en snel DNA-RNA FISH protocol, welke het mogelijk maakt om tegelijkertijd DNA en RNA moleculen in pre-implantatie embryo's van de muis te detecteren zonder de integriteit van het sample te compromiseren. Dit werd bewerkstelligd door bepaalde stappen toe te voegen en bestaande stappen te modificeren in gebruikte DNA FISH protocollen zoals incubatie van samples in HCl oplossingen. Het gebruik van ons DNA-RNA FISH protocol kan niet alleen een waardevolle toevoeging zijn voor fundamenteel onderzoek, bijvoorbeeld het bestuderen van verschillende aspecten van XCI in het vroege embryo, maar ook in een diagnostische setting, omdat het aangepast en toegepast kan worden voor ander materiaal (bijvoorbeeld weefsels van patiënten) waar zowel RNA transcripten (*Xist* of andere) en genomische locaties gedetecteerd moeten worden.

Ten slotte bediscussieer ik in **Hoofdstuk 6** de resultaten die behaald tijdens mijn promotie onderzoek in de context van de huidige kennis omtrent de epigenetische fenomenen die in mijn proefschrift zijn gepresenteerd. Ook presenteer ik suggesties voor verder toekomstig onderzoek, welke rekening houden met de experimentele restricties, maar ook de mogelijkheden wanneer schaars materiaal zoals PKCs of vroege embryo's worden bestudeerd. Deze suggesties zullen het verkrijgen van een beter overzicht van de epigenetische fenomenen die hier in dit proefschrift beschreven worden faciliteren.

LIST OF ABBREVIATIONS

Actb	actin b
AID/AICD	activation induced cytidine deaminase
AT	Acidic Tyrode's Solution
ATR	ataxia telangiectasia and Rad3-related protein (Serine/threonine-pro tein kinase)
ATRX	alpha thalassemia/mental retardation syndrome X-linked
BAC	bacterial artificial chromosome
BMI	B cell-specific Moloney murine leukemia virus integration site
BMP	bone morphogenetic protein
BRCA	breast cancer
BSA	bovine serum albumin
Canx	calnexin
CBX	chromobox
CD	chromodomain
cDNA	complementary DNA
CENP	centromere protein
ChIP	chromatin immunoprecipitation
CREST	calcium-responsive transactivator
Ct	theshold cycle
DAPI	4',6-Diamidino-2-Phenylindole
DAXX	death domain associated
DMR	differentially methylated region
DNA	deoxyribonucleic acid
DNMT	DNA methyltransferase
DSB	double strand breaks
E	embryonic day
Eif2s3y	eukaryotic translation initiation factor 2, subunit 3 (Y-linked)
Esrrb	estrogen related receptor
ExE	extra embryonic ectoderm
ERV	endogenous retroviruses
ESC	embryonic stem cells
FA	formamide
FACS	fluorescence-activated cell sorting
FISH	fluorescence in situ hybridisation

FITC	fluorescein isothiocyanate
fg	fully grown
FSH	follicle stimulating hormone
Gapdh	Glyceraldehyde 3-phosphate dehydrogenase
GFP	Green fluorescent protein
GLP	G9a-like protein
hCG	human chorionic gonadotropin
HCl	hydrochloric acid
HORMAD	HORMA domain containing 1
HP1	heterochromatin protein 1
IAP	intracisternal A particle
ICM	inner cell mass
ICSI	intracytoplasmic sperm injection
IVF	*in vitro* fertilisation
iXCI	imprinted X chromosome inactivation
iPSC	induced pluripotent stem cells
LH	luteneizing hormone
LTR	long terminal repeats
MNase	micrococcal nuclease
MSCI	meiotic sex chromosome inactivation
MSUC	meiotic silencing of unsynapsed chromatin
ng	non-growing
NIH-3T3	National Institute of Health 3-day transfer, inoculum 3 x 10^5 cells
NPB	nuclear precursor body
O.C.T.	Optimal cutting temperature compound
OCT4	octamer-binding transcription factor 4
P	postpatrum or placenta
PAR	pseudoautosomal region
PBS	phosphate buffered saline
PGC	primordial germ cell
Pgk1	phosphoglycerate kinase 1
PFA	paraformaldehyde
PHC	pericentric heterochromatin
PMSC	post meiotic sex chromosome
PRC	Polycomb repressive complex
PRDM	PR/SET domain
Prm	protamine

PRMT	Protein arginine methyltransferase
(q) PCR	(quantitative) polymerase chain reaction
PSCR	postmeiotic sex chromatin repression
Rex	Reduced expression
RNA	ribonuclei acid
RNA pol II	RNA polymerase II
RNF	RING finger protein
ROCK	Rho-associated, coiled-coil containing protein kinase
ROSI	round spermatid injection
RS	round spermatid
RT	reverse transcription
rXCI	random X chromosome inactivation
SOX	SRY (sex determining region Y)-box 2
SSC	or spermatogonial stem cells
PMSG	pregnant mare's serum gonadrotopin
P.Sp./S.Sp.	primary spermatocyte/secondary spermatocyte
Rsx	RNA-on-the-silent X
$StCl_2$	strontium chloride
SUMO	small ubiquitin-related modifier
SUV39H	suppressor of variegation 3-9 homolog
Tet	tet-eleven translocation
Tfap2	transcription factor AP-2
Tp	transition protein
TS	Tris-saline
Tsix	X inactive specific transcript, antisense
VRC	vanadyl ribosyc complex
WT	wild type
XCI	X chromosome inactivation
Xic	X inactivation center
Xm	maternal X chromosome
Xp	paternal X chromosome
ZGA	zygotic genome activation
γH2AX	phosphorylated H2AX
5mC/5hmC	5-methyl-cytosine/5-hydroxylmethyl-cytosine
5caC/5fC	5-carboxylcytosine/5-formylcytosine

CURRICULUM VITAE

Aristea Maria Magaraki was born on the 7th of May 1984, in Heraklion Crete, Greece. After finishing her secondary education in Heraklion, she moved to Thessaloniki to study biology in Aristotle University, where she obtained her B.Sc. degree with specialisation in genetics, developmental and molecular biology. With the completion of her undergraduate studies, she joined the programme “Cancer Genomics & Developmental biology” in Utrecht University (the Netherlands) in 2009, where she obtained her M.Sc. degree. During this period she joined laboratories of the Hubrecht Institute, the Developmental Biology division in Utrecht University, University Medical Center Utrecht (UMCU) and the Faculty of Veterinary Medicine Utrecht, where she participated in research projects related to mammalian and non-mammalian reproductive systems.

With the completion of her master studies she moved back to Heraklion, where she conducted research on breast metastatic cancer cells in the School of Medicine, in University of Crete.

Eventually, in 2011 she returned back to the Netherlands to join the department of Developmental Biology in Erasmus Medical Center (Rotterdam), in order to obtain a Ph.D. degree. During her Ph.D. period she worked on the research topics described in this thesis.

LIST OF PUBLICATIONS

1. **Aristea Magaraki**, Godfried van der Heijden, Esther Sleddens-Linkels, Antoine H. F. M. Peters, Joost Gribnau, Willy M. Baarends*# and Maureen Eijpe#. Silencing markers are retained on pericentric heterochromatin during murine primordial germ cell development. Submitted.

2. **Aristea Magaraki**, Agnese Loda, Joost Gribnau and Willy M. Baarends*, A robust protocol for simultaneous DNA-RNA FISH in mouse pre-implantation embryos. Invited manuscript (Springer Protocols).

3. **Aristea Magaraki#**, Agnese Loda#, Cristina Gontan Pardo, Stephen Meek, Willy M. Baarends, Tom Burdon[1] and Joost Gribnau*. Generation of a novel *in vitro* differentiation strategy to study the dynamics of X chromosome inactivation in rat. Manuscript in preparation.

4. Federica Federici#, **Aristea Magaraki#**, Evelyne Wassenaar, Catherina JH van Veen-Buurman, Christine van de Werken, Esther B Baart, Joop SE Laven, J Anton Grootegoed, Joost Gribnau and Willy M Baarends*, Round spermatid injection rescues female lethality of a paternally inherited *Xist* deletion in mouse. PLoS Genet. 7;12(10):e1006358, 2016 Oct.

5. K. S. Skaar#, R. H. Nóbrega#, **A. Magaraki**, L. C. Olsen, R. W. Schulz, and R. Male*, Proteolytically activated, recombinant Anti-Müllerian Hormone inhibits androgen secretion, proliferation, and differentiation of spermatogonia in adult Zebrafish testis organ cultures. Endocrinology. 152(9):3527-40, 2011 Sep.

# equal contribution, * corresponding author

Ph.D. PORTFOLIO

Summary of Ph.D. training and teaching

Name PhD student: Aristea Maria Magaraki
Erasmus MC Department: Developmental Biology
Research School: Biomedical Sciences
PhD period: March 2011- December 2016
Promotor(s): Prof.dr. Joost Gribnau
Supervisor(s): dr. M.Eijpe
dr. W.M.Baarends

1. PhD training

General courses	Year
- Genetics	2011
- Laboratory animal sciences (art.9/FELASA-C)	2012
- Handling of laboratory animals (IVC)	2012
- Biochemistry and Biophysics	2011
- Cell and Developmental Biology	2011
- Literature course	2012
- Biostatistical methods I: Basic	2014

Seminar and workshops	
- 18th MGC workshop, Maastricht	2011
- The Ensemble workshop	2012
- Adobe Photoshop and Illustrator CS6 workshop	2012
- 21st MGC Workshop, Münster, Germany	2014
- Indesign CS6 workshop	2015
- Winterschool Kleinwalserthal (oral presentation)	2016
- XCI retreat, Tinos, Greece	2016

(Inter)national conferences	
- Stem cells, development and regulation, Amsterdam	2013
- 12th Dutch Chromatin meeting, Utrecht, The Netherlands (poster)	2014
- Keystone symposium "Chromatin mechanisms and cell physiology", Oberstdorf (poster)	2014
- 13th Annual ISSCR meeting, Stockholm, Sweden (poster)	2015
- TRR81 International Chromatin Symposium, Marburg, Germany (poster)	2015

2. Teaching

- Teaching assistant in "VO Vroege embryos klonen en transgenese"	2015
- Assessing EvoDevo posters (2nd year Nanobiology students)	2016

ACKNOWLEDGEMENTS

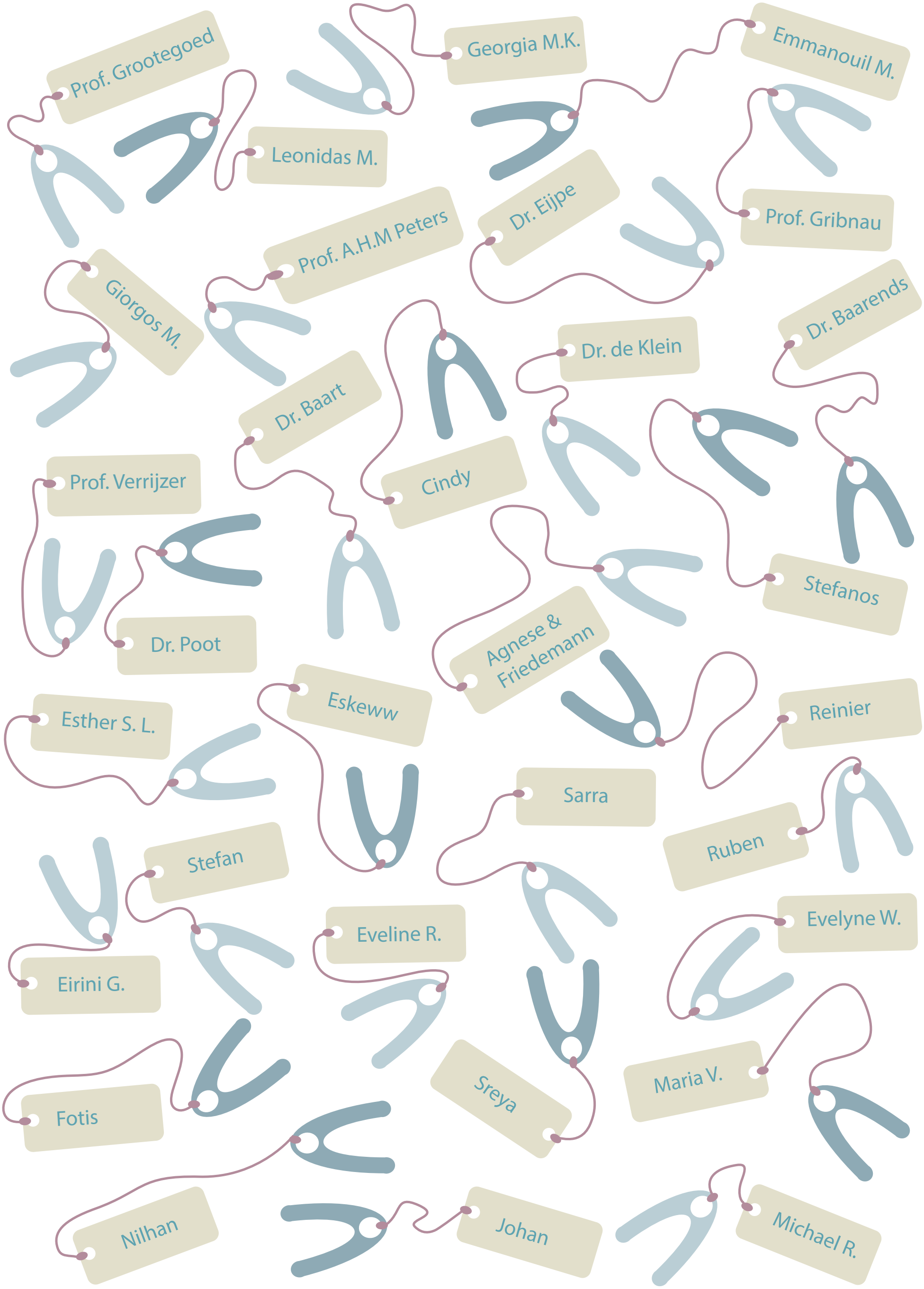
Prof. Grootegoed
Georgia M.K.
Emmanouil M.
Leonidas M.
Prof. Gribnau
Dr. Eijpe
Prof. A.H.M Peters
Giorgos M.
Dr. Baarends
Dr. de Klein
Dr. Baart
Cindy
Prof. Verrijzer
Stefanos
Dr. Poot
Agnese &
Friedemann
Esther S. L.
Eskeww
Reinier
Sarra
Ruben
Stefan
Eveline R.
Evelyne W.
Eirini G.
Maria V.
Sreya
Fotis
Nilhan
Johan
Michael R.

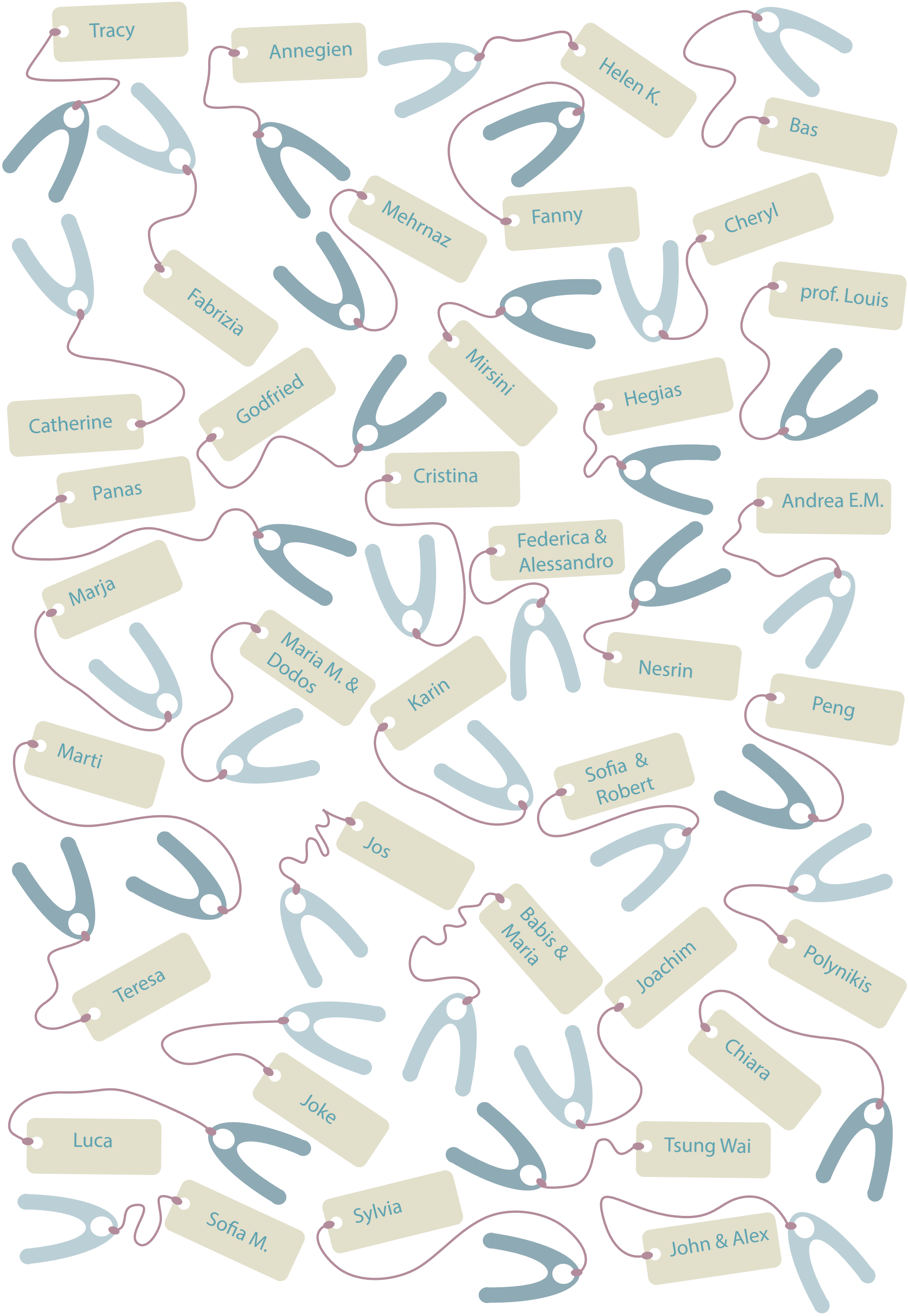
Tracy
Annegien
Helen K.
Bas
Mehrnaz
Fanny
Cheryl
Fabrizia
prof. Louis
Mirsini
Catherine
Godfried
Hegias
Cristina
Panas
Andrea E.M.
Federica & Alessandro
Marja
Maria M. & Dodos
Karin
Nesrin
Peng
Marti
Sofia & Robert
Jos
Babis & Maria
Joachim
Polynikis
Teresa
Chiara
Joke
Luca
Tsung Wai
Sofia M.
Sylvia
John & Alex